



CRANIAL ANATOMY OF KRYPTOBAATAR DASHZEVEGI (MAMMALIA, MULTITUBERCULATA), AND ITS BEARING ON THE EVOLUTION OF MAMMALIAN CHARACTERS

Authors: WIBLE, JOHN R., and ROUGIER, GUILLERMO W.

Source: Bulletin of the American Museum of Natural History, 2000(247) : 1-120

Published By: American Museum of Natural History

URL: [https://doi.org/10.1206/0003-0090\(2000\)247<0001:CAOKDM>2.0.CO;2](https://doi.org/10.1206/0003-0090(2000)247<0001:CAOKDM>2.0.CO;2)

BioOne Complete (complete.BioOne.org) is a full-text database of 200 subscribed and open-access titles in the biological, ecological, and environmental sciences published by nonprofit societies, associations, museums, institutions, and presses.

Your use of this PDF, the BioOne Complete website, and all posted and associated content indicates your acceptance of BioOne's Terms of Use, available at www.bioone.org/terms-of-use.

Usage of BioOne Complete content is strictly limited to personal, educational, and non - commercial use. Commercial inquiries or rights and permissions requests should be directed to the individual publisher as copyright holder.

BioOne sees sustainable scholarly publishing as an inherently collaborative enterprise connecting authors, nonprofit publishers, academic institutions, research libraries, and research funders in the common goal of maximizing access to critical research.

CRANIAL ANATOMY OF
KRYPTOBAATAR DASHZEVEGI
(MAMMALIA, MULTITUBERCULATA),
AND ITS BEARING ON THE EVOLUTION
OF MAMMALIAN CHARACTERS

JOHN R. WIBLE

Research Associate, Division of Vertebrate Zoology, American Museum of Natural History; Section of Mammals, Carnegie Museum of Natural History, 5800 Baum Boulevard, Pittsburgh, PA 15206

GUILLERMO W. ROUGIER

Research Associate, Division of Paleontology, American Museum of Natural History; Department of Anatomical Sciences and Neurobiology, School of Medicine, University of Louisville, Louisville, KY 40292

BULLETIN OF THE AMERICAN MUSEUM OF NATURAL HISTORY

Number 247, 124 pages, 39 figures, 3 tables

Issued February 28, 2000

Price: \$10.90 a copy

CONTENTS

Abstract	4
Introduction	5
Materials and Methods	9
Descriptions	16
Premaxilla	16
Nasal	19
Lacrimal	20
Frontal	21
Maxilla	23
Palatine	28
Pterygoid	30
Sphenoid Complex	31
Petrosal	36
Jugal	43
Squamosal	43
Parietal	46
Supraoccipital	46
Exoccipital	47
Basioccipital	48
Endocranium	48
Mandible	59
Vascular Reconstructions	62
Veins	62
Arteries	67
Comparisons	72
Snout and Palate	72
Prenasal Process of Premaxilla	72
Septomaxilla	74
Nasal Overhang and Anterior Nasal Notch	76
Nasal Foramina	76
Infraorbital Foramina	77
Palatine Foramina	77
Facial Process of Lacrimal	78
Orbitotemporal Region	78
Orbital Mosaic	78
Orbital Foramina	80
Postorbital Process	82
Nasoparietal Contact	83
Jugal	83
Basicranium and Lateral Braincase Wall	83
Pterygopalatine Ridges and Troughs	83
Ectopterygoid	84
Alisphenoid	85
Foramina for Branches of the Mandibular Nerve	86
Venous System	87
Arterial System	89
Pterygoid Canal	92
Petrosal	93
Hypoglossal Foramen	96

Endocranium	96
Cavum Epiptericum and Primary Braincase Wall	96
Hypophyseal Fossa, Tuberculum Sellae, and Jugum Sphenoidale	98
Cribriform Plate	99
Conclusions	99
Acknowledgments	104
References	105
Glossary	114
Index of Anatomical Terms	121

We affectionately dedicate this publication to Mike Novacek, for his years of encouragement, support, and friendship.

ABSTRACT

The cranial anatomy of the Mongolian Late Cretaceous multituberculate *Kryptobaatar dashzevegi* is described based on exquisitely preserved specimens collected from Ukhaa Tolgod and Tugrugeen Shireh in the Gobi Desert by joint expeditions of the American Museum of Natural History and the Mongolian Academy of Sciences. Most sutural relationships are preserved, enabling a bone-by-bone description of the skull and lower jaws exclusive of the nasal fossa and paranasal sinuses. A reconstruction of the principal components of the cranial nervous, arterial, and venous systems is facilitated by specimens with exposed endocranial surfaces.

Comparisons with previously described multituberculates, other Mesozoic mammaliaforms, and extant mammals allow an assessment of major topics in the evolutionary morphology of the multituberculate and mammaliaform skull, as well as identification of *Kryptobaatar* as an appropriate model regarding most aspects of the multituberculate skull for future phylogenetic studies. Elements previously unknown or poorly known in multituberculates are described. Included are a complete jugal on the internal surface of the zygoma; the orbital mosaic and foramina, including the optic foramen, the metoptic foramen, the transverse canal, and the foramen for the pituito-orbital vein; and the endocranium with an extensively ossified primary braincase wall formed by the pilae metoptica and antotica. The latter pila is very robust compared with its ossified remnants in non-mammalian cynodonts and monotremes, suggesting that it is a derived multituberculate condition. The co-occurrence of the pilae metoptica and antotica in multituberculates is thus far unique among mammaliaforms, but agrees with the morphology expected to be primitive for Mammalia. This in turn implies an independent loss of an ossified pila metoptica in monotremes, marsupials, and *Vincelestes* or the loss of the pila metoptica in the ancestry of multituberculates and therians combined with the independent reacquisition of a neomorphic pila metoptica in multituberculates and eutherians. The absence of several elements from the multituberculate skull, controversial in nature, is confirmed, including the prenasal process of the premaxilla, the septomaxilla, the ectopterygoid, and the orbital process of the palatine. Also confirmed is the presence of several controversial elements in the multituberculate skull, including an alisphenoid with a reduced contribution to the braincase and an anterior lamina expanded dorsal to the alisphenoid. Competing anatomical hypotheses for several elements are addressed, including the function of the lateral pterygo-palatine trough as muscle attachment and not for the auditory tube, the homology of the postorbital process on the parietal with that on the frontal, the identity of foramina in the anterior lamina as for mandibular nerve branches and not for the mandibular and maxillary nerves, and the function of the jugular fossa as primarily having housed a diverticulum of the cavum tympani and not large cranial nerve ganglia. The cranial arterial system in *Kryptobaatar* generally resembled that restored for other multituberculates and for other mammaliaforms, in particular the prototribosphenidan *Vincelestes*. Both *Kryptobaatar* and *Vincelestes* had a transpromontorial internal carotid artery, a stapedial artery that ran through a bicurrate stapes, ramus inferior, ramus superior, and an arteria diploëtica magna. The cranial venous system in *Kryptobaatar* resembled that described for other Mongolian Late Cretaceous multituberculates and for monotremes with the major exits of the dural sinuses having been the prootic canal and the foramen magnum.

A revised diagnosis of *Kryptobaatar* distinguishes it from other djadochtatherians (the grouping that includes 10 of the 11 genera of Mongolian Late Cretaceous multituberculates) by a pterygoid canal either confluent with or barely separated from the carotid canal and a separate hypoglossal foramen.

RESUMEN

Se describe la anatomía craneana del multituberculado *Kryptobaatar dashzevegi*, del Cretácico Tardío de Mongolia. Los especímenes, muy bien conservados, han sido colectados en las localidades Ukhaa Tolgod y Tugrugeen Shireh, en el desierto del Gobi por expediciones conjuntas del American Museum of Natural History y la Mongolian Academy of Sciences. La mayor parte de las suturas de *Kryptobaatar* están conservadas permitiendo una descripción hueso por hueso del cráneo y mandíbulas con excepción, de la fosa nasal y los senos para-

nasales. La reconstrucción de los principales nervios craneanos, sistema arterial y venoso que se presenta es facilitada por especímenes presentando la superficie endocranial expuesta.

La determinación de los tópicos más importantes en la evolución morfológica del cráneo de los multituberculados y otros mamaliaformes es posible a través de la comparación de *Kryptobaatar* con multituberculados descritos previamente, otros mamaliaformes y mamíferos vivientes. Estas comparaciones permiten identificar a *Kryptobaatar* como un modelo apropiado, en la mayoría de los caracteres craneanos, para representar a los multituberculados en análisis filogenéticos. Elementos previamente desconocidos, o mal representados en multituberculados, son descritos. Ellos incluyen: el jugal completo en la cara interna del arco cigomático, los elementos constituyentes de la órbita y sus forámenes, incluyendo el foramen óptico, metóptico, canal transverso y vena orbitopituitaria. Además de estos caracteres, se describe en detalle el endocranium. Este posee una pared primaria extensamente osificada, formada por las pilas metóptica y antótica. La última de ellas es muy robusta si se la compara con los restos osificados de esta estructura en cinodontes no mamalianos y monotremas. La ocurrencia simultánea de una pila metóptica y antótica en multituberculados es hasta ahora una característica única de multituberculados, pero está de acuerdo con la morfología que se presume primitiva para Mammalia. Esto a su vez implica una pérdida independiente de una pila metóptica osificada en monotremas, marsupiales y *Vincelestes*, o la pérdida de la pila metóptica en el ancestro común de multituberculados y terios, combinado con la readquisición de una pila metóptica neomórfica en euterios. Varios elementos del cráneo de los multituberculados cuya presencia ha sido discutida son aquí reconocidos como ausentes. Estos rasgos incluyen la ausencia de un proceso prenatal del premaxilar, septomaxila, ectopterigoides y la lámina orbital del palatino. Hemos confirmado también la presencia de varios elementos o rasgos controvertidos. Entre ellos se incluyen un aliesfenoides reducido y la presencia de una extensa lámina anterior expandida dorsalmente al aliesfenoides.

Hipótesis alternativas para diversos caracteres son discutidas, incluyendo la función de los surcos pterigopalatinos, aquí interpretados para inserción muscular y no para el tubo auditivo; la homología del proceso postorbitario en el parietal de los multituberculados de Mongolia con aquel del frontal de otros multituberculados; la identidad de los forámenes en la lámina anterior, interpretadas como salidas de las ramas mandibulares del trigémino y no para las ramas mandibulares y maxilares de este nervio. Además, la gran fosa jugular de los multituberculados habría albergado un divertículo de la cavidad auditiva y no grandes ganglios extracraneanos. El patrón general de las arterias craneanas de *Kryptobaatar* es semejante a aquel restaurado en otros multituberculados y algunos mamaliaformes, en particular el prototribosférido *Vincelestes*. Tanto *Kryptobaatar* como *Vincelestes* tienen una carótida interna de curso transpromontorial, una arteria estapedial que atraviesa un estribo con dos cruras; las ramas superior e inferior del sistema estapedial, y la arteria diploética magna están presentes. El sistema venoso del cráneo de *Kryptobaatar*, es similar a aquel descrito en otros multituberculados del Cretácico Tardío de Mongolia y en monotremas, en los cuales los senos duros drenados a través del canal proótico y el foramen magnum.

Se presenta aquí una nueva diagnosis de *Kryptobaatar*, agregando los siguientes caracteres diagnósticos: canal pterigoideo confluyente o estrechamente asociado al canal carotideo y un foramen hipogloso separado del foramen jugular. Estos caracteres lo distinguen de otros Djadochtatherians, el grupo que incluye con *Kryptobaatar* diez de los once géneros de multituberculados del Cretácico Tardío de Mongolia.

INTRODUCTION

Multituberculates are an extinct group of early mammals with a temporal range that probably spans from the Middle Jurassic (Freeman, 1976, 1979; McKenna and Bell, 1997) to the Late Eocene (Kristhalka et al., 1982; Prothero and Swisher, 1992). A purported multituberculate has been described from the Late Triassic by Hahn et al. (1987),

a determination accepted by some authors (e.g., Godefroit, 1997). However, one of us (G.W.R.) has studied the specimen and believes it to be a theropitid (see Sigogneau-Russell et al., 1986). Multituberculates also have a very wide geographic distribution and, with recent discoveries in Morocco (Sigogneau-Russell, 1991), are known from all

major land masses with the exception of South America, Australia, and Antarctica. If gondwanatheres from the Late Cretaceous of Argentina (Bonaparte, 1986; Krause et al., 1989; Kielan-Jaworowska and Bonaparte, 1996), Madagascar (Krause and Grine, 1996; Krause et al., 1997), and India (Krause et al., 1997) are multituberculates as considered by the above authors, but not in the most recent account by Pascual et al. (1999), then the geographic distribution of Multituberculata is even broader. Currently, more than 70 genera of multituberculates are recognized (McKenna and Bell, 1997), but the overwhelming majority of these are known only from isolated teeth and fragmentary jaws (Simmons, 1993).

Among Mesozoic multituberculates, the most notable exceptions to the usually incomplete morphological record for the group are taxa collected from the continental Late Cretaceous formations of Mongolia (Kielan-Jaworowska, 1970, 1971, 1974; Kermack and Kielan-Jaworowska, 1971; Kielan-Jaworowska and Gambaryan, 1994; Dashzeveg et al., 1995; Kielan-Jaworowska and Hurum, 1997; Kielan-Jaworowska et al., 2000). To date, 13 monospecific genera have been named from these formations, the majority of them by Zofia Kielan-Jaworowska, the leader of the Polish–Mongolian Paleontological Expeditions of the late 1960s and early 1970s. Two of the 13 genera, *Gobibaatar* and *Tugrigbaatar*, subsequently have been regarded as junior synonyms of a third, *Kryptobaatar* (see below). Another taxon, *Buginbaatar* (Kielan-Jaworowska and Sochava, 1969), has been said to be of Late Cretaceous or early Paleocene age (Trofimov, 1975; Clemens and Kielan-Jaworowska, 1979). However, Martinson (1982), followed by Jerzykiewicz and Russell (1991), considered the locality where *Buginbaatar* was collected to be of Late Cretaceous age, representing “Nemegt times.” The discovery of dinosaur eggshells at this locality by recent Joint Paleontological Expeditions from the Mongolian Academy of Sciences and the American Museum of Natural History supports a Late Cretaceous age for *Buginbaatar*. Therefore, we currently recognize 11 genera of Mongolian Late Cretaceous multituberculates from the Nemegt Formation, the Djadokhta Forma-

tion, and the probably equivalent Barun Goyot Formation (Novacek et al., 1996): *Buginbaatar* Kielan-Jaworowska and Sochava, 1969; *Bulganbaatar* Kielan-Jaworowska, 1974; *Catopsbaatar* Kielan-Jaworowska, 1994; *Chulsanbaatar* Kielan-Jaworowska, 1974; *Djadochtatherium* Simpson, 1925; *Kamptobaatar* Kielan-Jaworowska, 1970; *Kryptobaatar* Kielan-Jaworowska, 1970; *Nemegtbaatar* Kielan-Jaworowska, 1974; *Nesovbaatar* Kielan-Jaworowska and Hurum, 1997; *Sloanbaatar* Kielan-Jaworowska, 1971; and *Tombaatar* Rougier et al., 1997a. Regarding the state of preservation, 6 of the 11 genera are described from well-preserved, nearly complete skulls and lower jaws (Kielan-Jaworowska, 1970, 1971, 1974; Kielan-Jaworowska et al., 1986; Kielan-Jaworowska and Hurum, 1997), and 5 of these are also represented by some postcranial elements (Kielan-Jaworowska, 1969; Kielan-Jaworowska and Gambaryan, 1994). The most completely described taxa from the standpoint of anatomy are *Nemegtbaatar gobiensis* and *Chulsanbaatar vulgaris*. They are known from most aspects of cranial anatomy (Kielan-Jaworowska, 1974), including the brain endocast (Kielan-Jaworowska, 1983, 1986), the basicranium and the cranial vasculature (Kielan-Jaworowska et al., 1984, 1986; Hurum et al., 1995, 1996), the braincase (Hurum, 1998a), the inner ear (Hurum, 1998b), the nasal fossa and paranasal sinuses (Hurum, 1994), and the masticatory apparatus (Gambaryan and Kielan-Jaworowska, 1995); in addition, the postcranial skeleton of both is almost fully known (Kielan-Jaworowska and Gambaryan, 1994).

Although *Nemegtbaatar* and *Chulsanbaatar* are currently the most fully described Mongolian Late Cretaceous multituberculates, *Kryptobaatar dashzevegi*, the subject of this report, is the taxon represented by the most specimens. It is the most abundant mammal both in the traditional localities of the Djadokhta Formation (Kielan-Jaworowska, 1974) and in Ukhaa Tolgod (fig. 1), and, in fact, is represented by more skulls than any other Mesozoic mammal. Ukhaa Tolgod is the locality showing the highest concentration of mammalian skulls and skeletons from any Mesozoic site; it was discovered in July 1993 by the Joint Mongolian–American

Museum Expeditions (Dashzeveg et al., 1995). The Djadokhta Formation is thought to be of early Campanian age (Jerzykiewicz et al., 1993; Dashzeveg et al., 1995; Rougier et al., 1997a; Averianov, 1997). The age of Ukhaa Tolgod relative to Djadokhta and Barun Goyot is under study (Dingus et al., in prep.), but the faunal contents of these units are more uniform than previously thought (Novacek et al., 1996).

Kryptobaatar dashzevegi was named by Kielan-Jaworowska (1970) based on an incomplete skull (missing the braincase) and lower jaws recovered in the Djadokhta Formation, Bayn Dzak, Shabarakh Usu (the "Flaming Cliffs"; fig. 1). It was allocated to the suborder Taeniolabidoidea, family Eucosmodontidae, as were most of the other multituberculates from the Djadokhta and Barun Goyot Formations (Clemens and Kielan-Jaworowska, 1979). Recently, in fact, Rougier et al. (1997a) have suggested that nine of the Mongolian Late Cretaceous multituberculate genera are included in a monophyletic grouping along with *Pentacosmodon* from the North American Paleocene (see fig. 38); excluded was *Buginbaatar*, which was closer to the taeniolabidids, and *Nessovbaatar*, which had not yet been named. Kielan-Jaworowska and Hurum (1997) proposed a somewhat modified monophyletic Mongolian assemblage, which they named the Djadochtatheria. Included were the same taxa in the unnamed Mongolian clade of Rougier et al. (1997a) plus *Nessovbaatar* and *Paracimexomys* from the North American Cretaceous. *Kryptobaatar* was assigned by Kielan-Jaworowska and Hurum (1997) to the Djadochtatheriidae, along with *Djadochtatherium*, *Catopsbaatar*, and *Tombaatar*.

Based on additional specimens from Bayn Dzak, some additions and corrections to the original description of *Kryptobaatar dashzevegi* subsequently were made by Kielan-Jaworowska and co-authors. For example, the slender palatal vacuities included in the original diagnosis were found to be artificial (Kielan-Jaworowska and Dashzeveg, 1978). Comparisons were made by Kielan-Jaworowska and Dashzeveg (1978) with the skull of a new eucosmodontid, *Tugrigbaatar saichanensis*, from Tugrugen Shireh or Toogreeg (fig. 1), considered to be contempora-

neous with Bayn Dzak. These authors noted many resemblances between *Tugrigbaatar* and *Kryptobaatar*, and subsequently the former was declared a junior synonym of the latter (Rougier et al., 1997a; Kielan-Jaworowska and Hurum, 1997). In 1980, Kielan-Jaworowska recognized *Gobibaatar parvus* (Kielan-Jaworowska, 1970), originally described as the only ptilodontoid from the Late Cretaceous of Mongolia, to be a junior synonym of *K. dashzevegi*. Further remarks on the masticatory apparatus of *K. dashzevegi* have been published by Gambaryan and Kielan-Jaworowska (1995), and other incomplete skulls from Bayn Dzak have been figured by Kielan-Jaworowska and Gambaryan (1994) and Kielan-Jaworowska and Hurum (1997). A revised diagnosis of *K. dashzevegi* has been offered by Kielan-Jaworowska and Hurum (1997).

Regarding the postcranium, a partial skeleton, including nearly complete hindlimbs and pelvis, an incomplete scapulocoracoid, and some damaged cervical, lumbar, sacral, and caudal vertebrae, was collected in association with a skull of *Kryptobaatar dashzevegi* at Bayn Dzak during the 1968 Polish-Mongolian expedition. Described in this specimen for the first time in multituberculates were epipubic bones (Kielan-Jaworowska, 1969). Other details of the pelvis were reported by Kielan-Jaworowska (1979) and of the remaining postcranial elements by Kielan-Jaworowska and Gambaryan (1994). Partial humeri, an ulna, and ribs were found and described with the holotype skull of *Tugrigbaatar saichanensis* by Kielan-Jaworowska and Dashzeveg (1978), and a complete humerus of *Kryptobaatar* was described by Kielan-Jaworowska (1998). We add that *Kryptobaatar* also provides the first evidence of a tarsal spur in multituberculates. The bone that Kielan-Jaworowska and Gambaryan (1994: fig. 2A) labeled as a possible fragment of dentary between the distal ends of the tibia and fibula is a displaced tarsal spur (personal obs.) as occurs in monotremes (Griffiths, 1978), the gobiconodontid *Gobiconodon* (Jenkins and Schaff, 1988), and the symmetrodont *Zhangheotherium* (Hu et al., 1997).

The current report documents the anatomy of several well-preserved specimens of

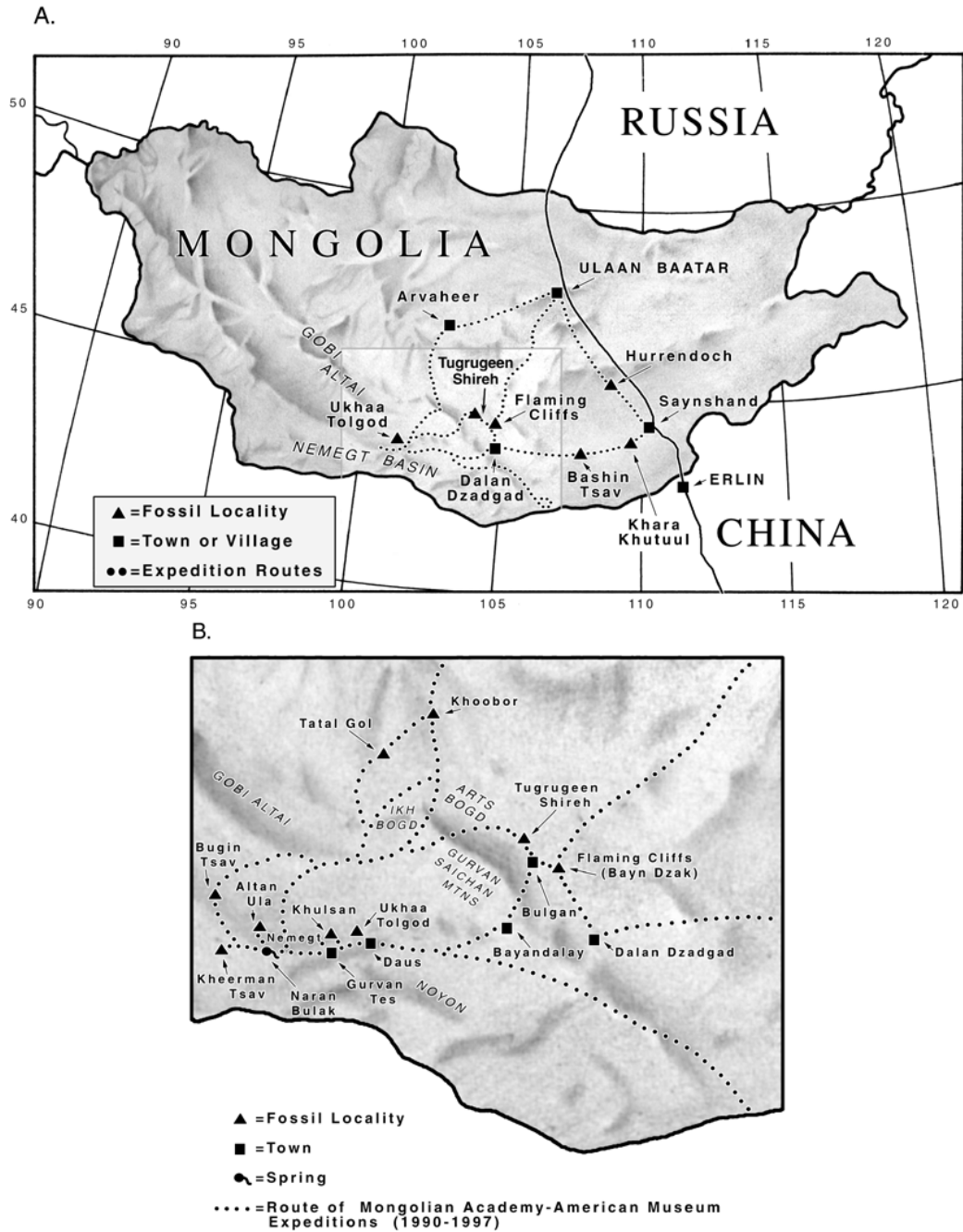


Fig. 1. Map of Mongolia (A) with inset of south-central region (B) indicating the major fossil localities visited by the joint expeditions of the Mongolian Academy of Sciences and the American Museum of Natural History. The specimens of *Kryptobaatar dashzevegi* described here come from Ukhaa Tolgod and Tugrueen Shireh.

Kryptobaatar dashzevegi collected over the last few years by the Joint Mongolian–American Museum Expeditions (fig. 2). Two specimens have been figured elsewhere (Novacek et al., 1994; Dashzeveg et al., 1995: fig. 3a, misidentified as *Chulsanbaatar*; Rougier et al., 1996c: figs. 1–4; Monastersky, 1996; Rose and Sues, 1996; Novacek, 1997: fig. 2), but thus far only the anatomy of the middle-ear ossicles has been described in detail (Rougier et al., 1996c). Although *K. dashzevegi* is known from more skulls than any other Mesozoic mammal, its entire cranial anatomy had yet to be documented in detail, and therefore we present a bone-by-bone description of the skull exclusive of the ear ossicles and reconstruct the course of the major cranial nerves and vessels. The dentition of *K. dashzevegi* has been described by Kielan-Jaworowska (1970) and Kielan-Jaworowska and Dashzeveg (1978), and will not be re-described here, although relevant dental measurements are presented in table 1.

Because postcranial and cranial remains (exclusive of teeth) are rarely recovered for multituberculates, the few well-preserved taxa that have been described are central to our understanding of the morphology and relationships of the group. Included among the most thoroughly studied multituberculates, in addition to several of the Mongolian Late Cretaceous taxa (e.g., *Nemegtbaatar gobiensis*, *Chulsanbaatar vulgaris*), is the taeniolabidid *Lambdopsalis bulla* from the Paleocene of China, whose anatomy has been the subject of several reports (e.g., Miao, 1986; Kielan-Jaworowska and Qi, 1990), including monographic treatment of the skull (Miao, 1988). *Lambdopsalis* is a highly specialized form, perhaps a burrower, with an expanded vestibular apparatus; it exhibits many apomorphic cranial features compared with the Mongolian Late Cretaceous taxa (Miao, 1988; Luo, 1996; Kielan-Jaworowska and Hurum, 1997). Despite its extreme specializations, *Lambdopsalis* has served as a model for Multituberculata in some phylogenetic studies (e.g., Wible, 1991; Meng, 1992; Meng and Wyss, 1995) because of the paucity of material and of comprehensive, detailed descriptions of other taxa. Therefore, a goal of our report on *Kryptobaatar dashzevegi* is to provide a detailed description of

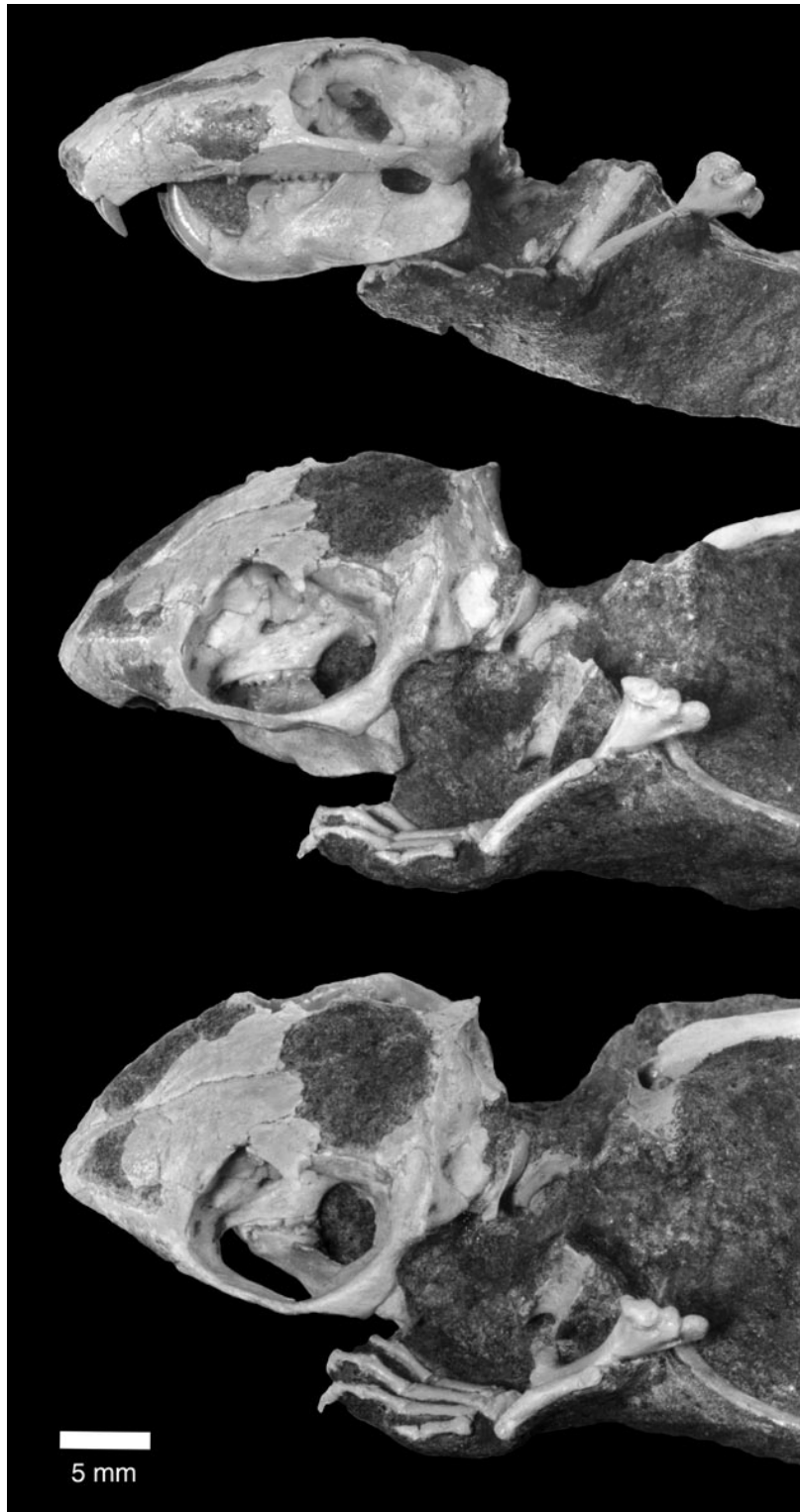
the skull and lower jaws that can serve as an appropriate model for future comparative morphological and phylogenetic studies on Multituberculata and on Mammaliaformes in general, the latter being the clade comprising the common ancestor of the Liassic taxon *Morganucodon* and Mammalia plus all its descendants (Rowe, 1988).

MATERIALS AND METHODS

To date, more than 400 multituberculate specimens have been collected by the Joint Mongolian–American Museum Expeditions. The majority are in the size range of *Kryptobaatar dashzevegi*, but only a handful have been prepared sufficiently to enable precise taxonomic determination. Our descriptions herein are based on the following specimens of *K. dashzevegi*, all of which are catalogued in the Institute of Geology, Ulaan Baatar. The first two specimens comprise the bulk of the descriptions of external surfaces and the measurements in tables 1 and 2; the remaining specimens reveal structures of the endocranium and/or selected external features.

(1) PSS-MAE 101 (figs. 2, 3): Anterior half of a fully articulated skeleton collected from Ukhaa Tolgod, including a pristine skull with lower jaws attached, the anterior portion of the vertebral column, and both shoulder girdles and forelimbs. Some external surfaces of the skull are not accessible; matrix has not been removed from part of the left ear region, the area of the foramen magnum, and part of the palate in order to preserve the stylohyal, atlas and axis, and lower jaws, respectively. The skull has been figured elsewhere in different views (Novacek et al., 1994; Rougier et al. 1996c: fig. 2; Dashzeveg et al., 1995: fig. 3a; Monastersky, 1996; Novacek, 1997: fig. 2), and the forelimb has been figured in dorsolateral view (Dashzeveg et al., 1995: fig. 3a; Rose and Sues, 1996).

(2) PSS-MAE 113 (figs. 4, 5): Skull and the left lower jaw collected in 1991 from Tugrueen Shireh. Missing are parts of the cranial vault, the left alisphenoid, part of the pterygoid, and the left zygomatic arch. The skull has been figured elsewhere in ventral view, as have closeups of the fragmentary left malleus-ectotympanic complex and the



fragmentary right stapes (Rougier et al., 1996c: figs. 1, 3, 4).

(3) PSS-MAE 123 (fig. 25): Partial skull with lower jaws collected in 1994 from Ukhaa Tolgod (Sugar Mountain). Missing are the braincase roof, right braincase wall, occiput, right zygomatic arch, and posterior part of the right lower jaw. Preparation has exposed the inner surfaces of the skull base and left braincase.

(4) PSS-MAE 124: Partial skull with lower jaws collected from Ukhaa Tolgod. Missing are the braincase roof and left zygomatic arch. Little matrix has been removed from the exterior of the skull, but the interior has been partially prepared. Exposed is the inner surface of part of the sphenoid complex. Specimen is not figured.

(5) PSS-MAE 125 (fig. 26): Partial skull with fragments of both lower jaws collected from Ukhaa Tolgod. Missing are the left zygomatic arch, left braincase wall, and most of the occiput. Preparation has exposed most of the left orbital wall, the braincase floor, and the inner surface of the right braincase wall.

(6) PSS-MAE 127: Skull and lower jaws collected in 1993 from Ukhaa Tolgod. Matrix has been removed only from selected external surfaces. Exposed is the tip of the rostrum, right upper and lower jaws, and the posterior part of the roof of the braincase and zygomatic arch. Specimen is not figured.

In addition, three other indeterminate skulls resembling *Kryptobaatar* from the Mongolian–American Museum Expeditions are included here for comparative purposes, but are not figured.

(1) PSS-MAE 126: Skull without lower jaws collected in 1994 from Gilbert Wash (locality 20) near Ukhaa Tolgod. Missing are both zygomatic arches and exoccipitals, as well as the tip of the rostrum. Also missing is part of the cranial vault, which exposes the posterior part of the brain endocast and vascular molds. Matrix has been removed from the right orbit, but not the from left.

(2) PSS-MAE 128: Partial skull without lower jaws collected in 1993 from Ukhaa Tolgod. Missing are the left braincase and zygomatic arch. Little matrix has been removed from the exterior of the skull, but the interior has been prepared. Exposed is the inner surface of the right petrosal and anterior lamina, as well as parts of the sphenoid complex.

(3) PSS-MAE 134: Natural nasal endocast collected in 1996 from Ukhaa Tolgod (Zofia's Hill).

Kielan-Jaworowska and Hurum (1997) recognized two species of *Kryptobaatar*, *K. dashzevegi* and *K. saichanensis*, with the most substantive difference being the cusp formula (in the labial and lingual rows) of the second lower molar (3:2 in *K. dashzevegi* versus 4:2 in *K. saichanensis*). We have inspected the single specimen of *K. saichanensis* (GI SPS 8-2 PST) and found three cusps in the labial row on the left second lower molar and three cusps plus an accessory cusp on the right side. Given that the other differences identified by Kielan-Jaworowska and Hurum (1997) are minor (e.g., the length of the mandibular ascending ramus), we recognize *K. saichanensis* as a junior synonym of *K. dashzevegi*. Our specimens of *Kryptobaatar* also exhibit differences. For example, in PSS-MAE 101, the sphenopalatine foramen lies between the frontal and maxilla, whereas in 113 it is wholly within the maxilla. Additionally, in PSS-MAE 101 the jugal is concealed in lateral view by the maxilla and squamosal, whereas in 113 a thin sliver of jugal is exposed along the dorsal edge of the zygomatic arch. PSS-MAE 113, collected in Tugrugeen Shireh, is slightly larger than 101 from Ukhaa Tolgod (see tables 1 and 2); this is in agreement with the purported larger size of *K. saichanensis* also from Tugrugeen Shireh compared to *K. dashzevegi* from Bayn Dzak (Kielan-Jaworowska and Dashzeveg, 1978). We believe that these and a few other differences in our specimens are minor and we treat the specimens as conspecific.

←

Fig. 2. *Kryptobaatar dashzevegi* PSS-MAE 101 in left lateral and two oblique dorsolateral views (from top to bottom), prior to removal of the skull and lower jaws from the block containing the postcranium.

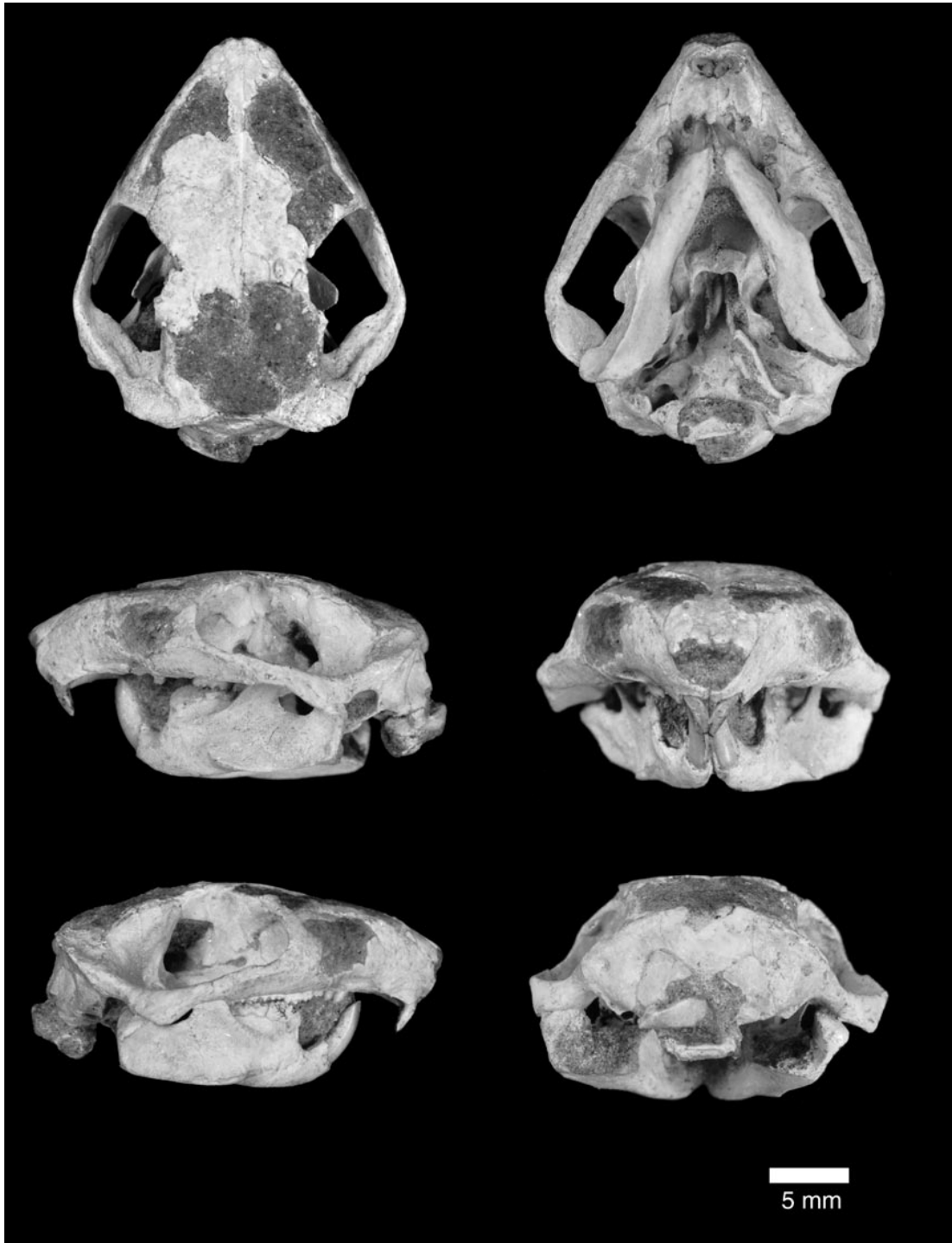


Fig. 3. The skull and lower jaws of *Kryptobaatar dashzevegi* PSS-MAE 101 in (clockwise from upper left) dorsal, ventral, anterior, posterior, right lateral, and left lateral views.

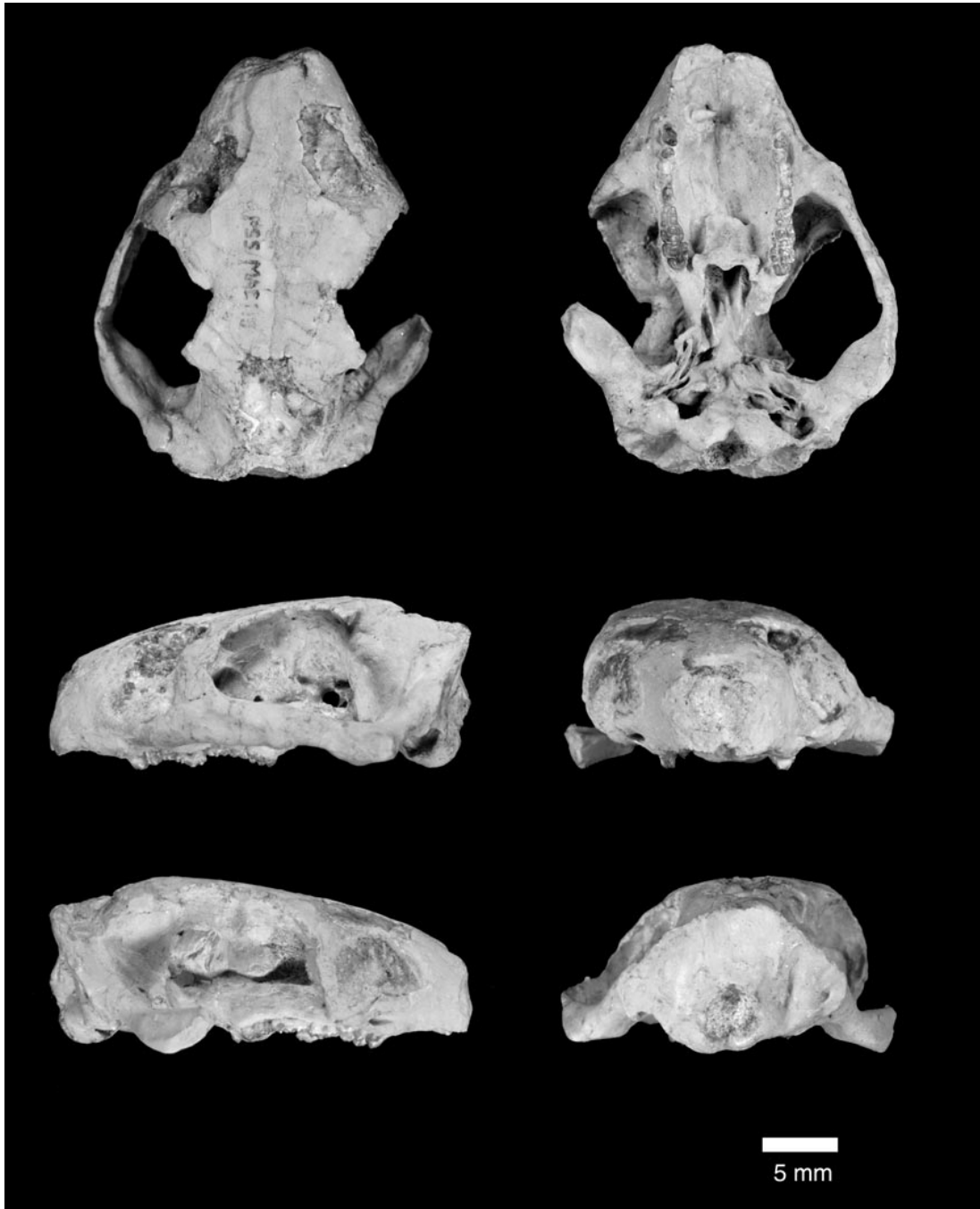


Fig. 4. The skull of *Kryptobaatar dashzevegi* PSS-MAE 113 in (clockwise from upper left) dorsal, ventral, anterior, posterior, right lateral, and left lateral views.



Fig. 5. The left lower jaw of *Kryptobaatar dashzevegi* PSS-MAE 113 in lateral and medial views.

Different authors (e.g., Kermack et al., 1981; Novacek, 1986; Miao, 1988) have used various organizational schemes in describing the skulls of fossil mammals. Here we provide a bone-by-bone description of the exterior of the skull of *Kryptobaatar*. In addition, the ventral endocranial surfaces visible in several specimens are described as a single anatomical unit. Also provided are reconstructions of the major cranial nerves, arteries, and veins. Following the descriptions, comparisons of individual regions of the skull are made with those of other multituberculates and mammaliaforms. Emphasis is on characters used in previous phylogenetic analyses (e.g., Simmons, 1993; Wible et al., 1995; Rougier et al., 1996a, 1996c).

Over the years, cranial remains of multi-

tuberculates have been described by numerous authors (e.g., Broom, 1914; Simpson, 1937; Hahn, 1969; Kielan-Jaworowska, 1970; Miao, 1988), and the anatomical terminology used has not always been consistent. In general, our usage of terminology agrees closely with that used by Kielan-Jaworowska and co-authors (e.g., Kielan-Jaworowska, 1970, 1974; Kielan-Jaworowska et al., 1986; Gambaryan and Kielan-Jaworowska, 1995), but for the auditory region and cranial vasculature we follow Wible (1987, 1990), Rougier et al. (1992, 1996a, 1996c), Wible and Hopson (1993, 1995), and Wible et al. (1995). In addition, for many of the endocranial structures not described previously in multituberculates, we follow the terminology in the dog (Evans and Christen-

sen, 1979). Our usages for the cranial foramina and canals are specified in a glossary at the end. We have also provided an index for the major page citations for most anatomical terms used. For the dentition, we use the abbreviations “I, P, M” and “i, p, m” to refer to upper and lower incisors, premolars, and molars, respectively. Regarding the numeration of the upper premolars, we follow Simmons (1993) and designate the five premolars present in primitive multituberculates (e.g., the Late Jurassic paulchoffatiines, Hahn, 1993) as P0–P4. The first upper premolar having been lost, the remaining four in *Kryptobaatar* are designated P1–4. However, our usage of the term premolars does not necessarily imply strict homology with the premolars of therians. There is no instance in which the multituberculate P4 is known to have a deciduous precursor (Greenwald, 1987; Hahn and Hahn, 1999); a deciduous p4 has only been reported for one form, *Kuehneodon dietrichi* (Hahn, 1978), but this was based on a single broken lower jaw that contained no replacement teeth. Given that there are no unequivocal examples of replacement of the upper and lower last premolars in multituberculates, it is possible that these teeth are molars, i.e., unreplaced permanent teeth (see Clemens and Lillegraven, 1986; Lockett, 1993).

Several authors (e.g., Bryant and Russell, 1992; Witmer, 1995) have recently proposed explicit methods for reconstructing soft tissues in fossils and for evaluating levels of confidence in those inferences. In formulating hypotheses about soft-tissue reconstruction here, we follow recent phylogenetic analyses (Rowe, 1988, 1993; Wible et al., 1995; Rougier et al., 1996a, 1996c; Hu et al., 1997; Ji et al., 1999) that identify multituberculates as members of Mammalia (fig. 39), the group including the last common ancestor of monotremes and therians plus descendants (Rowe, 1988). We acknowledge, however, that the relationships of multituberculates within Mammalia remain controversial (e.g., Rougier et al., 1996b; Sereno and McKenna, 1996; Meng and Wyss, 1996),

with some authors (e.g., Meng and Wyss, 1995) promoting a sister-group relationship for multituberculates and monotremes, and others (e.g., Rougier et al., 1996a, 1996c; Hu et al., 1997; Ji et al., 1999) allying multituberculates more closely with therians. Nevertheless, under the terminology proposed by Witmer (1995), the extant phylogenetic bracket (minimally, the first two extant outgroups) for multituberculates consists of monotremes and therians. Inferences that are based on soft-tissue structures and osteological correlates occurring in both extant outgroups are considered more decisive than those occurring in only one.

Institutional Abbreviations

AMNH	Department of Vertebrate Paleontology, American Museum of Natural History
FMNH	Department of Geology, Field Museum of Natural History, Chicago
GI	Geological Institute, Mongolian Academy of Sciences, Ulaan Baatar
IVPP	Institute of Vertebrate Paleontology and Paleoanthropology, Chinese Academy of Sciences, Beijing
MAE	Mongolian–American Museum Expedition
MCZ	Museum of Comparative Zoology, Harvard University, Cambridge
PIN	Institute of Paleontology, Academy of Sciences, Moscow
PSS (SPS)	Paleontological and Stratigraphic Section of the Geological Institute, Mongolian Academy of Sciences, Ulaan Baatar
USNM	Department of Paleobiology, National Museum of Natural History, Smithsonian Institution, Washington, D.C.
V.J.	Museum of the Geological Service, Lisbon
YPM-PU	Yale Peabody Museum, Princeton University Collection, New Haven
ZPAL	Institute of Paleobiology, Polish Academy of Sciences, Warsaw

DESCRIPTIONS

As accompaniment to the following descriptions, composite views of the skulls and lower jaws of PSS-MAE 101 and 113 are shown in figure 3 and 4–5, respectively. Stereophotographs of anterior, dorsal, lateral, ventral, and posterior views of these specimens are in figures 6–17. Enlargements of particular regions (i.e., orbit, basicranium, zygoma, endocranium, and mandible) are in figures 18–23, 25–26, 29, and 30. Reconstructions of the skull of *Kryptobaatar dashzevegi* in various views are in figures 27, 31–35, 36A, and 37A, with vascular reconstructions in figures 36B and 37B. Abbreviations used in the figures are listed in table 3.

PREMAXILLA

The premaxilla is a large bone with facial and palatal components of near equivalent size oriented approximately at right angles to

each other. It forms the walls of the anterior part of the nasal cavity and bears two incisors, a larger I2 and a smaller I3. The premaxilla is complete in PSS-MAE 101 (fig. 6), but its anterior portion is missing in PSS-MAE 113 (fig. 7).

In lateral view (figs. 10–13, 33), the facial component comprises approximately one-third of the preorbital skull length. It forms the anterolateral wall of the nasal cavity and the ventral half of the margin of the external nares. Facets for the septomaxilla on the external narial aperture are lacking. The anterior margin of the facial component is vertical, flush superiorly with the anterior tip of the nasal and inferiorly with the anterior edge of the I2 alveolus; consequently, the rim of the external nares is circular in outline and opens directly anteriorly without any lateral exposure. The facial component contacts the maxilla posteriorly and the nasal dorsally. The premaxillary–maxillary suture is vertical near the palatal margin, roughly halfway be-

TABLE 1
Dental Measurements (mm) of
Kryptobaatar dashzevegi

	Left			Right		
	Length	Max. width	Min. width	Length	Max. width	Min. width
PSS-MAE 101						
P1	—	—	—	0.8	0.7	—
P2	—	—	—	0.7	0.7	—
P3	0.8	0.7	—	0.8	0.8	—
P4	—	—	—	1.9	1.0	—
M1	2.7	—	—	2.7	—	—
M2	1.9	—	—	1.9	—	—
p3	0.2	—	—	0.2	—	—
p4	2.3	—	—	2.1	—	—
m1	2.5	—	—	2.4	—	—
m2	1.6	—	—	1.6	—	—
P4–M2	—	—	—	8.1	—	—
PSS-MAE 113						
P1	1.4	1.0	—	1.3	1.0	—
P2	0.9	1.0	—	0.9	1.0	—
P3	1.0	0.9	—	1.1	0.9	—
P4	2.4	1.2	—	2.4	1.1	—
M1	2.9	1.8	1.2	2.9	1.7	1.2
M2	2.1	1.9	1.5	2.1	1.9	1.5
p4	3.1	1.4	—	—	—	—
m1	2.4	1.4	—	—	—	—
m2	1.8	1.5	—	—	—	—
P4–M2	7.38	—	—	7.2	—	—

TABLE 2
Cranial Measurements (mm) of
Kryptobaatar dashzevegi

	PSS-MAE 101	PSS-MAE 113
Skull length	26.0	31.0
Maximum skull width	22.6	25.2
Premaxilla length (alveolar border)	3.8	5.03
Premaxilla length (nasal suture)	5.8	8.1
Premaxilla length (palatine process)	6.6	7.7
Maximum maxilla length (palatal view)	—	11.8
Palate length	14.5	17.9
Palate width (between P4)	6.5	7.5
Skull depth (above I2)	6.5	7.8
Skull depth (above M2)	9.9	12.0
Nasal length (maximum)	12.0	13.0
Nasal length (minimum)	9.7	10.3
Lower jaw length (from i base)	16.1 (R&L)	20.0 (L)
Lower jaw depth (below p3)	2.8 (R), 2.7 (L)	4.1 (L)
Lower jaw depth (below m1)	4.8 (R&L)	6.5 (L)

TABLE 3
List of Anatomical Abbreviations

aar	atlas arch	inf	incisive foramen	pet	petrosal
adm	arteria diploëtica magna	ioa	infraorbital artery	pfc	prefacial commissure
ais	anterior intercavernous sinus	iof	infraorbital foramen	pis	posterior intercavernous sinus
al	anterior lamina	ips	inferior petrosal sinus	pm	pila metoptica
ali	alisphenoid	izr	intermediate zygomatic ridge	pmx	premaxilla
ano	nasal notch	jf	jugular fossa	pop	postorbital process
aptca	artery of pterygoid canal	jfo	jugular foramen	pp	pila preoptica
ax	axis	jsp	jugum sphenoidale	ppr	paroccipital process
bo	basioccipital	ju	jugal	prc	prootic canal
bs	basisphenoid	juf	jugal facet	ps	prootic sinus
ce	cavum epiptericum	lac	lacrimal	psa	proximal stapedia artery
cev	capsuloparietal emissary vein	lacf	lacrimal foramen	pt	pterygoid
con	(mandibular) condyle	lhv	lateral head vein	ptc	posttemporal canal
cor	coronoid process	lpt	lateral pterygopalatine trough	ptca	pterygoid canal
cp	crista parotica	maf	masseteric fossa	ptr	pterygopalatine ridge
ctpp	caudal tympanic process of petrosal	mafo	masseteric fovea	pv	pituito-orbital vein
ds	dorsum sellae	man	mandible	ri	ramus inferior
ea	ethmoidal artery	mc	masseteric crest	rio	ramus infraorbitalis
ef	ethmoidal foramen	mef	metoptic foramen	rm	ramus mandibularis
en	ethmoidal nerve	mf	mental foramen	rs	ramus superior
er	epitympanic recess	mpf	minor palatine foramen	rso	ramus supraorbitalis
ev	ethmoidal vein	mpt	medial pterygopalatine trough	rt	ramus temporalis
exoc	exoccipital	msy	mandibular symphysis	rvnf	recess for vascular and nervous foramina
fbu	foramen buccinatorium	muf	muscular facet	sf	subarcuate fossa
fdac	foramen of dorsal ascending canal	mx	maxilla	sgf	supraglenoid foramen
fdv	foramen for frontal diploic vein	na	nasal	son	supraorbital notch
fhy	fragment of hyoid arch	naf	nasal foramen	spa	sphenopalatine artery
fica	foramen for internal carotid artery	nc	nasal capsule	spf	sphenopalatine foramen
fma	foramen masticatorium	oa	ophthalmic artery	sphf	sphenorbital fissure
foi	foramen ovale inferium	oc	otic capsule	sq	squamosal
fpv	foramen for pituito-orbital vein	oca	occipital artery	sth	stylohyal
fr	frontal	ocon	occipital condyle	sup	supraoccipital
frt	foramen for ramus temporalis	oiof	orbital aperture of infraorbital canal	tcv	transverse canal vein
fv	fenestra vestibuli	ompf	orbital opening of minor palatine foramen	tg	temporal groove
fv3	foramen for mandibular nerve	on	odontoid notch	th	tympanohyal
gica	groove for internal carotid artery	opf	optic foramen	tpmx	thickenings of premaxilla
gl	glenoid fossa	or	orbitosphenoid	tr	temporal ridge
gpsa	groove for proximal stapedia artery	otc	orbitotemporal canal	ttf	tensor tympani fossa
hf	hypophyseal fossa	P3	upper third premolar	tus	tuberculum sellae
hyf	hypoglossal foramen	pa	parietal	vo	vomer
i3a	alveolus for third upper incisor	pacc	posterior aperture of carotid canal	vv	vertebral vein
iam	internal acoustic meatus	pal	palatine	II	optic nerve
ica	internal carotid artery	pan	pila antotica	III	oculomotor nerve
		pat	postpalatine torus	IV	trochlear nerve
		pc	pterygoid crest	V	trigeminal nerve
		pef	perilymphatic foramen	VI	abducens nerve
				VII	facial nerve

tween I2 and P1. Near the nasal, the suture curves posteriorly, and a slender tongue of the premaxilla, the posterodorsal process, extends between the maxilla and nasal to the level of I3. In rostral view in PSS-MAE 101

(figs. 6, 31), the anterior part of the facial component, which is complete on both sides, is very narrow dorsoventrally and shows no sign of a prenasal process, which, if present, would have formed an internarial bar. Con-

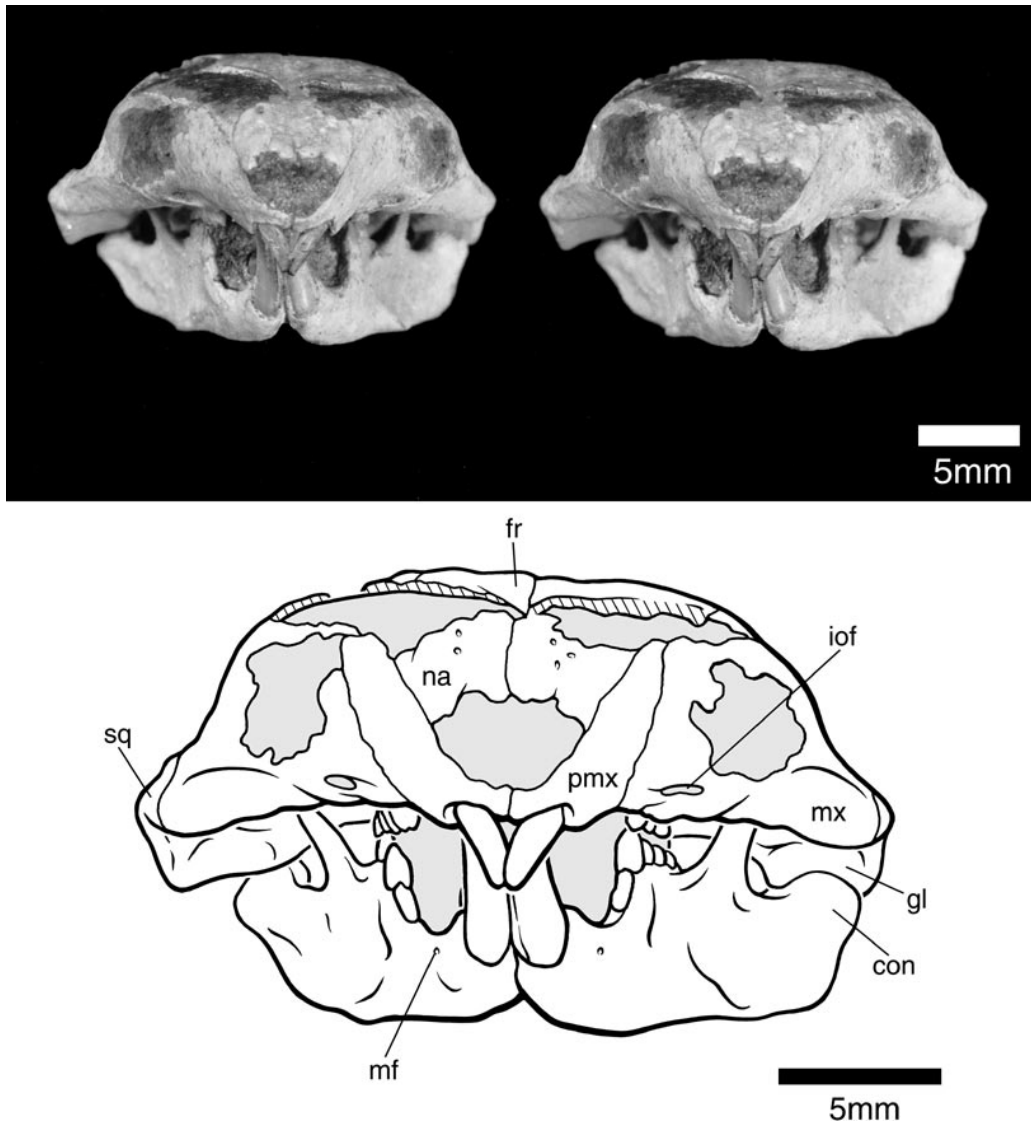


Fig. 6. Stereophotograph of the skull and lower jaws of *Kryptobaatar dashzevegi* PSS-MAE 101 in anterior view, with accompanying line drawing. Gray pattern represents matrix; parallel lines denote breakage. Abbreviations: **con** (mandibular) condyle; **fr** frontal; **gl** glenoid fossa; **iof** infraorbital foramen; **mf** mental foramen; **mx** maxilla; **na** nasal; **pmx** premaxilla; **sq** squamosal.

tained within the anterior part of the facial component is the alveolus of I2, and extending posteriorly from the anterior part to the premaxillary–maxillary suture is a small horizontal furrow, perhaps representing an attachment for facial musculature (“muf” in fig. 14). The most probable occupant of such a furrow was the musculus incisivus superio-

ris, which raised the upper lip (Evans and Christensen, 1979).

In ventral view (figs. 14, 15, 34), the premaxilla occupies roughly one-third of the palate, with the most conspicuous features being the alveolus of I2 anteriorly, and the alveolus of I3 and the incisive foramen posteriorly. The lateral margin is thickened to

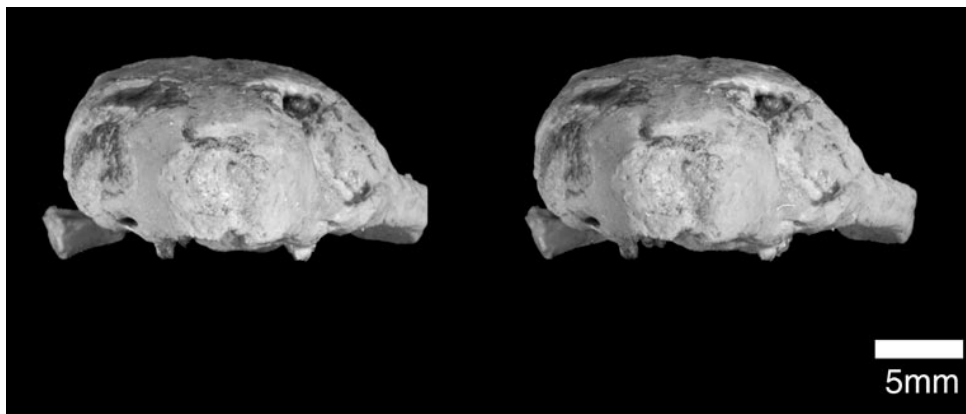


Fig. 7. Stereophotograph of the skull of *Kryptobaatar dashzevegi* PSS-MAE 113 in anterior view.

form a sharp, ventrally projecting ridge. The central portion of the palatal component, between the alveoli of I2 and I3, is very long and concave ventrally. Subdividing this part of the palatal component into two longitudinal depressions is a cord-shaped ridge, the thickening of the premaxilla (“tpmx” in fig. 14) of Kielan-Jaworowska et al. (1986). Of the two depressions divided by the thickening of the premaxilla, the medial is the deeper; it lies on the midline and meets its complement of the opposite side. The alveolus of I2 is large and although close to the midline, is separated from the I2 alveolus of the opposite side by considerable bone. The left and right I2s are directed ventromedially toward one another and come into contact ventrally, leaving a triangular space between them and the edge of the premaxilla visible in rostral view (figs. 6, 31). A similar arrangement with contact between the left and right I2s has been illustrated for *Sloanbaatar* from the Mongolian Late Cretaceous (Kielan-Jaworowska, 1971: fig. 9) and for *Taeniolabis taoensis* from the North American Paleocene (Granger and Simpson, 1929: figs. 5, 6). The portion of the premaxilla in front of the alveolus of I2 in *Kryptobaatar* slopes posteroventrally from the nasal aperture to the alveolus. The smaller alveolus for I3 lies roughly halfway between the median suture and the labial margin. The I3 alveolus is formed entirely by the premaxilla and is separated from the premaxillary–maxillary suture by bone approximating the diameter of the alveolus. Medial to the I3 alveolus and

of equivalent size is the incisive foramen (“inf” in fig. 14). This aperture is oval and lies between the premaxilla and maxilla (fig. 34). Separating the left and right incisive foramina and meeting on the midline are the broad palatal processes of the premaxillae.

NASAL

The nasals are elongate bones that form nearly the entire skull roof in the preorbital area. They are severely damaged in PSS-MAE 101, 113, 123, and 127, but the preservation is sufficient to restore their sutural relationships.

In dorsal view (figs. 8, 9, 32), the nasal on its lateral margin contacts the premaxilla and maxilla and on its posterior margin, the lacrimal and frontal. The sutural relationships of the nasal are as follows. Where the nasal contacts the premaxilla, the lateral margin of the nasal is subparallel to the medial margin. However, where the nasal contacts the maxilla, the nasal is strongly expanded laterally. The lateral three-quarters of the nasal’s posterior suture are roughly transverse, but in the medial quarter there is a slender tongue of frontal that projects into a short, broad U-shaped notch between the two nasals. The frontal is overlapped slightly by the nasal, as is evident on the right side of PSS-MAE 113 where the posterolateral part of the nasal is missing and the frontal is exposed (fig. 9). Nasal foramina (Simpson, 1937) are present on the dorsal surface (“naf” in figs. 8, 10). However, because of damage, the number

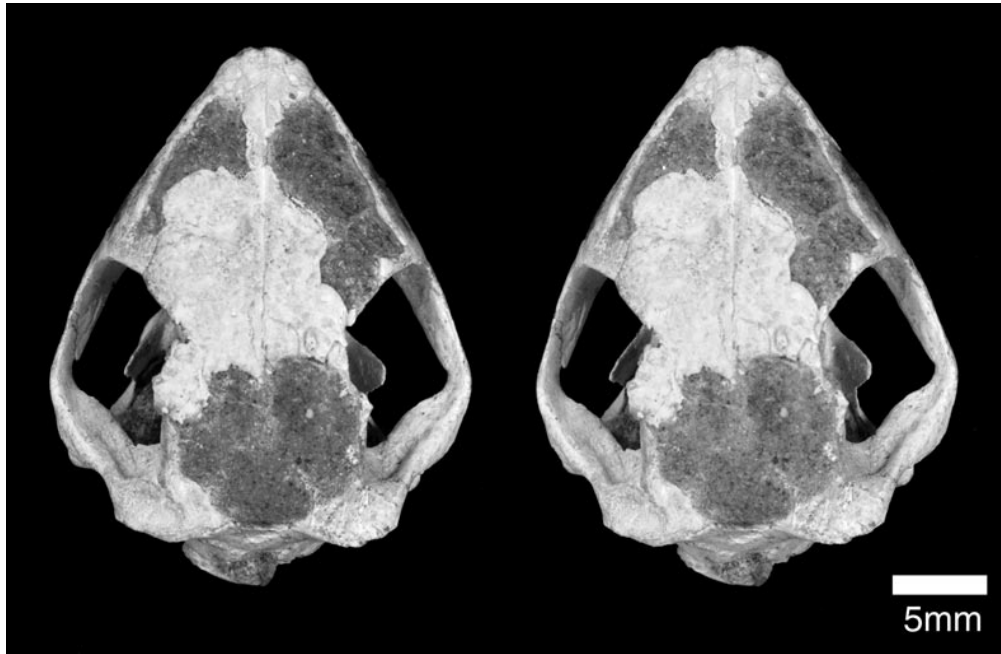


Fig. 8. Stereophotograph of the skull of *Kryptobaatar dashzevegi* PSS-MAE 101 in dorsal view, with accompanying line drawing. Gray pattern represents matrix; parallel lines denote breakage. Abbreviations: **al** anterior lamina; **ano** nasal notch; **con** (mandibular) condyle; **cor** coronoid process; **exoc** exoccipital; **fdac** foramen of dorsal ascending canal; **fr** frontal; **ftr** foramen for ramus temporalis; **ju** jugal; **juf** jugal facet; **lac** lacrimal; **mx** maxilla; **na** nasal; **naf** nasal foramen; **pa** parietal; **pmx** premaxilla; **sgf** supraglenoid foramen; **sq** squamosal; **sup** supraoccipital.

and position of the foramina cannot be fully ascertained. In the anterior third of the nasals in PSS-MAE 101, there are two foramina on the right side and three on the left, and they are not arranged symmetrically between the two sides (fig. 8). On the basis of more completely preserved nasals, Kielan-Jaworowska and Hurum (1997) reported two pairs of nasal foramina for *Kryptobaatar dashzevegi*. The anterior edge of the nasal is not fully preserved in any MAE specimens, but enough is present to report the presence of a notch there (“ano” in figs. 8, 12), especially in PSS-MAE 127, which we term the anterior nasal notch following Lillegraven and Krusat (1991). Additionally, enough is present to preclude a substantial nasal overhang of the external narial aperture and to exclude the presence of an internarial bar, as is also indicated by the morphology of the premaxilla.

LACRIMAL

The lacrimal occupies the anterior margin of the orbit and has orbital and facial processes, with the latter being the larger of the two. A complete lacrimal is not preserved in either PSS-MAE 101 or 113; the most complete is on the left side of the former (figs. 8, 18), which is missing only the anterior-most part.

The orbital exposure is wedge-shaped and does not extend ventrally far from the orbital rim, contributing mostly to the overhanging orbital roof (figs. 16, 18, 33). It contacts the maxilla laterally and inferiorly, and the frontal medially. The facial exposure (figs. 8, 32) is transversely convex and subrectangular in shape (see Kielan-Jaworowska and Hurum, 1997: figs. 2B, C). It contacts the maxilla anterolaterally, the nasal anteromedially, and the frontal posteromedially. The part of the lacrimal forming the orbital rim is thickened,

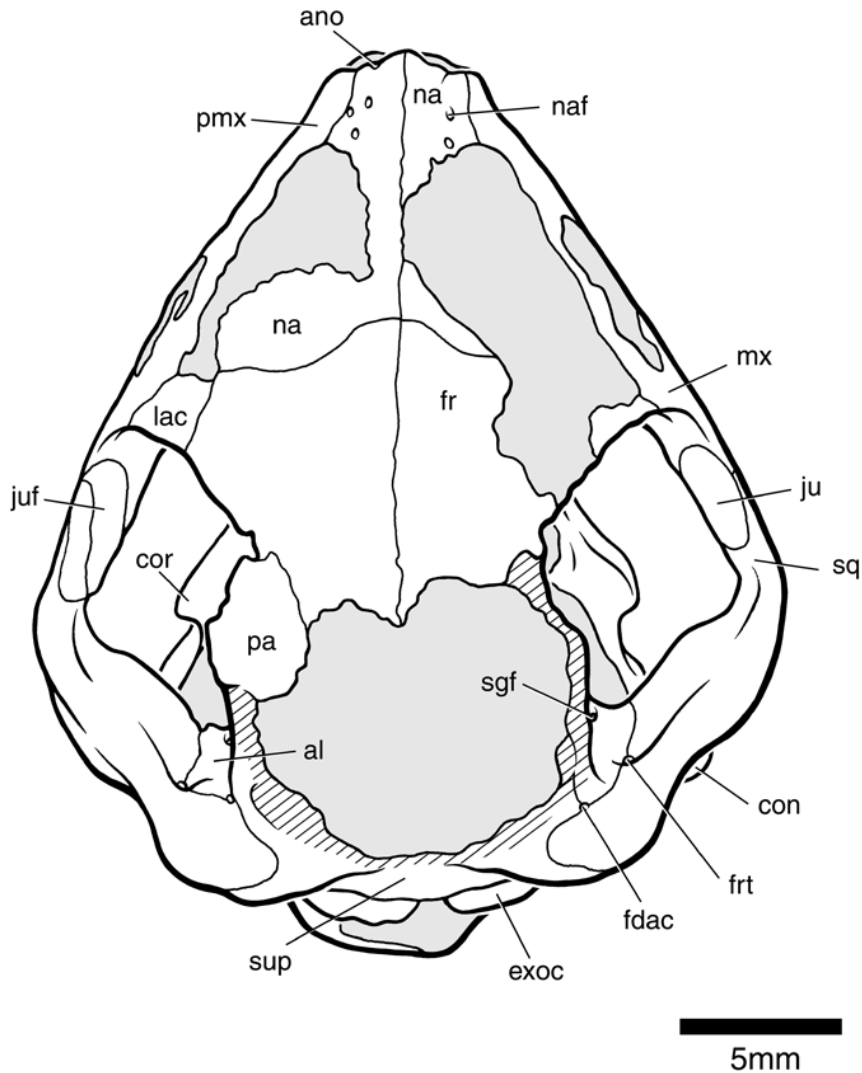


Fig. 8. Continued.

and on its ventrolateral aspect bears a single small lacrimal foramen, which is not subdivided (“lacf” in fig. 16). The foramen is high in the orbit, surrounded by strong crests, and opens near the contact between the lacrimal and the facial process of the maxilla.

FRONTAL

The frontal has a horizontal component in the skull roof and a vertical component in the orbit. Both components are well preserved in PSS-MAE 113, but the horizontal is damaged in PSS-MAE 101 (fig. 8).

The horizontal components of the frontals (figs. 8, 9, 32) are flat and meet on the dorsal midline at a slightly irregular suture. They roof the posterior part of the nasal cavity and the anterior part of the cranial cavity. Anteriorly, the frontals contact the lacrimals and send a tongue-shaped process anteromedially into the preorbital area between the nasals. Posteriorly, the frontals narrow, extending to the level of the postorbital processes on the parietals and contacting the parietals largely through a broad U-shaped suture; lateral to the arms of the U is a small prong of the

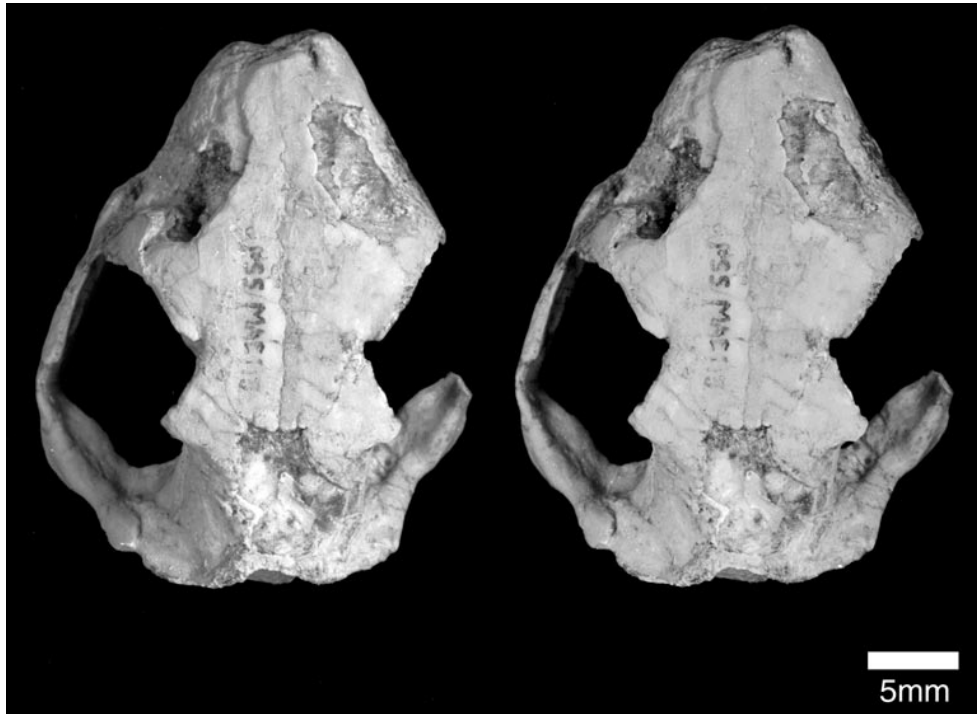


Fig. 9. Stereophotograph of the skull of *Kryptobaatar dashzevegi* PSS-MAE 113 in dorsal view.

frontal that projects posterolaterally, forming the medial rim of the supraorbital notch (“son” in figs. 10, 12). Along their suture, the frontal and parietal do not overlap. The lateral border of the horizontal component of the frontal forms a thickened ridge contributing to the orbital rim, the supraorbital crest of Miao (1988). In the orbital margin, the frontal is widest anteriorly where it contacts the lacrimal and tapers posteromedially, being narrowest where it contacts the anterior prong of the parietal in front of the postorbital process. At the frontal–parietal contact in the orbital margin, the frontal is indented by the supraorbital notch (see below).

In the orbit (figs. 10–13, 18, 19, 33), the vertical component of the frontal forms the dorsal third of the orbital mosaic, with its ventralmost projection extending to just above the sphenopalatine foramen. The frontal contacts the lacrimal and the maxilla anteroventrally, the orbitosphenoid posteroventrally, the anterior lamina posteriorly, and the parietal posterodorsally. Within the orbit, at a level just in front of the supraorbital notch,

there is a low, raised area directed dorsoventrally in the same position as is the well-defined, high orbital ridge of Kielan-Jaworowska et al. (1986) that occurs in some other Mongolian Late Cretaceous multituberculates (e.g., *Nemegtbaatar*). Interestingly, the orbital ridge is present in a specimen of *Kryptobaatar* from Tugrugeen Shireh, GISPS 8-2 PST (Kielan-Jaworowska, personal commun.), originally identified as *Tugrigbaatar saichanensis* by Kielan-Jaworowska and Trofimov (1980). Anterior to this raised area, the frontal is fairly flat in *Kryptobaatar*, PSS-MAE 101 and 113, whereas some other Mongolian Late Cretaceous taxa (e.g., *Nemegtbaatar*) have a small, rounded fossa, the orbitonasal fossa of Kielan-Jaworowska (1971). This part of the frontal bone is the posterodorsal end of a pocketlike structure (orbital pocket or theca orbitalis) occurring in many multituberculates that represents the origin for the pars anterior of the medial masseter muscle (Gambaryan and Kielan-Jaworowska, 1995). As noted by these authors, the orbital pocket is roofed

dorsally and laterally by the frontal, lacrimal, and maxilla in *Kryptobaatar*. Because the orbital pocket is open ventrally, its roof is visible in ventral view (figs. 14, 15).

Either in the frontal or between it and other bones are several nervous and vascular foramina and grooves (figs. 12, 18, 19, 36A). At the posterodorsal limit of the orbital plate of the frontal, beneath the postorbital process, is a well-developed, anteriorly facing foramen (“otc” in figs. 12, 36A). This is the anterior opening of the orbitotemporal canal of Rougier et al. (1992) for the ramus supraorbitalis of the stapedia artery and accompanying veins (postorbital foramen of Kielan-Jaworowska et al., 1986). The boundaries of this aperture are the frontal ventromedially, the anterior lamina ventrolaterally, and the parietal dorsally. In the right side of PSS-MAE 101 in which the postorbital process is missing, the frontal can be seen to contribute to the floor of the anteriormost part of the orbitotemporal canal. Running forward from the anterior opening of the orbitotemporal canal is a shallow longitudinal sulcus in the frontal. This sulcus turns dorsally ventral to the supraorbital notch and then continues onto the notch. Where the sulcus turns dorsally, a small foramen opens anteromedially into the frontal (“fdv” in figs. 18, 36A); this opening may have transmitted the frontal diploic vein, as does a similarly placed foramen in the frontal of the dog (Evans and Christensen, 1979). The frontal diploic vein has been described in only a handful of placentals and functions either as an emissary or diploic vein between the superior sagittal sinus or veins of the frontal paranasal air sinus and the ophthalmic vein (Thewissen, 1989). Given that the supraorbital notch is subdivided by a faint ridge, it transmitted at least two structures from the orbit to the skull roof: one ran anteriorly in a sulcus on the dorsal surface of the frontal, and the other ran posteriorly into a foramen between the parietal and frontal. The likely occupants of the notch, sulcus, and foramen are branches of the frontal artery, vein, and nerve derived from the ramus supraorbitalis, orbital veins, and ophthalmic nerve, respectively. The final aperture associated with the frontal is the ethmoidal foramen for the ethmoidal vessels and nerve (“ef” in figs. 12,

18, 19, 36A). It lies within the orbit on the suture between the frontal and orbitosphenoid, at the latter bone’s anterodorsal margin. Leading to the ethmoidal foramen from below is a broad sulcus whose anterior border is formed by a raised ridge along the frontal-orbitosphenoid contact.

MAXILLA

The maxilla is an enormous bone, extending from the snout and palate deep into the orbitotemporal fossa. In lateral view, its length is more than half that of the entire skull (fig. 33). It bears six cheekteeth, four premolars (P1–4) and two molars (M1–2), and it has four distinct processes: facial, zygomatic, orbital, and palatal.

The facial process (figs. 10–13, 33) occupies the preorbital region behind the premaxilla. It is incomplete in both PSS-MAE 101 and 113, but its outer margin is well preserved in the former. The facial process is tall and strongly convex laterally; dorsally, it bends medially such that its contact with the nasal and lacrimal tends toward the horizontal (fig. 8). As described by Kielan-Jaworowska (1970), the infraorbital canal opens to the rostrum between the embrasures of P1–P2 or slightly posterior to them (“iof” in fig. 10). The single infraorbital foramen is dorsoventrally compressed, and its roof is visible in ventral view (figs. 14, 15). Between the posterior margin of the infraorbital foramen and the root of the zygomatic arch is a small, horizontal shelf, visible in ventral view, that extends laterally from P2, P3, and the anterior half of P4 (figs. 14, 15). This shelf merges laterally with the zygomatic process of the maxilla and likely provided additional attachment area for the anterior part of the superficial masseter (Gambaryan and Kielan-Jaworowska, 1995).

The zygomatic process is preserved on both sides in PSS-MAE 101 (figs. 10, 12, 22) and on the left in PSS-MAE 113 (figs. 13, 23). It is a robust, posterolaterally trending lamina of bone that contacts the squamosal posteriorly and the feeble jugal medially. It is the main constituent of the zygomatic arch and, following the characterization of Kielan-Jaworowska (1970), is described as confluent with the snout, that is, there is no flare

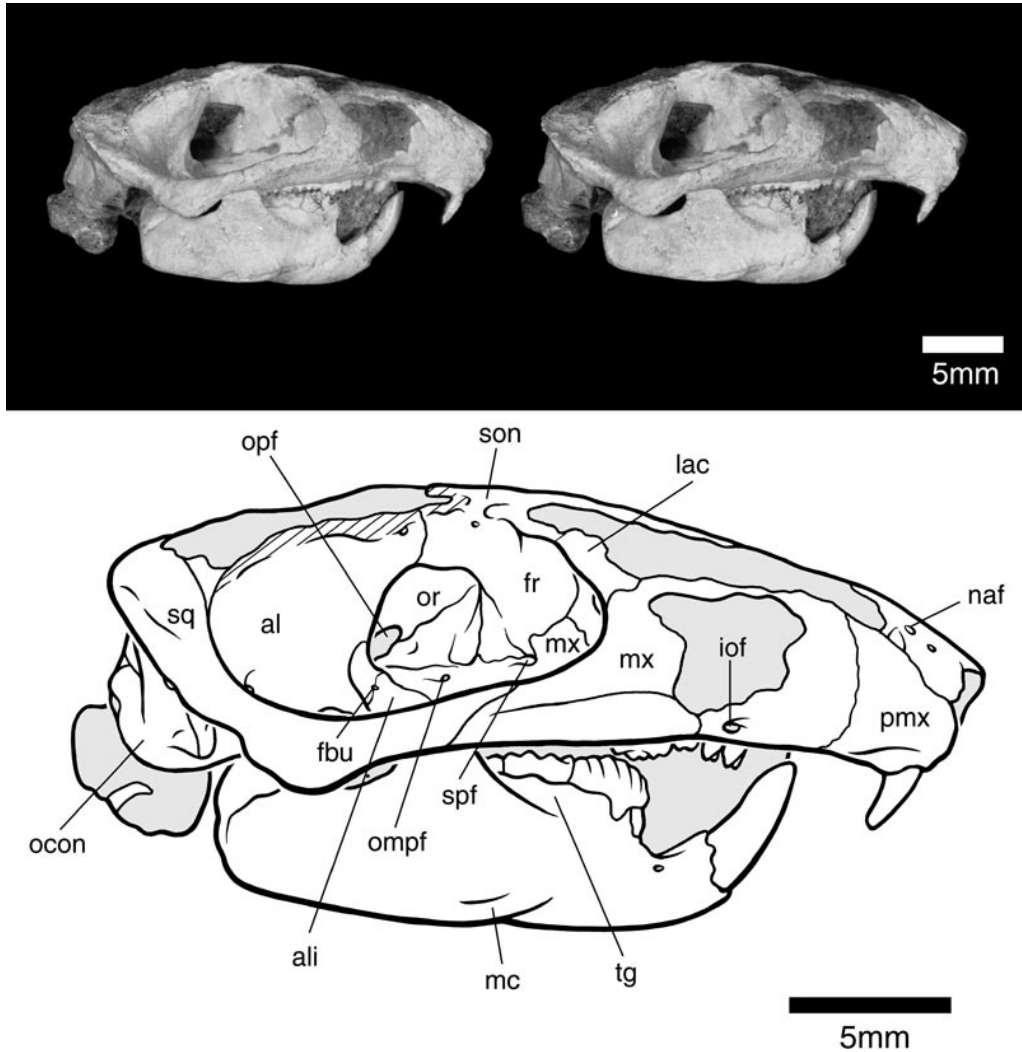


Fig. 10. Stereophotograph of the skull of *Kryptobaatar dashzevegi* PSS-MAE 101 in right lateral view. Gray pattern represents matrix; parallel lines denote breakage. Abbreviations: **al** anterior lamina; **ali** alisphenoid; **fbu** foramen buccinatorium; **fr** frontal; **iof** infraorbital foramen; **lac** lacrimal; **mc** masseteric crest; **mx** maxilla; **naf** nasal foramen; **ocon** occipital condyle; **ompf** orbital opening of minor palatine foramen; **opf** optic foramen; **or** orbitosphenoid; **pmx** premaxilla; **son** supraorbital notch; **spf** sphenopalatine foramen; **sq** squamosal; **tg** temporal groove.

in the zygomatic arch (figs. 8, 14). As noted by Kielan-Jaworowska (1970), the posterior edge of the root of the zygomatic process originates opposite the posterior half of P4. The ventral margin of the zygomatic process is fairly straight and horizontal, and posteriorly it stops short of the glenoid fossa; the dorsal margin does not extend posteriorly as far as the ventral margin, producing a diagonal suture between the maxilla and the

squamosal (figs. 10, 12, 33). On the lateral surface of the zygomatic process is a distinct, elongate, arcuate depression extending from the squamosal suture forward to the root of the zygomatic arch and being bordered dorsally by a crest. This depression and crest, the anterior zygomatic ridge (“azr” in fig. 14), provided attachment area for the anterior part of the superficial masseter muscle (Gambaryan and Kielan-Jaworowska, 1995). The

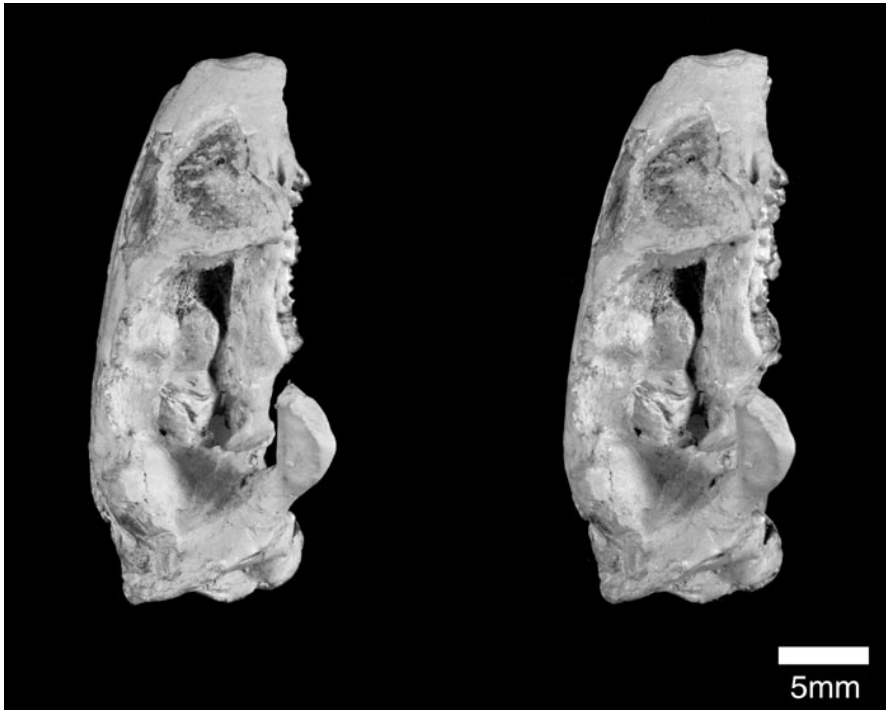


Fig. 11. Stereophotograph of the skull of *Kryptobaatar dashzevegi* PSS-MAE 113 in right lateral view.

anterior origin of this crest is on the ventral face of the shelf extending between the dental arcade, the posterior edge of the infraorbital foramen, and the root of the zygomatic process. The anterior origin is marked by a blunt, rounded process and a conspicuous kidney-shaped depression behind that. On the left zygomatic arch in PSS-MAE 101, the jugal is lost, exposing an elongate, shallow facet on the medial surface of the maxilla for this element (“juf” in figs. 8, 22).

The orbital process is complete in PSS-MAE 101 (fig. 18), but it is broken in PSS-MAE 113 (fig. 19). It is very extensive and represents the main constituent of the orbital mosaic. In the anterior part of the orbit (figs. 18, 19), the maxilla forms the wall and base of the roof, which is completed by the frontal and lacrimal; there is no floor to the orbit, which emphasizes the vertical nature of the maxilla here. In the posterior part of the orbit (figs. 10, 12), the maxilla is confined to the inferior one-fourth of the wall and forms the floor to the sphenorbital recess, the space medial to the lateral rim of the sphenorbital

fissure (“sphf” in fig. 36A), which is the aperture that transmitted nerves and vessels from the cavum epiptericum into the orbit. The posteromedial extent of the maxilla cannot be confidently identified, because it is deep within the sphenorbital recess. That recess is completed by the frontal and orbitosphenoid dorsomedially and by the alisphenoid posterolaterally. In the anteroventral corner of the orbital process of the maxilla, immediately above the root of the zygomatic arch, a circular opening into the infraorbital canal is present (“oiof” in fig. 18). Preparation of the infraorbital canal on the right side of PSS-MAE 113 exposed two openings leading medially into the maxilla (either to the maxillary sinus or nasal cavity), which may represent entrances into the alveolar canals, which transmitted alveolar branches of the infraorbital nerves and vessels (Rougier et al., 1997a). The presence of alveolar canals is confirmed by the study of high-resolution CT scans of PSS-MAE 101. In the orbital process at the level of the anterior part of M2 is a large, circular sphenopalatine fo-

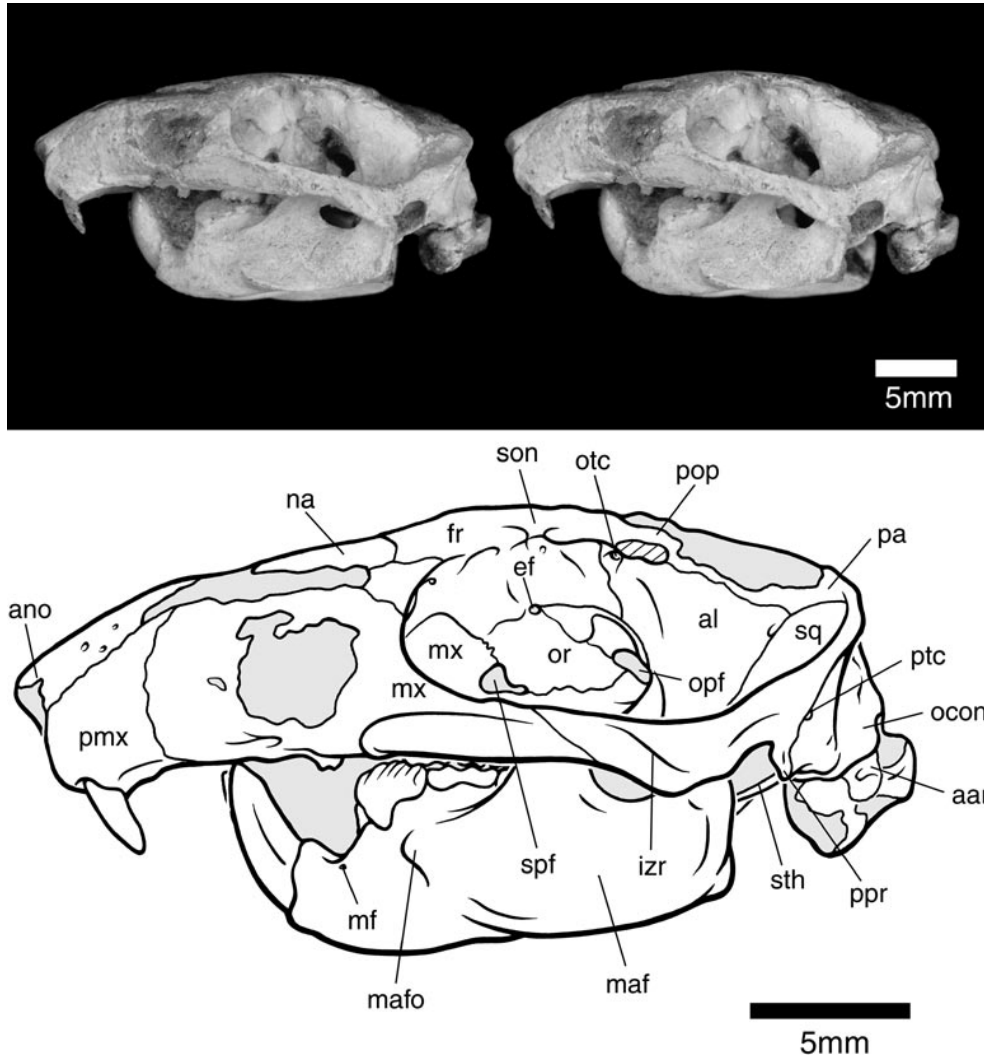


Fig. 12. Stereophotograph of the skull of *Kryptobaatar dashzevegi* PSS-MAE 101 in left lateral view, with accompanying line drawing. Gray pattern represents matrix; parallel lines denote breakage. Abbreviations: **aar** atlas arch; **al** anterior lamina; **ano** nasal notch; **ef** ethmoidal foramen; **fr** frontal; **izr** intermediate zygomatic ridge; **maf** masseteric fossa; **mafo** masseteric fovea; **mf** mental foramen; **mx** maxilla; **na** nasal; **ocon** occipital condyle; **opf** optic foramen; **or** orbitosphenoid; **otc** orbitotemporal canal; **pa** parietal; **pmx** premaxilla; **pop** postorbital process (broken); **ppr** paroccipital process; **ptc** posttemporal canal; **son** supraorbital notch; **spf** sphenopalatine foramen; **sq** squamosal; **sth** stylohyal.

ramen, the enclosing elements of which differ between the two specimens. In PSS-MAE 113 the foramen is entirely within the maxilla and the frontal approaches but does not contribute to the rim ("spf" in fig. 19). On the other hand, in PSS-MAE 101, the posterodorsal margin of the foramen is formed by the frontal (fig. 18). The sphenopalatine

foramen transmitted the sphenopalatine nerve and vessels, which went to the nasal cavity, and the major palatine nerve and vessels, which went to the hard palate. The dorsal aperture into the palatine canal, which transmitted the major palatine nerve and vessels to the palate, cannot be seen. Posterior to the sphenopalatine foramen, a sulcus, the

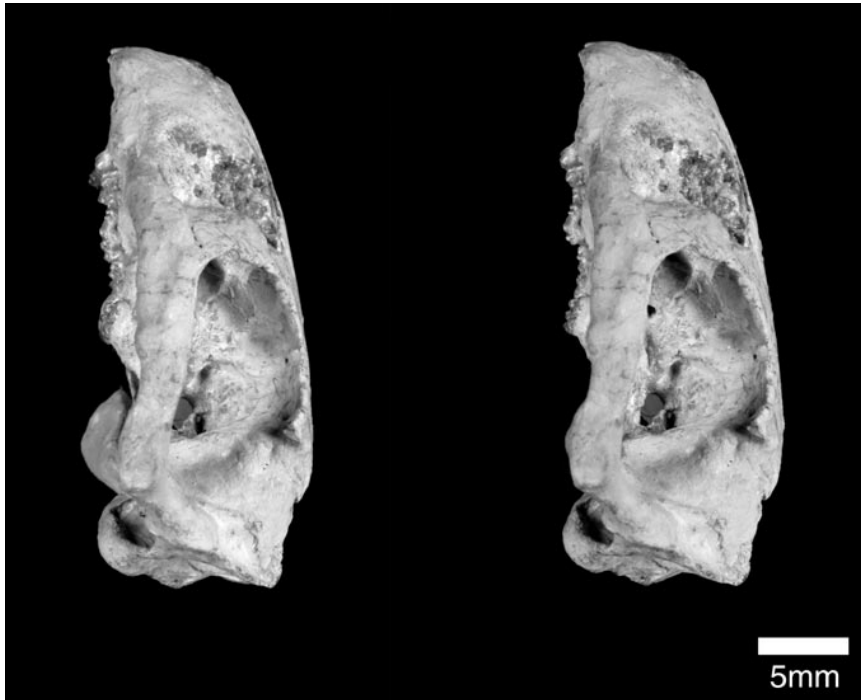


Fig. 13. Stereophotograph of the skull of *Kryptobaatar dashzevegi* PSS-MAE 113 in right lateral view.

sphenopalatine groove of Kielan-Jaworowska et al. (1986), extends posteriorly along the maxillary–frontal suture toward the sphenorbital fissure (fig. 19). Occupying this groove were the nerves and vessels destined for the sphenopalatine foramen. Near the posterior limit of the orbital process of the maxilla is a foramen that runs anteroventrally into the maxilla (“ompf” in figs. 10, 36A); we believe this is the dorsal opening into the minor palatine canal that transmitted the minor palatine nerves and vessels to the hard and soft palate.

The palatal processes, the largest elements of the hard palate (fig. 34), are fully accessible in PSS-MAE 113, where they are complete but distorted (fig. 15); in PSS-MAE 101, the lower jaws obscure all but the anterior- and posteriormost parts of the palatal processes (fig. 14). When restored to their natural positions, the palatal processes are moderately concave ventrally. As noted by Kielan-Jaworowska and Dashzeveg (1978), palatal vacuities are absent. The intermaxillary suture extends from the premaxilla to

the level of the anterior half of M1, where it meets the transverse suture with the palatines. The palatines have an essentially square-shaped exposure at the rear of the hard palate. Only a small splinter of the maxilla is interposed between the palatine and the medial alveolar margin. Despite distortion in PSS-MAE 113 (fig. 15), two medium-sized foramina (one on each side) are preserved that notch the transverse part of the maxillary–palatine suture (see fig. 34); these are the major palatine foramina, which transmitted the major palatine nerves and vessels. Where the longitudinal part of the maxillary–palatine suture meets the alisphenoid, lateral to the postpalatine torus, there is a slitlike foramen, called here the minor palatine foramen (“mpf” in fig. 14), that leads posterodorsally into a canal, the minor palatine canal. The alveolar portion of the maxilla projects ventrally below the level of the palate and extends posteriorly beyond the posterior margin of the hard palate to contact the alisphenoid.

A small triangular portion of the orbital

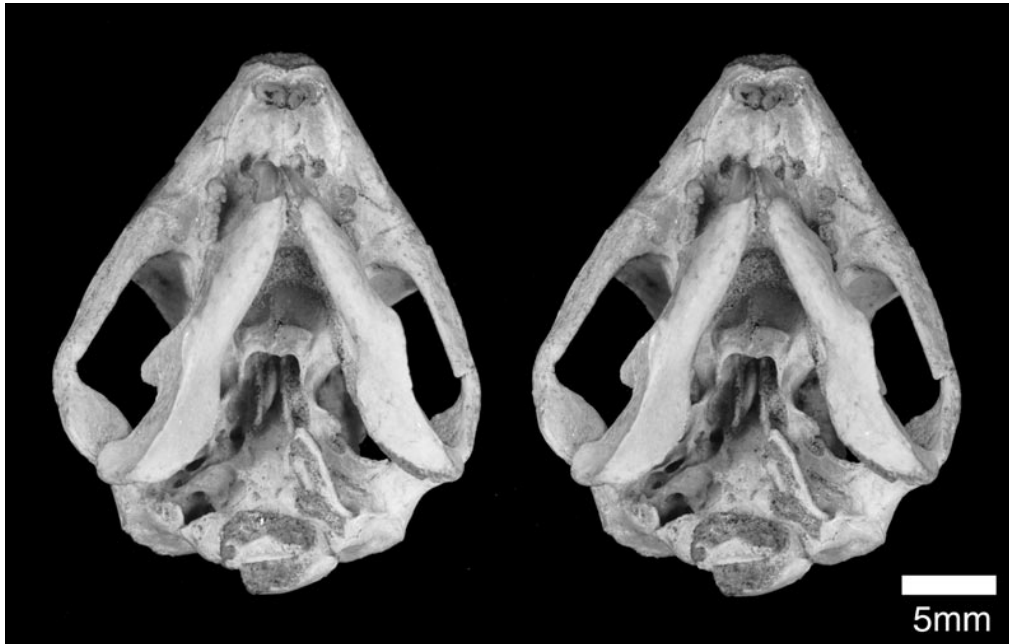


Fig. 14. Stereophotograph of the skull of *Kryptobaatar dashzevegi* PSS-MAE 101 in ventral view, with accompanying line drawing. Gray pattern represents matrix. Abbreviations: **ali** alisphenoid; **ax** axis; **azr** anterior zygomatic ridge; **bo** basioccipital; **cp** crista parotica; **fhv** fragment of hyoid arch; **foi** foramen ovale inferium; **fv** fenestra vestibuli; **gl** glenoid fossa; **i3a** alveolus for third upper incisor; **inf** incisive foramen; **iof** infraorbital foramen; **jf** jugular fossa; **mpf** minor palatine foramen; **msy** mandibular symphysis; **muf** muscular facet; **mx** maxilla; **oiof** orbital aperture of infraorbital canal; **P3** third upper premolar; **pal** palatine; **pat** postpalatine torus; **pef** perilymphatic foramen; **pmx** premaxilla; **ptc** posttemporal canal; **ptca** pterygoid canal; **rvnf** recess for vascular and nervous foramina (prootic canal, ventral ascending canal, canal for ramus inferior, and facial canal); **sth** stylohyal; **tpmx** thickenings of premaxilla; **tff** tensor tympani fossa; **vo** vomer.

process of the maxilla is exposed in the lateral wall and roof of the choana. It is limited anteroventrally by an oblique contact with the palatine, medially by the pterygoid, and posteroventrally by the alisphenoid.

PALATINE

The palatine lacks any orbital exposure and therefore can only be seen in ventral view, where it is fully exposed in PSS-MAE 113 (fig. 15), but is partially covered by matrix left on the palate to support the lower jaws in PSS-MAE 101 (fig. 14). The absence of the orbital exposure has been confirmed in PSS-MAE 101 via the study of high-resolution CT sections through the skull. The palatine contacts the maxilla on the palate, the alisphenoid at the ventrolateral edge of the choana, and the maxilla (and likely the

pterygoid) inside the choana. A contact with the vomer within the choana is not preserved and was probably absent.

The horizontal portion of the palatine is subrectangular (fig. 34). As seen in PSS-MAE 113 (fig. 15), the anterior limit of the palatine, at the level of the P4/M1 embrasure, is the transverse suture with the maxilla, which encloses the major palatine foramen. The lateral limit is the longitudinal suture with the maxilla, which encloses the minor palatine foramen, and the posterior limit is formed by the strong postpalatine torus. Parallel to the sides and close to the suture with the maxilla are four to five small foramina in the palatine in the position of accessory palatine foramina (fig. 34). No accessory palatine foramina are visible in the exposed area of the left palatine in PSS-MAE 101 (fig.

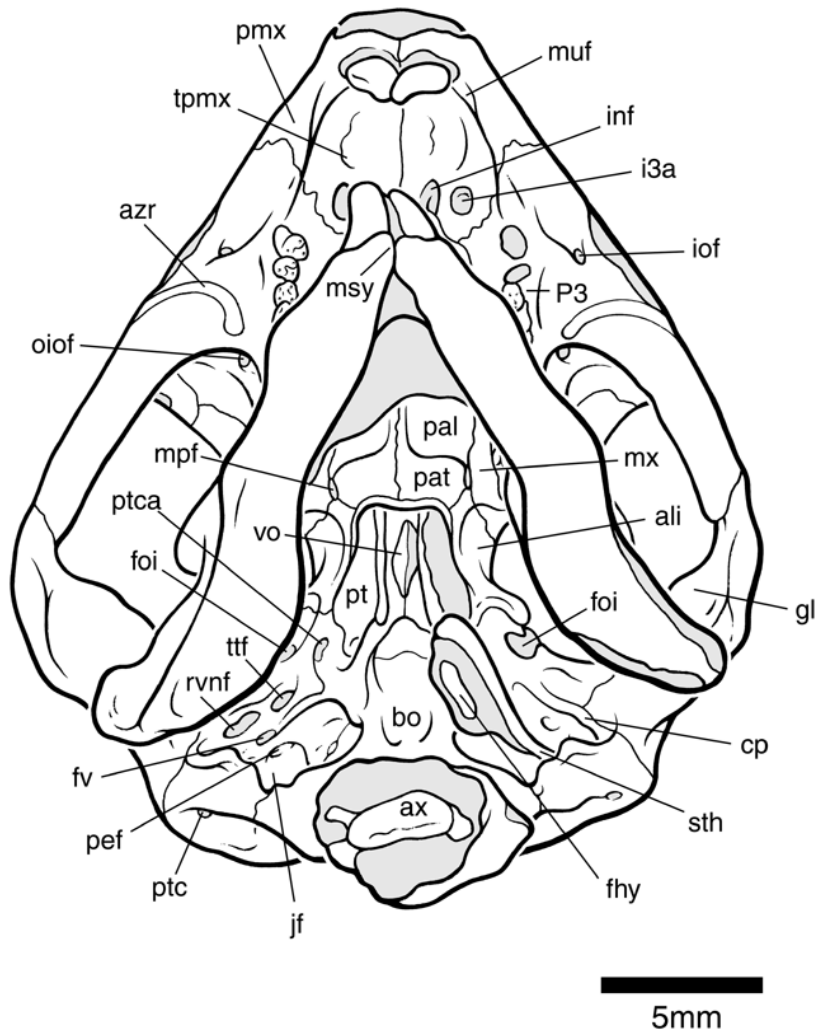


Fig. 14. Continued.

14); that portion of the right palatine is covered by matrix. In the midline, the palatine projects ventrally, forming a strong crest along the indistinguishable interpalatine suture. This crest is higher and thicker posteriorly and at the border of the choanae merges into the postpalatine torus ("pat" in fig. 14). The torus is massive, thick anteroposteriorly, projects strongly ventrally, and extends laterally to the suture with the maxilla and the alisphenoid. As preserved, the torus extends ventrally to the level of the occlusal surface of M2. The lateral part of the torus, at the level of the middle of M2, is continued

posteriorly by a wedge-shaped process that is covered laterally by the alisphenoid. This process marks the ventrolateral border of the choana.

The palatine forms the floor and a small part of the ventrolateral wall of the choana. Behind the palatine contribution to the ventrolateral choanal wall is the maxilla. These two bones are separated by an oblique suture that runs anterodorsally inside the choana above the minor palatine foramen. In the midline between the choanae, the palatine has a strong crest that projects dorsally, partially subdividing the air passageway.



Fig. 15. Stereophotograph of the skull of *Kryptobaatar dashzevegi* PSS-MAE 113 in ventral view.

PTERYGOID

The pterygoid lies on the skull base, extending from within the choana to the anterior pole of the ear region (fig. 34). It is preserved in both PSS-MAE 101 (fig. 14) and 113 (fig. 15), but is most complete on the right side of the former. The following description is based mostly on PSS-MAE 101, where the pterygoid appears to be essentially complete, although parts of its sutures are not very clear. The medial suture with the presphenoid and basisphenoid is distinct on PSS-MAE 113.

The pterygoid is elongate and underlies the presphenoid and basisphenoid, which are fused with the alisphenoid and orbitosphenoid to form the sphenoid complex. The pterygoid contacts the alisphenoid laterally, the basisphenoid posteriorly, and the presphenoid, vomer, and basisphenoid medially. It may reach as far posteriorly as the anterior pole of the promontorium of the petrosal and epitympanic recess, but the sutures are unclear. What is visible of the pterygoid shows

no contact across the midline, with the base of the vomer separating them. The pterygoids converge rostrally inside the choanae, but the full anterior extent cannot be ascertained because the interior of the nasal cavity cannot be accessed.

Each pterygoid bears a tall, longitudinal, ventrally directed crest, the pterygopalatine ridge (“ptr” in fig. 37A) of Barghusen (1986), that delimits a medial and lateral pterygopalatine trough (“mpt” and “lpt” in fig. 37A). As there is also a midline crest ventral to the presphenoid, likely formed by the vomer, four troughs extending within the choanae into the rear of the nasal cavity are present on the mesocranium. The two lateral troughs expand both anteriorly in the nasal cavity and posteriorly on the mesocranium, and their lateral wall likely included a contribution from the alisphenoid. However, the suture between the alisphenoid and pterygoid cannot be established. The two medial troughs are deeper and become only slightly wider posteriorly. They are confluent behind

the vomer where they are roofed by the sphenoid complex. The pterygopalatine ridge becomes taller posteriorly and ends at the level of the anterior portion of the epitympanic recess in a rounded, posteroventrally directed process. A similar process was described for *Kamptobaatar* by Kielan-Jaworowska (1971). As noted by her, this process is reminiscent of the pterygoid hamulus in modern mammals.

In PSS-MAE 113 (fig. 15), the pterygoids are broken posteriorly on both sides, exposing a groove for the internal carotid artery in the petrosal. The pterygoid likely formed the floor to an enclosed carotid canal (see Petrosal).

SPHENOID COMPLEX

The individual components of the sphenoid complex—presphenoid, basisphenoid, orbitosphenoid, and alisphenoid—are not delimited by sutures in any specimens of *Kryptobaatar*. Although these elements clearly form a unity in the adult skull, they are described here as separate entities that correspond with similar structures in living mammals for which the individual ossification centers are known. As sutures between the sphenoid and what we interpret as the vomer are lacking or cannot be identified, we describe the latter bone together with the presphenoid and basisphenoid.

PRESPHENOID/BASISPHENOID/VOMER

We describe this portion of the sphenoid complex and vomer as the elements lying on the midline in ventral view between the posterior edge of the choanae and the basioccipital (fig. 34). Based on the morphology in living mammals, the presphenoid comprises the anterior part of this complex, the basisphenoid the posterior part, with the vomer lying ventral to both. These three elements are most fully preserved in PSS-MAE 101 (fig. 14); however, additional details are shown in PSS-MAE 113, in which the midline crest (vomer) and parts of the pterygoids are not preserved (fig. 15).

The presphenoid and basisphenoid form the midline floor of the braincase in the mesocranium; their ventral surfaces are essentially flat. Laterally, they contact the ptery-

goids through a mostly longitudinal suture that diverges laterally toward the back of the skull; therefore, the basisphenoid is wider than the presphenoid. As mentioned above in relation to the pterygoids, the midline crest in the roof of the choanae is likely formed exclusively by the vomer. Its anterior terminus is obscured by the sediment still present inside the nasal cavity in both PSS-MAE 101 and 113. The midline crest becomes taller posteriorly, and at its terminus, approximately at the level of the anterior margin of the epitympanic recess, the ventral and posterior edges of the crest become quite massive. This enlargement makes the posterior portion of the crest a robust and prominent, ventrally projecting process; it does not, however, extend as far ventrally as the pterygopalatine ridges. Behind the midline crest, the basisphenoid exposure is wedge-shaped and slightly convex ventrally. Extending posteriorly from each of the pterygopalatine ridges to the suture between the basisphenoid and the basioccipital, there is a small, blunt, longitudinal crest. This crest marks the lateral boundary of the basisphenoid, but the bone(s) forming the crest as well as those immediately lateral to it cannot be confidently ascertained. Candidates include the pterygoid and the petrosal. In *Kamptobaatar* (ZPAL MgM-I/33), this crest is formed by the pterygoid.

In PSS-MAE 113 (fig. 15), the back part of the right pterygoid is missing, exposing the overlying basisphenoid. A large antero-medially directed foramen on the thick dorsolateral surface of the basisphenoid is found at the end of a vascular groove traceable back to the anterior pole of the promontorium. We interpret this foramen and groove as for the internal carotid artery. As stated above, the pterygoid likely formed the floor to an enclosed carotid canal and obscured the carotid foramen in the basisphenoid.

ORBITOSPHENOID

The orbitosphenoid is the most complicated portion of the sphenoid complex. It forms part of the posteromedial wall of the orbitotemporal fossa and is continuous posteriorly with the ossified primary wall of the braincase, the pilae antotica and metoptica (see

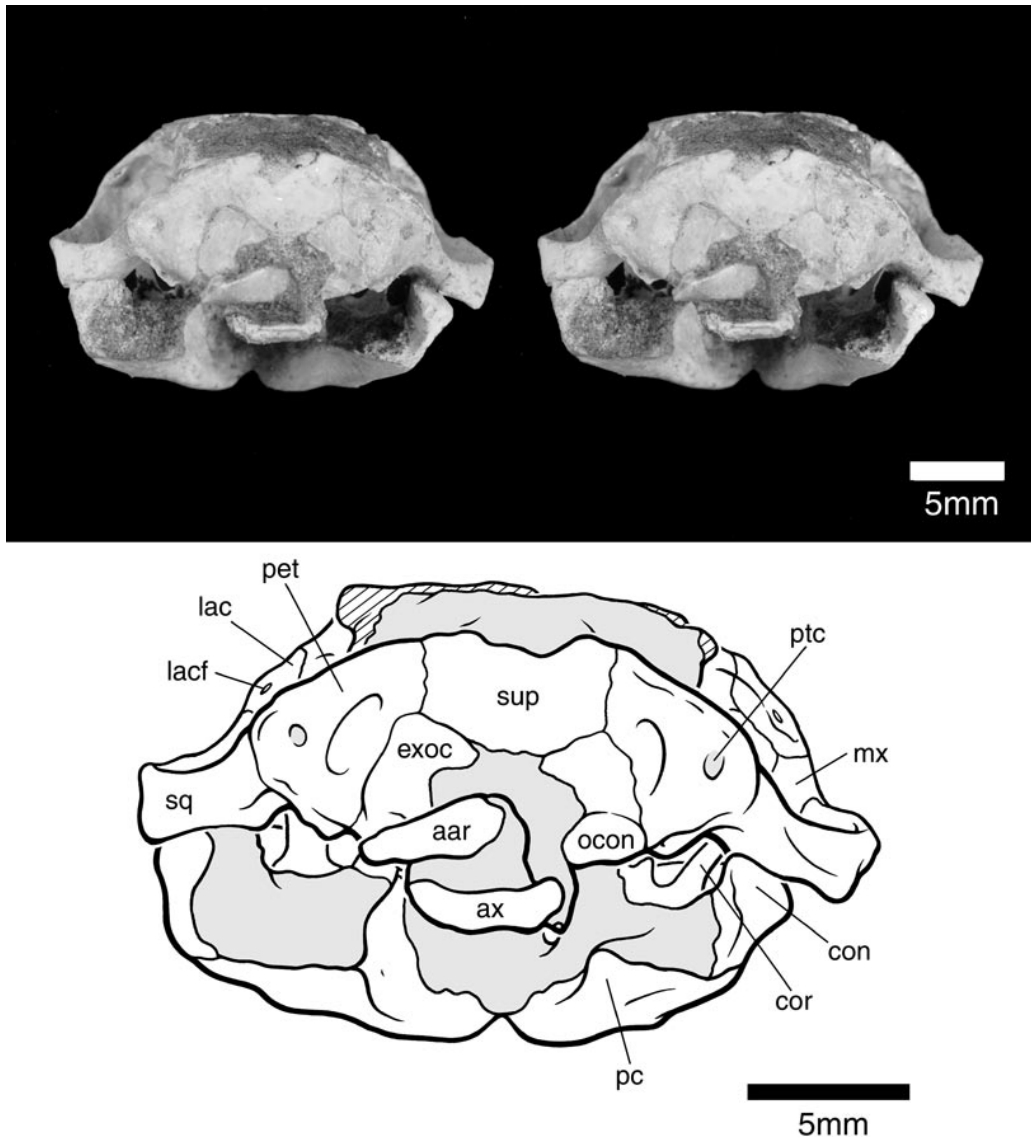


Fig. 16. Stereophotograph of the skull of *Kryptobaatar dashzevegi* PSS-MAE 101 in posterior view, with accompanying line drawing. Gray pattern represents matrix; parallel lines denote breakage. Abbreviations: **aar** atlas arch; **ax** axis; **con** (mandibular) condyle; **cor** coronoid process; **exoc** exoccipital; **lac** lacrimal; **lacf** lacrimal foramen; **mx** maxilla; **ocon** occipital condyle; **pc** pterygoid crest; **pet** petrosal; **ptc** posttemporal canal; **sq** squamosal; **sup** supraoccipital.

Endocranium). Additionally, the orbitosphenoid wholly or partially encloses the exits for the nerves and vessels that reached the orbit from the cranial cavity and constitutes the posteroventral edge of the ethmoidal foramen (figs. 33, 36A). The orbitosphenoid is a delicate element and is only partially preserved in both PSS-MAE 101 (figs. 10, 12, 18) and

113 (figs. 11, 13, 19). However, the specimens showing the endocranial surface of the skull provide additional information that enables a fairly complete reconstruction of the orbitosphenoid's external morphology.

As is visible in lateral view (figs. 10–13, 33, 36A), the orbitosphenoid contacts the frontal anteriorly and dorsally, the maxilla

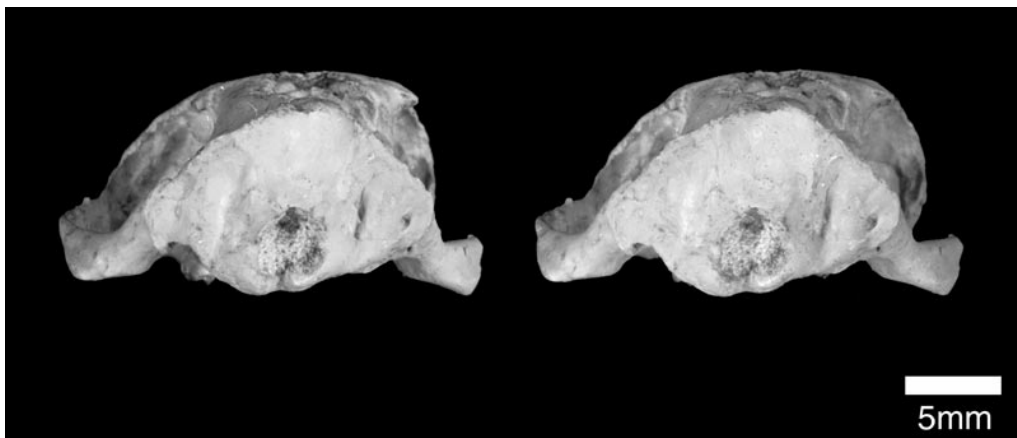


Fig. 17. Stereophotograph of the skull of *Kryptobaatar dashzevegi* PSS-MAE 113 in posterior view.

ventrally, and the anterior lamina posterolaterally. The orbitosphenoid is a laminar element with two major components, an oblique dorsal portion forming the floor of the cranial cavity and a subvertical ventral portion connecting the braincase to the skull base. Where these two portions meet is a broad groove leading into the ethmoidal foramen from behind and below. It transmitted nerves and vessels to the ethmoidal foramen and becomes deeper and broader dorsally as it approaches the foramen.

The dorsal portion of the orbitosphenoid has a slightly arched contact with the frontal dorsally and extends from the ethmoidal foramen in front to the anterior lamina behind. Ventral to its contact with the frontal, the dorsal portion of the orbitosphenoid bulges anterolaterally, reflecting the outer contour of the brain. Posteriorly, at the level of the rostral edge of the hypophyseal (pituitary) fossa, the dorsal portion flares laterally, contributing at least partially to the dorsomedial edge of the sphenorbital fissure. This aperture is completed laterally by the anterior lamina.

The ventral portion of the orbitosphenoid extends ventrally from the ethmoidal foramen in front and converges on the midline to contact the ventral portion of the orbitosphenoid of the opposite side. Together, in PSS-MAE 101, these elements form a midline structure, a broad, short crest that ventrally contacts the maxilla as well as the presphenoid and basisphenoid portions of the sphenoid complex. Anterodorsally, this crest

is notched on both sides. Upon comparison with the endocranial specimens, it is clear that the notches on the left and right sides constitute the anteroventral portions of the optic foramen (“opf” in figs. 10, 12), which would have been completely enclosed within the orbitosphenoid (figs. 33, 36A). On the right side of PSS-MAE 101 dorsomedial to the sphenorbital fissure is a small, circular foramen anterolaterally directed. A similar aperture seems to be present on the right side of PSS-MAE 113, but is not as clear. After comparison with the specimens showing the endocranial surfaces, this aperture is interpreted as the metoptic foramen for the oculomotor nerve (“mef” in fig. 36A).

ALISPHEOID

The alisphenoid is a small, laminar component of the sphenoid complex with contributions to the orbitotemporal region and the mesocranium. It is preserved on both sides of PSS-MAE 101 (fig. 14) and on the left side of 113 (fig. 15).

Despite its small size, the alisphenoid touches a number of bones on the skull base (figs. 14, 34, 37A) and in the orbitotemporal fossa (fig. 10). Its contacts are on the palate the maxilla and palatine anteriorly, on the choana the pterygoid medially, on the mesocranium the petrosal posteriorly and medially, and in the orbitotemporal fossa the anterior lamina posterodorsally, the remaining

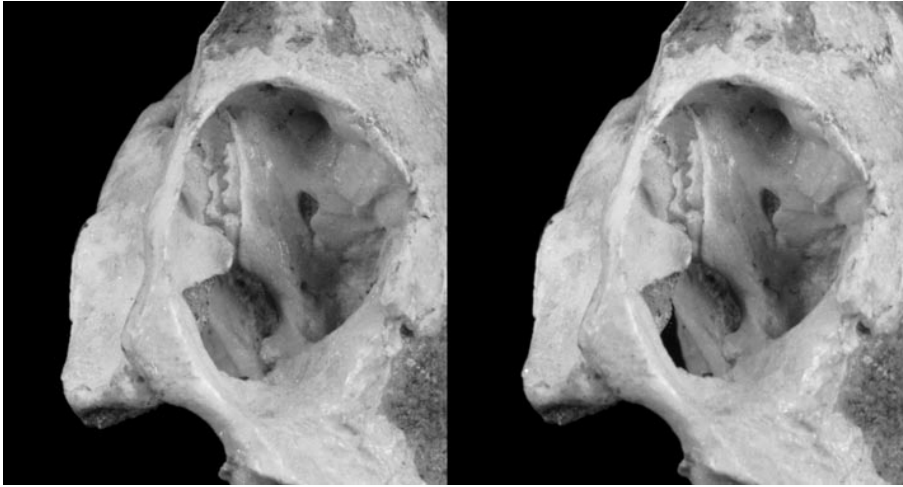


Fig. 18. Stereophotograph of the left orbitotemporal region of the skull of *Kryptobaatar dashzevegi* PSS-MAE 101 in oblique dorsolateral view, with accompanying line drawing. Gray pattern represents matrix; parallel lines denote breakage. Abbreviations: **al** anterior lamina; **ali** alisphenoid; **fdv** foramen for frontal diploic vein; **fr** frontal; **frt** foramen for ramus temporalis; **lac** lacrimal; **man** mandible; **mx** maxilla; **na** nasal; **oiof** orbital aperture of infraorbital canal; **or** orbitosphenoid; **pa** parietal; **sgf** supra-glenoid foramen; **spf** sphenopalatine foramen; **sq** squamosal.

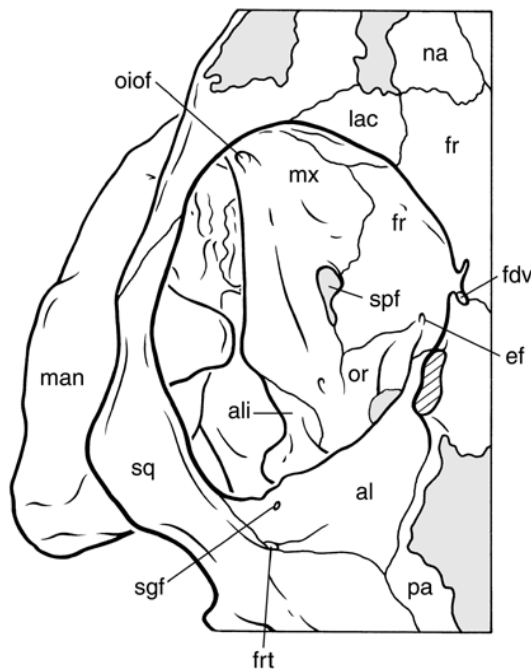


Fig. 18. Continued.

portions of the sphenoid complex medially, and the maxilla anteriorly.

The alisphenoid has the shape of a portion of a Möbius strip, so that its medial margin in the lateral wall of the choana through a continuous line becomes the lateral edge of the epitympanic recess in the ear region. Based on this shape, the alisphenoid can be divided into anterior and posterior portions. The anterior portion is exposed only on its ventral surface; the posterior portion is exposed ventrally and dorsally. The anterior portion (figs. 14, 34, 37A) contacts the palatine and maxilla in the wall of the choana. Lateral to this contact, there is a deeply recessed, semilunar area on the alisphenoid that probably housed the medial pterygoid muscle (Gambaryan and Kielan-Jaworowska, 1995: fig. 8B). The anterolateral part of this attachment area for the medial pterygoid is completed by the maxilla. From the anteromedial edge of this recess, a slender process of alisphenoid extends forward approximately to the level of M2 and contributes to the minor palatine foramen (fig. 14). Medially, the anterior portion of the alisphenoid meets the pterygoid in the lateral pterygo-palatine trough, but as already stated, the su-

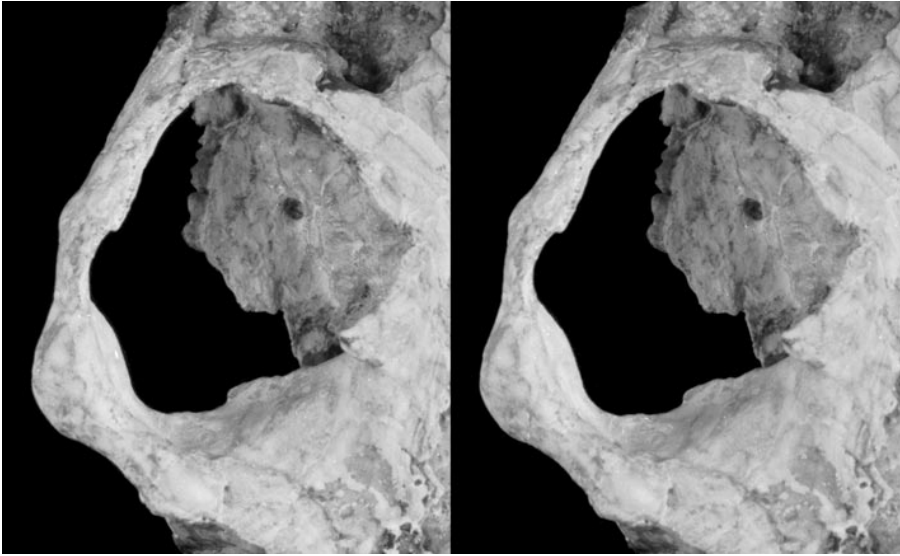


Fig. 19. Stereophotograph of the left orbitotemporal region of the skull of *Kryptobaatar dashzevegi* PSS-MAE 113 in oblique dorsolateral view, with accompanying line drawing. Gray pattern represents matrix; parallel lines denote breakage. Abbreviations: **al** anterior lamina; **ef** ethmoidal foramen; **fr** frontal; **ju** jugal; **lac** lacrimal; **mx** maxilla; **pa** parietal; **pop** postorbital process (broken); **spf** sphenopalatine foramen; **sq** squamosal.

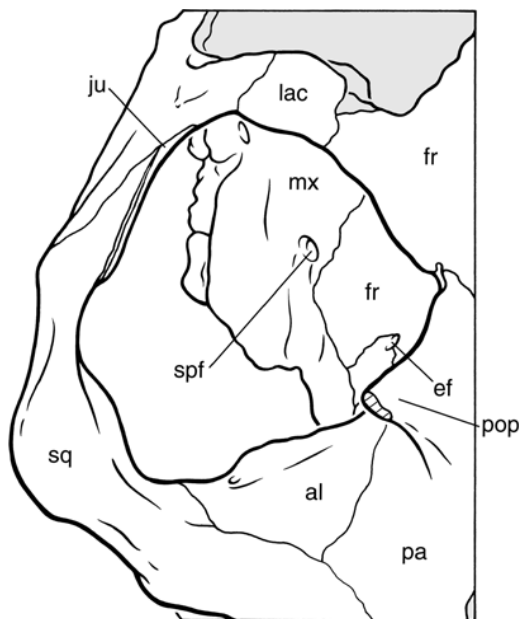


Fig. 19. Continued.

ture between these two bones is unclear (fig. 37A).

The posterior portion of the alisphenoid can be divided into two parts: one exposed ventrally and the other dorsally. The ventral exposure constitutes the anterior pole of the epitympanic recess (fig. 37A). It also forms the anterior part of the tall crest demarcating the lateral margin of the epitympanic recess; the bulk of this crest is formed by the anterior lamina. Extending medially from the anterior pole of the epitympanic recess is a tongue of alisphenoid that forms the anterolateral edge of the posterior aperture into the carotid canal (see Petrosal). The dorsal exposure of the posterior portion of the alisphenoid lies behind the maxilla and in front of the anterior lamina (fig. 10). This part of the alisphenoid forms the ventrolateral edge of the sphenorbital recess (figs. 10, 36A), the lateral limit of which is demarcated by a crest that continues anteroventrally in a ridge along the alisphenoid-maxillary suture. Inferior to this ridge is a concave surface on the dorsal exposure of the alisphenoid that is continuous with the surface described in ventral view as for the medial pterygoid muscle.

This concave surface likely represented an additional attachment area for pterygoid musculature, including the lateral pterygoid (Gambaryan and Kielan-Jaworowska, 1995: fig. 8B), which we term the pterygoid fossa of the alisphenoid.

Close to or within the suture between the dorsal exposure of the alisphenoid and the anterior lamina is a small, anteriorly directed foramen (“fbu” in figs. 10, 36A). We think that this foramen communicated with the cavum epiptericum, based on an as yet undescribed skull of a new species of Mongolian Late Cretaceous multituberculate (PSS-MAE 126). Among living mammals, comparably situated foramina (i.e., within the attachment area of the pterygoid musculature and connecting to the cavum epiptericum) are reported in some rodents and transmit branches of the mandibular nerve (Hill, 1935; Wahlerl, 1974). In fact, four apertures in or along the alisphenoid accommodating branches of the mandibular nerve are known to occur in rodents: the foramen ovale, the foramen ovale accessorius, the masticatory foramen, and the buccinator foramen (Wahlerl, 1974). Of the possible occupants of the anteriorly directed opening in the pterygoid fossa of *Kryptobaatar*, we think the most plausible was the buccal nerve, which is the most medial branch of the anterior division of the mandibular nerve and runs forward dorsal to the lateral pterygoid muscle in the dog (Evans and Christensen, 1979). Consequently, we identify this opening as the foramen buccinatorium (figs. 10, 36A).

PETROSAL

The petrosal is the most complex element of the basicranium; it houses the organs of hearing and balance, and contributes to the braincase wall on the lateral surface, floor, and occiput. In living therians, the petrosal is generally conceived as comprising two different regions: the pars cochlearis (housing the cochlea) and the pars canicularis (housing the vestibule and semicircular canals). In multituberculates, in addition to these two regions, an anterior lamina forms part of the lateral wall of the braincase and an extensive epitympanic recess. Among living mammals, an anterior lamina contributing to similar ar-

reas of the skull is found only in monotremes. The monotreme anterior lamina forms as the lamina obturans, an intramembranous ossification in the sphenoobturator membrane, that fuses with the endochondral petrosal proper in subsequent ontogeny (Kuhn, 1971; Presley, 1981; Zeller, 1989). Given that the monotreme lamina obturans is the only model for the anterior lamina in extinct taxa, it seems likely that the element in multituberculates and other mammaliaforms also forms intramembranously.

We describe the petrosal of *Kryptobaatar* in three views—ventral, lateral, and occipital—reserving the endocranial surface of the petrosal for a description of that space as a single unit (see Endocranium below). In PSS-MAE 101, both petrosals are preserved in situ, but the left is partially hidden in ventral view by the stylohyal and matrix left to support the stylohyal (figs. 14, 20). In PSS-MAE 113, the right petrosal is preserved in life position, but the left is displaced posteroventromedially and the anterior end of its epitympanic recess is missing (figs. 15, 21).

Ventral View (figs. 14, 20, 21, 34, 37A): In this view, the petrosal contacts medially the basisphenoid and basioccipital, postero-medially the exoccipital, laterally the squamosal, and anteriorly the alisphenoid and pterygoid. The most conspicuous feature of the petrosal is the promontorium (“pr” in fig. 37A), the tympanic surface of the cochlear housing, which is elongated, ventrally flattened, and anteromedially directed. In both PSS-MAE 101 and 113, the ventral surface of the promontorium is distinctly marked by grooves, presumably for the internal carotid and stapedial arteries, and it bears flanges along its medial aspect. However, these surface features do not mask the essential fingerlike contour of the promontorium, which in turn likely reflects the shape of the enclosed cochlear duct, known to be rodlike in other Late Cretaceous and Paleocene multituberculates (Miao, 1988; Luo and Ketten, 1991; Fox and Meng, 1997; Hurum, 1998b).

The grooves on the promontorium (fig. 37A) exhibit a Y-shaped pattern. The short stem of the Y, the medial groove, is oriented in a near transverse plane at a level posterior to the basisphenoid–basioccipital suture; it is interpreted as having housed the internal ca-

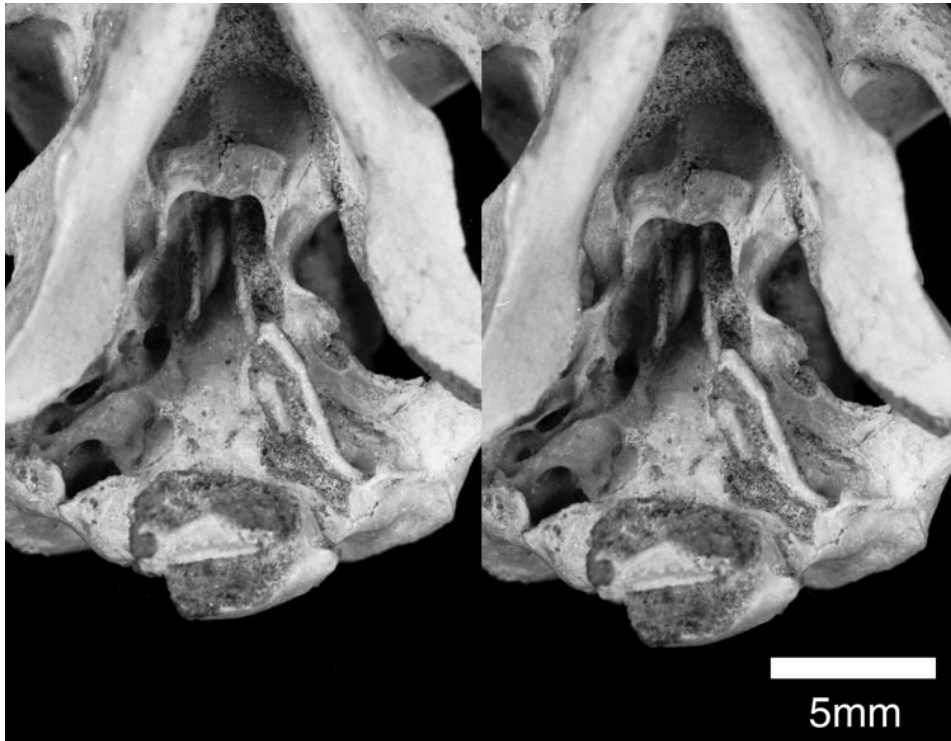


Fig. 20. Stereophotograph of the basicranium of *Kryptobaatar dashzevegi* PSS-MAE 101.

rotid artery. The anteriorly trending arm was for the rostral continuation of the internal carotid (“gica” in fig. 37A), and the posterolaterally directed arm was for the internal carotid’s main extracranial branch, the stapedia artery (“gpsa” in fig. 37A). Of these three grooves, the widest is the main stem of the internal carotid, and the longest is the one for the stapedia artery, which is subequal in diameter to the one for the rostral continuation of the internal carotid. This Y-shaped pattern is very rostrally positioned on the promontorium, which is unusual among living mammals (Wible, 1987) but is found in some other multituberculates (e.g., *Kamptobaatar*, ZPAL MgM-I/33).

From the point of the origin of the stapedia artery, the internal carotid groove extends anterolaterally close to the medial border of the epitympanic recess. On the right side of PSS-MAE 101 (fig. 20), the carotid groove leads anteriorly into a foramen situated between the lateral aspect of the anterior pole of the promontorium and the medial margin of the epitympanic recess. This fo-

ramen is formed jointly by the alisphenoid and petrosal and is called here the posterior aperture of the carotid canal (“pacc” in fig. 37A). The lateral position of this aperture determined a long course for the artery to the carotid foramen in the hypophyseal fossa, which is known from the specimens showing the endocranial surface. The exact course of the internal carotid artery from the posterior aperture of the carotid canal to the endocranium is not entirely clear, as it was hidden within bone, but the following reconstruction provides the best fit with the evidence available. On the right side of PSS-MAE 113 (fig. 21), the back part of the pterygoid is missing and the rostral continuation of the carotid groove can be followed as it curves medially on the anterior pole of the promontorium. From the promontorium, the carotid groove runs anteromedially to a foramen in the dorsolateral part of the basisphenoid that presumably represents the ventral aperture of the carotid foramen in the hypophyseal fossa. With the pterygoid in place, as on the right side of PSS-MAE 101 (fig. 20), the carotid

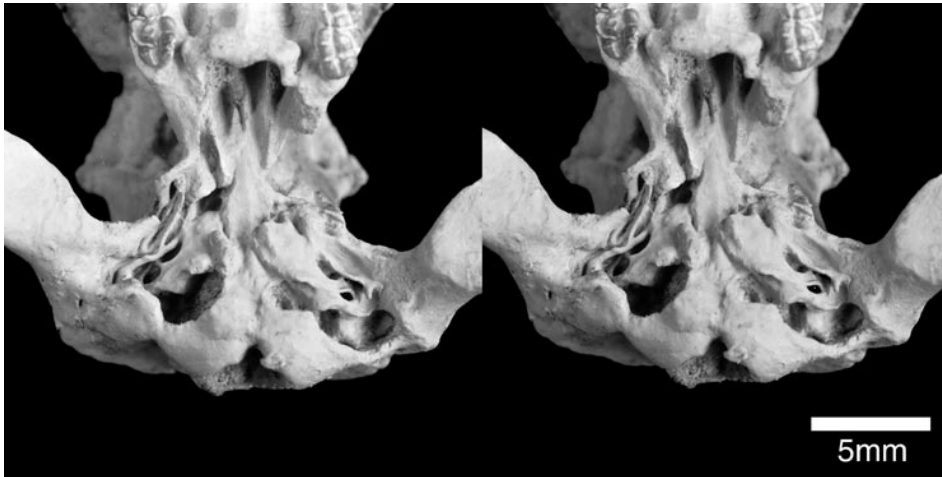


Fig. 21. Stereophotograph of the basicranium of *Kryptobaatar dashzevegi* PSS-MAE 113.

groove on the anterior pole of the promontorium was presumably enclosed in a canal, which left no visible trace on the ventral basicranial surface. The carotid canal appears to have been formed by the petrosal, alisphenoid, and pterygoid. The length of the carotid canal is a consequence of the lateral position of its posterior aperture and the very dorsal placement of the ventral aperture of the carotid foramen, which in turn implies a very thick basisphenoid from the floor of the hypophyseal fossa to the ventral surface of the skull base.

The absence of the pterygoid on the right side of PSS-MAE 113 exposes another groove in the alisphenoid that notches the dorsal surface of the ventral aperture of the carotid canal and leads anterolaterally toward the orbit (fig. 21). It is uncertain whether this second groove opened in the posterior aperture of the carotid canal or in a separate foramen anteromedial to it. The exact position of the orbital opening of this groove is uncertain, but was likely in the floor ventral to the foramen buccinatorium. This anterolaterally directed groove was likely enclosed in a canal by the pterygoid that is subequal to that for the internal carotid artery. In fact, on the right side of PSS-MAE 101, in which the pterygoid is in place, there is a ridge running forward from the posterior aperture of the carotid canal that likely marks the position of the enclosed canal (fig. 20). We interpret this canal as the pterygoid (Vidian) canal

(“ptca” in fig. 37A). Its usual occupant in modern mammals is the nerve of the pterygoid canal, which is formed by the greater and deep petrosal nerves, carrying parasympathetic and sympathetic fibers, respectively (Evans and Christensen, 1979; Williams et al., 1989). However, in some instances, there is also an accompanying artery off the internal carotid (McDowell, 1958; MacPhee, 1981). The relatively large size of the preserved groove on the alisphenoid in PSS-MAE 113 suggests that the pterygoid canal contained both an artery and nerve. The entrance of the deep petrosal nerve, a branch of the internal carotid nerve, into the pterygoid canal must have been from the carotid groove, but the entrance of the greater petrosal nerve is unclear. Given that there is no likely tympanic aperture for the greater petrosal nerve, we speculate that it must have entered the pterygoid canal through the suture (gap) between the petrosal and alisphenoid directly from the cavum epiptericum and/or cavum supracochleare.

From its origin, the groove for the stapedial artery runs posterolaterally on the promontorium toward the fenestra vestibuli or oval window (“fv” in figs. 14, 37A). The stapedial groove exhibits a slightly different relationship to the fenestra vestibuli in PSS-MAE 101 and 113. In the former, the groove notches the rim of the fenestra vestibuli, whereas in the latter it extends slightly posterior to the fenestra, with the crest forming

the ventral edge of the stapedial groove extending posteroventral to the ventral margin of the oval window.

On the medial aspect of the ventral promontorial surface, near the contact with the basisphenoid, is a fan-shaped flange trending anteroposteriorly. Running transversely on the surface of the flange is the groove for the main stem of the internal carotid described above. Extending rostrally from the sulcus on the flange is a low crest, which we call here the rostral tympanic process of the petrosal. It may mark the contact with either a membrane, cartilage, or bone contributing to the floor of the tympanic cavity, as it does in extant mammals (Novacek, 1977; MacPhee, 1981). However, the composition of this floor, whether membranous, cartilaginous, or bony, cannot be determined. To date, there is no evidence for a bony bulla in any nontherian mammal. On the right side of PSS-MAE 101, the rostral tympanic process of the petrosal is continuous with a low crest that extends rostrally to the base of the pterygopalatine ridge (fig. 20). At least the posterior part of this crest is petrosal.

At the posterior end of the promontorium (fig. 37A) are two apertures, the fenestra vestibuli and the perilymphatic foramen, separated by a narrow bridge of bone, the crista interfenestralis, that reaches posteriorly to the base of the paroccipital process. The perilymphatic foramen (“pef” in figs. 14, 37A) is roughly circular, and the subequal fenestra vestibuli has an average stapedial ratio (see Segall, 1970) of 1.39 in PSS-MAE 113. The fenestra vestibuli is oriented in a near vertical plane and faces anterolaterally with a slight ventral component. Immediately anterior to the fenestra vestibuli is a deeply excavated pocket (“tff” in figs. 14, 37A), the fossa for the tensor tympani muscle (fossa muscularis major of Kielan-Jaworowska et al., 1986). The lateral margin of the tensor tympani fossa is formed by the flaring medial edge of the epitympanic recess.

The perilymphatic foramen and environs are best shown on the right side of PSS-MAE 101 but are preserved on both sides in PSS-MAE 113. The foramen is posteriorly directed and only its ventral margin is well delimited; its roof lacks a definitive edge and is formed by the petrosal’s contribution to the

very conspicuous jugular fossa (“jf” in figs. 14, 37A), the large depression around the jugular foramen (“jfo” in fig. 37A). A sulcus for the cochlear aqueduct, which is present on the petrosal in some other multituberculates (Rougier et al., 1996c; Fox and Meng, 1997), is lacking. We term this aperture in *Kryptobaatar* a perilymphatic foramen, because observations on the endocranium of PSS-MAE 123 have failed to reveal a cochlear aqueduct (cochlear canaliculus), a bony canal that transported the perilymphatic duct. Consequently, the only possible channel for the perilymphatic duct from the inner ear to the jugular foramen was via the perilymphatic foramen.

Immediately behind the perilymphatic foramen and forming part of its posterodorsal edge is the prominent ventral bulge housing the posterior ampulla of the semicircular canals. Portions of the lateral and posterior semicircular canals can be traced posteriorly from the posterior ampulla. These, along with the crista interfenestralis, delimit two deep pits on either side of the posterior ampulla. The larger pit is the one lateral to the ampulla, which is encircled by the posterior extension of the crista interfenestralis and the posterior extension of the lateral semicircular canal. The small medial pit is subtriangular and is placed between the posterior extensions of the lateral and posterior semicircular canals. These pits likely housed the expanded middle-ear cavity.

Positioned medial and very near to the perilymphatic foramen is the jugular foramen (fig. 37A), which is about half the size of the former aperture. The jugular foramen lies on the suture between the petrosal and exoccipital; the basioccipital appears to be excluded, judging by a suture visible on the right side of PSS-MAE 101 (see Exoccipital). Also visible on the same side of this specimen is a smaller foramen just posterolateral to the jugular foramen completely encircled by the petrosal; the function of this opening is unknown and its presence in PSS-MAE 113 cannot be verified.

Directly in front of the anteromedial edge of the perilymphatic foramen is a niche on the promontorium, which is deeply recessed, more so in PSS-MAE 113 than in 101. This niche represents the anteromedial extent of

the greatly expanded jugular fossa, the large depression around the jugular foramen (figs. 14, 37A). A robust, long laminar process projects posteromedially from the medial side of the promontorium and forms a horizontal shelf that partially floors this part of the jugular fossa. This shelf is well developed in PSS-MAE 113 (fig. 21), but barely has any horizontal contribution in PSS-MAE 101 (fig. 20).

As stated above, the crista interfenestralis reaches posteriorly to contact the paroccipital process (“ppr” in fig. 37A). Lateral to the crista interfenestralis and in front of the paroccipital process (and hidden by that structure in the figures) is a broad depression in the tympanic roof, the fossa for the stapedius muscle. The limits of this depression are not conspicuous, but its ventral extension on the lateral face of the crista interfenestralis is very distinct. Nevertheless, this depression is at least twice the surface area of the fenestra vestibuli. The well-developed, triangular paroccipital process (fig. 37A) is preserved on both sides of PSS-MAE 101 (fig. 20) and on the right side of 113 (fig. 21). It is not a vertical structure, but is slanted somewhat anteroventrally. From the blunt apex of the paroccipital process two crests arise, one leading medially and the other laterally (fig. 37A). The medial one, the caudal tympanic process of the petrosal (“ctpp” in fig. 37A), is very short and marks the posteroventral limit of the conspicuous jugular fossa. The three bones encircling the jugular fossa (petrosal, exoccipital, and basioccipital) provide laminae that wall and partially floor this space. As one of these laminae, the caudal tympanic process of the petrosal is coplanar with the laminar projections from the other bones.

The lateral crest arising from the paroccipital process is the crista parotica (“cp” in fig. 37A). It is L-shaped with transverse and longitudinal components. The shorter transverse component is anteroposteriorly thick and smooth and runs from the tip of the paroccipital process to a scooped area housing the external acoustic meatus on the squamosal-petrosal suture. The posterior part of the longitudinal component is not well individualized, and sutures indicate that its lateral surface contacted the squamosal; it was

here that the external acoustic meatus likely entered the middle ear. The anterior part of the longitudinal component, beginning at the level of the posterior margin of the fenestra vestibuli, is more prominent. It runs antero-medially as a tall subvertical crest that limits the medial margin of the epitympanic recess and continues forward as the medial edge of the infolded lateral flange.

Slightly posterolateral to the level of the fenestra vestibuli, the crista parotica shows the attachment of a well-developed tympanohyal (“th” in fig. 37A). In ventral view, this pronglike element is posteriorly and only slightly medially directed; in medial view, it has a distinctly triangular outline. The tympanohyal appears completely preserved on the left side of PSS-MAE 113 (figs. 21) and has a hooklike profile for cradling the hyomandibular branch of the facial nerve. This nerve left the middle ear via a stylo-mastoid notch immediately posterior to the tympanohyal.

The epitympanic recess (“er” in fig. 37A), following Kielan-Jaworowska et al. (1986), is the fossa above the dorsal margin of the tympanic membrane that accommodated the body of the malleus and incus and housed the crus breve of the incus (fossa incudis). In *Kryptobaatar*, the epitympanic recess is a deeply excavated, elongated, ellipsoidal fossa trending roughly parallel to the crista parotica (figs. 20, 21, 37A). It has contributions from three bones: the petrosal forms the bulk with the alisphenoid at the anteriormost end. Additionally, the squamosal forms the posterolateral edge of the epitympanic recess where the fossa incudis is located. The medial wall of the fossa incudis is delimited by the prominent crista parotica and its rostral continuation, the lateral flange. This sharp, ventrally projecting crest forms a barrier between the fossa incudis and the fenestra vestibuli, and it severely constrained the likely positions of the stapes and incus. As in other multituberculates (Rougier et al., 1996a, 1996c), the lateral flange in *Kryptobaatar* is infolded such that its anterior end contacts the cochlear housing; in other Mesozoic taxa, such as *Morganucodon* and *Vincelestes*, the lateral flange runs parallel to and is separated from the promontorium by a depression

called the lateral trough (Wible and Hopson, 1993).

In the anterior part of the epitympanic recess are several foramina interpreted for branches of the mandibular nerve (“foi” and “fma” in fig. 37A); *Kryptobaatar*, as in all known multituberculates and some rodents (Hill, 1935; Wahler, 1974), has multiple apertures for this division of the trigeminal nerve, one of which, the buccinator foramen, was described already (see Alisphenoid). In PSS-MAE 101 (fig. 20), two foramina for the mandibular nerve are situated in the epitympanic recess: the foramen ovale inferium opens into the recess and faces anterovertrally, whereas the foramen masticatorium notches the lateral rim of the recess and faces ventrolaterally. The foramen ovale inferium is centrally placed in a deep fossa and dominates the anterior pole of the epitympanic recess; it is traversed by a broad sulcus, which anteriorly falls just short of the alisphenoid’s contribution to the recess. The foramen masticatorium is strongly elliptical with the anteroposterior axis longer than the dorsoventral and is placed lateral and slightly posterior to the foramen ovale inferium. A similar arrangement is present in PSS-MAE 113 (fig. 21) with the exception that the foramen masticatorium is subdivided into two foramina on the right side. The division is accomplished by a narrow bar of bone continuous with the lateral edge of the epitympanic recess. This delicate bar was complete, but was broken prior to illustration here and in Rougier et al. (1996c: fig. 3). The left side of PSS-MAE 113 is damaged, but only one foramen masticatorium seems to have been present. Variation in the number of exits for the mandibular nerve on different sides of the same skull is known in other multituberculates (e.g., *Kamptobaatar*, ZPAL MgM-I/33).

Medial and dorsal to the crista parotica, and anterior to the tympanohyal, is a recessed area (“rvnf” in figs. 14, 37A). On the left side of PSS-MAE 113, three foramina are visible in this recess. These foramina lead into canals presumably within the petrosal, the exact course of which could not be determined without damaging the available specimens. Our reconstruction of the occupants of these foramina and canals is based

on comparison with isolated petrosals of other Late Cretaceous multituberculates (see Kielan-Jaworowska et al., 1986; Luo, 1989; Wible and Hopson, 1995). Of the three foramina in the recess in PSS-MAE 113, the posterior two share a common space and are higher than the anterior one. The posterior-most foramen opens into a posterolaterally directed channel and likely transmitted one of the two end branches of the stapedia artery, the ramus superior, into the ventral ascending canal (the pterygoparoccipital foramen). The similarly sized middle foramen is posteroventrally directed and likely transmitted the prootic sinus; therefore, it represents the ventral aperture of the prootic canal. The dorsal aperture of the prootic canal will be described with the endocranial surfaces. The morphology of these two foramina, the ventral apertures of the ventral ascending and prootic canals, accords well with that reported in some other multituberculates (Wible and Hopson, 1995: fig. 7A). The anterior-most foramen in the recess in PSS-MAE 113, the largest, is anteromedially directed, horizontal, and elliptical in outline. We consider it to be a joint aperture leading to two canals, one for the hyomandibular branch of the facial nerve (the secondary facial foramen) and the second for the other end branch of the stapedia artery, the ramus inferior, an arrangement different from that in described ptilodontoid and taeniolabidoid multituberculates (Luo, 1989; Wible and Hopson, 1995). Supporting this interpretation is a distinct sulcus leading posteriorly from this aperture to the dorsal rim of the fenestra vestibuli that resembles the sulcus for the facial nerve in other multituberculates (Wible and Hopson, 1995: figs. 7A, 8A). Moreover, a second, well-developed foramen at the anterior edge of the petrosal, lateral to the promontorium, likely held the rostral continuation of a vessel that initially ran with the facial nerve. That this vessel was the ramus inferior is supported by the large size of the groove for the stapedia artery on the promontorium and the small size of the foramen for the ramus superior, implying that the other primary ramus of the stapedia artery was present. However, we cannot rule out that a vein, the post-trigeminal vein, accompanied the ramus inferior in its passage through the petrosal.

The positions of the foramina transmitting the superior and inferior rami and the stapedia groove on the promontorium in both PSS-MAE 101 and 113 suggest that the stapedia artery ran across the fenestra vestibuli and through the presumed bicurrate stapes (Rougier et al., 1996c).

Lateral View (figs. 10–13, 33, 36A): The most conspicuous feature of the petrosal in lateral view is the anterior lamina. It contacts dorsally the parietal, anteriorly the frontal, orbitosphenoid, and alisphenoid, and posteriorly it is overlapped by the squamosal; ventrally, it is continuous with the tympanic surface of the petrosal through the lateral flange. The anterior lamina formed wholly or partially a number of passageways for nerves and vessels leaving the braincase for the orbitotemporal fossa and also provided a major area of attachment for several muscles of mastication.

Dorsally, the anterior lamina overlaps the parietal as shown on the left side of PSS-MAE 101. From back to front, the suture between the anterior lamina and parietal runs slightly dorsally from the triple junction of parietal, squamosal, and anterior lamina to the anterior opening of the orbitotemporal canal between the parietal, frontal, and anterior lamina. Parallel and medial to this suture is a preserved endocast on both sides of PSS-MAE 101 (figs. 10, 12) and the right side of 113 (fig. 11), representing the filling of the orbitotemporal canal. The orbitotemporal canal appears to have been bounded laterally by the parietal only, with the anterior lamina lateral to that. Throughout most of its course, there is no distinct medial wall for the orbitotemporal canal, suggesting that the orbitotemporal vessels ran endocranially within a sulcus on the medial surface of the parietal. Toward the front, however, the frontal provides the medial wall of a true orbitotemporal canal, and the anterior lamina, parietal, and frontal complete the anterior opening of this canal. Directly lateral to the anterior opening of the orbitotemporal canal is a thickened lateral process of the anterior lamina that ventrally supports the large post-orbital process of the parietal. This process on the anterior lamina is incomplete on the left side of PSS-MAE 101, exposing dorsally

the deeply pitted articular surface of the parietal.

Slightly anteroventral to the anterior opening of the orbitotemporal canal is the suture between the anterior lamina and frontal (fig. 12). Along this arched junction, the anterior lamina lies lateral to the frontal. Farther ventrally, the anterior lamina meets the orbitosphenoid at a suture that is concave anteriorly (only the dorsal portion of which is preserved in PSS-MAE 101). As is apparent from one of the specimens showing the endocranial surface (fig. 25; PSS-MAE 123), the anterior lamina overlaps the orbitosphenoid laterally. In the area of the sphenorbital fissure, the anterior lamina is sharply inflected medially so that a portion of it faces anteriorly (figs. 10, 12). This surface has a deep fossa that is continuous ventrally with the surface for muscle attachment in the alisphenoid, the pterygoid fossa. The likely occupant of this area was the lateral pterygoid muscle. The suture between the alisphenoid and anterior lamina runs obliquely across this muscular fossa from the anteroventral margin of the sphenorbital fissure to the margin of the foramen masticatorium. Midway along its length, the suture is interrupted by an anteriorly facing foramen described above as having transmitted the buccal branch of the mandibular nerve (figs. 10, 36A).

The ventral edge of the anterior lamina (the lateral edge of the lateral flange) forms a gentle arch from the contact with the alisphenoid in front to the root of the zygomatic arch behind. Anteriorly, this margin is notched by the foramen masticatorium. Slightly dorsal and posterior to the edge of the foramen masticatorium is another small, anteriorly directed foramen, the supraglenoid foramen for a ramus temporalis of the ramus superior (“sgf” in figs. 8, 18, 36A). This foramen was likely continuous with the ventral ascending canal.

Posteriorly, the anterior lamina’s contact with the squamosal can be divided into two portions: a ventral one that is essentially horizontal, and a dorsal, essentially vertical one. Forming the horizontal portion is a flat flange of the anterior lamina that buttresses the front of the root of the zygoma and extends laterally toward, but falls short of, the glenoid fossa (“gl” in figs. 6, 14, 37A). The hori-

zontal portion of the suture is gently arched, concave posteriorly, and meets the dorsal portion in a small foramen, also for a ramus temporalis (“frt” in figs. 8, 36A). The dorsal portion runs along the course of the dorsal ascending canal, which, because of breakage in PSS-MAE 101, is shown to be formed by the squamosal and petrosal. On the left side of this specimen (fig. 12) there is a notch at the posterodorsal corner of the anterior lamina that opens to the dorsal ascending canal and probably was enclosed in a foramen by the squamosal posteriorly (“fdac” in figs. 8, 36A). This dorsal ascending canal foramen also transmitted a ramus temporalis. Similar foramina are found, for example, in *Kamptobaatar* (ZPAL MgM-I/33) and *Lambdopsalis* (Miao, 1988).

The external surface of the anterior lamina has a fairly complex topology and, in addition to the lateral pterygoid muscle, provided attachment for the temporalis muscle. The temporalis attachment can be divided into two major parts: an anterodorsal one that is convex and best expressed under the post-orbital process, and a ventral concave one. These two parts correspond to the attachment areas identified as for the pars anterior and pars posterior of the temporalis, respectively, in *Nemegtbaatar* by Gambaryan and Kielan-Jaworowska (1995).

Occipital View (figs. 16, 17, 35, 37A): Well preserved in both PSS-MAE 101 and 113, the mastoid exposure of the petrosal forms the lateral portion of the occiput and comprises approximately half of the occiput’s bony surface. The mastoid exposure is subtriangular with the base medially and with the apex laterally. It contacts the squamosal laterally on the ventral portion of the nuchal crest, the parietal dorsomedially on the dorsal portion of the nuchal crest, and the supraoccipital and exoccipital medially. The ventral edge of the mastoid exposure is formed by the paroccipital process and the crests arising from it, namely the caudal tympanic process of the petrosal medially and the crista parotica laterally.

There are three depressions on the mastoid exposure. The dorsomedial one continues onto the exoccipital and is subvertical with its deepest point along the suture between the petrosal and exoccipital; it lodges the atlas

when the skull is maximally extended (dorsiflexed) on the neck. The dorsolateral depression is shallow, roughly circular, and is separated from the atlantal fossa by a vertical ridge. Opening into the dorsolateral depression is the posterior opening of the posttemporal canal, which is wholly in the petrosal (“ptc” in figs. 14, 16, 36A). An elongated, ventral depression runs parallel to the crista parotica and probably represented the site of attachment for the sternomastoid muscle (Evans and Christensen, 1979).

JUGAL

The jugal is a thin, essentially oval, laminar bone on the inner surface of the zygomatic arch. In PSS-MAE 101, both zygomatic arches are preserved, but a nearly complete jugal is present only on the right side (fig. 22). In PSS-MAE 113, only the left arch is complete and the jugal preserved (fig. 23).

On the right side of PSS-MAE 101 (fig. 22A), the jugal is not as tall as the zygoma; it is recessed from both the ventral and dorsal margins of the zygomatic arch, but is closer to the latter. The anterior extent of the jugal is at the level of the posterior half of M1; posteriorly, it reaches almost to the same level as does the ventral margin of the zygomatic process of the maxilla. The zygomatic arch, and so the jugal, does not lie in a sagittal plane, but is tilted such that its dorsal margin is slightly lateral to the ventral. On the left side of PSS-MAE 101 (fig. 22B), the jugal is not preserved, and a shallow, oval facet is exposed. The bulk of the facet is on the maxilla, with only the posterodorsal fifth on the squamosal. In PSS-MAE 113 (fig. 23), the jugal conforms in most features to that in PSS-MAE 101, but the dorsal margin of the jugal is exposed in lateral view, forming the dorsal edge of the zygomatic arch (fig. 19). Moreover, the dorsal margin is slightly thicker than the portion of the jugal directly medial to the maxilla and squamosal.

SQUAMOSAL

The squamosal is appressed to the posterior part of the side wall of the braincase and can arbitrarily be divided into two parts: the zygomatic process and the dorsal flange. The squamosal is well preserved in both PSS-

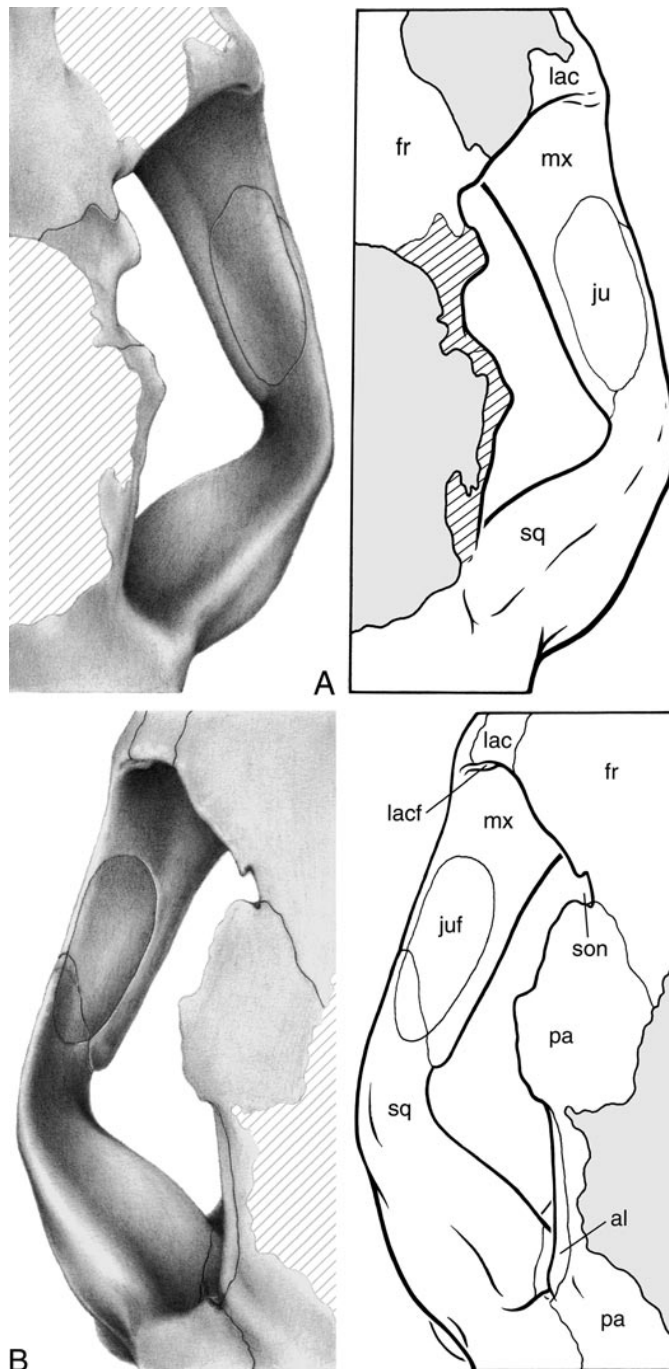


Fig. 22. Pencil drawings of the right and left zygomatic arches (A and B) of *Kryptobaatar dashzevegi* PSS-MAE 101 in dorsal view, with accompanying line drawings. Gray pattern represents matrix; parallel lines denote breakage. Abbreviations: **al** anterior lamina; **fr** frontal; **ju** jugal; **juf** jugal facet; **lac** lacrimal; **lacf** lacrimal foramen; **mx** maxilla; **pa** parietal; **son** supraorbital notch; **sq** squamosal.

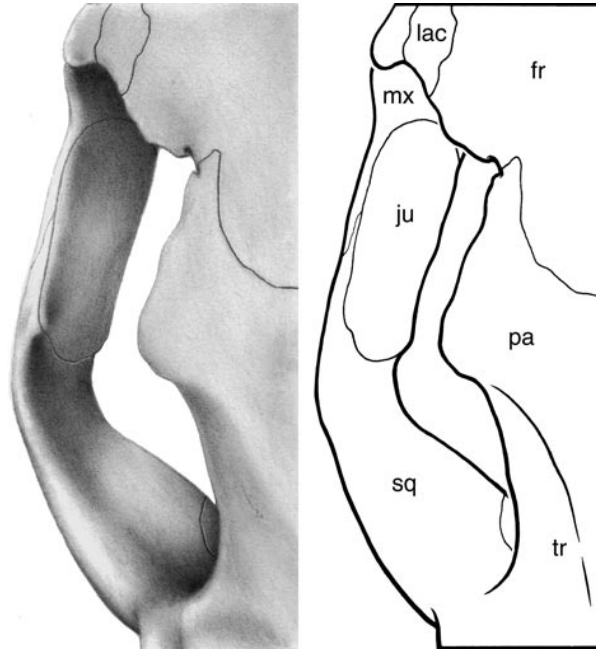


Fig. 23. Pencil drawing of the left zygomatic arch of *Kryptobaatar dashzevegi* PSS-MAE 113 in dorsal view, with accompanying line drawing. Abbreviations: **fr** frontal; **ju** jugal; **lac** lacrimal; **mx** maxilla; **pa** parietal; **sq** squamosal; **tr** temporal ridge.

MAE 101 and 113, although in the latter the zygomatic process is incomplete on the right side.

The squamosal's contacts are as follows (figs. 8, 12, 32–34): anteriorly, with the maxilla and the jugal via the zygomatic process, and with the anterior lamina via the dorsal flange; medially and posteriorly, with the petrosal via the dorsal flange; and dorsally, with the parietal via the dorsal flange. The squamosal has been partially lost in several specimens (PSS-MAE 113, 124, 125), exposing an extensive underlying facet on the petrosal. From this, it is evident that the squamosal has no direct contribution to the side wall of the braincase.

The dorsal flange of the squamosal is laminar, tongue-shaped, and appressed to the side wall of the braincase. In ventral view (figs. 20, 21, 34, 37A), the dorsal flange contacts the petrosal through an L-shaped suture, with the long arm oriented sagittally and the more anteriorly located short arm transversely. The short arm abuts a laterally directed, wedge-shaped projection from the lateral flange of the petrosal. In posterior view (figs.

16, 17, 35, 37A), the dorsal flange contacts the mastoid exposure of the petrosal to form the inferolateral extent of the nuchal crest, just lateral to the posterior opening into the posttemporal canal. In dorsal view (figs. 8, 9, 31), the chief contact is with the petrosal, in front with the anterior lamina and behind with the edge of the mastoid exposure forming the nuchal crest. The dorsal flange also has a narrow contact with the parietal dorsomedially. The suture with the anterior lamina can be divided into two arched portions: the anterior one is chiefly horizontal and is continuous with the front edge of the zygomatic process; the posterior one is vertically directed (fig. 8). Where these two portions of the squamosal–petrosal suture meet is a small foramen, probably for a ramus temporalis (“frt” in figs. 8, 36A). The posterior edge of the dorsal flange, together with the dorsal edge of the mastoid exposure of the petrosal, forms the inferolateral portion of the nuchal crest, which is low and sharp. The ventralmost portion of the nuchal crest partially delimits the notch that presumably lodged the external acoustic meatus.

The transition between the dorsal flange and zygomatic process of the squamosal is indicated by a neck projecting anterolaterally from the braincase to the glenoid fossa. In ventral view (figs. 15, 21), a shallow depression, likely marking the course of the external acoustic meatus, runs along the long axis of the neck and is continued medially on the petrosal. The anterior limit of the depression is marked by a blunt, low transverse ridge, which extends between the medial margin of the glenoid and the crista parotica on the petrosal. The glenoid fossa is essentially flat, with the anteromedial and posterolateral corners projecting slightly ventrally and the posteromedial corner being elevated. Its outline is slightly teardrop-shaped, with the major axis running from anterolateral to posteromedial. This axis forms an abrupt angle with the squamosal portion of the zygomatic arch, an unusual feature among mammals, which imparts a distinctive outline to the skull of *Kryptobaatar* and several other Mongolian Late Cretaceous multituberculates. In front of the glenoid, the zygomatic process is flangelike and has an extensive oblique contact with the maxilla; it is considerably shorter and weaker than is the maxilla's contribution to the zygoma. As described above, the squamosal and maxilla support the jugal, which lies medial to both bones but has the greater part of its contact with the maxilla. In external view, lateral to the glenoid fossa and extending anterior to it on the zygomatic process, there is an arched ridge, concave inferiorly, the intermediate zygomatic ridge ("izr" in fig. 12) of Gambaryan and Kielan-Jaworowska (1995). This ridge marks the dorsal border of a shallow depression, which these authors suggested was for the origin of the posterior part of the superficial masseter muscle. This intermediate ridge is confluent with the anterior zygomatic ridge on the maxilla, in contrast with the condition reported by Gambaryan and Kielan-Jaworowska (1995) in *Nemegtbaatar*, *Chulsanbaatar*, and *Catopsbaatar* where the anterior and intermediate ridges are not confluent. A third, more posterior ridge, the posterior zygomatic ridge, described for *Nemegtbaatar*, *Chulsanbaatar*, and *Catopsbaatar* (Gambaryan and Kielan-Jaworowska, 1995), is not discernible in *Kryptobaatar*.

PARIETAL

The parietals are laminar bones that form the bulk of the roof of the cranial cavity. They are essentially lacking in PSS-MAE 101 (fig. 8) and are considerably damaged in PSS-MAE 113 (fig. 9); however, enough is preserved to provide the major morphological details.

The parietals are limited to the dorsal portion of the braincase (figs. 8, 9, 32) and are only moderately convex. Anteriorly, they contact the frontals at a broad U-shaped suture; lateral to the arms of the U, a narrow anterior process of the parietal extends forward, nearly to the lacrimal in the orbital rim, to form the posterior part of the supraorbital notch and supraorbital crest. Behind the anterior process, level with the posterior border of the frontals, is the triangular, posterolaterally and ventrally directed postorbital process ("pop" in figs. 12, 19). As originally preserved, the process was long in PSS-MAE 113 but was damaged during preparation. It is completely preserved on both sides in a skull referred to *Kryptobaatar* (PSS-MAE 127). The posterior margin of the postorbital process is continuous with weakly developed temporal ridges ("tr" in fig. 23). The temporal ridges are not fully preserved in PSS-MAE 113, but in PSS-MAE 127 the temporal ridges do not meet on the midline to form a sagittal crest. Instead, the ridges approximate each other posteriorly, delimiting a broad middorsal ridge. Posteriorly, the parietals contact the supraoccipital at a mostly transverse suture, and together with the supraoccipital form the dorsal tip of the nuchal crest. An interparietal is not present. On its ventrolateral surface, the parietal contacts, from front to back, the frontal and the anterior lamina with an essentially straight suture, and the squamosal with a suture that is concave medially. The contact with the frontal and squamosal is fairly narrow, whereas that with the anterior lamina is extensive.

SUPRAOCCIPITAL

The supraoccipital is a laminar bone that is essentially confined to the occiput; it is well preserved in both PSS-MAE 101 (fig. 16) and 113 (fig. 17).

The supraoccipital is a hexagonal element

(fig. 35). Its contacts on the occiput are with the petrosals laterally and with the exoccipitals ventrolaterally. A small portion of the supraoccipital forms the dorsal margin of the foramen magnum and, with the parietal, the dorsal part of the nuchal crest. The nuchal crests flare out posterolaterally along the contact between the mastoid and squamosal; the medial continuation of these crests along the supraoccipital–parietal suture is less prominent and is moderately notched in the sagittal plane. The supraoccipital is slightly convex dorsoventrally and concave mediolaterally. The occipital plane in PSS-MAE 101 as determined by the supraoccipital inclines anteriorly at 35° from the vertical. In PSS-MAE 113, the supraoccipital is more concave mediolaterally and a little taller than in PSS-MAE 101.

EXOCCIPITAL

The exoccipital has contributions to the occiput and basicranium and can arbitrarily be divided into three parts: the occipital plate, the condyle, and the contribution to the jugular fossa. The sutures delimiting the exoccipital from its neighbors are distinct on the occiput, but are not as discernible in other areas. The exoccipital is well preserved in PSS-MAE 101 (figs. 14, 16) and 113 (figs. 15, 17), but its contribution to the jugular fossa has not been cleaned of matrix on the left side of the former.

The occipital plate of the exoccipital is a subrectangular bony lamina that forms one-third of the rim of the foramen magnum and extends anterolaterally from the edges of that aperture (fig. 35). Its contacts on the occiput are with the supraoccipital dorsomedially and with the petrosal ventrolaterally. The suture with the supraoccipital is straight and runs from dorsolaterally to ventromedially; the suture with the petrosal is arched and extends ventrolaterally from the point where the exoccipital, supraoccipital, and petrosal meet above the level of the condyle to the medial slope of the paroccipital process. Along the petrosal suture, there is a deep pit that is continuous with the atlantal fossa on the petrosal that probably lodged part of the atlas when the skull was maximally extended.

The condyle is a rounded structure

(“ocon” in figs. 10, 12, 16) with the major axis oriented from dorsolateral to ventromedial. The articular surface on the condyle can be divided into two parts: (1) a dorsal one contributing to the lateral margin of the foramen magnum and extending anterolaterally with a similar orientation as the occipital plate, and (2) a ventral one contributing to the floor of the foramen magnum and lying chiefly in a horizontal plane. The left and right condyles bound approximately half of the foramen magnum (figs. 16, 17). They do not contact each other in the midline, but are separated by a distinct odontoid notch (“on” in fig. 37A). Despite the fact that the sutures cannot be traced, it is likely that the medialmost portion of the condyles and the odontoid notch are actually formed by the basioccipital as, for example, in monotremes (Kuhn, 1971; Zeller, 1989).

The exoccipital is one of the major components of the jugular fossa, a deep excavation of the basicranium posterior to the promontorium of the petrosal (figs. 14, 15, 20, 21, 37A). The medial wall of the jugular fossa is formed by the exoccipital and basioccipital; the posterior wall largely by the exoccipital and the paroccipital process of the petrosal; and the lateral wall entirely by the petrosal, the crista interfenestralis in the posterior part and the promontorium anteriorly. In addition to contributing to the posterior wall, the anterior margin of the condyle projects as a thin lamina that partially floors the jugular fossa. In fact, the jugular fossa is deeply recessed into all the surrounding bones, so that its size is considerably larger than what is visible in ventral view. Inside the fossa, the exoccipital is the major constituent of the roof. It contacts the petrosal through an oblique suture running anteriorly from lateral to medial. Along this suture is the small jugular foramen, which occupies the posterolateral corner of the fossa, posteromedial to the perilymphatic foramen (fig. 37A). A possible suture between the basioccipital and exoccipital is visible in the roof of the jugular fossa on the right side of PSS-MAE 101; it begins just anteromedial to the jugular foramen and extends posteromedially but cannot be traced onto the condyle.

On the right side of PSS-MAE 101, deep in the jugular fossa and posterolateral to the

jugular foramen, is a small, circular foramen (not visible in the figures). An opening in a similar position may be present on the left side of PSS-MAE 113, but it is not as clear. The foramen in PSS-MAE 101 is interpreted as for the hypoglossal nerve. The right jugular fossa in PSS-MAE 113 seems to be well preserved, but in the area where a hypoglossal foramen is expected, no aperture is found. It is possible, although unlikely, that the foramina mentioned above are artifacts and that the true hypoglossal foramina are concealed by matrix in the caudalmost portion of the jugular fossa.

According to Kielan-Jaworowska et al. (1986), the large size of the jugular fossa in Mongolian Late Cretaceous multituberculates suggests the presence of large ganglia on the nerves below the jugular foramen. However, large ganglia alone cannot account for the immense jugular fossa in *Kryptobaatar*, especially considering the minute size of the jugular foramen. Therefore, we think that the structural continuity between the jugular fossa and the middle-ear space suggests that the fossa housed a diverticulum of the cavum tympani (see also Rougier et al., 1996c).

BASIOCCIPITAL

The basioccipital is a long, narrow, laminar bone that forms the base of the skull anterior to the foramen magnum and medial to the ear regions. It can be divided into two parts: one on the basicranial axis, and the other contributing to the jugular fossa. The basioccipital is best preserved in PSS-MAE 101 (fig. 14), having been distorted in PSS-MAE 113 in which the left petrosal is displaced (fig. 15).

The basioccipital contacts the exoccipital posterolaterally, the petrosal laterally, and the basisphenoid anteriorly (figs. 14, 34). In addition, there may even be a contact with the pterygoid along the lateral edge of the basioccipital in front of the petrosal contact, depending on the composition of the crest extending posteriorly from the pterygopalatine ridge (see Sphenoid Complex). The suture with the basisphenoid is straight and transverse, just behind the level of the back of the pterygopalatine ridges. The suture with the promontorium of the petrosal is gently

curved, with the basioccipital becoming slightly wider posteriorly along its petrosal contact. The maximum width of the basioccipital is at the level of the jugular fossa, and then it tapers posteriorly to the odontoid notch. As stated above, the suture between the basioccipital and exoccipital in the condylar region is not discernible, but it was likely oblique, running anterolaterally from the odontoid notch and the medial aspect of the condyle. A possible oblique suture separates these same two bones in the jugular fossa on the right side of PSS-MAE 101.

In the basicranial axis, the anterior part of the basioccipital is essentially flat, whereas posteriorly there is a concavity on the midline. In the jugular fossa, the basioccipital contributes a fairly vertical wall along the medial aspect and the anteromedial part of the roof. The ventral edges of the basioccipital's contribution to the jugular fossa strongly project laterally to form a partial floor for that depression.

ENDOCRANIUM

Described here are structures on the endocranial surface of the braincase preserved in three skulls of *Kryptobaatar*, PSS-MAE 123 (fig. 25), 124, and 125 (fig. 26). Comparative specimens also employed include two indeterminate skulls resembling *Kryptobaatar*, PSS-MAE 126 and 128. A reconstruction of the endocranial floor is shown in figure 27. As is evident from the exterior, the braincase in *Kryptobaatar* is formed by the exoccipitals, basioccipital, supraoccipital, petrosals, parietals, frontals, and the sphenoid complex; as stated above, the squamosal does not contribute directly to the braincase wall. With the exception of the petrosals, sutures delimiting the individual braincase elements are subject to some degree of uncertainty in the specimens showing the endocranium. Consequently, we base our descriptions on the internal morphology and attribute features to individual elements in light of our understanding of similar structures in extant mammals in which the boundaries are known. The dorsal components of the braincase (i.e., the frontal and parietal) were effectively missing in the specimens described herein, providing easy access to

the more complex floor and side wall of the endocranium.

Because endocrania are seldom preserved, let alone described, we add the following remarks by way of introduction to this anatomical region. The orbitotemporal region of the mammalian skull has a primary braincase wall formed by the chondrocranium and dura mater, and external to that, a secondary braincase wall formed by different patterns of several skeletal elements in different taxa (De Beer, 1937; Moore, 1981; Kuhn and Zeller, 1987). The extradural space between the primary and secondary wall is the cavum epiptericum (Gaupp, 1902, 1905), which houses the trigeminal and facial ganglia and is traversed by various cranial nerves and blood vessels. The cranial nerves enter the cavum epiptericum from the brain through specific gaps between near vertical bars or pillars of chondrocranial cartilage (fig. 24). The pattern of these gaps (i.e., how many are present and their contents) differs in monotremes, marsupials, and placentals (see below; Kuhn, 1971; Kuhn and Zeller, 1987).

There is a general consensus among morphologists (e.g., Starck, 1967, 1978; Kuhn, 1971; Moore, 1981) that the chondrocranium in the common ancestor of mammals had three pillars in the orbitotemporal region between the nasal and otic capsules, as occurs in most extant sauropsids (fig. 24A; De Beer, 1926, 1937; Bellairs and Kamal, 1981). From anterior to posterior, these are the pila preoptica, pila metoptica, and pila antotica (fig. 24B). These three pilae provide borders for the apertures that transmitted cranial nerves through the primary braincase wall (Kuhn and Zeller, 1987; Zeller, 1989). Anteriorly, between the nasal capsule and the pila preoptica is the orbitonasal foramen transmitting the ethmoidal branch of the ophthalmic nerve into the nasal cavity. Posterior to that, between the pila preoptica and metoptica is the optic foramen transmitting the optic nerve into the orbit. Next, between the pilae metoptica and antotica is the metoptic foramen transmitting the oculomotor nerve into the orbit (or into the front of the cavum epiptericum). Finally, the gap between the pila antotica and the otic capsule, the prootic foramen, transmitted the trochlear, trigeminal, and abducens nerves into the cavum

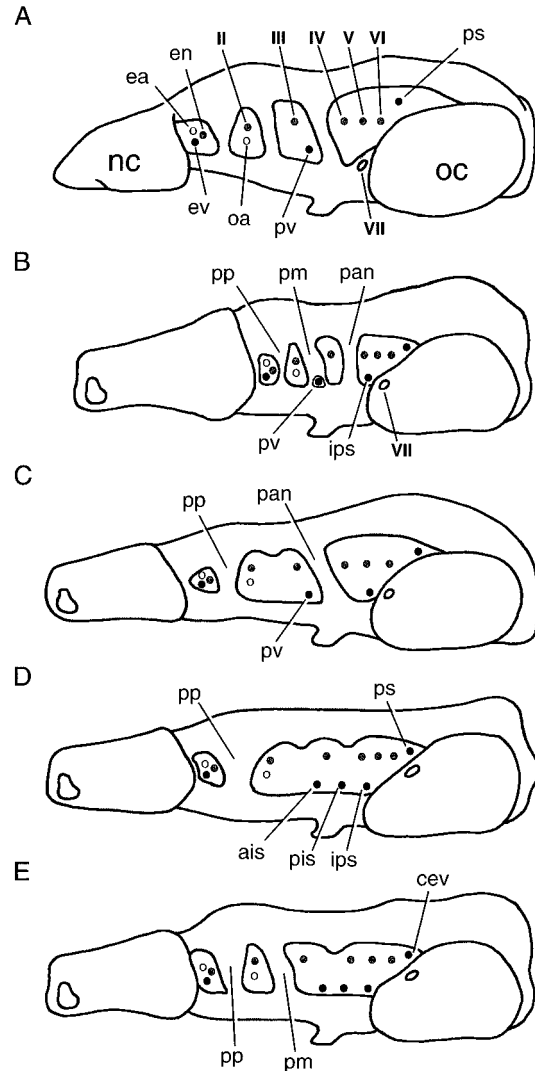


Fig. 24. Schematic drawings of embryonic chondrocrania in left lateral view. **A**, generalized sauropsid; **B**, generalized multituberculata, as reconstructed from here; **C**, generalized monotreme; **D**, generalized marsupial; **E**, generalized placental. Abbreviations: **ais** anterior intercavernous sinus; **cev** capsuloparietal emissary vein; **ea** ethmoidal artery; **en** ethmoidal nerve; **ev** ethmoidal vein; **ips** inferior petrosal sinus; **nc** nasal capsule; **oa** ophthalmic artery; **oc** otic capsule; **pan** pila antotica; **pis** posterior intercavernous sinus; **pm** pila metoptica; **pp** pila preoptica; **ps** prootic sinus; **pvt** pituito-orbital vein; **II** optic nerve; **III** oculomotor nerve; **IV** trochlear nerve; **V** trigeminal nerve; **VI** abducens nerve, **VII** facial nerve.

epiptericum. Immediately posterior to that, the facial nerve entered the back of the cavum epiptericum through a separate opening, the primary facial foramen, between the otic capsule and a bar of cartilage, the prefacial commissure, connected to the front of the otic capsule.

A reconstruction of the vessels passing through the primary wall in basal mammals has not yet been proposed, and we offer the following model here (fig. 24A, B). Judging from the anatomy of extant amniotes, blood vessels ran through all of the apertures in the primary wall named above except the primary facial foramen. Also in the orbitonasal foramen were ethmoidal arteries and veins; in the optic foramen, the ophthalmic branch of the internal carotid artery; in the metoptic foramen, the pituito-orbital vein; and in the prootic foramen, the prootic vein and inferior petrosal sinus. Our justification for this model is as follows.

(1) Ethmoidal vessels in the orbitonasal foramen: Vessels accompanying the ethmoidal nerve are typically present in both sauropsids (Shindo, 1914) and mammals (Tandler, 1899).

(2) Ophthalmic artery in the optic foramen: The ophthalmic artery has been reconstructed by Miao (1988), citing De Beer (1937), with the oculomotor nerve and the pituitary vein in the metoptic foramen in *Lambdopsalis*. However, we disagree with this placement of the ophthalmic artery in *Lambdopsalis* and in basal mammals. There are some sauropsids in which the ophthalmic artery enters the orbit via the metoptic foramen (e.g., *Crocodylus*, Shiino, 1914) or even via a separate foramen that secondarily fuses with the metoptic foramen (e.g., *Chrysemys*, Shaner, 1926; *Sphenodon*, Bellairs and Kamal, 1981). Yet, other sauropsids (e.g., *Lacerta*, Shindo, 1914; *Platydictylus*, Hafferl, 1921) and mammals (Tandler, 1899; Wible, 1984) have the ophthalmic artery and optic nerve intimately associated.

(3) Pituito-orbital vein in the metoptic foramen: A pituitary vein running from the pituitary (hypophysis) to the orbit is broadly distributed among sauropsids (Bruner, 1907), and is either in the metoptic foramen (e.g., *Lacerta*, De Beer, 1937) or in a separate foramen that secondarily fuses with the metop-

tic foramen (e.g., *Sphenodon*, Bellairs and Kamal, 1981). In mammals, a comparable vein drains medially from the cavernous sinus within the cavum epiptericum, immediately anterior to the pila antotica into the hypophyseal fossa in the echidna (Gaupp, 1908) and the platypus (personal obs.); in the latter, the vein exits the skull via the carotid foramen. This is not the only vein draining the pituitary, and, following a suggestion of one of our reviewers, Robert Presley, we refer to it as the pituito-orbital vein in light of its pathway. Marsupials and placentals do not have a strictly comparable vein, but it is possible that the stem of the anterior intercavernous sinus of therians (Shindo, 1915) is homologous with the pituito-orbital vein of monotremes and sauropsids.

(4) Prootic sinus and inferior petrosal sinus in the prootic foramen: The prootic sinus (middle cerebral vein) exits the prootic foramen to join the lateral head vein lateral to the otic capsule in sauropsids, monotremes, and some marsupials (Shindo, 1915; Wible, 1990; Wible and Hopson, 1995). Moreover, a canal housing this vessel is widely distributed among the extinct outgroups to mammals (Wible and Hopson, 1995; Rougier et al., 1996a). Among extant amniotes, an inferior petrosal sinus is known only in mammals, in which it runs posteriorly from the cavernous sinus within the cavum epiptericum, through the prootic foramen into the cranial cavity (Shindo, 1915; Rougier et al., 1996a).

As stated above, the pattern of the apertures in the primary braincase wall of basal mammals is altered in different ways in monotremes, marsupials, and placentals. All three retain the pila preoptica, but that is the extent of the resemblance between them.

(1) Monotremes (fig. 24C): In addition to the pila preoptica, a complete pila antotica forms in the chondrocranium of both the echidna (Gaupp, 1908; Kuhn, 1971) and platypus (Zeller, 1989). However, the pila antotica regresses during ontogeny, and in the adult it is represented by only its slender ossified base on the basisphenoid, the middle clinoid process ("mclp" in fig. 28; Kuhn, 1971; Zeller, 1989). The pila metoptica fails to form, leaving confluent the optic and metoptic foramina, which together are termed

the pseudoptic foramen (“psf” in fig. 28; Gaupp, 1908). The pseudoptic foramen transmits the optic and oculomotor nerves (Kuhn, 1971; Zeller, 1989), the pituito-orbital vein (Gaupp, 1908; personal obs.), and in the echidna the ophthalmic artery (Tandler, 1901); in the platypus, the ophthalmic artery branches off the maxillary artery in the orbit (Wible, 1984). The contents of the prootic foramen do not differ from that inferred for basal mammals.

(2) Marsupials (fig. 24D): The pila preoptica is the only pillar to form in the orbitotemporal region of the primary wall in marsupials (Kuhn and Zeller, 1987; Maier, 1987). Consequently, the optic, metoptic, and prootic foramina are confluent. Transmitted through this large gap are the second through sixth cranial nerves, the ophthalmic artery (Tandler, 1899), the anterior and posterior intercavernous sinuses, the inferior petrosal sinus, and the prootic sinus (Shindo, 1915). The prootic sinus is present during early ontogenetic stages in all marsupials investigated to date, but is retained only in adult didelphids, caenolestids, and some dasyurids (Wible, 1990; Wible and Hopson, 1995). This single large aperture transmitting all these structures in the marsupial chondrocranium has been referred to (e.g., Cords, 1915) as the sphenoparietal fenestra. Following most recent authors (e.g., Kuhn and Zeller, 1987), we reserve the similar term of sphenoparietal foramen for the opening in the chondrocranium of eutherians that transmits the third through sixth cranial nerves (see below).

(3) Placentals (fig. 24E): In addition to the pila preoptica, a complete pila metoptica forms in placentals and thus completes a true optic foramen in the orbitosphenoid of the adult (De Beer, 1937; Starck, 1967), which in most forms transmits the ophthalmic artery along with the optic nerve (Tandler, 1899, 1901; Wible, 1984). The pila antotica, however, fails to develop, leaving confluent the metoptic and prootic foramina, which together are termed the sphenoparietal foramen (Voit, 1909). The sphenoparietal foramen transmits the third through sixth cranial nerves, the anterior and posterior intercavernous sinuses, and the inferior petrosal sinus (Shindo, 1915). Unlike monotremes and

marsupials, the prootic sinus involutes in placentals and is replaced by a secondary vessel, the capsuloparietal emissary vein (Gelderen, 1924).

EXOCCIPITAL

In PSS-MAE 123 (fig. 25B), a small fragment of the left exoccipital has been preserved in articulation with the petrosal, posteromedial to the subarcuate fossa. Along the suture between the exoccipital and petrosal, a broad groove directed ventromedially is interpreted as having housed the sigmoid sinus. In PSS-MAE 125 (fig. 26), an even smaller portion of the right exoccipital completing the posteromedial margin of the jugular foramen has been preserved. The contribution of this bone to the jugular foramen is clearly indicated by sutures. Along the suture between the exoccipital and petrosal, directly posterior to the jugular foramen, is an anteriorly directed, digitiform process of the exoccipital that impinges on the lumen of the foramen. Also in this specimen, a longer segment of the sulcus for the sigmoid sinus is clearly preserved (“sss” in fig. 26). It does not approach the very small jugular foramen, but instead is directed toward the place where the missing foramen magnum would be expected. An endocast of the sigmoid sinus is preserved on both sides in the undescribed skull of multituberculate, n. sp. (PSS-MAE 126), and it follows the pattern described above in PSS-MAE 125.

BASIOCCIPITAL

In PSS-MAE 123, the rostral portion of the basioccipital is preserved; a smaller fragment is found in PSS-MAE 125; and the entire bone is likely present in PSS-MAE 124, but is not accessible for study. As preserved in PSS-MAE 123 (fig. 25), the basioccipital is a flat, slightly concave bone that is rather featureless. As gleaned from both specimens, the suture between the basioccipital and basisphenoid is situated immediately behind the dorsum sellae and runs transversely. The suture between the basioccipital and petrosal runs subparallel to the sagittal plane, converging slightly anteriorly. The basioccipital forms only a narrow portion of the skull base. In PSS-MAE 123, the basioccipital is

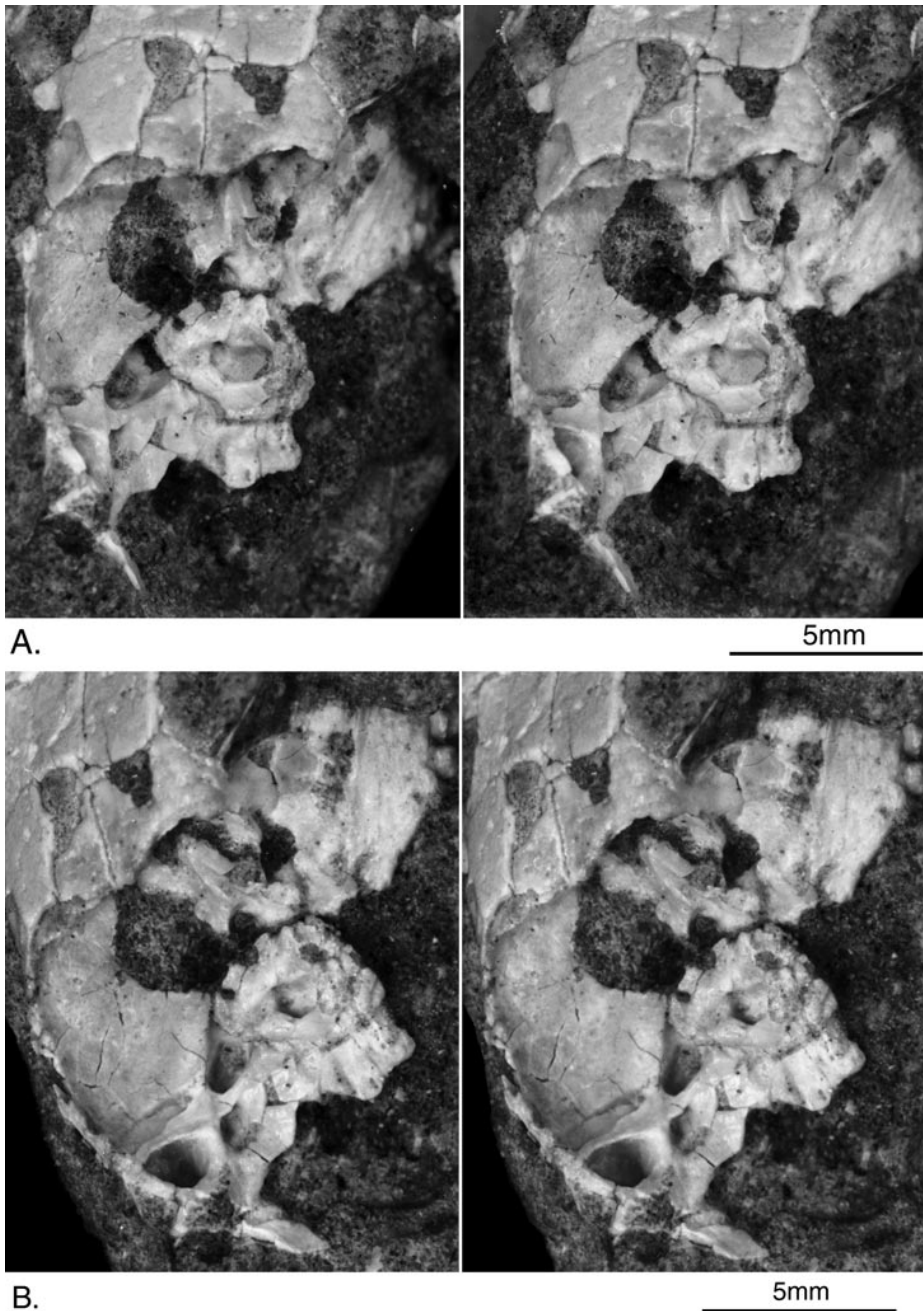


Fig. 25. Stereophotograph of the floor of the endocranium of *Kryptobaatar dashzevegi* PSS-MAE 123 in dorsal (A) and oblique dorsal (B) views, with accompanying line drawings. Gray pattern represents matrix; parallel lines denote breakage. Abbreviations: **al** anterior lamina; **bo** basioccipital; **ce** cavum epiptericum; **ds** dorsum sellae; **exoc** exoccipital; **ff** facial foramen; **fica** foramen for internal carotid artery; **fpv** foramen for pituito-orbital vein; **fr** frontal; **fv3** foramen for mandibular nerve; **hf** hypophyseal fossa; **iam** internal acoustic meatus; **jn** jugular notch; **jsp** jugum sphenoidale; **mef** metoptic foramen; **mx** maxilla; **na** nasal; **opf** optic foramen; **or** orbitosphenoid; **ow** orbital wing (pila preoptica); **pan** pila antotica; **prc** prootic canal; **pm** pila metoptica; **sf** subarcuate fossa; **sphf** sphenorbital fissure; **tus** tuberculum sellae.

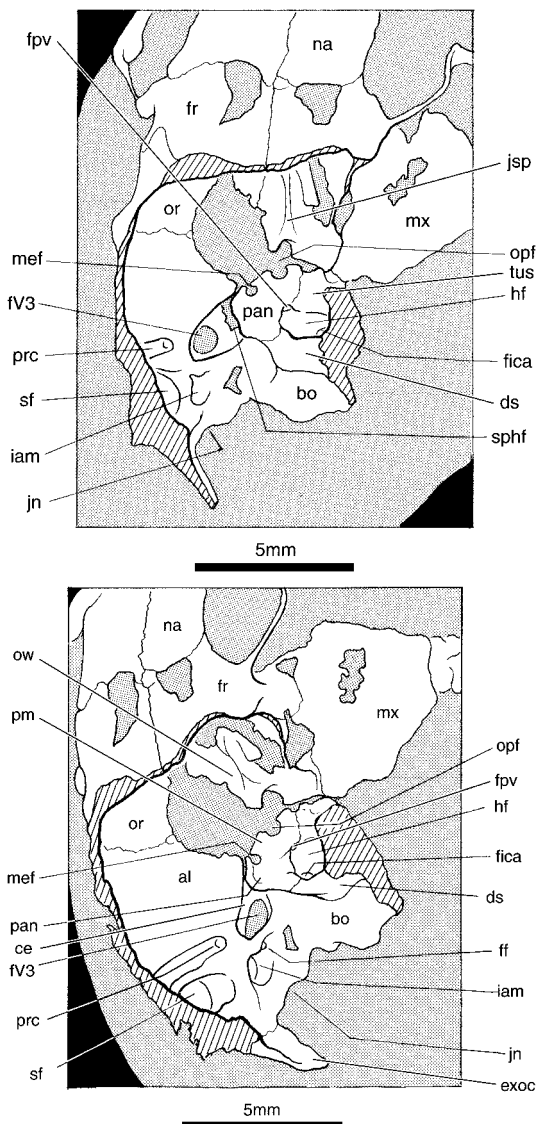


Fig. 25. Continued.

broken across the anteriormost portion of the jugular fossa, and the preserved fragment indicates that the fossa deeply excavates the basioccipital, leaving only a thin lamella separating the cranial cavity from the middle-ear cavity. Left and right jugular fossae also converge medially, being separated in the midline by a bridge of the basioccipital bone less than 1 mm in thickness. Along the basioccipital–petrosal suture is a shallow depression likely occupied by the inferior petrosal sinus.

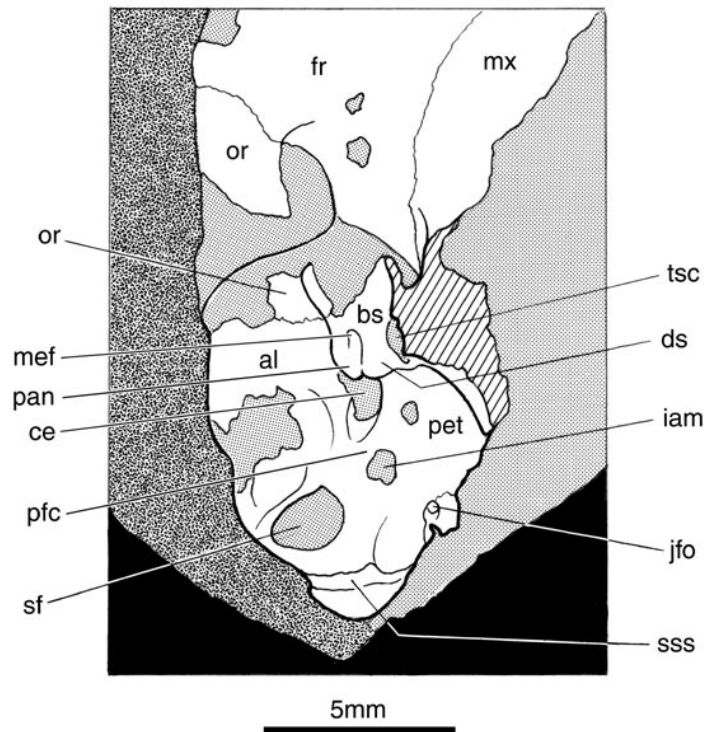
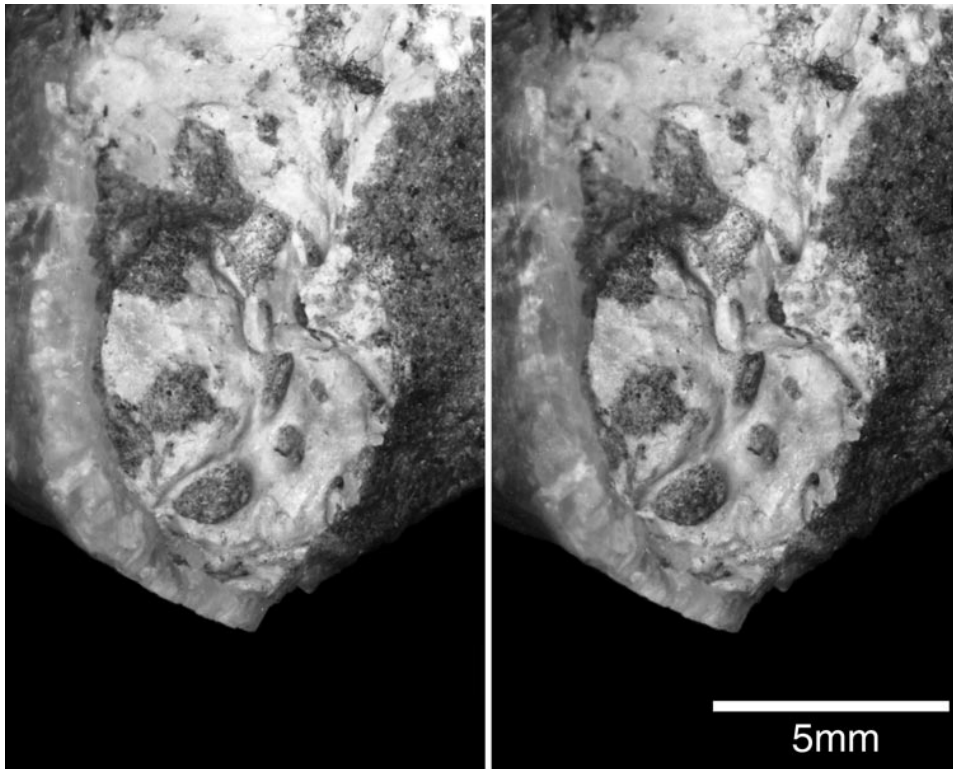
PSS-MAE 128, which is not *Kryptobaatar* but is referred here as an indeterminate multituberculate, conforms to the pattern of the skull base described above. The only substantive exception is that instead of a shallow depression, there is a deep trough on the basioccipital running to the basioccipital-petrosal suture. This unambiguously indicates the endocranial course of the inferior petrosal sinus.

PETROSAL

As was the case in our description of the exterior of the petrosal, when describing the interior, the anterior lamina is considered along with the petrosal proper. The following descriptions are based on the three specimens of *Kryptobaatar* with exposed the endocranial surfaces (i.e., PSS-MAE 123, 124, and 125).

The endocranial surface of the petrosal can be subdivided into four quadrants by two intersecting crests. One crest is the crista petrosa, which runs along the prefacial commissure (“pfc” in fig. 26) and the anterior margin of the subarcuate fossa (“sf” in figs. 25–27); the other crest separates the subarcuate fossa from the internal acoustic meatus (“iam” in figs. 25–27) and continues anteroventrolaterally as the dorsolateral margin of the cavum epiptericum (“ce” in figs. 25B, 26, 27). The crests intersect dorsolateral to the internal acoustic meatus in a rounded eminence. The four quadrants so delimited are identified by their most conspicuous features: the subarcuate fossa, the internal acoustic meatus, the cavum epiptericum, and the anterior lamina (fig. 27).

The subarcuate fossa, which accommodated the paraflocculus of the cerebellum, is a large, deep, subspherical depression that opens into the braincase through an elliptical aperture, the major axis of which is dorsoventrally oriented (figs. 25, 26). The dorsal-most margin of the subarcuate fossa is not preserved or fully prepared in any specimen. Considering the presence of the large vascular groove in the exoccipital already described, it is likely that a groove for the sigmoid sinus was present on the dorsal edge of the subarcuate fossa. A similar structure is present in the skull of multituberculate, n. sp.



(PSS-MAE 126). Along the posteroventral edge of the subarcuate fossa, in the crest separating the subarcuate fossa and the internal acoustic meatus, there is small foramen, the vestibular aqueduct, with a posterodorsally directed groove, interpreted as having housed the endolymphatic duct.

The quadrant housing the internal acoustic meatus is the part that contributes to the floor of the braincase, and it does so in an oblique fashion (figs. 25–27). Medially, the meatal quadrant contacts the basioccipital and exoccipital via a straight parasagittal suture; anteriorly, it cannot be differentiated from the sphenoid complex. Apparently, the sphenoid complex and petrosal are fused endocranially, although a distinct morphological discontinuity that forms the dorsum sellae probably indicates the anterior extent of the petrosal. A cochlear aqueduct is not identifiable in any specimen, and hence the aperture on the back of the promontorium is the perilymphatic foramen, as occurs in monotremes (Kuhn, 1971; Zeller, 1985, 1989, 1991). The posteromedial margin of the meatal quadrant is notched by the small jugular foramen (fig. 26). The internal acoustic meatus is a subcircular depression, although its medial wall is not very tall, and the meatus is continuous medially with the petrosal's contribution to the braincase floor. At the posteromedial edge of the meatus is an anteroventrally directed foramen, probably for the cochlear nerve. Separating this small foramen from the deeper part of the meatus is a low crest that forms the posteromedial margin of a second aperture, probably for the facial and vestibular nerves.

Lateral to the meatal quadrant is the cavum epiptericum (figs. 25–27), the very deep fossa that lodged the trigeminal or semilunar ganglion and provided passage to various nerves and vessels. The cavum opens anteriorly, ventrally, and laterally via several ap-

ertures. The ventral (“fv3” in fig. 25) and lateral openings transmitted branches of the mandibular nerve, and the large, subcircular anterior opening transmitted the trochlear, abducens, ophthalmic, and maxillary nerves, given that the cavum shows the same relationship to the pila antotica (see Sphenoid Complex below) as in monotremes (Kuhn and Zeller, 1987). The anterior opening, the sphenorbital fissure (“sphf” in figs. 25A, 27), probably also transmitted the ramus infraorbitalis of the stapedia artery and the ophthalmic veins (Rougier et al., 1992; Wible and Hopson, 1995). The cavum epiptericum is longer than wide, and its anterior portion is roofed by the laminar, laterally expanded pilae antotica and metoptica, which connect the medial and lateral crests delimiting the trigeminal fossa. Based on PSS-MAE 123, it is apparent that a separate cavum supracochleare for the facial ganglion is lacking in *Kryptobaatar*; the primary facial foramen opens directly into the back of the cavum epiptericum where the facial ganglion would have been located. The secondary exit of the facial nerve from the cavum epiptericum was likely in the posterior part of the cavum's floor, but it was inaccessible to preparation.

The anterior lamina quadrant is the largest and contributes to the side wall of the braincase (figs. 25–27). It is concave in medial view and extends from the subarcuate fossa forward to contact the primary wall of the braincase represented by the pila antotica/orbitosphenoid, which the anterior lamina overlaps laterally. Anterolateral to the subarcuate fossa in the anterior lamina quadrant is a deep, broad, anteroventrally directed sulcus leading into a foramen (“prc” in figs. 25, 27). This is the sulcus and foramen for the prootic sinus, which leads into the prootic canal. As preserved in the skull of PSS-MAE 123 (fig. 25), the foramen for the prootic si-

←

Fig. 26. Stereophotograph of the floor of the endocranium of *Kryptobaatar dashzevegi* PSS-MAE 125 in oblique dorsal view. Gray pattern represents matrix; parallel lines denote breakage. Abbreviations: **al** anterior lamina; **bs** basisphenoid; **ce** cavum epiptericum; **ds** dorsum sellae; **fr** frontal; **iam** internal acoustic meatus; **jfo** jugular foramen; **mef** metoptic foramen; **mx** maxilla; **or** orbitosphenoid; **pan** pila antotica; **pet** petrosal; **pfc** prefacial commissure; **sf** subarcuate fossa; **sss** sulcus for sigmoid sinus; **ts** transverse sinus canal.

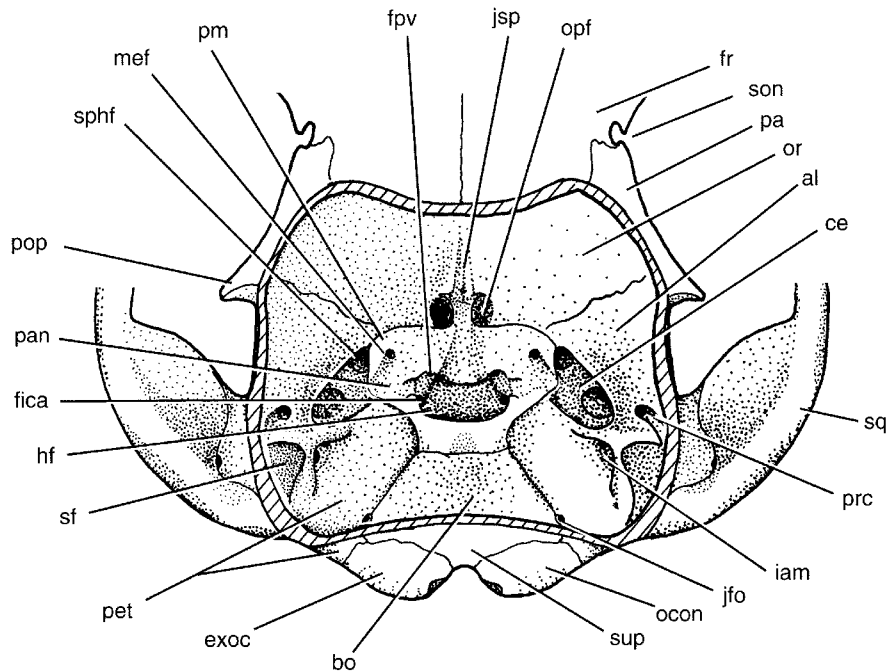


Fig. 27. Reconstruction of the floor of the endocranium of *Kryptobaatar dashzevegi*. Parallel lines represent the cut edge of the braincase. Abbreviations: **al** anterior lamina; **bo** basioccipital; **ce** cavum epiptericum; **ds** dorsum sellae; **exoc** exoccipital; **fica** foramen for internal carotid artery; **fpv** foramen for pituito-orbital vein; **fr** frontal; **hf** hypophyseal fossa; **iam** internal acoustic meatus; **jfo** jugular foramen; **jsp** jugum sphenoidale; **mef** metoptic foramen; **ocon** occipital condyle; **opf** optic foramen; **or** orbitosphenoid; **pa** parietal; **pan** pila antotica; **pet** petrosal; **pm** pila metoptica; **pop** postorbital process; **prc** prootic canal; **sf** subarcuate fossa; **son** supraorbital notch; **sphf** sphenorbital fissure; **sq** squamosal; **sup** supraoccipital.

nus opens at a level ventral to the lower margin of the subarcuate fossa. The anterior lamina in front of the prootic sulcus is very smooth and essentially featureless.

SPHENOID COMPLEX

Given that the hypophyseal or pituitary fossa is universally lodged in the basisphenoid among recent mammals (Starck, 1967), we identify the corresponding part of the sphenoid complex in *Kryptobaatar* as the basisphenoid. The hypophyseal fossa ("hf" in figs. 25, 27) is a deep, hemispherical depression on the skull base that is limited posteriorly by a prominent dorsum sellae, also on the basisphenoid ("ds" in figs. 25, 26). The dorsum sellae forms a steep angle with the floor of the braincase behind it; the dorsum is lower in the midline, and taller and thicker laterally where it becomes confluent with the

ossified pila antotica. Inside the hypophyseal fossa, the carotid foramina open in the posterolateral corner of the floor ("fica" in figs. 25, 27). Laterally on the anterior wall of the hypophyseal fossa, in front of each carotid foramen, there is a small foramen in PSS-MAE 123 ("fpv" in figs. 25, 27) and 125, the only specimens preserving the relevant area. This foramen connects the hypophyseal fossa with the orbitotemporal fossa, and in PSS-MAE 123 it is also connected to the carotid foramen via a distinct sulcus in the lateral floor of the hypophyseal fossa. The external aperture of this foramen is shown on the right side of PSS-MAE 101 (in addition to 123 and 125). Based on our observations of serially sectioned platypuses, as well as Gaupp's (1908) observations of the echidna, we interpret this foramen and sulcus as for the pituito-orbital vein.

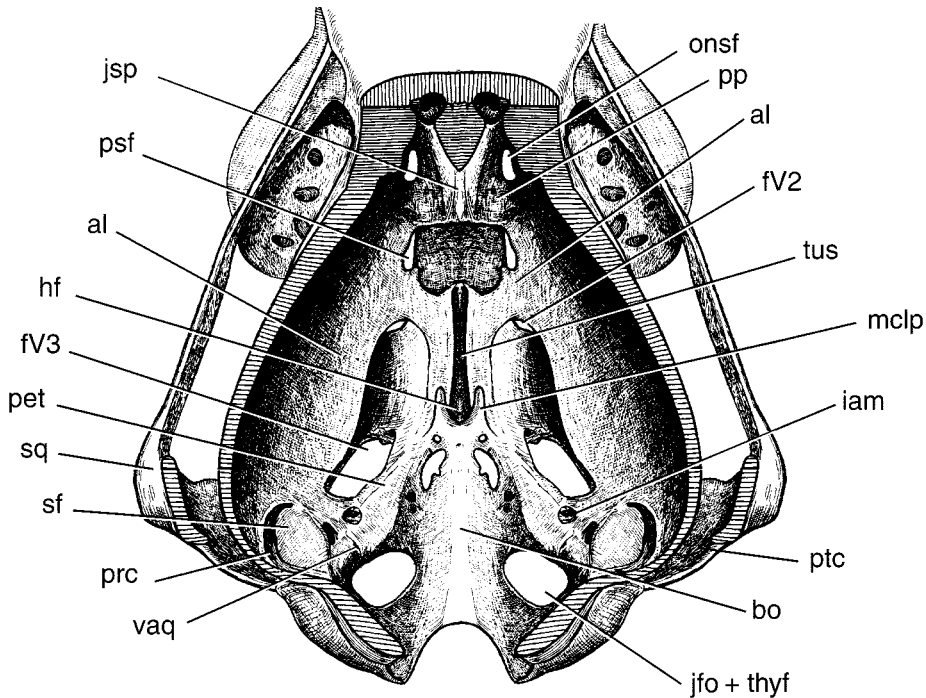


Fig. 28. The floor of the endocranium of the platypus *Ornithorhynchus anatinus* in dorsal view (modified from Zeller, 1989: fig. 6, with the author's permission). Parallel lines represent the cut edge of the braincase. Abbreviations: **al** anterior lamina; **bo** basioccipital; **fv2** foramen for maxillary nerve; **fv3** foramen for mandibular nerve; **hf** hypophyseal fossa; **iam** internal acoustic meatus; **jfo + hyf** confluent jugular and hypoglossal foramina; **jsp** jugum sphenoidale; **mclp** middle clinoid process (ossified remnant of pila antotica); **onsf** orbitonasal foramen; **pet** petrosal; **pp** pila preoptica; **prc** prootic canal; **psf** pseudoptic foramen (for II, III, IV, V₁, VI); **ptc** posttemporal canal; **sf** subarcuate fossa; **sq** squamosal; **tus** tuberculum sellae; **vaq** vestibular aqueduct.

The tall laminar walls forming the sides of the hypophyseal fossa are here considered as the ossified pila antotica ("pan" in figs. 25–27), a component of the primary wall of the braincase (fig. 24A–C). These walls project anteriorly and laterally as broad, winglike structures that connect the primary wall with the dermal elements that form the secondary wall; sutures demarcating the lateral extent of the pila are clearly visible in PSS-MAE 125 (fig. 26). The pila antotica is particularly thick posterodorsally, where in conjunction with the anterior lamina it roofs the cavum epiptericum. Running behind the pila antotica into the cavum epiptericum in *Kryptobaatar* were the trochlear, trigeminal, and abducens nerves, based on the relationships that these structures exhibit in monotremes (fig. 24C; Kuhn and Zeller, 1987; Zeller, 1989). In describing the similarly situated,

ossified pila antotica in other multituberculates, Kielan-Jaworowska et al. (1986), Miao (1988), and Hurum (1998a) have employed the term taenia clino-orbitalis. This term was originally coined by Gaupp (1902, 1908) for the well-developed pila antotica that he encountered in the chondrocranium of the echidna. Gaupp (1908: fig. 56) also applied the term to the remnant of the pila antotica in the adult echidna skull, but the primary usage was for a cartilaginous structure. Consequently, we continue to use the more general term pila antotica rather than the more restricted taenia clino-orbitalis.

Lateral to the hypophyseal fossa, on the laminar extension of the pila antotica, there is a deep trough that leads anteriorly to a sizable round foramen at the level of the anterior margin of the hypophyseal fossa ("mef" in fig. 25–27) that opens externally

into the orbitotemporal fossa (“mef” in fig. 36A). This foramen is present in the three specimens of *Kryptobaatar* with the endocranium exposed as well as in the indeterminate multituberculate (PSS-MAE 128). Miao (1988) interpreted a similarly placed aperture in *Lambdopsalis* as the metoptic foramen, the main occupant of which was the oculomotor nerve. We report here a similar opening in the right orbit of *Kamptobaatar* (ZPAL MgM-I/33). Even though a metoptic foramen is not known for any ontogenetic stage in extant mammals, we accept Miao’s interpretation for *Lambdopsalis* and extend it here for the same structures in *Kryptobaatar*, *Kamptobaatar*, and PSS-MAE 128. As stated above, the metoptic foramen is found in the chondrocranium of most extant sauropsids between the pila antotica and metoptica (fig. 24A; De Beer, 1926, 1937; Bellairs and Kamal, 1981) and is generally considered to have been present in the chondrocrania of the common ancestor of monotremes and therians (Kuhn, 1971; Kuhn and Zeller, 1987). Following this, the bone enclosing the anteromedial aspect of the foramen in *Kryptobaatar* is the ossified pila metoptica (“pm” in figs. 25B, 27).

In amniotes, the two most significant foramina in the interval between the passageways for the optic and trigeminal nerves are the metoptic foramen and the foramen for the abducens nerve (De Beer, 1926, 1937). Although the abducens nerve runs through the prootic foramen in monotremes and many sauropsids (fig. 24A, C), it pierces the base of the pila antotica at the level of the dorsum sellae in various sauropsids (De Beer, 1926, 1937; Säve-Söderburgh, 1947; Oelrich, 1956), and it has been similarly interpreted in various extinct forms, including the primitive non-mammalian cynodont *Thrinaxodon* (Parrington, 1946), the tritylodontid *Oligokyphus* (Kühne, 1956), and the tritheledontid *Diarthrognathus* (Crompton, 1958). The aperture in question in *Kryptobaatar*, however, is placed too far dorsally and forward, at the level of the front of the hypophyseal fossa, to be a foramen for the abducens nerve (figs. 25–27). Therefore, we reconstruct the abducens nerve in *Kryptobaatar* as having entered the cavum epiptericum with the trochlear and trigeminal nerves, posterior to

the pila antotica, and the oculomotor as having entered the orbit via a separate metoptic foramen.

The region anterior to the hypophyseal fossa is damaged in all available specimens, but a full restoration (fig. 27) can be offered based on the fragments preserved in two specimens of *Kryptobaatar* (PSS-MAE 123 and 125; figs. 25, 26) as well as in the indeterminate multituberculate (PSS-MAE 128). Extending forward from the hypophyseal fossa on the midline is a rodlike portion of the sphenoid complex, the tuberculum sellae (“tus” in fig. 25A). It extends anteriorly toward paired, laterally directed projections, the orbital wings or alae orbitales (“ow” in fig. 25B). These wings are part of the orbitosphenoid and represent the ossified pilae opticae. The edge of the wings, the orbitosphenoidal crest, dorsally delimits large, paired foramina that are not preserved intact in any specimen, although they are nearly preserved in PSS-MAE 123 (“opf” in fig. 25). These anterolaterally directed foramina, for the optic nerves and ophthalmic arteries, are situated between the orbital wings and the tuberculum sellae, close to the midline. The portion of the tuberculum sellae directly medial to the optic foramina is grooved transversely by a shallow sulcus, the chiasmatic sulcus for the optic chiasm.

In front of the optic foramina, the braincase floor between the right and left orbital wings is marked by a midline trough of uncertain function, which becomes narrower and shallower rostrally. This midline portion of the sphenoid complex in this region is the yoke or jugum sphenoidale (“jsp” in figs. 25A, 27). The overall orientation of the jugum sphenoidale is anterodorsally. Slightly rostral to the end of the midline trough, the cranial cavity is constricted, demarcating the posterior boundary of the olfactory bulbs. The rostralmost extent of the cranial cavity housing the olfactory bulbs is not prepared or preserved in any available specimens. In the indeterminate multituberculate (PSS-MAE 128), part of the floor in front of the olfactory bulb constriction is preserved on the left side. The surface is smooth, devoid of perforations, and corresponds to the lamina infracribrosa. Laterally, where the lamina infracribrosa contacts the jugum sphenoidale

behind, there is a foramen from which a sizable sulcus runs anterodorsally. This foramen and sulcus are interpreted as for the endocranial portion of the ethmoidal nerve and vessels. None of the available specimens exhibits any indication of an ossified cribriform plate. Our observation should be regarded as provisional, because the preservation of the available specimens hindered the investigation of this region of the endocranium.

In the three specimens of *Kryptobaatar* showing the endocranial surfaces (PSS-MAE 123, 124, and 125) and in the indeterminate multituberculate (PSS-MAE 128), a broad canal connects the right and left sphenorbital recesses, that is, the space medial to the walls demarcating the lateral rims of the sphenorbital fissures. This canal is low on the braincase floor and traverses the primary wall ventral to the tuberculum sellae; a thin wall separates this canal from the hypophyseal fossa (“tsc” in fig. 26). Among living mammals, the transverse canal is in a similar position, crossing the midline immediately anterior to the hypophyseal fossa, and it transmits a vein called the transverse canal vein in some marsupials (Archer, 1976; Marshall et al., 1990; Marshall and Muizon, 1995) and some placentals (McDowell, 1958; MacPhee, 1994). This is the only likely model for the similarly situated canal in *Kryptobaatar* (see fig. 36) and the indeterminate multituberculate.

The occurrence of turbinals or ridges for the turbinals on the appropriate bones in the nasal cavity could not be studied in any of the specimens of *Kryptobaatar* considered in this report. However, the natural nasal endocast of an indeterminate multituberculate from Ukhaa Tolgod (PSS-MAE 134) shows ridges in the maxillary, nasal, and frontal portions of the nasal cavity (Rougier et al., 1997b). These ridges correlate closely with similar structures present in living mammals supporting the turbinals (Paulli, 1900; Moore, 1981; Hillenius, 1994). PSS-MAE 134 confirms the presence of ethmoturbinals and nasoturbinals, and a crest running parallel to the sulcus for the nasolacrimal duct suggests the existence of maxilloturbinals. Also, fragments of turbinals appear to be preserved. Among multituberculates, turbinal ridges and fragments have been reported pre-

viously for *Lambdopsalis* (Miao, 1988) and *Nemegtbaatar* (Hurum, 1994), and fragments only for *Chulsanbaatar* (Hurum, 1994). Among Mesozoic mammaliaforms, turbinals have been preserved in the docodontid *Halldanodon* (Lillegraven and Krusat, 1991) and the zalambdalestid *Barunlestes* (Kielan-Jaworowska and Trofimov, 1980).

MANDIBLE

As is typical for the lower jaws or mandible in multituberculates, that of *Kryptobaatar* has a robust, deep horizontal ramus and an ascending ramus that is proportionally smaller. Housed in the lower jaw are five teeth: an enlarged, procumbent incisor (i1), two premolars (p3–p4) with the mesial one greatly reduced, and two molars (m1–2). Both lower jaws are complete and in place in PSS-MAE 101 (fig. 14). Only the left one is preserved in PSS-MAE 113; it is well preserved except that the ventral margin under the incisor alveolus is missing (fig. 5). We describe the lower jaw first in lateral and then in medial views; the terminology used follows that of Gambaryan and Kielan-Jaworowska (1995) unless noted otherwise.

In lateral view (figs. 10, 12, 29), the alveolus of the incisor is separated from p3 by a long, dorsally concave diastema. In PSS-MAE 113, in which the ventral margin of the lower jaw is broken, the root of the incisor can be traced posteriorly at least to the middle of m1. The mental foramen (“mf” in fig. 12) is positioned in front of the lateral bulge over the roots of the premolars; it lies closer to the superior than to the inferior margin of the lower jaw. In PSS-MAE 101 (fig. 10), it is even closer to the superior margin and to the lateral bulge over the premolar roots than in PSS-MAE 113 (fig. 29). The mental foramen is quite large and faces anterolaterally.

The area on the horizontal ramus between the lateral bulge over the premolar roots and the base of the coronoid process is very short and concave. This is the masseteric fovea (“mafo” in fig. 12), which Gambaryan and Kielan-Jaworowska (1995) interpreted as for the pars anterior of the medial masseter muscle. As noted by these authors, the masseteric fovea in *Kryptobaatar* is confluent posteriorly with the masseteric fossa. The masse-

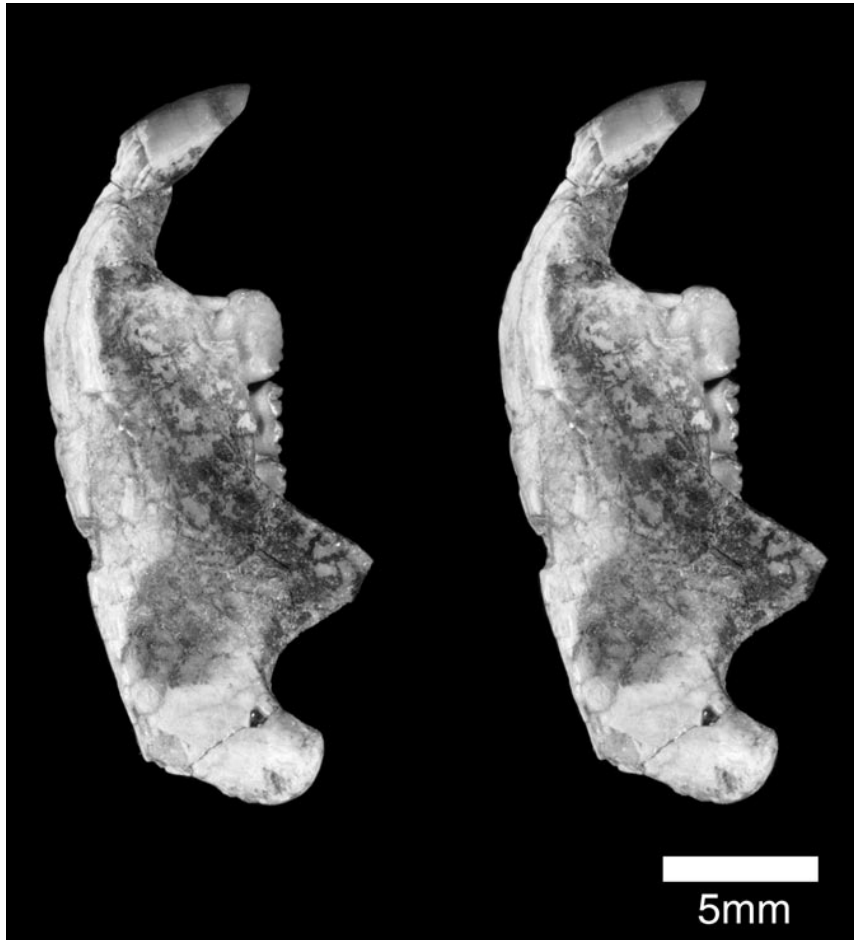


Fig. 29. Stereophotograph of the left lower jaw of *Kryptobaatar dashzevegi* PSS-MAE 113 in lateral view.

teric fossa (“maf” in fig. 12) is shallow, broad, and subdivided by a low, oblique ridge running anteroventrally from the condyle, which we call the condyloid crest following the terminology used for the dog (Evans and Christensen, 1979). The portion of the masseteric fossa anterodorsal to the condyloid crest is larger and deeper than the posteroventral one; these two fossae probably accommodated different parts of the masseter muscle (see Gambaryan and Kielan-Jaworowska, 1995). The anteroventral margin of the masseteric fossa is formed by the masseteric crest (“mc” in fig. 10), a well-developed ridge that is concave posteriorly and confluent posteriorly with the weaker masseteric line, as seen in PSS-MAE 101. The

masseteric line is nearly straight and is continuous posteriorly with the nearly vertical, straight rear edge of the condylar process.

The coronoid process (“cor” in figs. 8, 16) originates below the alveolar margin and its anterior extent lies at the back edge of the anterior root of m1 (fig. 29). Between the lateral alveolar margin and the coronoid process there is a trough running obliquely posterodorsally, the temporal groove (“tg” in fig. 10), which is said to be for the pars anterior of the temporalis muscle (Gambaryan and Kielan-Jaworowska, 1995). The coronoid process is subtriangular and only slightly higher than the condyle and the molar cusps (fig. 29). The angle of the anterior border of the coronoid process relative to the

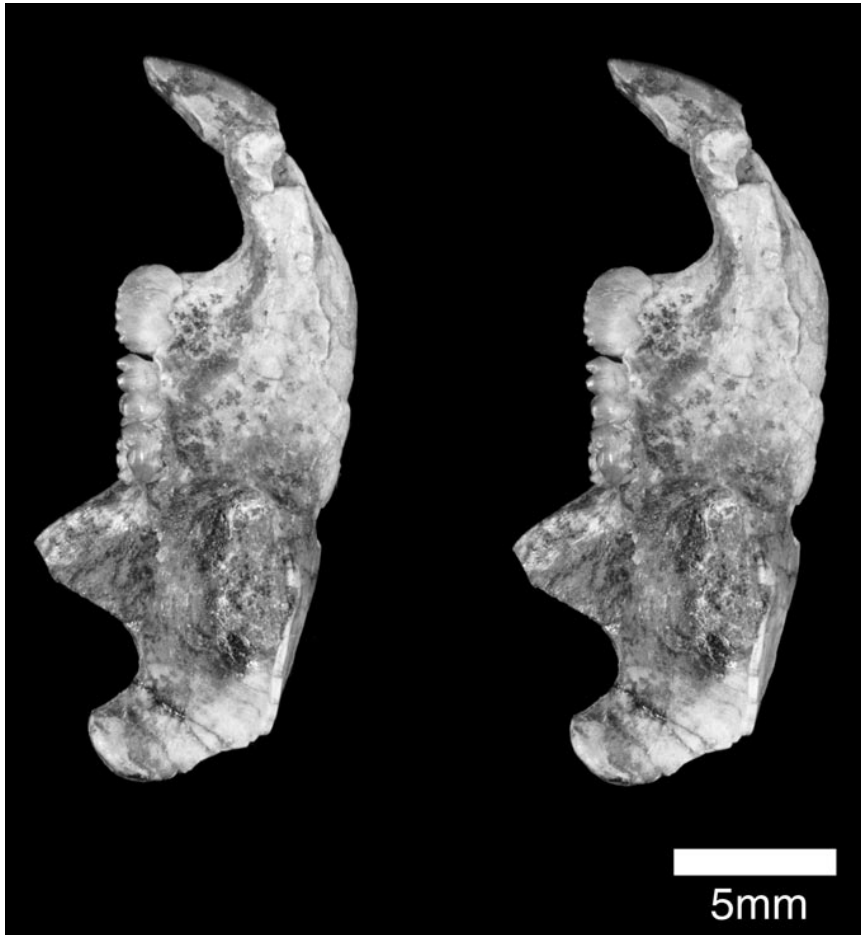


Fig. 30. Stereophotograph of the left lower jaw of *Kryptobaatar dashzevegi* PSS-MAE 113 in medial view.

toothrow is approximately 60° (contra Kielan-Jaworowska and Hurum, 1997, who report it as less than 45°). A sharp crest connects the tip of the coronoid process with the condyle, delimiting a shallow mandibular notch. The condyle (“con” in figs. 6, 16) is robust, lacks a distinct neck, and, as noted by Kielan-Jaworowska and Hurum (1997), is positioned at approximately the same level as the molars. The articular surface on the condyle is teardrop-shaped and directed posterodorsally. In posterior view, the articular surface is distributed symmetrically with respect to the plane of the dorsal border of the ascending ramus. This is in contrast to the condition in most mammals in which there

is an asymmetrical distribution (Crompton and Hylander, 1986).

In medial view (fig. 30), the area of the symphysis is only visible in the left lower jaw of PSS-MAE 113. Most of this surface has been lost, but enough remains to characterize the symphysis as vertical and narrow (“msy” in fig. 14). The dorsal surface of the diastema forms a roughly horizontal shelf that narrows posteriorly; the posterior narrowing of this shelf is a result of the oblique orientation of the alveoli of the premolars and molars in the lower jaw. The most distinctive feature of the medial side of the mandible is the very deep, enlarged pterygoid fossa located behind the alveolar pro-

cess. This fossa, for the medial pterygoid muscle (Gambaryan and Kielan-Jaworowska, 1995), is delimited anteriorly by the pterygoid crest (“pc” in fig. 16), which extends posteroventrally as the medial margin of the prominent pterygoid shelf. The dorsal margin of the pterygoid fossa is formed by a longitudinal, inconspicuous elevation, the transversal elevation, and the posterior margin is formed by a crest that is the medial equivalent of the condyloid crest described on the lateral surface. Continuing forward from the pterygoid fossa just behind the level of m2 is the mandibular canal. Behind the

pterygoid fossa is a concave area below the condyle, the pterygoid fovea for the lateral pterygoid muscle (Gambaryan and Kielan-Jaworowska, 1995). The fovea is both smaller and shallower than the pterygoid fossa and is delimited posteriorly by the posterior margin of the lower jaw.

Another measure of the lower jaw in multituberculates reported by Kielan-Jaworowska and Hurum (1997) is the angle between the lower margin of the mandible and the occlusal surface of the molars. In *Kryptobaatar*, this angle is very low, approximately 11°.

VASCULAR RECONSTRUCTIONS

Comprehensive reconstructions of the cranial vascular system in multituberculates were first attempted by Kielan-Jaworowska et al. (1984, 1986). These authors surveyed the relevant osteology in the then currently known Mongolian Late Cretaceous taxa, but they relied most heavily on cranial remains, endocasts, and sectioned skulls of two forms, *Nemegtbaatar* and *Chulsanbaatar*, along with isolated petrosals tentatively referred to the Late Cretaceous North American “*Catopsalis*” *joyneri* and *Mesodma thompsoni* (see Wible and Hopson, 1995). Kielan-Jaworowska et al. (1984, 1986) discovered that most of the presumed vascular channels in the multituberculates also occurred in other Mesozoic mammalian morphs, with Mammalian morphs being the clade comprising the last common ancestor of Tritylodontidae and Mammalia plus all descendants (Rowe, 1988). Given that remnants of these channels transport vessels in extant mammals, Kielan-Jaworowska et al. (1984, 1986) were able to offer reconstructions of the major cranial arteries and veins, including the dural sinuses, in the multituberculates. In general, these reconstructions have been followed by subsequent researchers and applied to other Mesozoic mammalian morphs, although some refinements have been proposed by Wible (1989) and co-workers (Rougier et al., 1992; Hopson and Wible, 1993; Wible and Hopson, 1995). With these refinements, vascular reconstructions have been offered for the following multituberculates: the Paleocene tae-

niolabidid *Lambdopsalis* (Miao, 1988), a generalized “taeniolabidoid” (Rougier et al., 1992), and “*Catopsalis*” *joyneri* and *Mesodma thompsoni* (Wible and Hopson, 1995).

The vascular reconstructions proposed here for *Kryptobaatar dashzevegi* (figs. 36B, 37B) are indebted to those already published, because the channels that previous authors identified in various multituberculates are, with minor amendments, repeated in *Kryptobaatar*. The basis for the reconstructions and the terminology employed is our own published and unpublished studies of the cranial vessels occurring in extant mammals (Wible, 1984, 1986, 1987, 1989, 1990; Rougier et al., 1992; Wible and Hopson, 1995; and references cited therein).

VEINS

In extant mammals, the veins of the head can be divided into the intracranial dural sinus system and the extracranial veins draining the dural sinuses and superficial structures. Although the components of the dural sinus system are conservative among extant mammals, the extracranial veins draining it vary considerably (Gelderen, 1924; Wible, 1990; Wible and Hopson, 1995). In monotremes, the principal drainage is through the prootic canal and foramen magnum (Hochstetter, 1896), whereas it is through the postglenoid foramen and foramen magnum in marsupials (Gelderen, 1924; Archer, 1976) and through the postglenoid and internal jug-

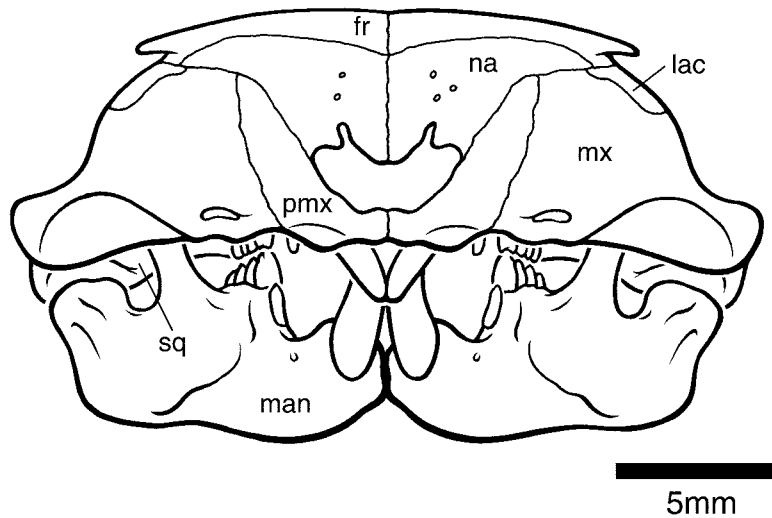


Fig. 31. Reconstruction of the skull of *Kryptobaatar dashzevegi* in anterior view. Abbreviations: **fr** frontal; **lac** lacrimal; **man** mandible; **mx** maxilla; **na** nasal; **pmx** premaxilla; **sq** squamosal.

ular foramina and foramen magnum in most placentals (Gelderen, 1924; Butler, 1967).

DURAL SINUS SYSTEM

The dural sinus system reconstructed for *Kryptobaatar* resembles in most regards that proposed for *Nemegtbaatar*, *Chulsanbaatar* (Kielan-Jaworowska, 1986; Kielan-Jaworowska et al., 1986), and *Lambdopsalis* (Miao, 1988). Included are superior (dorsal) sagittal, transverse, sigmoid, and prootic sinuses; the first three are nearly ubiquitous in their incidence among extant mammals (Gelderen, 1924), whereas the prootic sinus is known only for adult monotremes and some adult marsupials (Wible, 1990; Wible and Hopson, 1995). The evidence for these dural sinuses in *Kryptobaatar* is in the form of grooves on the endocranial surfaces and molds of vascular channels on the endocasts that resemble those occurring in extant mammals. The superior sagittal and transverse sinuses are visible in dorsal view in the exposed endocast of PSS-MAE 113; the superior sagittal sinus lies between the right and left cerebral hemispheres, and the paired transverse sinuses are between the cerebral hemispheres and the vermis (central lobe) of the cerebellum. Evidence for the sigmoid and prootic sinuses, the end distributaries of the transverse sinus, is found on the specimens

showing the endocranial surfaces. The prootic sinus is indicated by a groove and foramen into the prootic canal in the anterior lamina quadrant (figs. 25, 27), resembling those structures in monotremes (Wible and Hopson, 1995). The sigmoid sinus is indicated by grooves on the petrosal and exoccipital (fig. 26), and it is apparent that the sinus left the cranial cavity via the foramen magnum based on the extremely reduced size of the jugular foramen and the sulcus preserved in PSS-MAE 125 (fig. 26). This pattern is also clearly shown on the endocast of an undescribed skull of a new species of Mongolian Late Cretaceous multituberculate (PSS-MAE 126). *Kryptobaatar* shows no indication of a tentorial sinus, described as draining into the prootic sinus from in front in *Chulsanbaatar* and *Nemegtbaatar* (Kielan-Jaworowska et al., 1986).

Other major components of the dural sinus system that are ubiquitous among extant mammals are the cavernous sinus, the major venous pool in the cavum epiptericum, and its two principal conduits, the inferior (ventral) petrosal sinus (petrobasilar sinus) and the ophthalmic veins (Shindo, 1915; Gelderen, 1924). The cavernous sinus and ophthalmic veins are not indicated in *Kryptobaatar*, but were likely present, with the ophthalmic veins entering the cavernous sinus

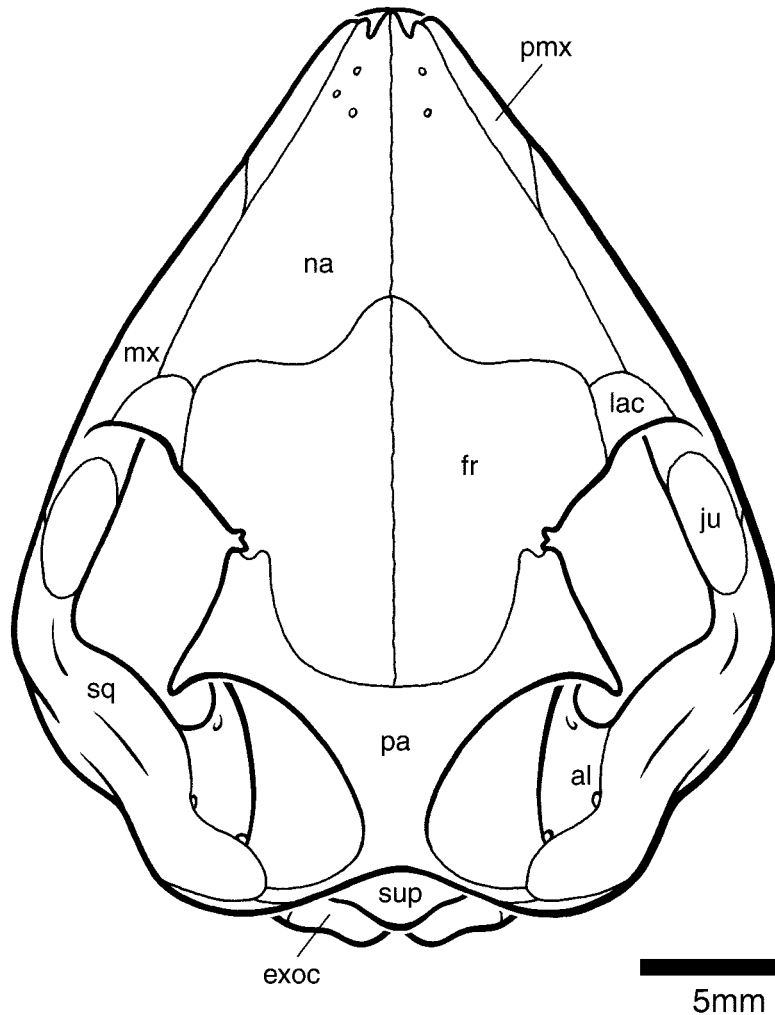


Fig. 32. Reconstruction of the skull of *Kryptobaatar dashzevegi* in dorsal view. Abbreviations: **al** anterior lamina; **exoc** exoccipital; **fr** frontal; **ju** jugal; **lac** lacrimal; **mx** maxilla; **na** nasal; **pa** parietal; **pmx** premaxilla; **sq** squamosal; **sup** supraoccipital.

via the sphenorbital fissure. The course of the inferior petrosal sinus is indicated by a shallow sulcus on the endocranial surface of the basioccipital–petrosal suture in PSS-MAE 123 (fig. 25) and by a trough in the same place in the indeterminate multituberculate PSS-MAE 128. Similarly situated sulci for the inferior petrosal sinus are found in many extant mammals, including both monotremes (Hochstetter, 1896; Kuhn, 1971; Zeller, 1989). Given the small size of the jugular foramen in *Kryptobaatar*, we think that the inferior petrosal sinus left the cranial cavity via the foramen magnum as vertebral veins

(“vv” in fig. 37B), as occurs in both monotremes (Hochstetter, 1896). A transverse groove on the back of the dorsum sellae in PSS-MAE 123 (fig. 25) and 124 likely held the posterior intercavernous sinus, as in the dog (Evans and Christensen, 1979) and various marsupials (Archer, 1976); this groove opens into the area of the sulcus for the inferior petrosal sinus along the basioccipital–petrosal suture.

LATERAL HEAD VEIN

In addition to the venous drainage from the sigmoid and inferior petrosal sinuses ex-

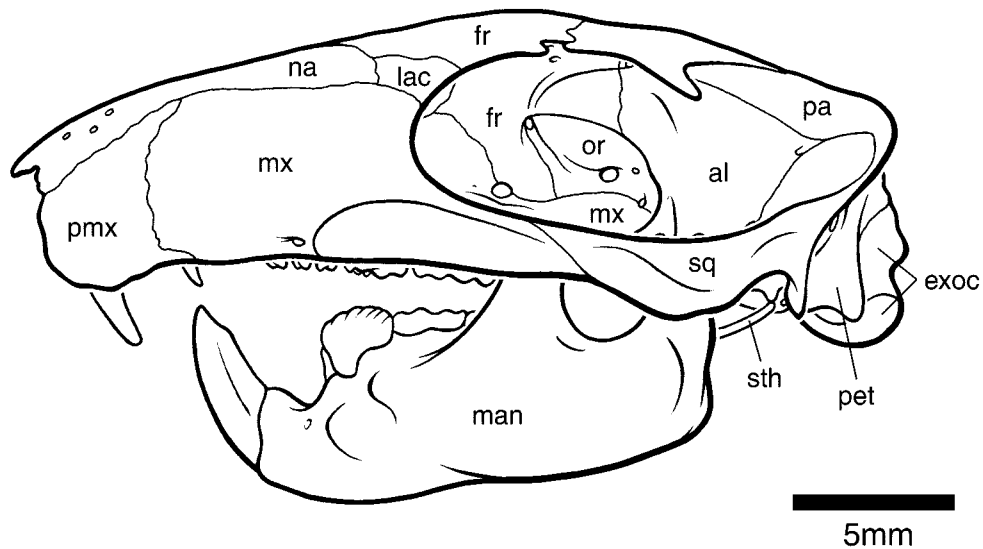


Fig. 33. Reconstruction of the skull of *Kryptobaatar dashzevegi* in lateral view. Abbreviations: **al** anterior lamina; **exoc** exoccipital; **fr** frontal; **lac** lacrimal; **man** mandible; **mx** maxilla; **na** nasal; **or** orbitosphenoid; **pa** parietal; **pet** petrosal; **pmx** premaxilla; **sq** squamosal; **sth** stylohyal.

iting the skull via the foramen magnum, the other major egress for the dural sinuses in *Kryptobaatar* was via the prootic canal. As in monotremes and some marsupials (Wible, 1990; Wible and Hopson, 1995), the prootic sinus in *Kryptobaatar* (“ps” in fig. 37B) drained into the lateral head vein (“lhv” in fig. 37B) in the middle-ear cavity through the prootic canal, which in extant taxa forms in the posterior aspect of the prootic foramen in the primary braincase wall (fig. 24A–C). Judging from the size of the endocranial aperture of the prootic canal (figs. 25, 27), the lateral head vein was well developed in *Kryptobaatar*; the tympanic aperture of the prootic canal is partially hidden within a recess. The intratympanic course of the lateral head vein (fig. 37B) was posteromedially, dorsal to the facial nerve. The vein then continued ventrally into the neck as the internal jugular vein. The lateral head vein probably did not leave the tympanic cavity with the facial nerve through the stylomastoid notch, contra Kielan-Jaworowska et al. (1986) and Miao (1988), but had a separate, more medial exit (Rougier et al., 1992; Wible and Hopson, 1995). Whether a post-trigeminal vein was present in *Kryptobaatar* is uncertain, although we have reconstructed one here (“ptv” in figs. 36B, 37B). Along with the

prootic sinus, the post-trigeminal vein is the other major tributary of the lateral head vein in the echidna, draining posteriorly from the cavernous sinus (Wible and Hopson, 1995); we have observed a small vein in a similar position accompanying the ramus inferior of the stapedial artery in the juvenile platypus described by Zeller (1989). We think that the ramus inferior was present in *Kryptobaatar* (see below), and a post-trigeminal vein has been reconstructed accompanying that artery in other multituberculates by Wible and Hopson (1995). However, given the absence of this vein in therians, without specific osteological evidence for it, the presence of the post-trigeminal vein in *Kryptobaatar* and other multituberculates is equivocal.

TRANSVERSE CANAL VEIN

A canal in front of the hypophyseal fossa connecting the right and left orbitotemporal regions is occupied among living mammals by a large vein known as the transverse canal vein (McDowell, 1958; Archer, 1976). Given that a similar canal is present in specimens of *Kryptobaatar* (figs. 26, 36A) and in PSS-MAE 128, we restore that vessel here (“tcv” in fig. 36B). Judging from the size of the

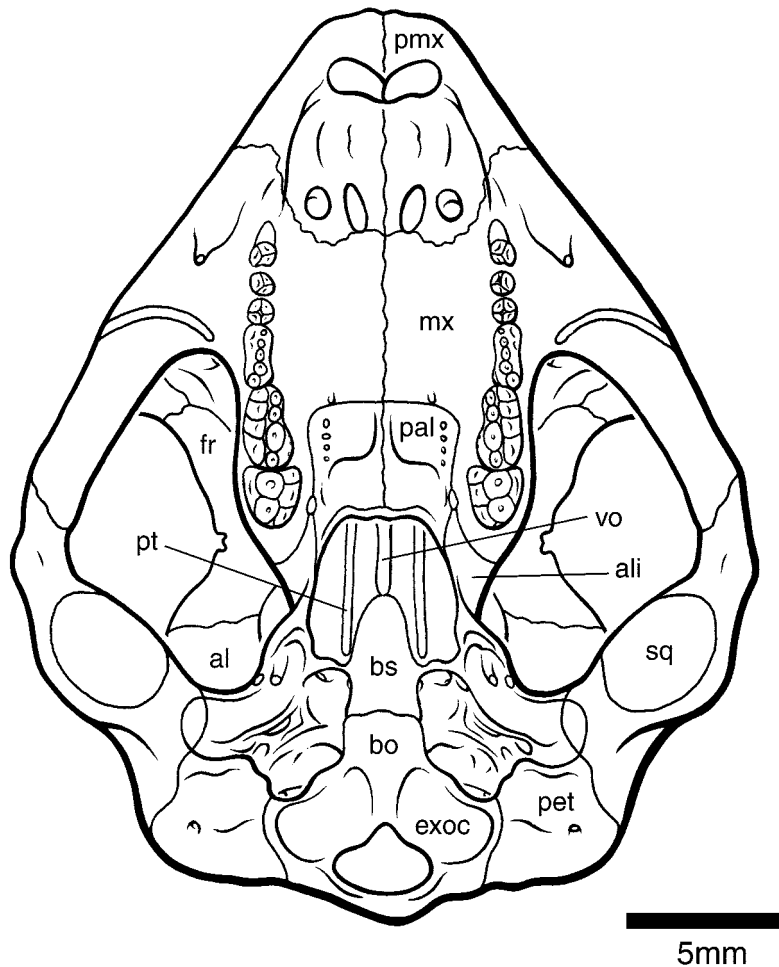


Fig. 34. Reconstruction of the skull of *Kryptobaatar dashzevegi* in ventral view. Abbreviations: **al** anterior lamina; **ali** alisphenoid; **bo** basioccipital; **bs** basisphenoid; **exoc** exoccipital; **fr** frontal; **mx** maxilla; **pal** palatine; **pet** petrosal; **pmx** premaxilla; **pt** pterygoid; **sq** squamosal; **vo** vomer.

transverse canal, the vein in *Kryptobaatar* was a substantial one.

PITUITO-ORBITAL VEIN

A vein to the pituitary gland from the orbital sinus, passing through the primary braincase wall, is known for various sauropods (Bruner, 1907; Bellairs and Kamal, 1981). Among mammals, monotremes have a similar vein (Gaupp, 1908), which in the platypus exits the hypophyseal fossa via the carotid foramen (personal obs.). *Kryptobaatar* has a foramen in the anterolateral wall of the hypophyseal fossa connecting to the or-

bitotemporal fossa, which in one specimen (PSS-MAE 123) leads into a sulcus running posteriorly to the carotid foramen (fig. 25). This arrangement resembles that which we have observed in the platypus. Consequently, we restore the pituito-orbital vein in this foramen in *Kryptobaatar*.

VEINS OF ASCENDING, ORBITOTEMPORAL, AND POSTTEMPORAL CANALS

Veins likely also accompanied at least some of the major arteries passing through the lateral braincase wall in *Kryptobaatar* (fig. 36B). Following a model proposed by

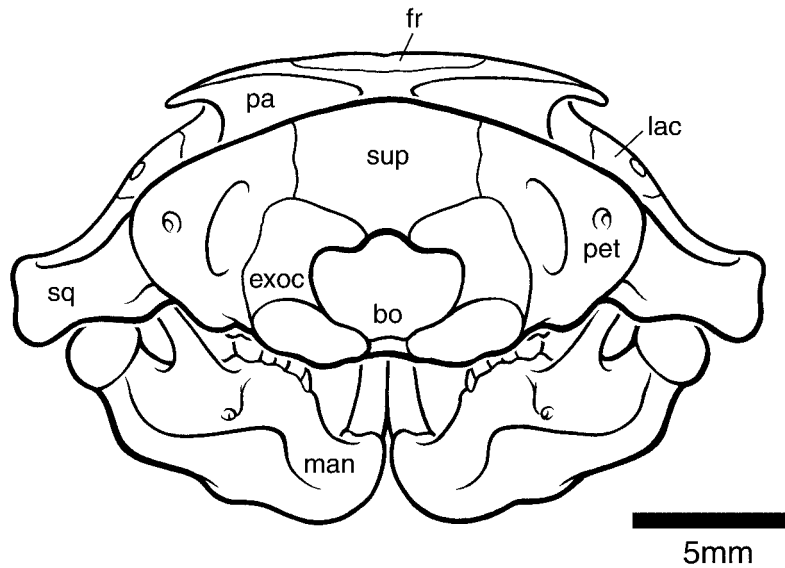


Fig. 35. Reconstruction of the skull of *Kryptobaatar dashzevegi* in posterior view. Abbreviations: **bo** basioccipital; **exoc** exoccipital; **fr** frontal; **lac** lacrimal; **man** mandible; **pa** parietal; **pet** petrosal; **sq** squamosal; **sup** supraoccipital.

Watson (1911, 1920), various authors (e.g., Kermack et al., 1981) have reconstructed veins as the sole occupants of the ascending, orbitotemporal, and posttemporal canals in Mesozoic mammaliaforms. However, Kielan-Jaworowska et al. (1984, 1986) argued effectively, on the basis of the anatomy of extant mammals, that arteries and not veins were the primary occupants of these canals in multituberculates and other Mesozoic synapsids (see also Wible, 1989). Following the model of Kielan-Jaworowska et al. (1984, 1986), we reconstruct in *Kryptobaatar* venae committantes with the ramus superior, ramus supraorbitalis, and arteria diploëtica magna in the ascending, orbitotemporal, and posttemporal canals, respectively (fig. 36B). These veins drained from the orbit to the middle ear and occiput, and they likely were substantial, as evidenced by the preserved endocast of the orbitotemporal canal showing two subequal vessels in the undescribed skull of a new species of Mongolian Late Cretaceous multituberculate (PSS-MAE 126).

SUBARCUATE FENESTRATION

In *Nemegtbaatar* and *Chulsanbaatar*, Kielan-Jaworowska et al. (1986) identified an-

other vascular canal between the subarcuate fossa and the posttemporal canal, which in the embryos of some extant bats and elephant shrews transmits a venous connection between the dural sinuses and the mastoid emissary system. These authors also reported a minute fenestration of the subarcuate fossa in "*Catopsalis*" *joyneri*. Luo (1989) found a large fenestration in *Ptilodus montanus* and *Mesodma*, and he (1996) proposed this condition as a synapomorphy of ptilodontids and eucosmodontids. In *Kryptobaatar*, the subarcuate fossa is very deep, hindering identification of a subarcuate fenestration; nevertheless, as far as we can tell, such an opening is lacking.

ARTERIES

In extant mammals, three major paired arteries supply blood to the head: the internal carotid, the external carotid, and the vertebral. In most forms, the internal carotid and vertebral supply the brain, whereas the external carotid along with the stapedial artery, the principal extracranial branch of the internal carotid, supply the meninges and superficial structures (Tandler, 1899, 1901). However, in the echidna, marsupials, and certain

placentals (e.g., xenarthrans, carnivorans, ungulates), the stapedia artery is lacking and most or all of its end branches are annexed to the external carotid (Bugge, 1978, 1979; Wible, 1984, 1987).

INTERNAL CAROTID ARTERY

In extant mammals, the internal carotid artery has an extracranial course ventral to the basicranium en route to the carotid foramen, which opens endocranially posterolateral to the hypophysis (pituitary). Both the position of the extracranial course and the foramen vary. The artery's course is either on the promontorium (transpromontorial), through the substance of the tympanic wall (perbullar), or medial to the tympanic wall (extrabullar); additionally, the extracranial course of the artery is not always indicated by a groove or canal (Wible, 1986). The carotid foramen is either within the basisphenoid or between the basisphenoid and petrosal (De Beer, 1937), and its endocranial aperture is either within the hypophyseal fossa or posterolateral to it.

In *Kryptobaatar* ("ica" in fig. 37B), the occupant of the well-developed groove on the anterior half of the promontorium, the canal between the petrosal, alisphenoid, and pterygoid, and the endocranial foramen within the hypophyseal fossa was the internal carotid artery, vein, and nerve. Among extant mammals, similar transpromontorial grooves are found only in certain placentals (e.g., lipotyphlans, aardvarks) and, with but one exception, are occupied by the internal carotid artery along with its companion vein and sympathetic nerve (Wible, 1986). The exception occurs in some strepsirhine primates, in which the artery is lost and the nerve is the principal occupant of the transpromontorial groove (Conroy and Wible, 1978). However, given that this is an unusual occurrence among extant mammals, we deem it more likely that both the internal carotid artery and nerve were present in *Kryptobaatar*. Additionally, the connections and sizes of the various sulci on the promontorium in *Kryptobaatar* strongly support a vascular interpretation. The internal carotid artery was likely not the sole supplier of blood to the brain in *Kryptobaatar*, given that the vertebral artery

is present in extant monotremes, marsupials, and the vast majority of placentals (Hochstetter, 1896; Tandler, 1899, 1901; Gillilan, 1972), with cetaceans being an exception (McFarland et al., 1979).

STAPEDIA ARTERY

During development in all but one of the extant mammals investigated, a well-developed stapedia artery arises from the extracranial portion of the internal carotid and sends branches with the trigeminal nerve (Tandler, 1902; Wible, 1984, 1987); the one exception is the echidna, in which the stapedia artery apparently does not form and the end branches accompanying the trigeminal nerve are supplied through the external carotid (Hochstetter, 1896). In placentals, there are two major branches of the embryonic stapedia system: the ramus superior, supplying a ramus supraorbitalis which accompanies the ophthalmic nerve, and the ramus inferior, supplying a ramus infraorbitalis and mandibularis in company with the maxillary and mandibular nerves, respectively (Tandler, 1902; Wible, 1984, 1987). The ramus superior fails to form in marsupials and is a late embryological addition in the platypus that does not extend rostrally as far as the ophthalmic nerve (Wible, 1984, 1987). The embryonic stapedia system is retained in few adult mammals, and in most, at least one of the end branches of the stapedia artery is annexed to a branch of the external carotid (Tandler, 1899, 1901; Bugge, 1974; Wible, 1984, 1987). In fact, the main stem of the stapedia (proximal stapedia) is retained only in the adult platypus and certain adult placentals (e.g., lipotyphlans, scandentians) (Tandler, 1899; Bugge, 1974; Wible, 1987). The two principal sites of anastomosis between the external carotid and stapedia systems are the maxillary artery, which connects to the ramus inferior of the stapedia below the mandibular nerve exit, and the arteria diploëtica magna, which connects to the ramus superior of the stapedia through the posttemporal canal (Wible, 1987).

Kryptobaatar has grooves, canals, and foramina that indicate the presence of a well-developed stapedia system, including the proximal stapedia artery, ramus inferior, ra-

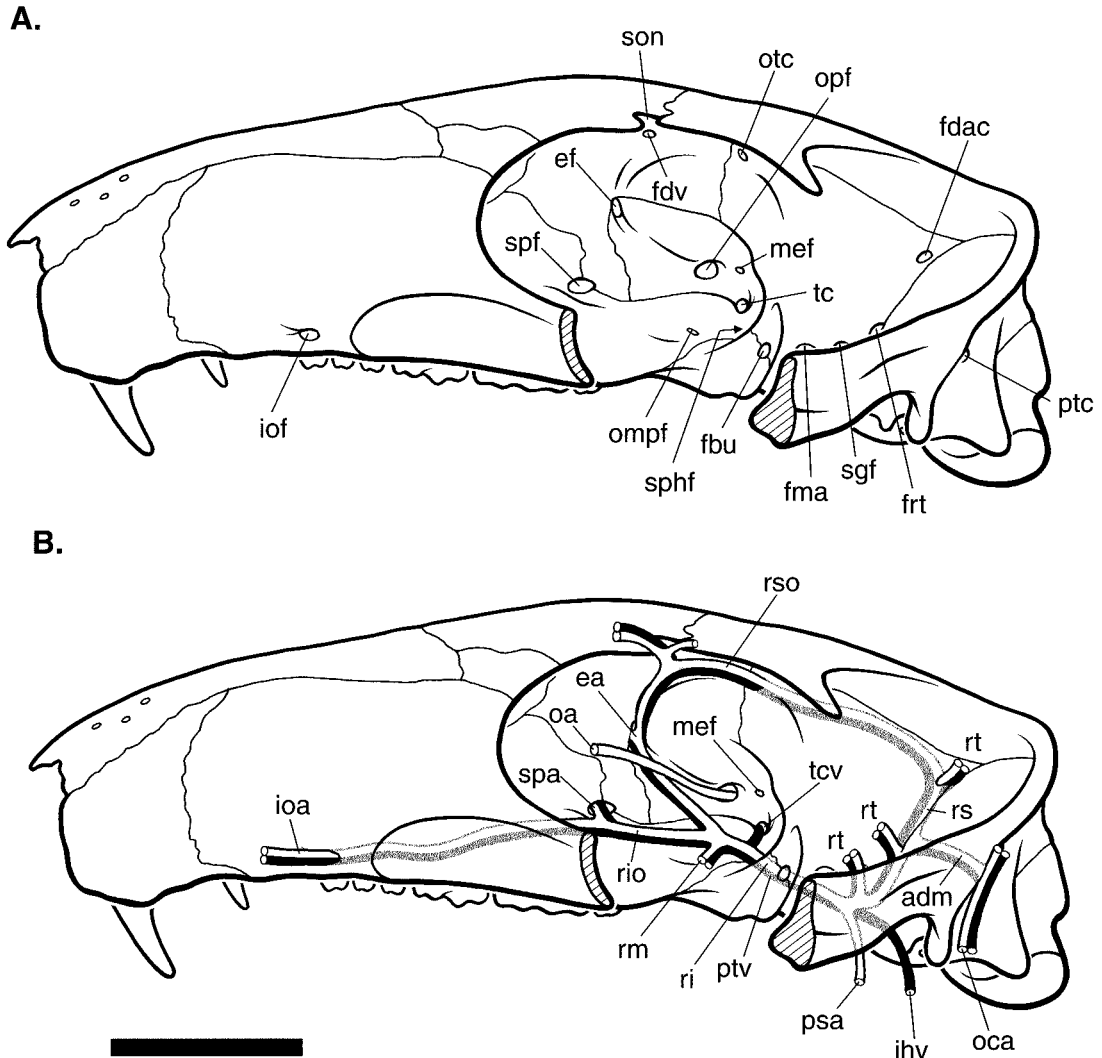


Fig. 36. Reconstruction of the skull of *Kryptobaatar dashzevegi* in left lateral view (A) with the major cranial arteries (white outline) and veins (black) added (B). Zygomatic arch is cut to show vessels in the floor of the orbit. Vessels in shadow pass through intramural canals, with the exception of the part of the ramus superior immediately rostral to the dorsalmost ramus temporalis branch which is endocranial. Abbreviations: **adm** arteria diploëtica magna (and accompanying vein); **ea** ethmoidal artery (and accompanying vein); **ef** ethmoidal foramen; **fbu** foramen buccinatorium; **fdac** foramen of dorsal ascending canal; **fdv** foramen for frontal diploic vein; **fma** foramen masticatorium; **frt** foramen for ramus temporalis; **ioa** infraorbital artery (and accompanying vein); **iof** infraorbital foramen; **ihv** lateral head vein; **mef** metoptic foramen (which transmitted pituito-orbital vein); **oa** ophthalmic artery; **oca** occipital artery (and accompanying vein); **ompf** orbital opening of minor palatine foramen; **opf** optic foramen; **otc** orbitotemporal canal; **psa** proximal stapelial artery; **ptc** posttemporal canal; **ptv** post-trigeminal vein; **ri** ramus inferior; **rio** ramus infraorbitalis (and accompanying vein); **rm** ramus mandibularis (and accompanying vein); **rs** ramus superior (and accompanying vein); **rso** ramus supraorbitalis (and accompanying vein); **rt** ramus temporalis (and accompanying vein); **sgf** supraglenoid foramen; **son** supraorbital notch; **spa** sphenopalatine artery (and accompanying vein); **spf** sphenopalatine foramen; **sphf** sphenorbital fissure; **tc** transverse canal; **tcv** transverse canal vein.

mus superior, and arteria diploëtica magna (figs. 36, 37). The proximal stapedial artery occupied the groove on the promontorium that runs posterolaterally from the groove for the internal carotid artery toward the fenestra vestibuli (“psa” in fig. 37B). In extant mammals, grooves on the promontorium directed at the fenestra vestibuli invariably contain the proximal stapedial artery, but such grooves are only found in some placentals retaining that artery in the adult (e.g., lipotyphlans; Wible, 1987). From the rim of the fenestra vestibuli, the proximal stapedial artery in *Kryptobaatar* ran through what appears to be a bicurrate stapes (Rougier et al., 1996c); this is the artery’s course in the placentals that retain it, but in the platypus the artery runs posterodorsal to the columnar stapes (Wible, 1987).

Two canals lateral to the fenestra vestibuli in *Kryptobaatar* indicate that beyond the stapes the proximal stapedial divided into the ramus superior and the ramus inferior (“rs” and “ri” in figs. 36B, 37B), as occurs in the platypus and certain placentals (Wible, 1987). The canal for the ramus inferior in *Kryptobaatar* is directed anteriorly and lies dorsal to the epitympanic recess on the in-folded lateral flange. Posteriorly, this canal is confluent with the canal for the facial nerve, and anteriorly it presumably opens into the cavum epiptericum. In extant mammals, similarly situated canals are found in the echidna and certain placentals (e.g., scandentians, macroscelidids). In the placentals, the main occupant is arterial, with the ramus inferior in front and sometimes the proximal stapedial behind; the course of the facial nerve is very close to the arterial canal, and, in fact, in macroscelidids, the facial nerve and proximal stapedial share a canal (MacPhee, 1981). In the echidna, in which the ramus inferior is lacking, the main occupant is venous, the post-trigeminal in front and the lateral head vein behind, with the posterior part of the canal also transmitting the facial nerve (Wible and Hopson, 1995). The only form in which the ramus inferior and post-trigeminal vein co-occur is the platypus, and these structures travel together in an open sulcus (Wible and Hopson, 1995; personal obs.). We think that in *Kryptobaatar* the ramus inferior was the major vascular occupant of the canal

in question, because the large size of the groove for the proximal stapedial on the promontorium and the small size of the foramen for the ramus superior suggest that the other major end branch of the proximal stapedial, the ramus inferior, was present. The evidence for the occurrence of the post-trigeminal vein in *Kryptobaatar* has been discussed above.

The course of the ramus inferior rostral to the petrosal bone in *Kryptobaatar* was presumably through the cavum epiptericum and then the sphenorbital fissure (fig. 36B), because other suitable foramina of exit in the mesocranium are lacking. An endocranial course for the ramus inferior (or its rostral continuation, the ramus infraorbitalis) is unusual among extant mammals, but is known for some chiropterans (Kallen, 1977; Wible and Davis, 2000) and dipodoid rodents (Bugge, 1971). Within the orbit, the ramus inferior, now the ramus infraorbitalis (“rio” in fig. 36B), ran forward in the sphenopalatine groove along the suture between the maxilla and frontal. En route, it likely supplied the minor palatine artery into a foramen in the orbital process of the maxilla, the major palatine and sphenopalatine artery in the sphenopalatine foramen (“spa” in fig. 36B), and its terminal branch, the infraorbital artery into the infraorbital canal (“ioa” in fig. 36B). It also likely provided a ramus orbitalis connecting with the rostral continuation of the ramus superior (see below).

Isolated petrosals of Late Cretaceous multituberculates, in particular “*Catopsalis*” *joyneri*, have been critical for reconstructing the ramus superior in *Kryptobaatar*, as much of this vessel is hidden within the lateral wall of the braincase. In “*C.*” *joyneri*, en route from the middle ear to the orbit, the ramus superior passed through a complex canal, which for descriptive purposes is treated as three successive canals: the ventral ascending, dorsal ascending, and orbitotemporal (Rougier et al., 1992; Wible and Hopson, 1995). The ventral ascending canal begins in the middle ear, runs back posteriorly in a horizontal plane, and then turns dorsally; opening into it from the temporal fossa is the supra-glenoid foramen, which transmitted a ramus temporalis to the temporalis muscle. The dorsal ascending canal is essentially vertical,

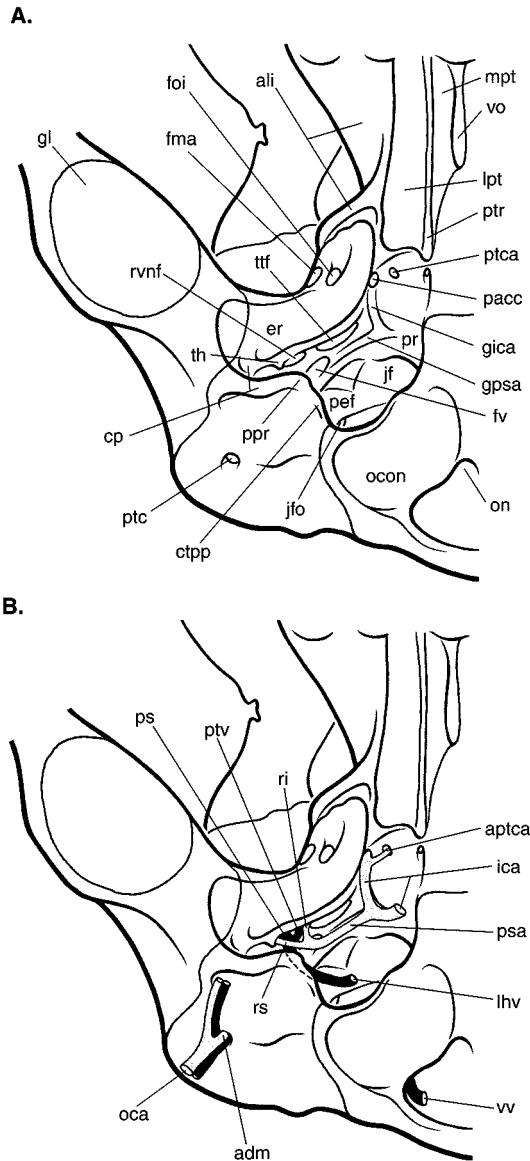


Fig. 37. Reconstruction of the right basicranium of *Kryptobaatar dashzevegi* in ventral view (A) with the major cranial arteries (white outline) and veins (black) added (B). Abbreviations: **adm** arteria diploëtica magna (and accompanying vein); **ali** alisphenoid; **aptca** artery of pterygoid canal; **cp** crista parotica; **ctpp** caudal tympanic process of petrosal; **er** epitympanic recess; **fma** foramen masticatorium; **foi** foramen ovale inferium; **fv** fenestra vestibuli; **gica** groove for internal carotid artery; **gl** glenoid fossa; **gpsa** groove for proximal stapedia artery; **ica** internal carotid artery; **jf** jugular fossa; **jfo** jugular foramen; **lhv** lateral head vein; **lpt** lateral pterygopalatine trough;

curving forward into the anteriorly directed orbitotemporal canal. Opening from behind and marking the limits of the ventral and dorsal ascending canals is the posttemporal canal, which transmitted the arteria diploëtica magna from the occiput. The ventral ascending canal is largely within the anterior lamina, the dorsal ascending canal is between the petrosal and presumably the squamosal, and the posttemporal canal is entirely in the petrosal. The reconstruction of arteries into these various canals is based largely on the pattern in monotremes; between the platypus and echidna all the canals present in “*C. joyneri*” can be found (Rougier et al., 1992; Wible and Hopson, 1995).

The ramus superior in *Kryptobaatar* exhibited essentially the same pattern as in “*Catopsalis joyneri*”, as reconstructed from the various surface foramina into this system of canals (figs. 36A, 37A). The ventral ascending canal in *Kryptobaatar* is indicated by its tympanic aperture and by two foramina in the anterior lamina on the lateral braincase wall, which transmitted rami temporales from the canal (“rt” in fig. 36B). The position of these three foramina suggests that the ventral ascending canal runs posteriorly in a largely horizontal plane. Breakage in one specimen, PSS-MAE 101, provides access to the near vertical dorsal ascending canal between the petrosal and squamosal and shows a notch that was probably enclosed to complete a foramen, which transmitted a third ramus temporalis from the canal (fig. 36). The anteriorly directed orbitotemporal canal is indicated by a horizontal endocast representing its filling and by its anterior aperture in the orbit. The

←

mpt medial pterygopalatine trough; **oca** occipital artery (and accompanying vein); **ocon** occipital condyle; **on** odontoid notch; **pacc** posterior aperture of carotid canal; **pef** perilymphatic foramen; **ppr** paroccipital process; **pr** promontorium of petrosal; **ps** prootic sinus; **psa** proximal stapedia artery; **ptc** posttemporal canal; **ptca** pterygoid canal; **ptr** pterygopalatine ridge; **ptv** post-trigeminal vein; **ri** ramus inferior; **rs** ramus superior; **rvnf** recess for vascular and nervous foramina (prootic canal, ventral ascending canal, canal for ramus inferior, and facial canal); **th** tympanohyal; **ttf** tensor tympani fossa; **vo** vomer; **vv** vertebral vein.

endocast reveals that the anterior part of the orbitotemporal canal was enclosed, but that the posterior part had no medial wall and therefore is an endocranial orbitotemporal groove. Finally, the posttemporal canal is indicated by its posterior aperture on the occiput, entirely within the petrosal (figs. 16, 17). Judging from the size of this aperture, the *arteria diploëtica magna* was of substantial size (“adm” in figs. 36B, 37B).

The rostral continuation of the ramus superior within the orbit is the ramus supraorbitalis (“rso” in fig. 36B). In the extant mammals retaining this vessel (i.e., monotremes and some placentals), it provides up to four sorts of branches: the lacrimal, frontal, and ethmoidal arteries running with the ophthalmic nerve branches of the same name, and the ramus orbitalis anastomosing with the ramus infraorbitalis (Tandler, 1899, 1902; Bugge, 1974; Wible, 1987). Given that all four branches are present in both the platypus and echidna and in diverse placentals (e.g., armadillos, lemurs), it is probable that *Kryptobaatar* exhibited the same condition.

ARTERY OF THE PTERYGOID CANAL

An artery accompanies the nerve of the pterygoid canal in many extant mammals, but in most it is derived from the external carotid system and runs posteriorly into the canal from the orbit (Wible, 1984). In only a

few instances (e.g., some lipotyphlans, McDowell, 1958; MacPhee, 1981; Novacek, 1986) is the artery derived from the internal carotid, running anteriorly into the canal from behind. Given the large size of the sulcus running forward from the carotid canal visible in PSS-MAE 113 (fig. 21), it seems likely that *Kryptobaatar* exhibited the pattern as some lipotyphlans (“aptca” in fig. 37B). However, in light of the rare occurrence of this origin for the artery of the pterygoid canal among extant mammals, we are less confident in this particular aspect of the vascular reconstruction. Moreover, note that the major occupant of the pterygoid canal in extant mammals is the nerve (Wible, 1984).

OPHTHALMIC ARTERY

An ophthalmic artery derived from the internal carotid (circulus arteriosus) and accompanying the optic nerve is widely distributed among extant mammals, including the echidna, all marsupials investigated, and most placentals (Tandler, 1899, 1902; Bugge, 1974; Archer, 1976; Wible, 1984). In light of this distribution, an ophthalmic artery probably ran with the optic nerve in the optic foramen in *Kryptobaatar* as well (“oa” in fig. 36B). It may have anastomosed with branches of the ramus supraorbitalis within the orbit via a ramus orbitalis (not shown in fig. 36B).

COMPARISONS

The following section is devoted to highlighting particular characters or character systems of the multituberculate skull to which our descriptions of *Kryptobaatar* are relevant or have prompted reevaluation of current evidence. An ongoing project beyond the scope of this report is our reevaluation of the phylogenetic interrelationships within Multituberculata. In conducting this reevaluation, we have observed many of the relevant multituberculate specimens, and some of our observations are included here. To place these taxa in a phylogenetic context, we have reproduced a recent hypothesis of multituberculate interrelationships (fig. 38) and of the higher-level relationships of multituberculates (fig. 39).

As a cautionary note, the taxonomy of the Late Jurassic Paulchoffatiidae has been revised recently by Hahn (1993), who has been publishing on this group for more than a quarter century. Hahn (1993) has created several new genera for previously described specimens and reassigned other specimens to previously named genera. We follow Hahn’s (1993) revision in our taxonomic usages.

SNOUT AND PALATE

PRENASAL PROCESS OF THE PREMAXILLA

The tip of the rostrum is rarely preserved in multituberculates. PSS-MAE 101 (fig. 6) is an exception and clearly shows that a pre-

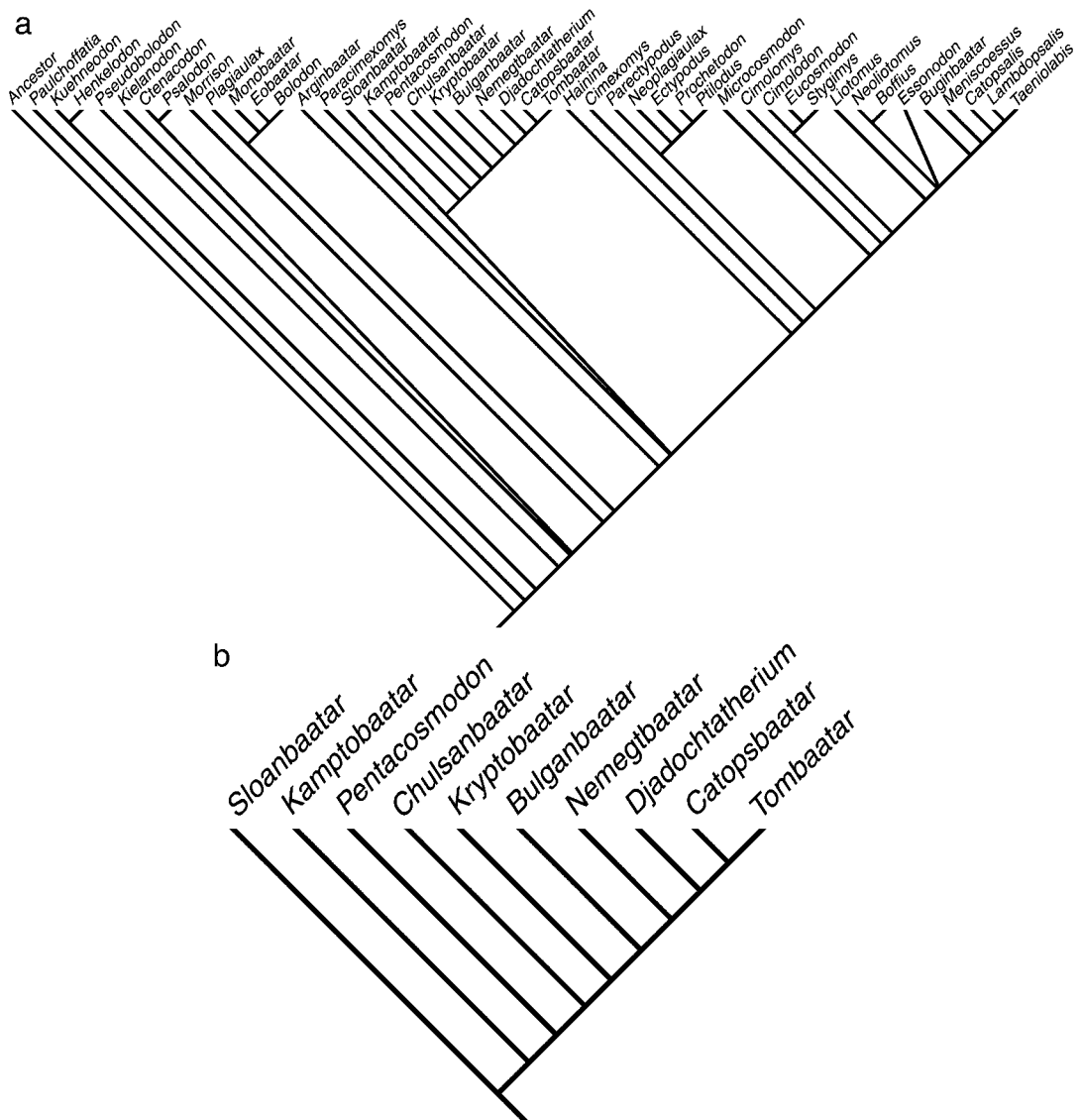


Fig. 38. Cladogram of phylogenetic relationships within Multituberculata (a), based on the analysis in Rougier et al. (1997), with an enlargement of the tree section containing *Kryptobaatar* and its nearest relatives, all of which are Mongolian Late Cretaceous taxa with the exception of *Pentacosmodon* from the North American Paleocene (b). A similar Mongolian Late Cretaceous grouping was called Djadochtatheria by Kielan-Jaworowska and Hurum (1997). In their phylogeny, *Kryptobaatar* is in a clade, Djadochtatheriidae, with *Djadochtatherium*, *Catopsbaatar*, and *Tombaatar*.

nasal process of the premaxilla (internarial bar) is lacking in *Kryptobaatar*. A prenasal process dividing the external nares is found in the outgroups to Mammalia, such as *Haldanodon* (Lillegraven and Krusat, 1991), *Morganucodon* (Miao, 1988; Wible, 1991) and *Sinoconodon* (Wible et al., 1990; Cromp-

ton and Luo, 1993), but is lacking in extant mammals and the prototribosphenidan *Vincelestes* (Rougier, 1993).

To date, an internarial bar has been reconstructed for only one multituberculate, the Paleocene taeniolabidid *Lambdopsalis*. Miao (1988) based this on the presence of a wedge

of bone between the anterior ends of the nasals, which he interpreted to be the broken dorsal tip of the prenasal process. Miao (1988) speculated that the prenasal process in *Lambdopsalis* either was an evolutionary reversal or that the process was more widespread in multituberculates than indicated in previously described specimens. In support of the latter, Miao (1988: 9) suggested that the left nasal in stereophotographs of *Chulsanbaatar* (ZPAL MgM-I/89) published in Kielan-Jaworowska et al. (1986: fig. 16) appeared "indicative of a sutural facet at the anterior end," presumably for the prenasal process. However, we interpret the left nasal in this specimen as broken, in light of other specimens of *Chulsanbaatar* (e.g., ZPAL MgM-I/139) that show a more complete nasal with no sutural facets at the anterior end (see Kielan-Jaworowska, 1974: pl. XI). Therefore, we find no evidence of an internarial bar in *Chulsanbaatar* or other multituberculates described to date. The presence of an internarial bar in *Lambdopsalis* is controversial (see below), and the absence of this structure primitively in multituberculates is corroborated by our observations of snouts of Late Jurassic paulchoffatiids, including two species of *Pseudobolodon* (V.J. 111-155, V.J. 450-155) and one of *Kuehneodon* (V.J. 112-155).

The element in question in *Lambdopsalis* is illustrated in two rostra (Miao, 1988; figs. 1, 2), but it exhibits differences in size and position between the two, as well as between the right and left sides of the same individual. Given these differences, the purported prenasal process of the premaxilla may be a broken part of the nasal. Despite our doubt about the element in *Lambdopsalis*, it is largely irrelevant as a systematic feature, because it is not shared with any other multituberculate and was absent primitively in the group.

Although the internarial bar is lacking in adult extant mammals, remnants of it occur during development in monotremes and marsupials. In the platypus, it forms prenatally as a dorsal outgrowth from the rostral part of the premaxilla (os carunculae of Wilson, 1900), which supports the egg-tooth; it persists in young individuals after the egg-tooth is shed and is subsequently resorbed (Green,

1930; Hill and De Beer, 1949; Zeller, 1989). This element does not come into contact with the nasals. In the echidna, the os carunculae forms independent of, but in contact with, the prenasal process of the premaxilla (Gaupp, 1908; Kuhn, 1971). Among marsupials, an independent ossification in the cleft between the anterior cupulae of the nasal capsule, also called the os carunculae, has been reported in embryos of the didelphid *Caluromys philander* (Denison and Terry, 1921). In addition, condensed connective tissue in the same region has been reported and homologized with the prenasal process of the premaxilla in *Trichosurus vulpecula* (Broom, 1909), *Didelphis marsupialis* (Toeplitz, 1920), *Didelphis aurita*, and *Perameles nasuta* (Hill and De Beer, 1949). Remnants of an egg-tooth papilla beneath the premaxilla have also been discovered in *Trichosurus* and *Phascolarctos cinereus* (De Beer, 1937; Hill and De Beer, 1949). Finally, in placentals, remnants of the os carunculae, egg-tooth, and internarial bar are unknown (De Beer, 1937). In light of the distribution of the characters associated with the os carunculae, egg-tooth, and internarial bar, as well as the phylogenetic position of multituberculates (fig. 39; Rowe, 1988, 1993; Rougier et al., 1996a, 1996c; Hu et al., 1997; Ji et al., 1999), it is likely that an os carunculae and egg-tooth, or remnants thereof, were at least temporarily present in multituberculates at some point in ontogeny. The implications of these features for assessing whether multituberculates were oviparous or viviparous are inconclusive, because different conditions for the os carunculae, egg-tooth, and internarial bar are present in the extant phylogenetic bracket for multituberculates (i.e., monotremes and therians). Based on the reconstructed small size of the pelvic outlet in *Kryptobaatar* (ZPAL MgM-I/41) relative to that in monotremes, Kielan-Jaworowska (1979) proposed that multituberculates were viviparous with extremely small neonates. Lillegraven et al. (1987) argued that the same condition was found in the common ancestor of marsupials and placentals.

SEPTOMAXILLA

In multituberculates, the premaxilla has a large dorsal process that forms the lateral

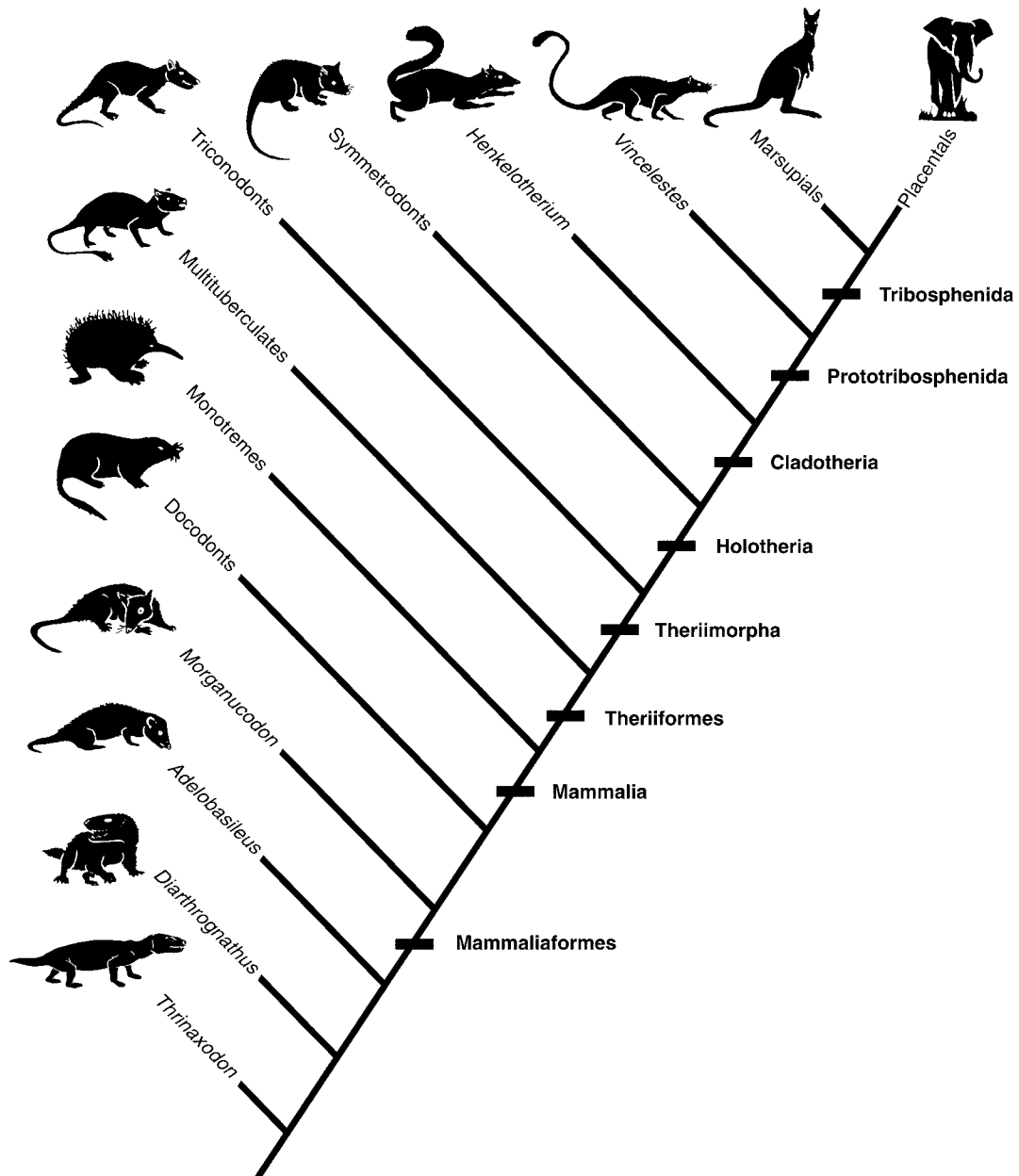


Fig. 39. Cladogram of phylogenetic relationships within Mammaliaformes based on analyses by Rougier et al. (1996a) and Hu et al. (1997).

margin of the external nares (fig. 33), as in most therians. In contrast, in monotremes and most groups of Mesozoic mammals, this position is occupied by a separate bone, the septomaxilla. Based on recent phylogenetic hypotheses of multituberculate relationships (e.g., Rougier et al., 1996a, 1996c; Hu et al.,

1997; Ji et al., 1999), the presence of a septomaxilla in the group would be expected. In fact, such a bone has been recently described for the Late Jurassic paulchoffatiid *Pseudobolodon krebsi* (Hahn and Hahn, 1994). Its purported septomaxilla is cuneiform and lies between the dorsal process of the premaxilla,

the nasal, and the maxilla; that is, it is excluded entirely from the external nares. This would be a unique position for the septomaxilla among synapsids, which otherwise have the septomaxilla in the margin of the external nares (Wible et al., 1990). Our observations of the specimen of *Pseudobolodon krebsi* (V.J. 451-155) described by Hahn and Hahn (1994) suggest that the bone in question is likely part of the premaxilla and that what is illustrated by these authors (1994: tables 1, 2) as a suture between the purported septomaxilla and premaxilla is merely a crack within the premaxilla. Therefore, pending new information, we consider the septomaxilla to be absent in multituberculates. It is also absent in marsupials and placentals (Wible et al., 1990), although the homologies of the purported septomaxilla of some xenarthrans remain controversial (Zeller et al., 1993).

NASAL OVERHANG AND ANTERIOR NASAL NOTCH

In primitive mammaliaforms (e.g., *Haldanodon*, Lillegraven and Krusat, 1991; *Sinoconodon*, Crompton and Luo, 1993), the anterior end of the nasal extends rostrally beyond the septomaxilla and the posterodorsal process of the premaxilla, dorsal to the external narial aperture. We call this condition the nasal overhang of the nares. Additionally, at least in *Haldanodon*, there is a deep anterior nasal notch in the rostral margin that, according to Lillegraven and Krusat (1991), may have transmitted ethmoidal vessels.

Among multituberculates, a nasal overhang of the nares is illustrated for the Late Jurassic paulchoffatiid *Pseudobolodon krebsi* (Hahn and Hahn, 1994: fig. 2b), and we observed it in *Kuehneodon simpsoni* (V.J. 112-155) and *Henkelodon nais* (V.J. 401-155); these three taxa also have an anterior nasal notch. In contrast, a nasal overhang is absent or greatly reduced in all younger taxa preserving the anterior tip of the nasal: *Kryptobaatar* (fig. 33), *Kamptobaatar* (Kielan-Jaworowska, 1971: pl. III), *Nemegtbaatar* (Kielan-Jaworowska, 1974: pl. IX), *Chulsanbaatar* (ibid.: pl. XII), *Catopsbaatar* (ibid.: pl. XIX), and *Lambdopsalis* (Miao, 1988: fig. 4). However, the anterior nasal notch is re-

tained, at least in *Kryptobaatar* ("ano" in figs. 8, 12), *Kamptobaatar* (Kielan-Jaworowska, 1969: pl. XVI), and *Catopsbaatar* (Kielan-Jaworowska, 1974: pl. XVIII).

NASAL FORAMINA

Once considered to be highly unusual among mammals (Kielan-Jaworowska, 1971; Miao, 1988), nasal foramina are now known to be distributed widely among Mammaliaformes, including *Sinoconodon* (Crompton and Luo, 1993), *Haldanodon* (Lillegraven and Krusat, 1991), *Vincelestes* (Rougier, 1993), and *Ornithorhynchus* (Zeller, 1989). Nasal foramina have also been described widely among Late Cretaceous and Cenozoic multituberculates. However, until recently they had not been reported for any Late Jurassic paulchoffatiid. In 1994, Hahn and Hahn reported a single pair of small nasal foramina in *Pseudobolodon krebsi* (V.J. 451-155), and we have seen the same condition in another species of the same genus, *P. oreas* (V.J. 461-155). However, we report here that nasal foramina are not ubiquitous among paulchoffatiids, as they are wholly lacking in *Kuehneodon dryas* (V.J. 454-155). Another feature of the nasal foramina that varies considerably among multituberculates is the number of pairs present (Kielan-Jaworowska and Hurum, 1997), from a single pair in *Pseudobolodon* to seven or eight pairs in *Lambdopsalis* (Miao, 1988). Kielan-Jaworowska and Hurum (1997) reported two pairs of nasal foramina in *Kryptobaatar* and in *Chulsanbaatar*, *Catopsbaatar*, *Tombaatar*, and the ptilodontoid *Ptilodus*. However, we found only one pair in *Catopsbaatar* (ZPAL MgM-I/78), and in *Ptilodus*, we found three pairs in *P. gracilis* (USNM 6076) and two pairs, asymmetrically placed on the right and left sides, in *P. montanus* (AMNH 35490). Finally, in *Kryptobaatar* PSS-MAE 101, we found two foramina on the right and three on the left ("naf" in figs. 6, 8).

Foramina in the nasals were first described in multituberculates by Simpson (1925) in *Djadochtherium matthewi*. However, it was not until 1937 that Simpson applied the term nasal foramina to these apertures in his description of *Ptilodus*. Miao (1988) cited

Simpson (1937) as employing two different terms for these foramina: either vascular foramina or nasal foramina. From our reading of Simpson (1937), we think that the term he intended for these apertures was nasal foramina, and that vascular foramina was meant as a descriptor of their function and not an alternative term. Rather than vascular, a nervous function was suggested for the nasal foramina by Kielan-Jaworowska (1971).

INFRAORBITAL FORAMINA

Some Jurassic multituberculates have two infraorbital foramina on the facial process of the maxilla, which vary in size from subequal to the anterior one being considerably the larger (Hahn, 1985). The latter condition is also found in Early Cretaceous *Arginbaatar* from Khoobur in Mongolia (Kielan-Jaworowska et al., 1987). The smaller posterior foramen is absent in *Kryptobaatar* (fig. 33) and other Mongolian Late Cretaceous multituberculates, and in Cimolodonta (sensu Simmons, 1993; i.e., ptilodontoids and taeniolabidoids), except for *Meniscoessus robustus* (Archibald, 1982; Simmons, 1993).

Multiple facial exits for the infraorbital canal system are present in basal mammaliaforms (Kermack et al., 1981; Lillegraven and Krusat, 1991; Crompton and Luo, 1993), monotremes (Kuhn, 1971; Zeller, 1989), and in members of the therian lineage, including paurodontids (personal obs. of an undescribed new genus from the Morrison Formation) and *Vincelestes* (Rougier, 1993). A foramen for the lacrimal branch of the infraorbital system is present in most forms with multiple exits; it opens between the maxilla, the lacrimal, and sometimes the jugal. Some Jurassic multituberculates and monotremes have multiple exits, but lack the foramen for the lacrimal branch.

Miao (1988) questioned the utility of characters of the infraorbital foramina in phylogenetic analyses, because there are instances of individual variability. For example, on one side of a maxilla of *Lambdopsalis* of the 13 maxillae reported by Miao (1988), two rather than a single infraorbital foramina were present, though the smaller posterior foramen was distinguished by only a tiny bridge. However, as pointed out by Rougier et al.

(1997a), the discrepancies noted by Miao (1988) have no bearing when considered in a wider phylogenetic framework, because the variations occur in only a few very disparate groups. We add here that after review of the major collections of Mongolian Late Cretaceous multituberculates (MAE and ZPAL), we have found no instances of more than a single infraorbital foramen.

Another feature of the infraorbital system preserved in *Kryptobaatar* is several small foramina linking the infraorbital canal with either the maxillary sinus or nasal cavity. Rougier et al. (1997a) reported similar apertures in another form from Ukhaa Tolgod, *Tombaatar*, and speculated that they may lead into alveolar canals and have carried nerves and vessels to the upper teeth. Confirmation of the presence of alveolar canals for *Kryptobaatar* is provided by high-resolution CT scans of PSS-MAE 101.

PALATINE FORAMINA

There is considerable confusion about the foramina in and around the palatine's contribution to the palate because different terms have been used by various authors. As our point of reference, we have used the dog (Evans and Christensen, 1979), which has three sets of palatine foramina: a large anterior one transmitting the major palatine nerve and vessels, a small one behind it transmitting the accessory palatine nerve and artery, and at the back of the palate a notch or large foramen for the minor palatine nerve and vessels (see figs. 15, 34). Additionally, we have named these foramina based on their occupants (contra Evans and Christensen, 1979): that is, major, accessory, and minor palatine foramina, respectively. Similarly placed foramina are widely distributed among mammaliaforms, but all three do not necessarily occur together. For example, among primitive mammaliaforms, *Sinocodon* (Crompton and Luo, 1993) has all three, but *Morganucodon* (Kermack et al., 1981) and *Haldanodon* (Lillegraven and Krusat, 1991) have only the major and minor palatine foramina.

Among multituberculates, paulchoffatiids appear to have only the major and minor foramina (Hahn, 1987). Most of the Mongolian

Late Cretaceous taxa with well-preserved palates (*Kryptobaatar*; *Kamptobaatar*, Kielan-Jaworowska, 1971; *Chulsanbaatar*, *Nemegtbaatar*, Kielan-Jaworowska et al., 1986) have all three (fig. 15), although the number of accessory foramina varies. Another variant is presented by *Ptilodus montanus*, which seems to have only the major and accessory palatine foramina (Simpson, 1937; AMNH 34590). This is the same condition reported for *Lambdopsalis*, although all three foramina are visible in stereophotographs and reconstructions in Miao (1988: figs. 3, 14, 18).

According to Kielan-Jaworowska et al. (1986), the opening we call the minor palatine foramen does not penetrate bone fully in *Nemegtbaatar* as shown from their study of a sectioned specimen. To distinguish this opening from a true foramen, Kielan-Jaworowska et al. (1986) employed the term palatonasal notch. Additionally, they generalized from their observations of *Nemegtbaatar*, suggesting that the purported foramen present in other multituberculates is also merely a palatonasal notch. We cannot say unequivocally that the minor palatine foramen in *Kryptobaatar* penetrates bone, because full preparation of this passageway is essentially impossible. However, *Kryptobaatar* has a foramen in the orbital process of the maxilla (fig. 12) that closely resembles the one leading into the minor palatine canal in various therians (Novacek, 1986). Consequently, we are fairly confident that the minor palatine foramen on the palate transmitted the same named nerves and vessels in *Kryptobaatar*. We also think that a true minor palatine foramen is more widespread among multituberculates, but justification awaits better preserved orbital processes of the maxilla.

FACIAL PROCESS OF LACRIMAL

In their phylogenetic analysis of selected multituberculate taxa, Kielan-Jaworowska and Hurum (1997) reported a large, roughly rectangular facial process of the lacrimal separating the frontal and the maxilla as characteristic of Djadochtatheria, the monophyletic clade that includes 10 Mongolian Late Cretaceous genera. This is in contrast to the small, arcuate facial process of some other

multituberculates. We offer the following amendments to Kielan-Jaworowska and Hurum's scoring.

Among Djadochtatheria, whereas the typical djadochtatherian facial process is said to be present in *Sloanbaatar*, *Catopsbaatar*, and *Bulganbaatar* (Kielan-Jaworowska and Hurum, 1997), we were not able to unequivocally identify a lacrimal in the specimens of these taxa housed in Warsaw. According to Kielan-Jaworowska (personal commun.), the typical djadochtatherian facial process is present on the *Catopsbaatar* specimen housed in Moscow (PIN 4537-5).

Among Taeniolabidae, Kielan-Jaworowska and Hurum (1997) reported a small, arcuate facial process in *Lambdopsalis* and *Taeniolabis*. However, the lacrimal is wholly lacking in *Lambdopsalis* (Miao, 1988), and if one was present in *Taeniolabis*, it had no facial exposure (Broom, 1914).

Among Ptilodontoidea, for the observation of a small facial process of the lacrimal in *Ptilodus*, Kielan-Jaworowska and Hurum (1997) cited Simpson (1937). Although Gidley (1909) originally identified a lacrimal in *P. gracilis*, Simpson (1937: 740), in reanalyzing the same specimen and other specimens of *P. montanus*, stated that "the anterior orbital rim is not perfectly preserved in any case and certainty is impossible, but there is no suggestion of facial exposure of the lacrimal and the maxilla probably forms this rim." In our observations of the specimens of *P. montanus* and *P. gracilis* described by Simpson (1937), we were unable to either deny or confirm the presence of a lacrimal. This is also the case in the skull of the ptilodontoid *Ectypodus tardus* (YPM-PU 14724), which was originally described by Sloan (1979) as having no lacrimal.

Among Paulchoffatiidae, a small, arcuate facial process contacting the posteriorly expanded nasals has been reported for *Pseudobolodon krebsi* (Hahn, 1969; Hahn and Hahn, 1994), but we have also seen it in *P. oreas* (V.J. 460-155), *Kuehneodon dryas* (V.J. 454-155), and *Meketichoffatia krausei* (V.J. 446-155).

ORBITOTEMPORAL REGION

ORBITAL MOSAIC

The sutural pattern of the bony elements contributing to the orbital mosaic has been

reported for fewer than a handful of multituberculates. The two with the most evident sutures are *Kryptobaatar* (this report; figs. 18, 19, 33) and *Lambdopsalis* (Miao, 1988). In both taxa, the palatine is wholly excluded from the orbit, and the major contributing elements are the frontal and the maxilla, with the latter forming the anterior part of the orbital roof and extending posteriorly through the orbit to floor the sphenorbital recess. However, the proportions of several elements are strikingly different between the two taxa. In *Lambdopsalis*, there is no lacrimal; the orbitosphenoid has a restricted orbital exposure; and the alisphenoid is expanded dorsally, contacting the frontal and parietal and excluding the anterior lamina from the orbital mosaic. In contrast, in *Kryptobaatar* (figs. 18, 19, 33), there is a lacrimal with a small orbital process, the orbitosphenoid has a more extensive orbital exposure; the anterior lamina contacts the frontal, and the alisphenoid is confined to the sphenorbital recess.

How widespread these patterns are among multituberculates is not entirely clear because of preservational problems. A lacrimal was primitively present in multituberculates, given its distribution reported above in paulchoffatiids and Mongolian Late Cretaceous taxa, but the extent of the orbital contribution is uncertain. A maxilla resembling that in *Kryptobaatar* and *Lambdopsalis* is also reported in *Chulsanbaatar* and *Nemegtbaatar* (Hurum, 1994, 1998a), but the maxilla does not form a bony roof over the anterior orbital space in the paulchoffatiids *Pseudobolodon* (V.J. 447-155, 451-155, 460-155) and *Mekitchoffatia* (V.J. 446-155) or in the ptilotontoids *Ectypodus* (Sloan, 1979) and *Ptilodus* (Simpson, 1937). The orbital exposure of the orbitosphenoid in *Pseudobolodon* (originally described as *Kuehneodon* in Hahn, 1977), *Kamptobaatar* (Kielan-Jaworowska, 1971), *Chulsanbaatar*, and *Nemegtbaatar* (Hurum, 1994, 1998a) appears to be more substantial than that in *Kryptobaatar*. Finally, as in *Kryptobaatar*, the alisphenoid is confined to the sphenorbital recess in *Kamptobaatar* and *Nemegtbaatar* (see below), and the anterior lamina sends a process forward that contacts the frontal high in the orbit in *Nemegtbaatar* and *Chulsanbaatar* (Hurum, 1998a).

The primitive condition of the palatine for multituberculates is still controversial, but Miao's (1988, 1993) suggestion that the absence of an orbital process may be primitive is still viable. In addition to *Kryptobaatar*, an orbital process of the palatine is lacking in *Catopsbaatar* (ZPAL MgM-I/78) and *Kamptobaatar* (ZPAL MgM-I/33) (contra Kielan-Jaworowska, 1971, and Hurum, 1994), but it is said to be present in a sectioned skull of *Nemegtbaatar* (Hurum, 1994, 1998a) and is illustrated in *Ectypodus* (Sloan, 1979: fig. 1). We have not had the opportunity to study the specimen of *Nemegtbaatar* described by Hurum (1994, 1998a); however, we were not able to identify sutures distinguishing any orbital elements in *Ectypodus tardus* (YPM-PU 14724). If Hurum's (1994, 1998a) interpretations of the orbital sutures in *Nemegtbaatar* are correct, then the Mongolian Late Cretaceous taxa would be polymorphic regarding the presence of the palatine in the orbit. Because an orbital process has been reported in *Nemegtbaatar* and *Ectypodus*, we carefully scrutinized the condition in *Kryptobaatar*. On the left side of PSS-MAE 101 (fig. 12) and possibly also 113, there is a line along the ventral edge of the part of the orbit bulging over the frontal lobe that we interpret as a fracture within the orbitosphenoid. The bone anteroventral to this line is the only orbital element that conceivably could be palatine, but the high-resolution CT sections of PSS-MAE 101 do not support this interpretation. Interestingly, this is not the position the palatine is reported to exhibit in *Nemegtbaatar*, which is in the anteroventral corner of the orbit (Hurum, 1998a). In *Kryptobaatar*, the corresponding part of the orbit is most assuredly maxilla.

One feature of the orbit that clearly varies within multituberculates is the orbital pocket of Gambaryan and Kielan-Jaworowska (1995), the depression in the orbital process of the frontal for the pars anterior of the medial masseter muscle. Among Mongolian Late Cretaceous taxa, an orbital pocket is reported for *Kamptobaatar* (Kielan-Jaworowska, 1971), *Catopsbaatar* (Gambaryan and Kielan-Jaworowska, 1995), *Tombaatar* (Rougier et al., 1997a), *Nemegtbaatar*, *Chulsanbaatar*, *Sloanbaatar* (Kielan-Jaworowska et al., 1986), and *Kryptobaatar* (figs. 10–14).

Among ptilodontoids, an orbital pocket is reported for *Ectypodus* by Sloan (1979), but it has not been noted in *Ptilodus* (Simpson, 1937; Wall and Krause, 1992). Among taeniolabidids, Sloan (1981) noted that the large orbital pocket in *Taeniolabis taoensis* had been misidentified as the orbit proper by Broom (1914) and Granger and Simpson (1929). In *Lambdopsalis*, an orbital pocket is not apparent in the reconstructions in Miao (1988), but a reduced one was said to be present in a personal communication by that author to Gambaryan and Kielan-Jaworowska (1995: 65) dated December 1994. Finally, an orbital pocket is absent in the paulchoffatiids *Meketichoffatia* (V.J. 443-155) and *Pseudobolodon* (V.J. 447-155, 451-155, 460-155).

ORBITAL FORAMINA

Given that few orbits are known in detail for multituberculates, it is not surprising that information concerning orbital foramina is also limited. The reported distributions of various orbital foramina in multituberculates are treated below.

Lacrimal Foramen: A lacrimal foramen has been noted thus far for only the paulchoffatiids *Meketichoffatia* (originally described as *Paulchoffatia* by Hahn, 1969) and *Pseudobolodon* (Hahn and Hahn, 1994), *Lambdopsalis* (1988), *Nemegtbaatar* (Hurum, 1994), and *Kryptobaatar* ("lacf" in fig. 16). In the mammaliaforms *Morganucodon* (Kermack et al., 1981), *Haldanodon* (Lillegraven and Krusat, 1991), and *Vincelestes* (Rougier, 1993), there are two lacrimal foramina in the orbital process of the lacrimal, although *Sinoconodon* has only one (Crompton and Luo, 1993). The paulchoffatiids have a single opening in the ventral part of the orbital process (Hahn and Hahn, 1994), whereas in *Nemegtbaatar* (Hurum, 1994) and *Kryptobaatar* the foramen is in the ventral part of the lacrimal's contribution to the orbital rim. *Lambdopsalis*, in which the lacrimal is absent, has a single lacrimal foramen in the orbital process of the maxilla (Miao, 1988). The lacrimal is also lacking in monotremes, and their lacrimal foramen is between the maxilla and frontal (Kuhn, 1971; Zeller, 1989). As reported above, the presence of the lacrimal is uncertain in *Ptilodus*;

however, we found a lacrimal foramen in the orbital process of the isolated maxillae of *P. montanus* (USNM 9735).

Sphenopalatine Foramen: A sphenopalatine foramen in the anteroventral portion of the orbital wall is widely distributed among multituberculates. What may differ among taxa are the enclosing bony elements. According to Kielan-Jaworowska et al. (1986), the foramen is at the junction of the maxilla, frontal, orbitosphenoid, and palatine in taeniolabidoids, based presumably on *Kamptobaatar* (Kielan-Jaworowska, 1971) and *Nemegtbaatar* (see also Hurum, 1994), whereas it lies in or near the frontomaxillary suture in *Lambdopsalis* (Miao, 1988) and *Kryptobaatar* ("spf" in figs. 10, 12, 18, 19), the two forms whose orbital mosaics are known best. A true characterization of the borders of the sphenopalatine foramen among multituberculates awaits better preserved orbits.

Foramen for Frontal Diploic Vein: An aperture in the frontal near the dorsal orbital rim resembling that described here in *Kryptobaatar* for the frontal diploic vein ("fdv" in figs. 18, 36A) is also found in *Catopsbaatar* (ZPAL MgM-I/78), *Chulsanbaatar* (ZPAL MgM-I/168), *Ptilodus* (AMNH 35490, USNM 6076), and the paulchoffatiids *Kuehneodon* (V.J. 454-155), *Meketichoffatia* (V.J. 446-155), and *Pseudobolodon* (V.J. 447-155, 451-155, 458-155, 460-155). Miao (1988) did not report one in *Lambdopsalis*, and we did not see any in the specimens of *Kamptobaatar* and *Nemegtbaatar* available for study. Among primitive mammaliaforms, there are two foramina in the frontal in *Morganucodon* (Kermack et al., 1981) and one in *Haldanodon* (Lillegraven and Krusat, 1991) that may have transmitted the frontal diploic vein.

Anterior Opening of Orbitotemporal Canal: *Kamptobaatar* (ZPAL MgM-I/33) and *Nemegtbaatar* (Kielan-Jaworowska et al., 1986) have a foramen below the postorbital process at the anterior end of the orbitotemporal canal, which transmitted the orbitotemporal vessels, resembling that reported here in *Kryptobaatar*. According to Kielan-Jaworowska et al. (1986), this aperture (their postorbital foramen) is in the parietal in *Nemegtbaatar*; it is between the parietal, frontal, and anterior lamina in *Kryptobaatar*

("otc" in fig. 12). *Lambdopsalis* (Miao, 1988) also has an opening at the anterior end of the orbitotemporal canal, but it lies well posterior to the reduced postorbital process, between the parietal, frontal, and alisphenoid. Hahn and Hahn (1994) reported a post-orbital foramen in *Pseudobolodon krebsi*, but the relevant specimen (V.J. 451-155) shows no communication between this aperture and an orbitotemporal canal. If this is a vascular foramen, it served a nutritive function only. The only basal mammaliaform in which an anterior opening of the orbitotemporal canal has been reported is *Adelobasileus*, in which the aperture is positioned in the parietal well posterior to the orbit (Lucas and Luo, 1993). In addition, although the foramen has not been described, orbitotemporal vessels entering the orbit have been restored for *Morganucodon* (Kermack et al., 1981; Rougier et al., 1992).

Ethmoidal Foramen: Simmons (1993) employed the presence/absence of an ethmoidal foramen in her phylogenetic analysis of Multituberculata, noting its absence in only two taxa, the ptilodontoids *Ptilodus* and *Ectypodus*. This result is surprising, given that an ethmoidal foramen to our knowledge is universally present among living mammals, representing the only pathway for branches of the ophthalmic nerve to reach the nasal cavity from the orbit. However, our inspection of the relevant specimens reveals an ethmoidal foramen to be present in both *P. montanus* (AMNH 35490; see also Simpson, 1937) and *E. tardus* (YPM-PU 14724). Therefore, an ethmoidal foramen is now known for all multituberculates preserving the relevant portion of the orbit, including *Kryptobaatar* ("ef" in figs. 12, 18, 19, 36A).

Optic Foramen: *Lambdopsalis* (Miao, 1988), *Kamptobaatar* (ZPAL MgM-I/33), and *Kryptobaatar* ("opf" in figs. 10, 12, 36A) have a foramen in the orbitosphenoid that, given its position, likely transmitted the optic nerve. An optic foramen has been reported for two other multituberculates, but these do not resemble the openings in the three taxa named above. The supposed optic foramen in *Meketichoffatia* (originally described as *Pseudobolodon* by Hahn, 1981) is too small and too far forward, whereas that in *Nemegtbaatar* (Kielan-Jaworowska et al.,

1986) connects to the upper part of the cavum epiptericum rather than to the orbit. Beyond excluding these openings as optic foramina, we are uncertain of their function. Among cynodonts, an optic foramen occurs in *Probainognathus* (MCZ 4274), *Sinocynodon* (Crompton and Luo, 1993), *Adelobasileus* (Lucas and Luo, 1993), and eutherians (Novacek et al., 1997), and was likely more widespread among multituberculates and mammaliaforms than is currently known.

Metoptic Foramen: Among mammaliaforms, a metoptic foramen has thus far been identified in only five taxa, all of them multituberculates. In *Kryptobaatar*, the metoptic foramen is anteromedial to the sphenorbital fissure ("mef" in fig. 36A), and on the endocranial surface is anterolateral to the hypophyseal fossa, with a deep sulcus on the ossified pila antotica running into the foramen from behind ("mef" in figs. 25–27). In *Lambdopsalis* (Miao, 1988), the metoptic foramen is also anterolateral to the hypophyseal fossa, but is posterior to the sphenorbital fissure. The metoptic foramen in *Kamptobaatar* (ZPAL MgM-I/33) is only known from the orbital surface; as in *Kryptobaatar*, it is anteromedial to the sphenorbital fissure. Finally, the metoptic foramen in *Nemegtbaatar* and *Chulsanbaatar* has only been described from the endocranial surface, and it lies posterolateral to the hypophyseal fossa (Hurum, 1998a). Miao (1988) also suggested that tiny pores in the anterior floor of the hypophyseal fossa reported in *Meketichoffatia* (originally described as *Pseudobolodon* by Hahn, 1981) may represent metoptic foramina. In our study of this specimen (V.J. 443-155), we think these pores are artifactual. A metoptic foramen is a primitive amniote feature that was likely more widespread among multituberculates and other mammaliaforms than is currently known, although the ossification of the pila metoptica or lack thereof may be a variable feature.

Sphenorbital Fissure: The opening of the cavum epiptericum into the orbit, the sphenorbital fissure, reported for *Lambdopsalis* (Miao, 1988), *Ptilodus* (Simpson, 1937), *Ectypodus* (Sloan, 1979), and other Mongolian Late Cretaceous multituberculates (Kielan-Jaworowska et al., 1986), resembles that described here for *Kryptobaatar* ("sphf" in

fig. 36A). It is not directly visible in lateral view, but is concealed behind the alisphenoid and/or anterior lamina (figs. 10, 12, 36A). One potential difference is the occupants of the sphenorbital fissure. As mentioned above, *Lambdopsalis* (Miao, 1988) and *Kryptobaatar* have separate optic and metoptic foramina; if these apertures are truly lacking in other multituberculates, the optic and oculomotor nerves and the ophthalmic artery probably left the cranial cavity through the cavum epiptericum via the sphenorbital fissure.

Miao (1988) noted that the multituberculate sphenorbital fissure is unusual in that it is concealed in lateral view. This differs from the condition in basal mammaliaforms, such as *Sinoconodon* (Crompton and Luo, 1993) and *Haldanodon* (Lillegraven and Krusat, 1991), and in modern mammals in which the foramen is generally visible from the side. Miao (1988: 54) speculated that "this is due to the retention of a medially bony walled cavum epiptericum in multituberculates, among early mammals, which prevents the orbitosphenoid from articulating with the alisphenoid in most parts." As an alternative explanation, this concealment may result from the apparent foreshortening of the temporal region in the multituberculates for which the position of the sphenorbital fissure is known.

POSTORBITAL PROCESS

The postorbital process on the frontal bone is a widespread feature of the mammalian skull (Novacek, 1986). Presumably, as in the dog (Evans and Christensen, 1979), it serves as an attachment for the orbital ligament, delimiting the back of the orbit, and marks the anterior limit of the temporalis muscle attachment.

In multituberculates, the postorbital process has been said by Miao (1988, 1993) to be reduced or absent. Gambaryan and Kielan-Jaworowska (1995) pointed out, contra Miao (1988, 1993), that a parietal postorbital process is characteristic of taeniolabidoids. In our preliminary comparisons among multituberculates, we have identified three conditions for the postorbital process: on the frontal and inconspicuous, on the parietal and

short, and on the parietal and long. An inconspicuous postorbital process on the frontal is found in paulchoffatiids (*Meketichoffatia krausei*, V.J. 446-155; *Pseudobolodon oreas*, V.J. 460-155; *Pseudobolodon krebsi*, V.J. 451-155), *Ptilodus* (Simpson, 1937), and *Ectypodus tardus* (YPM-PU 14724). In contrast, in those Mongolian Late Cretaceous taxa preserving the postorbital process, it is on the parietal. It is short in *Chulsanbaatar*, *Kamptobaatar*, and *Nemegtbaatar* (Kielan-Jaworowska and Hurum, 1997) and is long in *Catopsbaatar* (Kielan-Jaworowska and Sloan, 1979) and *Kryptobaatar*. Kielan-Jaworowska and Hurum (1997) characterized the postorbital process of *Kryptobaatar* as short, but PSS-MAE 113 had long ones prior to preparation damage (see reconstruction in fig. 33). The only non-Mongolian multituberculate with a postorbital process on the parietal, and a short one at that, is *Taeniolabis taoensis* from the Paleocene of North America (Broom, 1914). We are uncertain of the condition in *Lambdopsalis*, which has been said to have a short but distinct postorbital process on the frontal (Miao, 1988) and on the parietal (Meng, personal commun. cited in Gambaryan and Kielan-Jaworowska, 1995).

Miao (1988) suggested that a true postorbital process is lacking in Mongolian Late Cretaceous multituberculates and that the process on the parietal in these forms does not delimit the back of the orbit. In support, he noted that the postorbital constriction is on the posterior side of the parietal process, whereas it is on the anterior side of a true postorbital process on the frontal. Based on *Kryptobaatar*, however, we think that the element on the parietal represents a true postorbital process that has shifted onto a different skull roof bone. In the dog (Evans and Christensen, 1979) and the platypus (Zeller, 1989; personal obs.), anterior to the postorbital process, are the foramen for the frontal diploic vein and the passageway by which the supraorbital nerve and vessels leave the orbit. The same structures are found immediately in front of the process in question on the parietal in *Kryptobaatar* (fig. 18). Additionally, Miao (1988) has misidentified the position of the postorbital constriction in the Mongolian Late Cretaceous taxa; it does lie

posterior to the process on the parietal, in the very foreshortened temporal fossa (fig. 32). Incidentally, the postorbital process is not invariably on the frontal in extant mammals; in hyracoids, for example, both the frontal and the parietal contribute to the formation of this process (Fischer, 1986: fig. 27; MacPhee, 1994: fig. 6).

NASOPARIETAL CONTACT

One of the more unusual features of the skull roof above the orbit in the taeniolabidids *Taeniolabis* (Broom, 1914; Simpson, 1937) and *Lambdopsalis* (Miao, 1988) is the long anterior process of the parietal that overlies the frontal and extends forward to contact the nasal. The absence/presence of this feature has been used in recent phylogenetic analyses within Multituberculata by Simmons (1993), Rougier et al. (1997a), and Kielan-Jaworowska and Hurum (1997). We restudied the incidence of nasoparietal contact in paulchoffatiids, following a suggestion from J. A. Hopson, and offer the following amendments to the scoring of this feature. Whereas nasoparietal contact has been widely held to be a unique feature of taeniolabidids, we have also observed it in several paulchoffatiids: *Kuehneodon dryas* (V.J. 454-155), *Pseudobolodon krebsi* (V.J. 447-155, 451-155), and *Pseudobolodon*, n. sp. (V.J. 400-155, 450-155). The condition in *Meketichoffatia krausei* (V.J. 445-155, 446-155) is uncertain.

JUGAL

Until recently, the jugal was widely considered (e.g., Clemens and Kielan-Jaworowska, 1979; Hahn, 1983) to be wholly lacking in multituberculates. J. A. Hopson (personal commun. cited in Kielan-Jaworowska et al., 1986) noted the presence of a jugal or a facet for it on the medial side of the zygomatic arch in several previously described specimens. From Hopson's observations, Hahn (1987) reported the presence of a jugal facet on the medial side of the zygomatic process of the maxilla in several paulchoffatiids, *Kuehneodon dryas*, *Pseudobolodon oreas*, and ?*Pseudobolodon*, sp. indet., and we have observed this facet in *Meketichoffatia krausei* (V.J. 446-155). Hopson et al. (1989) re-

ported displaced, broken jugals in *Ptilodus montanus*, which contacted the medial surface of both the maxilla and the squamosal in the zygomatic arch and extended forward into the anteroventral part of the orbit. They also reported an incomplete jugal in *Nemegtbaatar*, which contacted both the maxilla and the squamosal, as well as small fragments of a jugal in *Chulsanbaatar*. The jugals described here in *Kryptobaatar* (PSS-MAE 101 and 113) are the first complete ones reported for multituberculates (figs. 22, 23). They conform with the jugals in *Ptilodus montanus*, except that they do not extend as far forward into the anteroventral part of the orbit.

Outside of multituberculates, monotremes are the only other mammaliaform group in which replacement of the jugal in the zygomatic arch by an elongate maxillary process extending nearly to the squamosal glenoid is likely primitive (Hopson et al., 1989). However, rather than internal to the maxilla and squamosal as in multituberculates, the reduced jugal is dorsal to them in the platypus (Zeller, 1989). The jugal is wholly absent in the echidna (Kuhn, 1971).

BASICRANIUM AND LATERAL BRAINCASE WALL

PTERYGOPALATINE RIDGES AND TROUGHS

In the mesocranium, *Kryptobaatar* has paired medial and lateral pterygopalatine troughs ("mpt" and "lpt" in fig 37A) separated by the paired pterygopalatine ridges ("ptr" in fig. 37A) and on the midline by the vomer (figs. 14, 15, 20, 21, 34, 37A). A similar arrangement is known for other Mongolian Late Cretaceous multituberculates (e.g., *Kamptobaatar*, Kielan-Jaworowska, 1971; *Nemegtbaatar*, Kielan-Jaworowska et al., 1986) and for Late Jurassic paulchoffatiids (e.g., *Pseudobolodon oreas*, Hahn, 1981), except in the latter the lateral trough is significantly narrower and shallower than the medial. We have seen a similar arrangement in *Ptilodus* (USNM 6076). Medial and lateral pterygopalatine troughs are also found in primitive mammaliaforms (e.g., *Morganucodon*, Kermack et al., 1981; *Sinoconodon*, Crompton and Luo, 1993). In contrast, in *Lambdopsalis*, pterygopalatine ridges are

lacking, and a single trough bordered by a very low, midline crest enters the choana (Miao, 1988).

Regarding the occupants of the medial and lateral troughs, the former held the air passageway, whereas there are two hypotheses for the occupants of the lateral in multituberculates. According to Barghusen (1986), the auditory (Eustachian) tube connecting the nasopharynx and the cavum tympani occupied the lateral trough. Other authors have reconstructed muscle there: tensor veli palatini by Kielan-Jaworowska (1971) and Hahn (1981), and medial pterygoid by Gambaryan and Kielan-Jaworowska (1995). We think that the morphology in *Kryptobaatar* eliminates the auditory tube as a possible occupant; the pterygopalatine ridge extends far rostrally into the choana, an arrangement that required the auditory tube to empty into the nasal cavity and not into the nasopharynx as it does in extant mammals (Starck, 1995). The more likely course for the auditory tube was one posterior to the pterygopalatine ridge to join the nasopharynx in the medial trough. On the other hand, the morphology of the lateral trough in *Kryptobaatar*, in particular the fossa at its anterior end, appears appropriate for muscle attachment. However, we are uncertain what the muscular occupant could have been. The tensor veli palatini arises more posteriorly in living therians (see Evans and Christensen, 1979), and the medial pterygoid would seem to have been at a mechanical disadvantage within the lateral trough, with the medially inflected, lateral choanal wall constraining the direction of the muscle's pull. As a third hypothesis, we propose that a parallel channel to the main air passageway may have occupied the lateral trough. Either such a channel and/or muscle seem to be the only viable options. Perhaps evaluating these options in light of the morphology of other mammaliaforms and mammaliaform outgroups, which is beyond the scope of this report, may resolve this problem.

The pterygopalatine ridges in *Kryptobaatar* and *Kamptobaatar* (ZPAL MgM-I/33) end as a rounded, posteroventrally directed process that is reminiscent of the pterygoid hamulus of living therians. Kielan-Jaworowska (1971) suggested that it served a sim-

ilar function, directing the pull of the tendon of the tensor veli palatini. However, she doubted its homologies with the therian hamulus because the two are formed from different parts of the pterygoid. We agree with Kielan-Jaworowska (1971), noting that the therian hamulus is formed from the posterolateral part of the pterygoid, whereas the process in *Kryptobaatar* and *Kamptobaatar* is off the posteromedial part of the bone.

ECTOPTYERGOID

A separate ectopterygoid bone in the posterolateral corner of the palate has been described for one specimen of *Morganucodon oehleri* (Kermack et al., 1981) and in the mesocranium of various non-mammalian cynodonts (e.g., *Thrinaxodon*, Fourie, 1974). An ectopterygoid has also been said (e.g., Partridge and Westoll, 1940; Presley and Steel, 1978) to be present in monotremes, but the homologies of this element have been questioned (Wible, 1991). At one time, an ectopterygoid was also thought to be present in the lateral wall of the choana in certain Mongolian Late Cretaceous multituberculates (Kielan-Jaworowska, 1971; Clemens and Kielan-Jaworowska, 1979), although the suture delimiting it from the alisphenoid behind was said to be indistinct (Kielan-Jaworowska et al., 1986). A separate ectopterygoid has also been reconstructed in the early Eocene pilodontoid *Ectypodus* (Sloan, 1979). Miao (1988, 1993) suggested that the purported multituberculate ectopterygoid may merely be part of the alisphenoid, which is how it was restored in *Chulsanbaatar* by Rougier et al. (1992: fig. 8C) and in subsequent reconstructions by Kielan-Jaworowska and co-workers (e.g., Gambaryan and Kielan-Jaworowska, 1995; Kielan-Jaworowska and Hurum, 1997; Hurum, 1998a). This view is supported by the morphology of the alisphenoid in *Kryptobaatar* and our observations of the multituberculates in the ZPAL collections.

Miao (1988) also suggested that although the ectopterygoid was not present as a separate element in multituberculates, it was fused with the pterygoid to form the equivalent of the therian hamulus. The basis for this hypothesis is that the ventrolateral portion of the therian pterygoid, which forms

from cartilage separate from the intramembranous dorsomedial portion of the pterygoid, is homologous with the ectopterygoid bone of other amniotes (Presley and Steel, 1978). This is not the only view on the homologies of these elements; Kuhn (1971) and Zeller (1989) treated the pterygoid cartilage as a derivative of the palatoquadrate. This controversy is beyond the scope of our report, but we have stated above that a hamulus as occurs in therians is not present in *Kryptobaatar* or other multituberculates.

ALISPHENOID

The alisphenoid in multituberculates has been said (e.g., Kermack and Kielan-Jaworowska, 1971; Kielan-Jaworowska et al., 1986) to be a small element with little contribution to the side wall of the braincase. This is in contrast to the usual condition in mammaliaforms in which the alisphenoid is expanded dorsally and contacts the frontal (Novacek, 1986; Wible and Hopson, 1993; Hopson and Rougier, 1993). Miao (1988, 1993) has questioned the purported small size of the alisphenoid in multituberculates, noting that there are few specimens that unambiguously detail the extent of the alisphenoid in the braincase wall; one is *Lambdopsalis*, which has an alisphenoid extending dorsally to meet the parietal in the skull roof, according to Miao (but see below). In addition, Miao (1993: 69) included under his category of multituberculate apomorphies an “elastic ossification pattern in the orbitotemporal region as reflected by the variability in extent of the alisphenoid and the so-called ‘anterior lamina of the petrosal’.”

A review of recent reconstructions of the multituberculate braincase would seem to support Miao’s (1993) observation of alisphenoid variability. At one extreme is *Lambdopsalis*, in which the alisphenoid is said to extend to the skull roof (Miao, 1988); at the other extreme is *Kryptobaatar*, in which the alisphenoid has very little contribution to the braincase (fig. 10). Intermediate between these two extremes, according to Hurum (1998a), is the alisphenoid in *Nemegtbaatar*, with *Chulsanbaatar* showing an element intermediate between *Nemegtbaatar* and *Kryptobaatar*. In *Kryptobaatar*, the su-

tures delimiting the alisphenoid from the anterior lamina are very distinct and show without doubt that the alisphenoid is a small element. Moreover, the suture between the alisphenoid and anterior lamina in *Kryptobaatar* closely resembles that tentatively identified for *Kamptobaatar* by Kielan-Jaworowska (1971), with which we concur based on ZPAL MgM/I-33, and for *Nemegtbaatar* by Kielan-Jaworowska et al. (1986). Hurum (1998a) has provided a new reconstruction for *Nemegtbaatar* based on a sectioned specimen in which the contribution of the alisphenoid to the braincase is more substantial than that reconstructed by Kielan-Jaworowska et al. (1986). Because we have not seen the sectioned skull of *Nemegtbaatar* (or *Chulsanbaatar*), we are not able to evaluate Hurum’s reconstruction. Regarding *Lambdopsalis*, we have not had access to the entire collection of specimens studied by Miao (1988), but we identified a possible suture in the anterior portion of the epitympanic recess of IVPP V7151.80 (see Miao and Lillegraven, 1986; Rougier et al., 1996c). This possible suture is in the same place that the alisphenoid contacts the petrosal in *Kryptobaatar*, suggesting that *Lambdopsalis* also might have a small alisphenoid. This single observation does not refute Miao’s reconstruction for *Lambdopsalis*, but it does raise doubts about it, in particular in light of the fragmentary nature of the material. In summary, we are skeptical about the extreme variability reported for the multituberculate alisphenoid, and we think that Miao’s (1993) inclusion of an elastic ossification pattern in the orbitotemporal region as a multituberculate apomorphy seems unwarranted.

Kielan-Jaworowska et al. (1986) claimed that the alisphenoid in multituberculates is not pierced by any foramina. However, Miao (1988) described in *Lambdopsalis* a foramen ovale inferium and foramen masticatorium wholly within the alisphenoid and an alisphenoid canal between the alisphenoid and anterior lamina. Additionally, we report here for *Kryptobaatar* and various other Mongolian Late Cretaceous forms, a buccinator foramen between the alisphenoid and anterior lamina (see below; “fbu” in figs. 10, 36A).

FORAMINA FOR BRANCHES OF THE
MANDIBULAR NERVE

Most Mesozoic mammaliaforms, including multituberculates, have two foramina in the anterior lamina and/or petrosal that are interpreted for branches of the trigeminal nerve (Wible and Hopson, 1993; Luo, 1994). Recently, we (Rougier et al., 1996a) have raised doubts about which branches of the trigeminal nerve occupied these various apertures. To date, two models of nerve restoration have been proposed. First, Simpson (1937) restored branches of the mandibular nerve in the two foramina in *Ptilodus montanus*, citing Hill's (1935) observation of two foramina for the mandibular nerve in the alisphenoid of some extant rodents. Second, Patterson and Olson (1961) restored the maxillary and mandibular nerves respectively in the two foramina in the anterior lamina of *Sinoconodon*. This model has been followed by Kermack (1963, 1967) in reconstructing nerves in *Morganucodon* and by most subsequent authors considering Mesozoic mammaliaforms other than multituberculates. In contrast, authors researching multituberculates (e.g., Kielan-Jaworowska, 1971; Sloan, 1979) invariably have followed the model proposed by Simpson (1937). In describing *Kryptobaatar*, we too have followed Simpson's model. However, we have accepted it because the pattern of the foramina in *Kryptobaatar* fits the arrangement of the mandibular nerve foramina in some living rodents (Hill, 1935; Wahlert, 1974). Specifically, the two foramina in *Kryptobaatar* are roughly at the same level, with the medial one anteroventrally directed and the lateral one ventrolaterally directed ("foi" and "fma" in fig. 37A); this does not correspond to the positions of the maxillary and mandibular nerve exits in any extant mammals. As detailed below, there is some variation in the position of the two foramina in question in other multituberculates; however, the variation is not extreme enough in any taxon to warrant an alternative nerve restoration. The implications of this for non-multituberculate mammaliaforms are beyond the scope of this report, and what is required is careful comparison of the relevant extinct taxa with the morphology of extant mammals and the es-

tablishment of morphological criteria to recognize the different branches of the trigeminal system based on osteology.

All multituberculates known to date with one exception have at least two apertures in the anterior lamina and/or petrosal that have been interpreted as for branches of the mandibular division of the trigeminal nerve: the foramen ovale inferium and the foramen masticatorium. The exception is *Lambdopsalis* in which the two foramina are said to be in the alisphenoid (Miao, 1988). In our preliminary comparisons, we have noted that the positions of the foramina in the petrosal vary with regard to each other and to the epitympanic recess. In Late Jurassic paulchoffatiids (e.g., *Kuehneodon dryas*, V.J. 454-155; *Pseudobolodon*, n. sp., V.J. 450-155), the foramen ovale inferium is at a level posterior to the foramen masticatorium, and both foramina are lateral to the epitympanic recess. In ptilodontoids (e.g., *Ptilodus montanus*, AMNH 35490; *Mesodma thompsoni*, Wible and Hopson, 1995), the two foramina are at the same level and the foramen ovale inferium traverses the epitympanic recess. Among Mongolian Late Cretaceous multituberculates, the foramen ovale inferium traverses the epitympanic recess in *Sloanbaatar* (ZPAL MgM-I/20), whereas both foramina traverse it in *Kryptobaatar* (fig. 37A), *Kamptobaatar* (ZPAL MgM-I/33), *Nemegtbaatar* (ZPAL MgM-I/81), *Chulsanbaatar* (ZPAL MgM-I/168), and *Catopsbaatar* (ZPAL MgM-I/78). The foramina are roughly at the same level in *Kryptobaatar*, *Kamptobaatar*, and *Nemegtbaatar*, but the foramen ovale inferium is more posterior in *Sloanbaatar*, *Chulsanbaatar*, and *Catopsbaatar*. Finally, in *Lambdopsalis*, the two foramina are at the same level, lateral to the epitympanic recess, but supposedly enclosed in the alisphenoid (Miao, 1988). Another variant is found in *Kamptobaatar* (ZPAL MgM-I/33) in which there are more than two foramina in the epitympanic recess (five on the right side and four on the left) that likely held branches of the mandibular nerve (Kielan-Jaworowska, 1971).

We have identified in *Kryptobaatar* another foramen in the pterygoid fossa of the alisphenoid between that bone and the anterior lamina as for the buccal branch of the man-

dibular nerve (“fbu” in figs. 10, 36A). This foramen is not unique to *Kryptobaatar*, but also occurs in *Catopsbaatar* (ZPAL MgM-I/78), *Chulsanbaatar* (ZPAL MgM-I/168), *Kamptobaatar* (ZPAL MgM-I/33), *Nemegtbaatar* (ZPAL MgM-I/81), and *Sloanbaatar* (ZPAL MgM-I/20). Kielan-Jaworowska et al. (1986) described for *Chulsanbaatar* (ZPAL MgM-I/168; see also Hurum, 1998a: ZPAL MgM-I/84, the sectioned skull) and *Nemegtbaatar* (ZPAL MgM-I/82 and 76, the sectioned skull) another more dorsally situated foramen wholly within the anterior lamina, as possibly for the deep temporal branch of the mandibular nerve. We have not yet studied the sectioned skulls, and we were not able to confirm the presence of this dorsal foramen of the anterior lamina in the other cited specimens.

VENOUS SYSTEM

Our reconstruction of the venous system has considered only a few vessels. We treat these below, with the exception of the frontal diploic vein, which has already been discussed above (see Orbital Foramina).

Superior Sagittal and Transverse Sinuses: A superior sagittal sinus connecting with paired transverse sinuses is nearly ubiquitous among extant mammals (Gelderen, 1924), and the multituberculates for which the relevant anatomy is known are no exception. Endocasts of *Kryptobaatar*, *Ptilodus* (Simpson, 1937; Krause and Kielan-Jaworowska, 1993), *Lambdopsalis* (Miao, 1988), *Nemegtbaatar*, *Chulsanbaatar* (Kielan-Jaworowska et al., 1986), and an undescribed new species of Mongolian Late Cretaceous multituberculate (PSS-MAE 126) show evidence that this dural sinus pattern was present.

Sigmoid Sinus: In *Kryptobaatar*, the sigmoid sinus does not exit the skull via the small jugular foramen, but likely left through the foramen magnum in the vertebral veins (“vv” in fig. 37B). The same arrangement has been reported for *Chulsanbaatar* and *Nemegtbaatar* by Kielan-Jaworowska et al. (1986) based on clear evidence from endocranial casts (contra Miao, 1988). A foramen magnum exit for the sigmoid sinus is not the universal pattern in multituberculates. Grooves indicate that the sigmoid sinus ex-

ited through the jugular foramen in *Lambdopsalis* (Miao, 1988) and through both the jugular foramen and foramen magnum in paulchoffatiids (Lillegraven and Hahn, 1993).

Miao (1988) questioned the taxonomic significance of differences in the sigmoid sinus's egress in multituberculates, because this vessel exhibits considerable diversity among extant and extinct mammals. However, at least some of this diversity falls along taxonomic lines; for example, the principal exit of the sigmoid sinus in all extant marsupials is via the foramen magnum (Archer, 1976; Wible, 1990). Consequently, this character should not be eliminated a priori from phylogenetic analyses. In fact, Rougier et al. (1996a, 1996c) have used the egress of the sigmoid sinus in their analyses of mammaliaform interrelationships. They observed that in addition to paulchoffatiids, the sulcus for the sigmoid sinus extends to the jugular foramen in *Morganucodon* and *Haldanodon*. In contrast, in the other taxa for which the sigmoid sulcus is known, it does not reach the jugular foramen.

Inferior Petrosal Sinus: Among extant mammals, the inferior petrosal sinus follows a course along the basioccipital-petrosal suture that may be largely either endocranial, intramural, or extracranial (Wible, 1983). We reconstruct the inferior petrosal sinus in an endocranial course in *Kryptobaatar* in part because there is a shallow sulcus in the appropriate location in PSS-MAE 123 (fig. 25) and in part because there is no bony passageway appropriate for an extracranial or intramural route. Moreover, given the small size of the jugular foramen (figs. 26, 37A), it seems likely that this vessel exited the cranial cavity via the foramen magnum in the vertebral veins (“vv” in fig. 37B). We believe that *Nemegtbaatar* and *Chulsanbaatar* likely exhibited the same pattern; there is no likely route other than an endocranial one, and the jugular foramen in these forms is also small (Kielan-Jaworowska et al., 1986). The inferior petrosal sinus was not reconstructed for *Lambdopsalis* by Miao (1988), but we think it likely occupied a deep sulcus on the endocranial surface between the petrosal and the basioccipital (Miao, 1988: fig. 23). In contrast to the Late Cretaceous taxa,

the jugular foramen in *Lambdopsalis* is large (Miao, 1988) and may have transmitted the inferior petrosal sinus, as occurs in most extant therians (Wible, 1983). As noted by Rougier et al. (1996a), canals in the petrosal of some paulchoffatiids indicate that the inferior petrosal sinus had an intrapetrosal course to the jugular foramen as occurs in all mammaliaforms with the exception of extant mammals. We have also observed such canals in *Ptilodus montanus* (AMNH 35490).

The small size of the jugular foramen in *Kryptobaatar*, *Nemegtbaatar*, and *Chulsanbaatar* suggests an unusual pattern for the drainage of the dural sinuses. As stated above, it is likely that neither the inferior petrosal sinus nor the sigmoid sinus exited through the jugular foramen. Consequently, the lateral head vein was the major constituent of the internal jugular vein. The only extant mammal exhibiting this same pattern is the echidna (Hochstetter, 1896). The platypus has a minor variant in that a part of the inferior petrosal sinus drains into the internal jugular vein through the enormous metotic fissure, which is formed by the confluent jugular and hypoglossal foramina (fig. 28), and part is into the vertebral veins via the foramen magnum (Rougier et al., 1992). In contrast, in marsupials and placentals, the major contributor to the internal jugular vein (the inferior petrosal and/or sigmoid sinuses) exits the cranial cavity via the jugular foramen.

Lateral Head Vein and Prootic Sinus: A well-developed prootic canal that transmitted the prootic sinus to the lateral head vein is known for all multituberculates preserving the relevant portion of the petrosal bone. Several characters of this vessel have been employed in phylogenetic analyses among mammaliaforms: most recently, the position of the cranial and tympanic apertures of the prootic canal (Rougier et al., 1996a, 1996c). In multituberculates, the cranial aperture is said by Rougier et al. (1996a, 1996c) to lie at the anterodorsal margin of the subarcuate fossa, whereas the tympanic aperture is confluent with the pterygoparoccipital foramen (ventral ascending canal). The prootic canal in *Kryptobaatar* conforms with these observations (figs. 27, 37A). However, we add here that in some paulchoffatiids (V.J. 73-155, 82-155) the cranial aperture of the pro-

otic canal lies between the cavum epiptericum and the subarcuate fossa (see also Lillegraven and Hahn, 1993: figs. 1, 6). Also, the tympanic aperture is not confluent with the pterygoparoccipital foramen in *Chulsanbaatar* (ZPAL MgM-I/168) and in an isolated petrosal tentatively assigned to *Meniscoessus* (Luo, 1989; Wible and Hopson, 1995). Additionally, the condition in paulchoffatiids and *Nemegtbaatar* is uncertain.

Post-trigeminal Vein: In multituberculates, the vascular canal in the petrosal above the epitympanic recess and lateral flange has been called variously the canal for the ?maxillary artery (Kielan-Jaworowska et al., 1986), the post-trigeminal canal (Rougier et al., 1996a, 1996c), and the canal for the ramus inferior (Miao, 1988; Wible and Hopson, 1995). In "*Catopsalis*" *joyneri* and *Mesodma thompsoni*, the canal is wide enough that it likely had two occupants, the ramus inferior and the post-trigeminal vein (Wible and Hopson, 1995). We are confident that a ramus inferior occupied the canal in question in *Kryptobaatar*, given the size of the groove for the stapedial artery and the ventral ascending canal; however, we cannot exclude the presence of a post-trigeminal vein as well ("ptv" in figs. 36B, 37B). A canal for the ramus inferior is also present in *Lambdopsalis*, but the incidence of this structure among other multituberculates is uncertain due to preservational problems. The only other mammaliaform with a post-trigeminal vein enclosed in a canal is the echidna (Wible and Hopson, 1995).

Pituito-orbital Vein: In *Kryptobaatar*, we have identified a separate foramen in the anterolateral wall of the hypophyseal fossa for the pituito-orbital vein ("fpv" in figs. 25, 27, 36A). Miao (1988), in his description of *Lambdopsalis*, is the only other author to discuss this vein (his pituitary vein) in Mesozoic mammals. He concluded that this vein shared the metoptic foramen with the oculomotor nerve, based on the co-occurrence of these structures in the chondrocranium of some living sauropsids (e.g., *Lacerta*, De Beer, 1937). This restoration was the only logical one for Miao, because a separate foramen for the vein, as occurs in the chondrocranium of some other sauropsids (e.g., *Sphenodon*, Bellairs and Kamal, 1981), was

not identified in *Lambdopsalis* (although he did report a nutrient foramen in the midline of the anterior wall of the hypophyseal fossa). In the case of *Kryptobaatar*, there are two distinct foramina, and in our restoration we follow the model provided by those sauropsids where the nerve and vein occupy separate foramina. A likely candidate for a separate foramen for the pituito-orbital vein does not appear to be present in *Meketichoffatia* (V.J. 446-155), although it should be noted that this region is not in pristine condition.

Transverse Canal Vein: Here is reported for the first time in multituberculates the presence of a transverse canal vein. This vein in *Kryptobaatar* ("tcv" in fig. 36B) is an unexpected occurrence among Mammaliaformes, because a similar canal is only known for some metatherians (Marshall et al., 1990; Marshall and Muizon, 1995) and placentals (McDowell, 1958; MacPhee, 1994). The absence of this canal in other multituberculates may be an artifact of preservation or related to the relative inaccessibility of the medial wall of the sphenorbital recess for preparation. In fact, two of the sections of *Nemegtbaatar* published by Hurum (1998a: figs. 2, 4) show gaps across the midline dorsal to the horizontal portion of the basisphenoid in the skull base that are reminiscent of the canal in *Kryptobaatar*. The meaning of these gaps awaits further consideration. The phylogenetic implications of the transverse canal vein are unclear, and we are uncertain about the homology of the transverse canal of multituberculates with that of later therians.

ARTERIAL SYSTEM

The arterial reconstructions presented here for *Kryptobaatar* do not differ in principle from that offered previously for *Lambdopsalis* (Miao, 1988), "*Catopsalis*" *joyneri* (Rougier et al., 1992; Wible and Hopson, 1995), and a generalized taeniolabidoid (Rougier et al., 1992). The most striking differences among these reconstructions concern the positions of particular osseous passageways (e.g., supraglenoid foramen, ventral ascending canal). The pattern reconstructed here for *Kryptobaatar* also generally agrees with that interpreted for such diverse

mammaliaforms as *Morganucodon* and *Vincelestes* (Rougier et al., 1992). In fact, one specific feature of the arterial pattern, a horizontal ventral ascending canal, supports the grouping of multituberculates with triconodontids and prototribosphenidans (Rougier et al., 1996a).

Internal Carotid Artery: *Kryptobaatar* has provided information about certain arteries not included in other vascular reconstructions of multituberculates. Probably the most noteworthy of these is the basicranial portion of the internal carotid artery, which has proven to be of systematic value among some groups of extant mammals (Wible, 1986). The groove on the promontorium in *Kryptobaatar* clearly indicates that the internal carotid followed a transpromontorial course en route to the cranial cavity ("ica" in fig. 37B). Among multituberculates, a similar course has been described previously from sulci only in *Ectypodus* (Sloan, 1979), and outside of multituberculates, only in *Vincelestes* (Rougier et al., 1992) and certain eutherians (MacIntyre, 1972; Wible, 1986). However, the basicranial course of the internal carotid in *Kryptobaatar* is atypical in two regards: first, it does not run the length of the promontorium but is confined to the rostral half (also in *Ectypodus*), and second, its rostral-most part is enclosed in a long canal between the petrosal, alisphenoid, and pterygoid that leads to the carotid foramen in the basisphenoid. Both of these derived conditions occur only rarely among certain placentals (MacPhee, 1981; Wible, 1984; MacPhee and Cartmill, 1986). Among multituberculates, a transpromontorial course confined to the rostral half of the promontorium like that in *Kryptobaatar* and *Ectypodus* is also indicated by promontorial grooves in *Meketichoffatia* (V.J. 446-155), *Ptilodus* (AMNH 35490), *Chulsanbaatar* (ZPAL MgM-I/168), *Kamptobaatar* (ZPAL MgM-I/33), *Nemegtbaatar* (ZPAL MgM-I/82), and *Sloanbaatar* (ZPAL MgM-I/20). A carotid groove is lacking in *Pseudobolodon oreas* (V.J. 460-155), *Kuehneodon dryas* (V.J. 454-155), *Lambdopsalis* (Miao, 1988), and the isolated petrosals referred to "*Catopsalis*" *joyneri* and *Mesodma thompsoni* (Wible and Hopson, 1995). Given that carotid foramina are putatively lacking in *Lambdopsalis* (Miao, 1988), its internal

carotid artery apparently did not reach the cranial cavity, and the vertebral arteries must have been the principal supplier of blood to the brain. Noted, however, that given the vascular pattern reconstructed for *Lambdopsalis* by Miao (1988), including the presence of a well-developed stapedia artery, the absence of a carotid foramen is surprising.

In *Kryptobaatar*, the carotid foramen is entirely within what we think is the basisphenoid (“pacc” in fig. 37A); its ventral aperture is not on the basicranial surface but is recessed somewhat dorsally at the end of the carotid canal (fig. 14), and its dorsal aperture is in the posterolateral part of the hypophyseal fossa (“fica” in figs. 25, 27). Among multituberculates, the location of the dorsal aperture of the carotid foramen has been reported only in *Meketichoffatia krausei* (Hahn, 1981), *Nemegtbaatar* (Kielan-Jaworowska et al., 1986; Hurum, 1998a), and *Chulsanbaatar* (Hurum, 1998a). As in *Kryptobaatar*, the carotid foramen is in the posterolateral part of the hypophyseal fossa in *M. krausei* and *Nemegtbaatar*. However, in *Chulsanbaatar*, it is illustrated (Hurum, 1998a: fig. 12) in the anterolateral part of the hypophyseal fossa, although no basis for this position is provided. Among other mammaliaforms, the dorsal aperture of the carotid foramen is in the anterolateral part of the hypophyseal fossa in *Triconodon* (Kermack, 1963) and *Morganucodon* (Kermack et al., 1981) and in the posterolateral part in monotremes (Zeller, 1989). In contrast, the dorsal aperture appears to be wholly lateral to the hypophyseal fossa in marsupials (see Archer, 1976) and placentals (see Ellenberger and Baum, 1908; Cooper and Schiller, 1975; Evans and Christensen, 1979; Novacek, 1986). Among multituberculates, the ventral aperture of the carotid foramen is on the basicranial surface within the basisphenoid in *Meketichoffatia krausei* (Hahn, 1981) and *Ptilodus* (Simpson, 1937), and between the basisphenoid and the petrosal in *Ectypodus* (Sloan, 1979), *Kamptobaatar* (ZPAL MgM-I/33), *Sloanbaatar* (ZPAL MgM-I/20), *Nemegtbaatar*, and *Chulsanbaatar* (Kielan-Jaworowska et al., 1986). Noted, however, that the position of the carotid foramen in the Mongolian taxa implies a long intraosseous course for the artery, which approximates the

morphology of the carotid canal in *Kryptobaatar*. Among other mammaliaforms, the ventral aperture is generally within the basisphenoid (Archer, 1976; Rougier et al., 1992; Luo, 1994) except in some placentals (De Beer, 1937; Wible, 1984).

Stapedial Artery: A stapedial groove running posterolaterally on the promontorium to the oval window like that in *Kryptobaatar* (“gpsa” in fig. 37A) has been reported previously for multituberculates in *Ectypodus* (Sloan, 1979) and in various isolated petrosals, including those referred to “*Catopsalis*” *joyneri* (Kielan-Jaworowska et al., 1986; Wible and Hopson, 1995) and *Meniscoessus* (Luo, 1989), as well as unreferred specimens from the Bug Creek Anthills (Fox and Meng, 1997). We have also observed such a stapedial groove in *Meketichoffatia* (V.J. 446-155), *Ptilodus* (AMNH 35490), *Chulsanbaatar* (ZPAL MgM-I/168), *Kamptobaatar* (ZPAL MgM-I/33), *Nemegtbaatar* (ZPAL MgM-I/82), and *Mesodma thompsoni* (FMNH 53904). In light of the position of the groove in these taxa, it seems likely that their stapedial artery ran through a bicurrate stapes, as reconstructed for *Kryptobaatar*. A groove for the stapedial artery is also present in *Lambdopsalis*, but it differs in that it runs wholly posterior to the oval window; therefore, the artery did not perforate the stapes but ran behind it (Miao, 1988), a fact subsequently confirmed by Meng’s (1992) description of a columnar stapes in *Lambdopsalis*. A stapedial groove is not ubiquitous among multituberculates, being absent for example in paulchoffatiids (Lillegraven and Hahn, 1993) other than *Meketichoffatia*. Among other mammaliaforms, a stapedial groove is known only for *Vincelestes* (Rougier et al., 1992) and certain eutherians (Wible, 1987). However, among these taxa, the artery’s course to the oval window is usually a lateral or anterolateral one; a posterolateral course is known only for the tarsier (MacPhee and Cartmill, 1986).

All multituberculates for which the relevant anatomy is preserved have a lateral flange that is bent medially to contact the promontorium (Rougier et al., 1996a), except for *Lambdopsalis* in which, according to Miao (1988), the alisphenoid accomplishes this. It is the infolded lateral flange that

forms the floor of the canal for the ramus inferior (post-trigeminal canal). Because of preservational problems, the canal for the ramus inferior has been described in only a few multituberculates; in addition to *Kryptobaatar*, these include *Nemegtbaatar* (Luo, 1989), *Lambdopsalis* (Miao, 1988), and various isolated petrosals, including those referred to “*Catopsalis*” *joyneri* (Kielan-Jaworowska et al., 1986), *Mesodma thompsoni* (Wible and Hopson, 1995), and *Meniscoessus* (Luo, 1989). To date, we have found only one multituberculate in which the canal for the ramus inferior is without a doubt absent (*Ptilodus montanus*, AMNH 35490), although the absence of the canal does not necessarily imply the absence of the artery, which could have run ventral to the tympanic roof. Among other mammaliaforms, similar canals in the tympanic roof are known only for the echidna and certain placentals (e.g., scandentians, macroscelidids), where they are formed by appositional bone growth from the petrosal (Kuhn, 1971; MacPhee, 1981). In the echidna, the major occupant is venous (Wible and Hopson, 1995), whereas in placentals, it is the ramus inferior of the stapedial artery (MacPhee, 1981).

Miao’s (1988) interpretation of the osseous structures associated with the course of the ramus inferior in *Lambdopsalis* differs substantially from that presented here for other multituberculates. He proposed that the ramus inferior en route to the cavum epiptericum passed through an alisphenoid canal, indicated by a groove on the medial side of the alisphenoid and an opening anterior to the foramen ovale inferium. Additionally, the ramus inferior was exposed laterally through an elongated fenestra slightly larger than the foramen ovale inferium. Behind this fenestra, the ramus inferior was enclosed in a second canal that Miao terms “canal of maxillary artery,” following Kielan-Jaworowska et al. (1986). Although we have not seen all the relevant specimens of *Lambdopsalis*, we speculate that the fenestra is an artifact and that the ramus inferior was fully enclosed in an osseous canal as in other multituberculates, except *Ptilodus*. The relationships of the osseous canal in *Lambdopsalis* (i.e., to the facial nerve, prootic canal, and stapedial system) are the same as the canal for the ramus

inferior in other multituberculates, and we interpret them as homologous. The homogeneity of this region across Multituberculata, invariably formed by the petrosal, casts additional doubts on Miao’s (1988) interpretation of the alisphenoid in *Lambdopsalis* (see above). What Miao (1988) terms the alisphenoid canal, we think merely reflects the course of the ramus inferior through the cavum epiptericum en route to the sphenorbital fissure.

A pattern for the canals associated with the ramus superior and arteria diploëtica magna resembling that described here for “*Catopsalis*” *joyneri* and *Kryptobaatar* (fig. 36A) has been described for other multituberculates, including *Chulsanbaatar*, *Nemegtbaatar* (Kielan-Jaworowska et al., 1986; Rougier et al., 1992), *Lambdopsalis* (Miao, 1988), *Ptilodus* (Wible and Hopson, 1995), and isolated petrosals referred to *Meniscoessus* (Luo, 1989) and *Mesodma thompsoni* (Wible and Hopson, 1995). Differences among taxa concern the positions of foramina, the communications between canals, and the enclosing bony elements. For example, the tympanic aperture of the ventral ascending canal (pterygoparoccipital foramen of non-mammalian cynodonts) for the ramus superior is confluent with that for the prootic canal in most taxa including *Kryptobaatar* (fig. 37), but is posterior to the prootic canal in *Chulsanbaatar* (ZPAL MgM-I/168) and *Meniscoessus* (Luo, 1989). The ventral ascending canal has a communication with the prootic canal intramurally in *Nemegtbaatar* (Kielan-Jaworowska et al., 1986) and *Lambdopsalis* (Miao, 1988), but remains separate in “*Catopsalis*” *joyneri* and *Mesodma thompsoni* (Wible and Hopson, 1995); the condition in *Kryptobaatar* is unknown. The supraglenoid foramen for a ramus temporalis opens in the anterior lamina at a level anterior to the fenestra vestibuli in most taxa, including *Kryptobaatar* and the paulchoffatiids *Meketichofatia* (V.J. 446-155), *Kuehneodon* (V.J. 454-155), and *Pseudobolodon* (V.J. 450-155), but is level with the fenestra vestibuli in *Chulsanbaatar* (ZPAL MgM-I/168), *Sloanbaatar* (ZPAL MgM-I/20), *Lambdopsalis* (Miao, 1988), and *Mesodma thompsoni* (Wible and Hopson, 1995). As in most mammaliaforms (Luo, 1994), the posterior opening into the

posttemporal canal for the arteria diploëtica magna is between the squamosal and petrosal in paulchoffatiids (Lillegraven and Hahn, 1993), *Nemegtbaatar* (Hurum, 1998a), and *Kamptobaatar* (ZPAL MgM-I/33), but is within the petrosal in other multituberculates including *Kryptobaatar* (figs. 35, 36A). Also, the posterior opening is located low on the occiput in most taxa, including *Kryptobaatar* and *Pseudobolodon* (V.J. 460-155), but is dorsally situated in *Ptilodus* (AMNH 35490) and *Lambdopsalis* (Miao, 1988); the position of the posterior opening into the posttemporal canal dictates the length of ventral ascending canal. A foramen of the dorsal ascending canal for a ramus temporalis is found, in addition to *Kryptobaatar*, in *Kamptobaatar* (ZPAL MgM-I/33), *Chulsanbaatar* (ZPAL MgM-I/168), *Ptilodus* (AMNH 35490), and *Lambdopsalis* (Miao, 1988), but is lacking in specimens of *Nemegtbaatar*. Finally, as discussed above, an orbitotemporal channel that transmitted the ramus superior to the orbit has yet to be identified in paulchoffatiids, but it was likely present given the widespread presence of this structure.

The general pattern for the ramus superior and arteria diploëtica magna that occurs in multituberculates is repeated in most regards in other mammalian morphs (Rougier et al., 1992, 1996a; Wible and Hopson, 1995). The most striking differences among taxa concern the course of the ramus superior and its rostral continuation, the ramus supraorbitalis, which may have been wholly or partially extracranial, intramural, or endocranial. The taxon that most closely resembles the multituberculate pattern is the prototribosphenidan *Vincelestes* (Rougier et al., 1992, 1996a). Like multituberculates, *Vincelestes* has an intramural ventral ascending canal within the anterior lamina that initially runs posteriorly in a horizontal plane; it also has multiple foramina for rami temporales, including a foramen of the dorsal ascending canal on the suture between the anterior lamina, squamosal, and parietal (Rougier et al., 1992). The only other taxa with a horizontal course for the ventral ascending canal are triconodontids (Rougier et al., 1996a, 1996c), but their canal differs in that it is intramural between the petrosal and squamosal (Rougier et al., 1996a).

PTERYGOID CANAL

Arising from the carotid groove on the anterolateral pole of the promontorium in *Kryptobaatar* is a canal of subequal diameter that is directed anterolaterally toward the orbit; we have interpreted this as the pterygoid canal ("ptca" in fig. 37A) based on the resemblance to that, for example, in lipotyphlans (McDowell, 1958; MacPhee, 1981; Novacek, 1986). We think that some other Mongolian Late Cretaceous taxa have a similar arrangement, with the only difference being that the posterior aperture of the pterygoid canal is farther away from the posterior aperture of the carotid canal, and these two openings are connected by a groove for the contents of the pterygoid canal. The morphology in question was described for *Chulsanbaatar* and *Nemegtbaatar* by Kielan-Jaworowska et al. (1986). In these forms, the carotid groove leads to the posterior aperture of the carotid canal situated more posteriorly than in *Kryptobaatar*. Originating at the posterior aperture of the carotid canal is a narrower groove that curves anteromedially across the lateral and anterior surface of the promontorium's anterior pole and ends at the pterygoid canal between the petrosal and basisphenoid. Kielan-Jaworowska et al. (1986) interpreted what we think to be the posterior aperture of the carotid canal as the 'hiatus Fallopii' (quotes in original) and the pterygoid canal as the carotid foramen. That the 'hiatus Fallopii' of Kielan-Jaworowska et al. (1986) is not homologous with that of other mammals was recognized by these authors and has been discussed by others (e.g., Miao, 1988; Luo, 1989; Wible and Hopson, 1995), but there is no consensus on alternative occupants for this aperture in *Chulsanbaatar* and *Nemegtbaatar*. Given the remarkable positional similarity with the posterior aperture of the carotid canal in *Kryptobaatar*, we think that it served the same function in *Chulsanbaatar* and *Nemegtbaatar*. We have seen the same arrangement, that is, a pterygoid canal arising from the carotid groove, in *Sloanbaatar* (ZPAL MgM-I/20) and *Kamptobaatar* (ZPAL MgM-I/33). Given the size of the aperture into the pterygoid canal in these forms, its occupants likely included an artery and nerve (i.e., the deep petrosal

nerve). As with *Kryptobaatar*, the greater petrosal nerve must have entered the canal directly from the cavum epiptericum and/or cavum supracochleare.

PETROSAL

During the last few years, we have published several phylogenetic analyses of Mesozoic mammaliomorphs relying principally on features of the petrosal bone (Wible and Hopson, 1993; Wible et al., 1995; Rougier et al., 1996a, 1996c). Among multituberculates, the petrosal has been described in some detail in various paulchoffatiids (Hahn, 1988; Lillegraven and Hahn, 1993), *Ptilodus* (Simpson, 1937; Luo, 1989; Wible and Hopson, 1995), *Chulsanbaatar*, *Nemegtbaatar* (Kielan-Jaworowska et al., 1986; Hurum, 1998a, 1998b), *Lambdopsalis* (Miao, 1988; Meng and Wyss, 1995), and from an array of isolated elements from the Late Cretaceous of North America (Kielan-Jaworowska et al., 1986; Luo, 1989, 1996; Luo and Ketten, 1991; Fox and Meng, 1997), including those referred to "*Catopsalis*" *joyneri* and *Mesodma thompsoni* (Wible and Hopson, 1993, 1995). A striking result of these studies has been how uniform the petrosal morphology is across Multituberculata, a conclusion reinforced by our descriptions of *Kryptobaatar*. However, the only derived petrosal feature shared by all multituberculates known to date is an infolded bony flange that contacts the promontorium and housed the epitympanic recess (Rougier et al., 1996a, 1996c). This bony flange is continuous with the anterior lamina and crista parotica in all multituberculates with the sole exception of *Lambdopsalis*, following Miao's (1988) interpretation (but see our comments in the Alisphenoid section above). Some of the petrosal features discussed below may be diagnostic of Multituberculata but are dependent on the phylogenetic positions of the exceptions. Other petrosal features have been discussed already under the Venous System and Arterial System sections.

Despite the general uniformity/similarity in petrosal morphology within Multituberculata, our comparisons of *Kryptobaatar* with other multituberculates have also highlighted differences (see also Kielan-Jawo-

rowska et al., 1986; Luo, 1989, 1996; Lillegraven and Hahn, 1993; Wible and Hopson, 1995; Kielan-Jaworowska and Hurum, 1997). Some of these differences are discussed here.

Jugular Fossa: Kielan-Jaworowska and Hurum (1997) used the size and depth of the jugular fossa in their phylogenetic analysis of selected multituberculate taxa. They reported it to be "small and shallow" in the hypothetical ancestor, based on Late Jurassic Plagiaulacoidea and *Ptilodus*, and "large and deep" in *Kryptobaatar* ("jf" in fig. 37A), *Nemegtbaatar*, *Chulsanbaatar*, *Catopsbaatar*, *Kamptobaatar*, and *Lambdopsalis*. To their list we add *Sloanbaatar* (ZPAL MgM-I/20). The only plagiaulacoid for which we could confirm a small, shallow jugular fossa was *Pseudobolodon* (V.J. 450-155, 460-155). In *Ptilodus gracilis* (USNM 6076) and *Ectypodus* (YPM-PU 14724), the jugular fossa is shallow but not small. Finally, we could not confirm the size and depth of the jugular fossa in *Catopsbaatar*.

Channel for Perilymphatic Duct: Prior to our description of *Kryptobaatar*, two character states of the channel for the perilymphatic duct in multituberculates had been identified by us (Rougier et al., 1996a, 1996c): (1) an open sulcus, and (2) a sulcus partially enclosed by bony lappets. The former state occurs in *Ptilodus* and *Mesodma thompsoni*, the latter in "*Catopsalis*" *joyneri*. We have subsequently seen bony lappets on the perilymphatic channel in *Mekechhoffatia krausei* (V.J. 446-155) and *Pseudobolodon oreas* (V.J. 460-155). *Kryptobaatar* exhibits a third state: no indication of the perilymphatic channel whatsoever.

Recessus Scalae Tympani: *Ornithorhynchus* possesses a distinct depression immediately external to the perilymphatic foramen, the recessus scalae tympani (perilymphatic recess of Fox and Meng, 1997), where the perilymphatic duct contacts the cavum tympani (Zeller, 1991, 1993). We have observed a similar depression in the triconodontid *Priacodon* (Rougier et al., 1996a). We also report a conspicuous recessus scalae tympani in the following multituberculates (see also Fox and Meng, 1997): *Ptilodus montanus* (AMNH 35490), *Ectypodus* (YPM-PU 14724), *Mesodma thompsoni*

(FMNH 53904), “*Catopsalis*” *joyneri* (AMNH 119445), and *Kamptobaatar* (ZPAL MgM-I/33). In contrast, the depression is inconspicuous in *Kryptobaatar*, *Pseudobolodon* (V.J. 460-155), *Meketichoffatia krausei* (V.J. 446-155), *Nemegtbaatar* (ZPAL MgM-I/81), *Sloanbaatar* (ZPAL MgM-I/20), and *Lambdopsalis* (Miao, 1988).

Post-promontorial Tympanic Recess: Our analyses (e.g., Wible and Hopson, 1993; Rougier et al., 1996a, 1996c) have indicated that the tall, horizontal crista interfenestralis marks the posterior boundary of the cavum tympani in multituberculates and that a post-promontorial tympanic recess behind the perilymphatic foramen was lacking. However, the crista interfenestralis is not very tall in any multituberculates, and at least in a few forms (e.g., *Pseudobolodon*, V.J. 450-155, 460-155) it seems likely that the cavum tympani extended into a post-promontorial recess. Moreover, if the depression identified above as the recessus scalae tympani had the same function as in *Ornithorhynchus* (i.e., housing a diverticulum of the perilymphatic duct that contacted the cavum tympani, Zeller, 1991), then the crista interfenestralis did not prevent the cavum tympani from reaching the perilymphatic duct in those multituberculates with a conspicuous recessus scalae tympani. A post-promontorial recess has heretofore been known only for prototribosphenidans (Wible, 1990) and isolated petrosals from the Early Cretaceous Khoobur locality (Wible et al., 1995). In light of the morphology in multituberculates, this character needs to be reevaluated before use in future phylogenetic studies.

Caudal Tympanic Process: Until recently, our analyses (e.g., Wible et al., 1995; Rougier et al., 1996a) had shown that a crest medial to the paroccipital process forming the posterior wall of the tympanic cavity was a synapomorphy of prototribosphenidans plus isolated petrosals from the Early Cretaceous Khoobur locality. In addition, a caudal tympanic process has been reported in the symmetrodont *Zhangheotherium* (Hu et al., 1997). A caudal tympanic process had been unknown for multituberculates, but Rougier et al. (1996a, 1996c) reported one in *Kryptobaatar* (“ctpp” in fig. 37A; PSS-MAE 113) and *Kamptobaatar* (ZPAL MgM-I/33).

To the list of multituberculates with a caudal tympanic process, we now add *Meketichoffatia krausei* (V.J. 446-155), *Chulsanbaatar* (ZPAL MgM-I/145), *Nemegtbaatar* (contra Rougier et al., 1996a; ZPAL MgM-I/82), and *Ptilodus gracilis* (USNM 6076). On the list of those without this process are *Pseudobolodon* (V.J. 450-155, 460-155) and *Ectypodus* (YPM-PU 14724).

Paroccipital Process: The form of the paroccipital process varies among multituberculates. We have described it above as triangular in *Kryptobaatar* (“ppr” in fig. 37A); this shape also occurs in *Meketichoffatia krausei* (V.J. 446-155), *Chulsanbaatar*, *Nemegtbaatar*, *Sloanbaatar*, and *Kamptobaatar* (see Kielan-Jaworowska and Hurum, 1997: fig. 11). The paroccipital process is a finger-like projection in *Ectypodus* (YPM-PU 14724), and is expanded posterolaterally in *Pseudobolodon* (V.J. 450-155) and *Ptilodus montanus* (AMNH 35490). Two of these conditions appear to characterize the paroccipital process of *Lambdopsalis*, where it is both triangular and posterolaterally expanded (Miao, 1988).

Medial Wall of Epitympanic Recess: Rougier et al. (1996c) reported that the medial wall of the epitympanic recess in *Kryptobaatar* (fig. 21; PSS-MAE 113) is formed by a sharp, ventrally projecting crest composed of the crista parotica posteriorly (“cp” in fig. 37A) and the lateral flange anteriorly. They also noted that the vertical nature of this wall would have severely constrained the possible positions of the stapes and incus. Hurum et al. (1996) observed a similar arrangement to the medial wall of the epitympanic recess in *Kamptobaatar* and *Chulsanbaatar* and suggested “that there must have been a significant vertical component in the plane of the manubrium and therefore of the tympanic membrane” (p. 269). We add here that a tall medial wall of the epitympanic recess also occurs in *Meketichoffatia* (V.J. 110-155), *Ptilodus* (AMNH 35490), *Mesodma thompsoni* (FMNH 53904), *Nemegtbaatar* (ZPAL MgM-I/82), *Catopsbaatar* (ZPAL MgM-I/78), and *Lambdopsalis* (Miao, 1988). In fact, the only multituberculate preserving the relevant anatomy that has a low medial wall is *Ectypodus* (YPM-PU 14724). We have not seen similarly developed medial

walls of the epitympanic recess in other Mesozoic mammaliaforms.

Lateral Wall of Epitympanic Recess: We found two different conditions for the lateral wall of the epitympanic recess in multituberculates: (1) either it is a low crest and the epitympanic recess is not sharply demarcated, so that the lateral braincase wall and epitympanic recess are confluent, or (2) prominent ridges separate the epitympanic recess from the lateral braincase wall. The former condition is found in *Meketichoffatia krausei* (V.J. 446-155), *Kuehneodon dryas* (V.J. 454-155), *Ectypodus* (YPM-PU 14724), *Mesodma thompsoni* (FMNH 53904), and *Kamptobaatar* (ZPAL MgM-I/33); the latter condition is found in *Kryptobaatar* (figs. 20, 21), *Pseudobolodon* (V.J. 450-155), *Ptilodus montanus* (AMNH 35490), *Chulsanbaatar* (ZPAL MgM-I/168), *Nemegtbaatar* (ZPAL MgM-I/76), *Sloanbaatar* (ZPAL MgM-I/20), *Catopsbaatar* (ZPAL MgM-I/78), “*Catopsalis*” *joyneri* (AMNH 119445), and *Lambdopsalis* (Miao, 1988).

Tensor Tympani Fossa: Our analyses (e.g., Wible and Hopson, 1993; Rougier et al., 1996a, 1996c) have indicated that the tensor tympani muscle occupied a deep recess in multituberculates (“ttf” in figs. 14, 37A). This remains true for most taxa, but a few (e.g., *Pseudobolodon*, V.J. 450-155, 460-155) have a shallow tensor tympani fossa.

Facial Ganglion Floor: In Rougier et al. (1996a, 1996c), we characterized the facial ganglion floor in multituberculates as a narrow petrosal bridge beneath the primary facial foramen. There are only a few forms in which this morphology can be verified, most notably various isolated petrosals from the North American Late Cretaceous studied by Luo (1989) and Wible and Hopson (1993, 1995). However, *Kryptobaatar* exhibits a different morphology; the apparent confluence of the facial canal with the canal for the ramus inferior produces a broad petrosal bridge beneath the facial ganglion. It is uncertain how widespread this morphology is within Multituberculata.

Cavum Supracochleare: Our analyses (e.g., Wible and Hopson, 1993; Rougier et al., 1996a, 1996c) have characterized multituberculates as having a cavum supracochleare, which housed the facial (geniculate)

ganglion, continuous with the cavum epiptericum. As with the facial ganglion floor, there are few taxa in which this morphology can be verified, most notably paulchoffatiids (Lillegraven and Hahn, 1993), “*Catopsalis*” *joyneri* (AMNH 119445), *Mesodma thompsoni* (FMNH 53904), and *Kryptobaatar* (PSS-MAE 123). Luo (1996: 49A) reported that a “geniculate ganglion completely enclosed in the cavum supracochleare” is a synapomorphy of Cimolomyidae and Taeniolabididae. Given that this statement was taken from a published abstract, we cannot evaluate the supporting evidence. However, Miao (1988, 1993) clearly has described the cavum supracochleare continuous with the cavum epiptericum in the taeniolabidid *Lambdopsalis*. The only cimolomyid represented by a petrosal is *Meniscoessus* (Luo, 1989), and the pattern of its cavum supracochleare has not yet been described. In our comparisons, we have discovered one multituberculate in which the cavum supracochleare is partially walled off from the cavum epiptericum and enclosed within the petrosal (i.e., *Ptilodus montanus*, AMNH 35490). A partially enclosed cavum supracochleare has been reported previously for *Vincelestes*, isolated petrosals from the Early Cretaceous of Mongolia, and a few marsupials, and a completely enclosed one was reported only in triconodontids, *Tachyglossus*, and most therians (Wible et al., 1995; Rougier et al., 1996a).

Hypertrophied Vestibule: Miao (1988) reported a greatly expanded vestibular apparatus in the Paleocene taxon *Lambdopsalis* and suggested it represented an adaptation to the perception of low-frequency vibrations, as has been posited for certain extant vertebrates with enlarged vestibules. Luo and Ketten (1991) examined isolated petrosals from the North American Late Cretaceous *Meniscoessus* and “*Catopsalis*” *joyneri* with CT and reported a more than 10-fold expansion in vestibular size over the condition in opossums and humans. They proposed that this extraordinary inflation was a diagnostic feature of known Cretaceous and Tertiary multituberculates and a possible synapomorphy of Multituberculata. The latter is unlikely in light of Lillegraven and Hahn’s (1993; see also Hurum et al., 1996; Fox and Meng,

1997) observation that the vestibule is not enlarged in the Late Jurassic paulchoffatiids. Moreover, we have seen no evidence of vestibular inflation from the outer contour of the petrosal in *Kryptobaatar*. Hurum et al. (1996) and Hurum (1998b) reported from analyses of serial sections that the vestibule in *Nemegtbaatar* and *Chulsanbaatar* is not much expanded, and Hurum (1998b: 90) stated that the dimensions of the inner ear “are within the limits expected for an extant, small mammal.” Therefore, the hypertrophied vestibule seen in *Lambdopsalis* (Miao, 1988), *Meniscoessus*, and “*Catopsalis*” *joyneri* (Luo and Ketten, 1991) most likely is a unique adaptation of these taxa for low-frequency hearing, as would be anticipated, for example, in burrowing forms.

HYPOGLOSSAL FORAMEN

Most Mesozoic mammaliaforms and near outgroups have a single hypoglossal foramen, although two are present in *Adelobasileus* (Luo, 1994). Hahn (1969) reported two small openings behind the jugular foramen in *Meketichoffatia krausei*, both of which he termed condyloid foramina. He (see also Hahn, 1988) reconstructed the spinal accessory nerve in the more anterior opening and the hypoglossal nerve in the posterior one. We are aware of no instance among extant mammals where the spinal accessory nerve has such a course, and in forms with two foramina (e.g., *Didelphis*, Wible, 1990) both transmit components of the hypoglossal nerve. Among other multituberculates, a single hypoglossal foramen has been described for *Ptilodus* (Simpson, 1937) and *Lambdopsalis* (Miao, 1988) and was illustrated for *Ectypodus* (Sloan, 1979: fig. 1). Among Mongolian Late Cretaceous taxa, the hypoglossal foramen is reported to be either absent, confluent with the jugular foramen (as in monotremes; “jfo + hyf” in fig. 28), or indiscernible (Kielan-Jaworowska et al., 1986). *Kryptobaatar* (PSS-MAE 101) is the exception, with a small aperture in the appropriate place that we have tentatively identified as a hypoglossal foramen.

ENDOCRANIUM

CAVUM EPIPTERICUM AND PRIMARY BRAINCASE WALL

Among multituberculates, the structure of the cavum epiptericum has been considered in detail in *Kryptobaatar*, *Meketichoffatia krausei* (Hahn, 1981), *Lambdopsalis* (Miao, 1988), *Nemegtbaatar* and *Chulsanbaatar* (Hurum, 1998a). In *Kryptobaatar*, the cavum epiptericum is an oval endocranial space outside the primary wall of the braincase, posterolateral to the hypophyseal fossa (“ce” in figs. 25B, 26, 27). Contributing to the walls of the cavum epiptericum in *Kryptobaatar* are: posteriorly, the petrosal; laterally, the anterior lamina and alisphenoid; medially, the orbitosphenoid, presphenoid, and basisphenoid, as well as the ossified pilae antotica and metoptica; dorsally, the orbitosphenoid and ossified pilae antotica and metoptica; and ventrally, the petrosal, alisphenoid, and perhaps maxilla. As reconstructed here, the cavum epiptericum in *Kryptobaatar* contained the trigeminal and facial ganglia and the cavernous sinus; traversing the cavum were the divisions of the trigeminal nerve, the trochlear and abducens nerves, the greater petrosal nerve, the ramus infraorbitalis of the stapedial artery, and the ophthalmic veins.

The cavum epiptericum in *Lambdopsalis*, *Nemegtbaatar*, and *Chulsanbaatar* resembles that in *Kryptobaatar* in most regards. Differences exhibited by *Lambdopsalis* include the presence of a conspicuous recess for the facial ganglion in the posterior part of the cavum epiptericum; the large alisphenoid in the lateral wall of the cavum epiptericum, enlarged at the expense of the anterior lamina; and the exclusion from the cavum epiptericum of the ramus infraorbitalis at least in part by its course through an alisphenoid canal (but see above). Also, given the more posterior position of the metoptical foramen, the oculomotor nerve in *Lambdopsalis* would have run through the front part of the cavum epiptericum.

Hahn (1981) illustrated and described the cavum epiptericum in a specimen of *Pseudobolodon oreas*, which he later identified (Hahn, 1993) as *Meketichoffatia krausei*. Its cavum epiptericum was shown to be a long, narrow, roofless space lateral to the hypo-

physeal fossa and tuberculum sellae that ended anteriorly at the sphenorbital canal. As described by Hahn (1981), the absence of a roof distinguishes the cavum of *Meketichoffatia* from that of *Kryptobaatar*, *Lambdopsalis*, *Nemegtbaatar*, and *Chulsanbaatar* in which an extensive roof is formed by the ossified primary wall of the braincase. We have had the opportunity to study the basisphenoid of *Meketichoffatia* (V.J. 443-155) in light of that in *Kryptobaatar*. We think that a roof formed by the primary wall was present, although not as thick and extensive as in *Kryptobaatar*, *Lambdopsalis*, *Nemegtbaatar*, and *Chulsanbaatar*; however, the roof has been damaged in *Meketichoffatia* through compression. In fact, there is evidence of breaks in what we interpret to be the medial edge of the roof at the level of the anterior extent of the hypophyseal fossa. Additionally, what Hahn (1981) described as the sphenorbital canal is really just the anterior part of the roofed cavum epiptericum. Also distinguishing the cavum of *Meketichoffatia* is a small longitudinal canal running through the floor, within which Hahn (1981) placed a blood vessel and which Miao (1988) subsequently identified as an alisphenoid canal resembling that purported for *Lambdopsalis*. We are uncertain of the nature of this canal in *Meketichoffatia*. However, because of the canal's length, extreme medial position, and small diameter, it is unlikely an alisphenoid canal. Finally, a metoptic foramen is not indicated in *Meketichoffatia*, but may have been damaged along with the bulk of the roof of the cavum epiptericum.

The structure of the cavum epiptericum in other mammaliaforms and near outgroups differs in various ways from that in multituberculates. First, there is only a partial floor below the cavum epiptericum in *Adelobasileus*, *Sinoconodon*, *Dinnetherium*, *Megazostrodon*, and *Morganucodon* (Luo, 1994). Second, the cavum supracochleare is separated wholly or partially from the cavum epiptericum in triconodontids, isolated petrosals from the Early Cretaceous Khoobur locality, *Vincelestes*, *Tachyglossus*, and therians (Rougier et al., 1996a). Third, a course for the oculomotor nerve separate from the other contents of the cavum epiptericum is not known for any other mammaliaforms, al-

though as discussed below this may be a preservational artifact and is likely primitively present in Mammalia. Finally, perhaps the most striking difference is the presence of a massive roof over the cavum epiptericum formed by the primary braincase in multituberculates, and its absence in all other mammaliaforms known thus far, as noted by Kielan-Jaworowska et al. (1986). According to Lucas and Luo (1993), only a very small remnant of the primary wall, the slender ossified base of the pila antotica, occurs in *Adelobasileus*, *Sinoconodon*, *Megazostrodon*, *Morganucodon*, and monotremes. In the first three taxa, the pila antotica has only been described from the ventral view, where it is visible through the open floor of the cavum epiptericum, and the pila may have been more substantial than thus far reported. However, the massive ossified pila antotica of *Kryptobaatar* ("pan" in figs. 25–27), *Lambdopsalis*, *Nemegtbaatar*, and *Chulsanbaatar* exceeds any other ossified pila reported thus far among cynodonts, suggesting that this is a secondary specialization of these multituberculates. This thickening and extension of the pila antotica might be a derived feature for Multituberculata, of which the condition in *Meketichoffatia* might represent an early stage.

Considering that the common ancestor of all mammals is thought (e.g., Starck, 1967, 1978; Kuhn, 1971; Zeller, 1989) to have had a fully developed primary wall (the pilae preoptica, metoptica, and antotica; fig. 24A, B), the presence of these structures is expected at least in all pre-mammalian synapsids if these elements are homologous across Amniota. However, the term pila refers to a chondrocranial structure that need not be ossified in the adult, as occurs in most adult sauropsids (De Beer, 1937; Bellairs and Kamal, 1981). In Mammaliaformes, the orbital region both externally and internally is rarely preserved or accessible for preparation, hampering the recognition of the presence of the primary wall and its foramina. Based on the presence of an optic foramen in the orbitosphenoid of *Probainognathus*, *Sinoconodon*, and *Adelobasileus*, we expect the optic foramina to have been present in the orbitosphenoid of the mammaliaforms occupying a phylogenetic position between these Triassic/

Early Jurassic forms and Mammalia. This in turn implies an independent loss of an ossified pila metoptica in monotremes, marsupials, and *Vincelestes*, or the absence of the pila metoptica in the ancestry of multituberculates and therians, with the reacquisition of a neomorphic pila metoptica in eutherians as suggested by Maier (1987) and in multituberculates. Accepting the phylogenetic position for multituberculates (fig. 39) proposed by Rowe (1988, 1993), Sereno and McKenna (1995), Rougier et al. (1996a, 1996c), Hu et al. (1997), and Ji et al. (1999), the latter scenario is favored. The loss of the pila antotica in marsupials and eutherians can be considered a synapomorphy (Rowe, 1988). The problem of the presence/absence of a metoptic foramen is more complex because even if perfectly preserved in most cases, it will be confined deep within the cavum epiptericum and hidden in lateral view by the secondary braincase wall. As noted by Miao (1988), given the presence of a metoptic foramen in multituberculates, it is likely that this foramen was also present in pre-multituberculate mammaliaforms.

HYPOPHYSEAL FOSSA, TUBERCULUM SELLAE, AND JUGUM SPHENOIDALE

The entire structure of the hypophyseal fossa is known for only five multituberculates: *Kryptobaatar* ("hf" in figs. 25, 27), *Meketichoffatia krausei* (originally described as *Pseudobolodon oreas* by Hahn, 1981), *Lambdopsalis* (Miao, 1988), *Nemegtbaatar*, and *Chulsanbaatar* (Hurum, 1998a). In all taxa, the hypophyseal fossa is a very deep excavation in the dorsal surface of the braincase floor, bordered laterally by tall walls formed by the primary wall of the braincase. The dorsum sellae, which forms the posterior wall, is also very prominent in *Kryptobaatar* ("ds" in figs. 25, 26), *Meketichoffatia*, *Nemegtbaatar*, and *Chulsanbaatar*, but is low in *Lambdopsalis*. Well-developed carotid foramina enter the posterolateral aspect of the hypophyseal fossa in *Kryptobaatar* ("fica" in figs. 25, 27), *Nemegtbaatar*, and, as interpreted here, *Meketichoffatia*; Hahn (1981) incorrectly identified the endocranial entrance of the carotid as in the dorsum sellae in *Meketichoffatia*. Carotid foramina are more an-

teriorly placed in the hypophyseal fossa in *Chulsanbaatar* (Hurum, 1998a) and are described by Miao (1988) as wholly lacking in *Lambdopsalis*.

Among Mesozoic mammaliaforms, the structure of the hypophyseal fossa is known only in *Morganucodon* and *Triconodon*. In the former, as reconstructed from several incomplete basisphenoids by Kermack et al. (1981), the hypophyseal fossa is bordered by tall anterior and lateral walls, with the dorsum sellae being very low; the carotid foramina enter the anteriormost aspect of the fossa's floor. A single basisphenoid is known for *Triconodon* (Kermack, 1963; Kermack et al., 1981); it shows a fairly shallow hypophyseal fossa with anteriorly placed carotid foramina in the floor, but this specimen has been compressed, hindering evaluation. Among extant mammals, the hypophyseal fossa is generally shallow, with the dorsum sellae being the most prominent wall (Kuhn, 1971; Archer, 1976; Novacek, 1986; Zeller, 1989); the carotid foramina enter the posterior aspect of the hypophyseal fossa in monotremes but tend to lie wholly lateral to the fossa in therians.

In addition to *Kryptobaatar*, the endocranial surface anterior to the hypophyseal fossa, that is, the tuberculum sellae and the jugum sphenoidale ("tus" and "jsp" in fig. 25A), has been described in detail only in *Meketichoffatia* by Hahn (1981). The major difference between *Kryptobaatar* and *Meketichoffatia* is the proportional shortening of the mesocranium in the former. In *Meketichoffatia*, the tuberculum sellae, hypophyseal fossa, and cavum epiptericum are long, whereas in *Kryptobaatar* these structures are shorter and broader (fig. 27). Damage to the area labeled as the fossa hypochiasmatica in *Meketichoffatia* (Hahn, 1981: fig. 4) obscures the morphology of the rostral portion of the tuberculum sellae; crushing has collapsed the orbital wings over this region. This is the area where the optic foramina and chiasmatic sulcus would be expected. Consequently, crushing may account for the apparent absence of structures in *Meketichoffatia* that we have found in *Kryptobaatar*.

The jugum sphenoidale in *Meketichoffatia* has a broad, shallow sulcus on the midline, whereas the jugum is narrow in *Kryptobaa-*

tar and even narrower in PSS-MAE 128. The orbital wings in *Meketichoffatia* are broad and continue anterodorsally into the lamina infracribrosa, much as in *Kryptobaatar*. Hahn (1981) describes the cranial aperture of the ethmoidal foramen in *Meketichoffatia*, which seems to occupy a position similar to that in *Kryptobaatar*.

CRIBRIFORM PLATE

An ossified cribriform plate is ubiquitous in living mammals except for the platypus, which is known to have a cartilaginous one that resorbs during ontogeny (Zeller, 1988). The cribriform plate is seldom preserved in fossils, because of its delicate nature and its inaccessibility to preparation. Among multituberculates, a purported cribriform plate has

been reported in a serially sectioned *Nemegtbaatar* (Kielan-Jaworowska et al., 1986; Hurum, 1994) based on tiny bone fragments in the appropriate region. *Kryptobaatar* and *Lambdopsalis* (Miao, 1988), which show pristine preservation of delicate endocranial structures, have failed to provide any evidence of an ossified cribriform plate. However, given the extant phylogenetic bracket for multituberculates, the presence of a cartilaginous or ossified cribriform plate is expected. In fact, the presence of at least a cartilaginous cribriform plate has been suggested in *Diarthrognathus* and *Thrinaxodon* based on differential matrix preservation in the nasal and cranial cavities (Crompton, 1958). Consequently, the presence of a cribriform plate cartilaginous and/or osseous is likely an ancient trait in cynodont history.

CONCLUSIONS

The cranial anatomy of Mongolian Late Cretaceous multituberculates, in particular *Nemegtbaatar* and *Chulsanbaatar*, has previously been evaluated in some detail in a series of papers by Kielan-Jaworowska (e.g., 1974) and various co-workers (e.g., Kielan-Jaworowska et al., 1986; Gambaryan and Kielan-Jaworowska, 1995; Hurum et al., 1996). In the tradition of these studies, our descriptions of *Kryptobaatar dashzevegi* present the first bone-by-bone treatment of cranial anatomy in the most abundant Mongolian Late Cretaceous multituberculate, which is derived from specimens revealing most of the osseous sutural relationships as well as most of the grooves, canals, and foramina relevant to the cranial nervous, arterial, and venous systems. The only significant components of the skull of *Kryptobaatar* lacking from our description are the nasal fossa and paranasal sinuses. Yet, without recourse to serial sectioning, which allowed the description of this region in *Nemegtbaatar* and *Chulsanbaatar* (Hurum, 1994), or high-resolution CT scanning, which has revealed details of internal anatomy in the skull of, for example, the primitive non-mammalian cynodont *Thrinaxodon* (Rowe et al., 1995), none of the available specimens of *Kryptobaatar* exhibited sufficient exposure of the

nasal fossa to enable description. The specimens of *K. dashzevegi* studied by us provided little new information on brain structure to address the questions raised by Kielan-Jaworowska (1997) concerning neglected characters of the multituberculate brain.

The exquisite state of preservation of specimens of *Kryptobaatar dashzevegi* has offered us a rare glimpse of details of cranial anatomy that are seldom preserved in an undistorted manner in Mesozoic mammaliaforms, with *Morganucodon* (Kermack et al., 1981) and *Vincelestes* (Rougier et al., 1992; Rougier, 1993; Hopson and Rougier, 1993) being among the more noteworthy exceptions. The anatomical details uncovered by our study impact knowledge of the skull of multituberculates, and of Mesozoic mammaliaforms in general, in various ways.

(1) We have been able to describe osseous elements poorly known or not known at all for other multituberculates or other Mesozoic mammaliaforms. Elsewhere (Rougier et al., 1996c), we have provided descriptions of the stylohyal and partial stapes, malleus, and ectotympanic, the first for some of these elements among Multituberculata and for the stylohyal among Mesozoic Mammaliaformes.

Although partial jugals have been reported

for *Ptilodus*, *Nemegtbaatar*, and *Chulsanbaatar* (Hopson et al., 1989), those in *Kryptobaatar* are the first complete jugals known for multituberculates. In all instances, the jugal is a reduced element lying internal to the maxilla and the squamosal in the zygomatic arch. Among other mammaliaforms, monotremes resemble multituberculates in that the jugal is replaced in the zygomatic arch by the maxilla and the squamosal (Hopson et al., 1989). However, the pattern of replacement differs somewhat; in the platypus, the reduced jugal is situated dorsal to the maxilla and the squamosal (Zeller, 1989), and in the echidna, the jugal is wholly absent (Kuhn, 1971).

The orbital mosaic and foramina and the endocranium were largely unknown in multituberculates prior to our study, with the major exceptions being *Lambdopsalis* (Miao, 1988), *Nemegtbaatar*, and *Chulsanbaatar* (Hurum, 1994, 1998a), and were also poorly known in other Mesozoic mammaliaforms. We have confirmed Miao's (1988) observation in *Lambdopsalis* of an optic foramen, a metoptic foramen, and an extensive, thick ossified primary wall of the braincase including the pila metoptica and antotica; the latter two also occur in *Nemegtbaatar* and *Chulsanbaatar* (Hurum, 1998a). The presence of these structures in these taxa, as well as embryological evidence, suggests that the optic foramen, the metoptic foramen, and an extensive ossified primary wall may be more widespread among Multituberculata and Mammaliaformes. The robust nature of the pila antotica in *Kryptobaatar*, *Lambdopsalis*, *Nemegtbaatar*, *Chulsanbaatar*, and perhaps *Meketichoffatia* may be a derived feature of Multituberculata, because the ossified remnants of the pila in the outgroups are not as substantive. We have also described for the first time in multituberculates a foramen for the pituito-orbital vein, unknown in other mammaliaforms, and a transverse canal, occurring only in some metatherians and placentals (McDowell, 1958; Archer, 1976).

(2) We have been able to confirm the absence of several elements from the multituberculate skull whose incidence has been controversial. *Kryptobaatar* clearly lacks an ectopterygoid, a prenasal process of the premaxilla, and a septomaxilla, all of which

have been posited for multituberculates (see, respectively, Kielan-Jaworowska, 1971; Miao, 1988; Hahn and Hahn, 1994). These elements now appear to be ubiquitously absent in multituberculates or, at the minimum in the case of the prenasal process, not present primitively in the group. Multituberculates share the absence of an ectopterygoid with other mammaliaforms except apparently *Morganucodon* (Kermack et al., 1981), the absence of a prenasal process with other mammals (Wible, 1991), and the absence of a septomaxilla with marsupials and placentals (Wible et al., 1990), with the possible exception of some xenarthrans (Zeller et al., 1993).

Kryptobaatar also clearly lacks an orbital exposure of the palatine, which may represent a synapomorphy of multituberculates as suggested by Miao (1988, 1993). Hurum (1994, 1998a) argued against this interpretation, in light of his description of the palatine in the orbit of *Nemegtbaatar*. However, it appears that Hurum's interpretation of *Nemegtbaatar*, if correct, is unusual among multituberculates.

(3) We have been able to confirm the presence of several elements in the multituberculate skull whose incidence has been controversial. Miao (1988, 1993) questioned whether any multituberculate really has an alisphenoid with a reduced contribution to the lateral wall of the braincase, as initially described by Kermack and Kielan-Jaworowska (1971) and Kielan-Jaworowska (1971). *Kryptobaatar* clearly has such a reduced alisphenoid, and its presence confirms the tentative observations of such an element in other Mongolian Late Cretaceous taxa (Kielan-Jaworowska, 1971; Kielan-Jaworowska et al., 1986). *Kryptobaatar* also clearly shows that the anterior lamina is expanded forward dorsal to the alisphenoid, again confirming previous observations in other Mongolian Late Cretaceous taxa (Kielan-Jaworowska, 1971; Kielan-Jaworowska et al., 1986; Hurum, 1998a). Both of these elements, a reduced alisphenoid and expanded anterior lamina, are shared by Mongolian Late Cretaceous multituberculates and monotremes (Wible and Hopson, 1993). Moreover, these characters have been used to support a monotreme-multituberculate clade (Wible

and Hopson, 1993; Meng and Wyss, 1995), which more recent analyses, some of which include this feature, do not support (fig. 39; Rougier, 1996a, 1996c; Hu et al., 1997; Ji et al., 1999).

(4) We have been able to resolve competing anatomical hypotheses for several elements of the multituberculate and mammaliaform skull. The troughs lateral to the pterygopalatine ridges that occur in *Kryptobaatar* and most Mesozoic mammaliaforms have been said to have accommodated the auditory tube (Barghusen, 1986) or to have provided muscle attachment (Kielan-Jaworowska, 1971; Hahn, 1981; Gambaryan and Kielan-Jaworowska, 1995). The morphology in *Kryptobaatar* eliminates the auditory tube as a possible occupant, because the troughs extend too far anteriorly into the nasal cavity rather than ending in the nasopharynx, the site of origin for the auditory tube in extant mammals (Starck, 1995). We think that the lateral troughs provided muscle attachment and/or an accessory route for air in *Kryptobaatar* and other Mesozoic mammaliaforms.

Miao (1988) has argued that the element identified (e.g., Kielan-Jaworowska et al., 1986) as a postorbital process on the parietal in Mongolian Late Cretaceous multituberculates is not a true postorbital process, which, he suggested, is reduced or absent in Multituberculata. However, the process on the parietal in question in *Kryptobaatar* has the same positional relationship to the frontal diploic vein and the supraorbital nerves and vessels, as does the true postorbital process on the frontal in extant mammals. Consequently, the postorbital process, which is inconspicuous and on the frontal in other multituberculates, has shifted onto the parietal and become enlarged in Mongolian Late Cretaceous taxa.

Kielan-Jaworowska et al. (1986) have argued, on the basis of serial sections of *Nemegtbaatar*, that the aperture at the back of the palate identified (e.g., Kielan-Jaworowska, 1971) as a minor palatine (palatonasal) foramen in multituberculates is merely a notch that does not fully penetrate bone. Along with a minor palatine foramen, we have found a second aperture in the orbital process of the maxilla in *Kryptobaatar* resembling that leading into the minor palatine

canal in therians (Novacek, 1986). Therefore, we deem it likely that the palatal aperture in question in *Kryptobaatar* is a true foramen that transmitted the minor palatine nerve and vessels, as occurs in most mammaliaforms including other multituberculates (except possibly *Nemegtbaatar*).

Most Mesozoic mammaliaforms, including multituberculates, have multiple apertures in and around the anterior lamina that have been interpreted as having transmitted branches of the trigeminal nerve (Luo, 1994). Two models for the nerves in these apertures have been proposed: branches of the mandibular nerve transmitted in multituberculates (Simpson, 1937; Kielan-Jaworowska, 1971), and the maxillary and mandibular nerves transmitted as in other mammaliaforms (Patterson and Olson, 1961; Kermack et al., 1981). The morphology in *Kryptobaatar* and the vast majority of multituberculates support the former restoration for multituberculates, because the foramina in question are at the same anteroposterior level, which is not the pattern that the maxillary and mandibular nerve exits exhibit in any extant mammal. The implications of this for the reconstruction of nerves in other Mesozoic mammaliaforms are yet to be explored, but at a minimum legitimate concerns have been raised (see also Rougier et al., 1996a).

Kielan-Jaworowska et al. (1986) suggested that the enormous jugular fossa in Mongolian Late Cretaceous multituberculates housed large ganglia on the cranial nerves below the jugular foramen. The exceedingly large dimensions of the jugular fossa and its connection with the middle-ear cavity in *Kryptobaatar* suggest that this recess housed a diverticulum of the cavum tympani (Rougier et al., 1996c). We think that this interpretation can be extended to other multituberculates with large jugular fossae.

(5) We have been able to reconstruct the major components of both the cranial arterial and venous patterns in *Kryptobaatar*. The cranial vascular system of *Kryptobaatar* in general resembled that restored previously for multituberculates (e.g., Kielan-Jaworowska et al., 1986; Miao, 1988; Wible and Hopson, 1995) or for other Mesozoic mammaliaforms (e.g., Rougier et al., 1992). However,

the specimens of *Kryptobaatar* have provided insight into the course of several vessels previously unreconstructed for multituberculates. *Kryptobaatar* clearly had a transpromontorial internal carotid artery, and based upon this observation, we have discovered transpromontorial carotid grooves in a variety of other multituberculates. A groove for a transpromontorial internal carotid is a feature that multituberculates share with *Vincelestes* (Rougier et al., 1992) and certain eutherians (Wible, 1986), but it is absent in basal mammaliaforms, symmetrodonts, triconodontids, monotremes, and marsupials. Consequently, a transpromontorial sulcus has been acquired convergently in multituberculates and prototribosphenidans.

The endocranial aperture of the carotid foramen is in the posterolateral aspect of the deep hypophyseal fossa in *Kryptobaatar*, *Pseudobolodon* (Hahn, 1981), and *Nemegtbaatar* (Kielan-Jaworowska et al., 1986; Hurum, 1998a), whereas it is more anteriorly placed in *Chulsanbaatar* (Hurum, 1998a). Our comparisons with other Mesozoic mammaliaforms have led us to an additional observation of potential phylogenetic impact: the endocranial aperture of the carotid foramen is in the hypophyseal fossa in most taxa with the exception of marsupials and placentals, in which it is wholly lateral to the fossa.

The positions of the groove for the stapedial artery and the foramina for its end branches, along with the partial bicurrate stapes described for *Kryptobaatar* elsewhere (Rougier et al., 1996c), support a course for the artery through the stapes. We have found a similar arrangement of sulci and foramina in a wide variety of other multituberculates, with the exception being *Lambdopsalis*, in which the artery ran posterodorsal to the oval window (Miao, 1988), as in the platypus (Wible, 1987). Consequently, the vast majority of multituberculates exhibited the same relationship between the stapedial artery and stapes as in all extant eutherians in which the artery is present in the adult (Wible, 1987). The same pathway has been inferred for *Vincelestes* (Rougier et al., 1992). Multituberculates differ, however, from *Vincelestes* and most eutherians in the course of the stapedial artery beneath the promontorium of the petrosal. The multituberculate vessel ran pos-

terolaterally to reach the fenestra vestibuli, whereas it had a lateral or anterolateral course in the remaining taxa.

The cranial venous system of *Kryptobaatar* and other multituberculates resembled that in monotremes, with the primary exits from the cranial cavity being the prootic canal and the foramen magnum. However, *Kryptobaatar* is unique among mammaliaforms known to date in having a separate foramen for the pituitary-orbital vein and is unique among non-therians in having a transverse canal vein.

Lambdopsalis, whose cranial anatomy has been described in detail (Miao, 1988), has served as a model for Multituberculata in several phylogenetic analyses (e.g., Wible, 1991; Meng, 1992; Meng and Wyss, 1995), despite this taxon's extreme specializations for burrowing and numerous apomorphic cranial features compared with Mongolian Late Cretaceous taxa (Miao, 1988; Luo, 1996). A goal of our report on *Kryptobaatar* has been to provide a detailed description of the skull and lower jaws of a less specialized form that can serve as an appropriate model for future comparative morphological and phylogenetic studies on Multituberculata and on Mammaliaformes in general. In most aspects of its cranial anatomy, *Kryptobaatar*, and not *Lambdopsalis*, resembles the vast majority of other multituberculates. Cranial features that *Kryptobaatar* shares with most multituberculates, but which differ in *Lambdopsalis*, include: the absence of the prenasal process of the premaxilla; an anterior nasal notch; fewer nasal foramina; the presence of a lacrimal; a more extensive orbital exposure of the orbitosphenoid; a foramen for the frontal diploic vein; the anterior opening of the orbitotemporal canal below the postorbital process; the presence of a jugal; the presence of pterygopalatine ridges; a reduced alisphenoid; mandibular nerve foramina in the anterior lamina; a transpromontorial internal carotid artery; carotid foramina in the posterolateral hypophyseal fossa; a stapedial artery that ran through a bicurrate stapes; a supraglenoid foramen opening at a level anterior to the oval window; the posterior opening of the posttemporal canal low on the occiput; an epitympanic recess on the lateral flange; a crista parotica continuous with the

lateral flange; a caudal tympanic process of the petrosal; a triangular paroccipital process; a nonhypertrophied vestibule; and a tall dorsum sellae. In contrast, there are only a few features in which *Lambdopsalis*, and not *Kryptobaatar*, exhibits the likely primitive multituberculate condition. These include: an inconspicuous postorbital process on the frontal; the absence of a buccinator foramen between the anterior lamina and alisphenoid; the absence of a transverse canal foramen; and a large jugular foramen that transmitted the sigmoid sinus.

In our descriptions of *Kryptobaatar* and comparisons with other multituberculates, a number of features of the cranial anatomy have been identified that are shared at various levels within Multituberculata. Evaluating the phylogenetic significance of these features both within Multituberculata and within Mammaliaformes is beyond the scope of the current report and awaits an in-depth analysis of multituberculate interrelationships.

In lieu of a such an analysis, we compare our descriptions of *Kryptobaatar* to the recent diagnoses of Djadochtatheria, Djadochtatheriidae, and *Kryptobaatar* published by Kielan-Jaworowska and Hurum (1997), based on their cladistic analysis of 43 characters, (18 dental and 25 cranial). Djadochtatheria includes 10 of the 11 Mongolian Late Cretaceous multituberculate genera (with the exception being *Buginbaatar*) and tentatively 2 North American genera (*Paracimexomys* and *Pentacosmodon*). Djadochtatheriidae includes *Kryptobaatar*, *Djadochtatherium*, *Catopsbaatar*, and *Tombaatar*. Rougier et al. (1997a) have also placed *Kryptobaatar* within a monophyletic Mongolian Late Cretaceous clade, which also includes *Pentacosmodon* (fig. 38). However, the characters supporting the interrelationships of these taxa are largely from the dentition and, therefore, less relevant to our consideration of the cranial anatomy of *Kryptobaatar*.

For Djadochtatheria, Kielan-Jaworowska and Hurum (1997: 206) cited the following cranial synapomorphies: "large frontals, pointed anteriorly in the middle, deeply inserted between the nasals; U-shaped frontoparietal suture; a sharp edge between the lateral and palatal walls of premaxilla (rounded

in other multituberculates). A large roughly rectangular facial surface of the lacrimal, exposed on the cranial roof, separating the frontal from the maxilla is also characteristic for Djadochtatheria, but this may be a plesiomorphy." Of these proposed synapomorphies, only two are found exclusively in djadochtatherians: the frontoparietal suture is V-shaped in non-djadochtatherians, including the paulchoffatiid *Pseudobolodon* (V.J. 447.155, 451-1255, 460-155), *Ptilodus* (Simpson, 1937), and taeniolabidids (Granger and Simpson, 1929; Miao, 1988); and the facial exposure of the lacrimal is arcuate in non-djadochtatherians, including the paulchoffatiids *Kuehneodon* (V.J. 454-155), *Meketichoffatia* (V.J. 446-155), and *Pseudobolodon* (Hahn and Hahn, 1994; V.J. 460-155). However, given that a V-shaped process of the frontals also contacts the nasals in the paulchoffatiids *Kuehneodon* (V.J. 454-155), *Meketichoffatia* (V.J. 446-155), and *Pseudobolodon* (V.J. 447.155, 451-1255, 460-155), this purported djadochtatherian feature may be plesiomorphous for Multituberculata. In addition to djadochtatherians, the sharp edge between the lateral and palatal walls of the premaxilla occurs in *Lambdopsalis* (Miao, 1988).

For Djadochtatheriidae, Kielan-Jaworowska and Hurum (1997: 208) cited the following: ". . . differs from all other multituberculates (and all other mammals) in having a subtrapezoidal snout in dorsal view, with the anterior and lateral margins confluent with the zygomatic arches rather than incurved in front of the arches . . . [differs] from other members of Djadochtatheria in having the snout extending for 50% or more of the skull length, anterior part of promontorium (*sensu* Hurum et al., 1996) irregular, with incurvatures on both sides rather than oval (a character shared with *Lambdopsalis*)." As noted by Kielan-Jaworowska and Hurum (1997), the features of the snout distinguish *Kryptobaatar*, *Djadochtatherium*, and *Catopsbaatar* from other multituberculates, but the promontorial feature is known only for *Kryptobaatar* and *Catopsbaatar*. None of these djadochtatheriid characters has yet been described for *Tombaatar*.

For *Kryptobaatar*, Kielan-Jaworowska and Hurum (1997: 208) provided the following

revised diagnosis: “The smallest member of the Djadochtatheriidae nov. (skull length 25–32 mm), most similar to *Djadochtatherium*, with which it shares an arcuate (rather than trapezoidal as in *Catopsbaatar*) p4. The p4 in *Kryptobaatar* is relatively longer than in *Djadochtatherium* and has eight serrations (number unknown in *Djadochtatherium*). Differs from *Catopsbaatar* in having smaller facial surface of the lacrimal; differs from *Djadochtatherium* and *Catopsbaatar* in having a shorter postorbital process. Shares with MLCM [Mongolian Late Cretaceous multituberculates] except *Tombaatar* the alveolus for I3 formed by premaxilla, rather than by both premaxilla and maxilla (autapomorphy of *Tombaatar*). Differs from *Catopsbaatar* and *Tombaatar* in having four upper premolars. Differs from *Catopsbaatar* in having an inner row of cusps in M1 extending for less than a half, or a half of the tooth length, rather than a long row; shares short inner row of cusps in M1 with *Tombaatar* and the North American *Paracimexomys* (Lillegraven 1969; Archibald 1982). Differs from *Chulsanbaatar* and *Sloanbaatar* in having cusps on the inner ridge in M1, rather than a smooth ridge. Differs from *Tombaatar* in having M1 cusp formula 4–5:4:3–5 rather than 5:5:2. Differs from *Djadochtatherium* and *Catopsbaatar* in having a shorter snout (but longer than in non-djadochtatheriid djadochtatherians), a relatively less robust lower incisor, and less prominent masseteric and parietal crests.”

Our additions and amendments to their revised diagnosis follows: Differs from other djadochtatherians in having either confluent carotid and pterygoid canals or a very short separation between the two, a separate hypoglossal foramen, a foramen for the pituito-orbital vein, and a transverse canal. Differs from *Nemegtbaatar* in that the anterior opening of the posttemporal canal is between the parietal, frontal, and anterior lamina. Differs from *Nemegtbaatar*, *Chulsanbaatar*, and *Kamptobaatar* in having a smaller orbital exposure of the orbitosphenoid. Differs from *Nemegtbaatar*, *Chulsanbaatar*, and *Catopsbaatar* in that the anterior and intermediate zygomatic ridges are confluent and the posterior ridge is absent. Differs from *Nemegtbaatar* and *Kamptobaatar* in that the poste-

rior opening into the posttemporal canal is within the petrosal. Differs from *Chulsanbaatar* and *Sloanbaatar* in that the supraglenoid foramen is at a level anterior to the fenestra vestibuli. Resembles *Sloanbaatar* in having I2s directed ventromedially and in contact with each other, leaving a triangular open space between them and the edge of the premaxilla. Resembles *Djadochtatherium* and *Catopsbaatar* in having a long postorbital process on the parietal (contra Kielan-Jaworowska and Hurum, 1997). Resembles *Nemegtbaatar* and *Sloanbaatar* in the absence of a conspicuous recessus scalae tympani. Resembles *Nemegtbaatar* and *Chulsanbaatar* in having a sigmoid sinus that exits via the foramen magnum and not the jugular foramen. Resembles *Kamptobaatar* and *Chulsanbaatar* in having a foramen of the dorsal ascending canal. Resembles *Kamptobaatar*, *Nemegtbaatar*, *Chulsanbaatar*, and *Catopsbaatar* in having both the foramen ovale inferium and foramen masticatorium traverse the epitympanic recess.

ACKNOWLEDGMENTS

For the great privilege of studying the exquisite MAE skulls of *Kryptobaatar*, we are grateful to Dr. Demberelyin Dashzeveg of the Geological Institute of the Mongolian Academy of Sciences, Ulaan Baatar, Mongolia, and Dr. Michael J. Novacek of the American Museum of Natural History. For the high-resolution CT scans of *Kryptobaatar*, we thank Dr. Timothy Rowe of the University of Texas, Austin. For access to comparative materials, we thank G. Hahn, Institut für Geologie und Paläontologie, Philipps-Universität, Marburg; J. A. Hopson, University of Chicago, Chicago; Z. Kielan-Jaworowska, Institute of Paleobiology, Polish Academy of Sciences, Warsaw; B. Krebs and T. Martin, Institut für Paläontologie, Freie Universität, Berlin; R.D.E. MacPhee and N.B. Simmons, Department of Mammalogy, AMNH; W. Maier, Lehrstuhl für Spezielle Zoologie, Karl-Universität, Tübingen; M.J. Novacek and M.C. McKenna, Department of Vertebrate Paleontology, AMNH; and U. Zeller, Museum für Naturkunde, Berlin. For amassing the vast collection of *Kryptobaatar* specimens described above, we thank all the

members of the MAE field crews. The description of *Kryptobaatar* was made possible through the skilled preparation completed by Amy Davidson at the AMNH. Also at the AMNH, Edward Heck produced figures 1–23 and 29–37, Lorraine Meeker produced figures 25–26, and G.W.R. produced the remainder. Discussions over the years with E.F. Allin, G. Hahn, J.A. Hopson, J. Hurum, Z. Kielan-Jaworowska, Z. Luo, J. Meng, D. Miao, M.J. Novacek, and R. Presley have enhanced our comprehension of the multituberculate skull. For comments on an earlier

version of this manuscript, we are extremely grateful to E.F. Allin, J.A. Hopson, Z. Kielan-Jaworowska, J. Meng, and R. Presley. This research was supported by NSF Grants BSR 91-19212, DEB 93-0070, DEB 94-0799, DEB 95-27811, DEB 96-25431, DEB 99-96051, and DEB 99-96172. GRW's research has also been supported by a Ralph E. Powe Junior Faculty Award from Oak Ridge Associated Universities. Finally, we acknowledge the extreme patience and understanding of our spouses, Stephanie Davis and Adela Reale.

REFERENCES

- Archer, M.
1976. The basicranial region of marsupicarnivores (Marsupialia), interrelationships of carnivorous marsupials, and affinities of the insectivorous perame-lids. *Zool. J. Linn. Soc.* 59: 217–322.
- Archibald, J. D.
1982. A study of Mammalia and geology across the Cretaceous–Tertiary boundary in Garfield County, Montana. *Univ. California Publ. Geol. Sci.* 122: 1–286.
- Averianov, A. O.
1997. New Late Cretaceous mammals of southern Kazakhstan. *Acta Palaeontol. Pol.* 42: 243–256.
- Barghusen, H. R.
1986. On the evolutionary origin of the therian tensor veli palatini and tensor tympani muscles. *In* N. Hotton III, P. D. MacLean, J. J. Roth, and E. C. Roth (eds.), *The ecology and biology of mammal-like reptiles*: 253–262. Washington, D.C.: Smithsonian Institution Press.
- Bellairs, A. d'A., and A. M. Kamal
1981. The chondrocranium and the development of the skull in recent reptiles. *In* C. Gans and T. S. Parsons (eds.), *Biology of the Reptilia*: 1–263. London: Academic Press.
- Bonaparte, J. F.
1986. Sobre *Mesungulatum houssayi* y nuevos mamíferos Cretácicos de Patagonia. *Actas IV Congr. Argent. Paleontol.* 2: 48–61.
- Broom, R.
1909. Observations on the development of the marsupial skull. *Proc. Linn. Soc. N.S.W.* 34: 195–214.
1914. On the structure and affinities of the Multituberculata. *Bull. Am. Mus. Nat. Hist.* 33: 115–134.
- Bruner, H. L.
1907. On the cephalic veins and sinuses of reptiles, with description of a mechanism for raising the venous blood-pressure in the head. *Am. J. Anat.* 7: 1–117.
- Bryant, H. N., and A. P. Russell
1992. The role of phylogenetic analysis in the inference of unpreserved attributes of extinct taxa. *Philos. Trans. R. Soc. London B337*: 405–418.
- Bugge, J.
1971. The cephalic arterial system in mole-rats (Spalacidae), bamboo rats (Rhizomyidae), jumping mice and jerboas (Dipodoidea) and dormice (Gliroidea) with special reference to the systematic classification of rodents. *Acta Anat.* 79: 165–180.
1974. The cephalic arterial system in insectivores, primates, rodents and lagomorphs, with special reference to the systematic classification. *Ibid.* 87 (suppl. 62): 1–159.
1978. The cephalic arterial system in carnivores, with special reference to the systematic classification. *Ibid.* 101: 45–61.
1979. Cephalic arterial pattern in New World edentates and Old World pangolins with special reference to their phylogenetic relationships and taxonomy. *Ibid.* 105: 37–46.
- Butler, H.
1967. The development of the mammalian dural venous sinuses with especial reference to the post-glenoid vein. *J. Anat.* 102: 33–56.

- Clemens, W. A., and Z. Kielan-Jaworowska
1979. Multituberculata. In J. A. Lillegraven, Z. Kielan-Jaworowska, and W. A. Clemens (eds.), Mesozoic mammals, the first two-thirds of mammalian history: 99–149. Berkeley: Univ. California Press.
- Clemens, W. A., and J. A. Lillegraven
1986. New Late Cretaceous, North American advanced therian mammals that fit neither the marsupial nor eutherian molds. In K. M. Flanagan and J. A. Lillegraven (eds.), Vertebrates, phylogeny, and philosophy. Contrib. Geol. Univ. Wyoming Spec. Pap. 3: 55–85.
- Conroy, G. C., and J. R. Wible
1978. Middle ear morphology of *Lemur variegatus*: implications for primate paleontology. *Folia Primatol.* 29: 81–85.
- Cooper, G., and A. L. Schiller
1975. Anatomy of the guinea pig. Cambridge, MA: Harvard Univ. Press.
- Cope, E. D.
1880. On the foramina perforating the posterior part of the squamosal bone of the Mammalia. *Proc. Am. Philos. Soc.* 18: 452–461.
- Cords, E.
1915. Über das Primordialcranium von *Perameles* spec.? unter Berücksichtigung der Deckknochen. *Anat. Hefte* 52: 1–84.
- Crompton, A. W.
1958. The cranial morphology of a new genus and species of ictidosaurian. *Proc. Zool. Soc. London* 130: 183–216.
- Crompton, A. W., and W. L. Hylander
1986. Changes in mandibular function following the acquisition of a dentary-squamosal jaw articulation. In N. Hotton III, P. D. MacLean, J. J. Roth, and E. C. Roth (eds.), The ecology and biology of mammal-like reptiles: 263–282. Washington, D.C.: Smithsonian Institution Press.
- Crompton, A. W., and Z. Luo
1993. Relationships of the Liassic mammals *Sinoconodon*, *Morganucodon oehleri*, and *Dinnetherium*. In F. S. Szalay, M. J. Novacek, and M. C. McKenna (eds.), Mammal phylogeny: Mesozoic differentiation, multituberculates, monotremes, early therians, and marsupials: 30–44. New York: Springer.
- Dashzeveg, D., M. J. Novacek, M. A. Norell, J. M. Clark, L. M. Chiappe, A. Davidson, M. C. McKenna, L. Dingus, C. Swisher, and A. Perle
1995. Extraordinary preservation in a new vertebrate assemblage from the Late Cretaceous of Mongolia. *Nature* 374: 446–449.
- De Beer, G. R.
1926. Studies on the vertebrate head. II. The orbitotemporal region of the skull. *Q. J. Microsc. Sci.* 70: 263–370.
1937. The development of the vertebrate skull. Oxford: Clarendon Press.
- Denison, W., and R. J. Terry
1921. The chondrocranium of *Caluromys*. *Washington Univ. Stud.* 8: 161–181.
- Eisthen, H. L.
1992. Phylogeny of the vomeronasal system and of receptor cell types in the olfactory and vomeronasal epithelia of vertebrates. *Microsc. Res. Tech.* 23: 1–21.
- Ellenberger, W., and H. Baum
1908. Handbuch der vergleichenden Anatomie der Haustiere. Berlin: Verlag Von August Hirschwald.
- Evans, H. E., and G. C. Christensen
1979. Anatomy of the dog. Philadelphia: W. B. Saunders.
- Fischer, M. S.
1986. Die Stellung der Schliefer (Hyracoidea) im phylogenetischen System der Eutheria. *Cour. Forschungsinst. Senckenb.* 84: 1–132.
- Fourie, S.
1974. The cranial morphology of *Thrinaxodon liorhinus* Seeley. *Ann. S. Afr. Mus.* 65: 337–400.
- Fox, R. C., and J. Meng
1997. An X-radiographic and SEM study of the osseous inner ear of multituberculates and monotremes (Mammalia): implications for mammalian phylogeny and evolution of hearing. *Zool. J. Linn. Soc.* 121: 249–291.
- Freeman, E. F.
1976. A mammalian fossil from the Forest Marble (Middle Jurassic) of Dorset. *Proc. Geol. Assoc.* 87: 231–235.
1979. A Middle Jurassic mammal bed from Oxfordshire. *Palaeontology* 22: 135–166.
- Gambaryan, P. P., and Z. Kielan-Jaworowska
1995. Masticatory musculature of Asian taeniolabidoid multituberculate mammals. *Acta Palaeontol. Pol.* 40: 45–108.
- Gaupp, E.
1902. Über die Ala temporalis des Säugetierschädels und die Regio orbitalis einiger anderer Wirbeltierschädels. *Anat. Hefte* 19: 155–230.
1905. Neue Deutungen auf dem Gebiete der

- Lehre vom Säugetierschädel. *Anat. Anz.* 27: 273–310.
1908. Zur Entwicklungsgeschichte und vergleichenden Morphologie des Schädels von *Echidna aculeata* var. *typica*. *Semon Zool. Forschungsreisen in Australien* 6: 539–788.
- Gauthier, J. A., A. G. Kluge, and T. Rowe
1988. Amniote phylogeny and the importance of fossils. *Cladistics* 4: 105–208.
- Gelderen, C. van
1924. Die Morphologie der Sinus durae matris. Zweiter Teil. Die vergleichende Ontogenie der neurokranialen Venen der Vögel und Säugetiere. *Z. Anat.-Entwicklungsgesch.* 74: 432–508.
- Gidley, J. W.
1909. Notes on the fossil mammalian genus *Ptilodus*, with descriptions of a new species. *Proc. U.S. Natl. Mus.* 36: 611–626.
- Gillilan, L. A.
1972. Blood supply to primitive mammalian brains. *J. Comp. Neurol.* 145: 209–222.
- Godefroit, P.
1997. Reptilian, therapsid and mammalian teeth from the Upper Triassic of Vangéville (northeastern France). *Bull. Inst. R. Sci. Nat. Belg. Sci. Terre* 67: 83–102.
- Granger, W., and G. G. Simpson
1929. A revision of the Tertiary Multituberculata. *Bull. Am. Mus. Nat. Hist.* 56: 601–676.
- Green, H. L.
1930. A description of the egg-tooth of *Ornithorhynchus*, together with some notes on the development of the palatine processes of the premaxillae. *J. Anat.* 64: 512–522.
- Greenwald, N. S.
1987. Patterns of tooth eruption and replacement in multituberculate mammals. *J. Vertebr. Paleontol.* 8: 265–277.
- Gregory, W. K.
1910. The orders of mammals. *Bull. Am. Mus. Nat. Hist.* 27: 1–524.
- Griffiths, M.
1978. The biology of monotremes. New York: Academic Press.
- Hafferl, A.
1921. Zur Entwicklungsgeschichte der Kopfgefäße des Gecko. (*Platydictylus annularis*). *Anat. Hefte* 59: 1–42.
1933. Das Arteriensystem. In L. Bolk, E. Göppert, E. Kallius, and W. Lubosch (eds.), *Handbuch der vergleichenden Anatomie der Wirbeltiere*, vol. 6: 563–684. Reimpression 1967. Amsterdam: Ascher.
- Hahn, G.
1969. Beiträge zur Fauna der Grube Guimarota Nr. 3. Die Multituberculata. *Palaeontogr. Abt. A* 133: 1–100.
1977. Neue Schädel-Reste von Multituberculaten (Mamm.) aus dem Malm Portugals. *Geol. Palaeontol.* 11: 161–186.
1978. Milch-Bezahnungen von Paulchoffatiidae (Multituberculata; Ober-Jura). *Neues Jahrb. Geol. Paläontol. Mh.* 1978: 25–34.
1981. Zum Bau der Schädel-Basis bei den Paulchoffatiidae (Multituberculata; Ober-Jura). *Senckenb. Lethaea* 61: 227–245.
1983. Überblick über die Erforschungsgeschichte der Multituberculaten (Mammalia). *Schriftenr. Geol. Wiss.* 19/20: 217–246.
1985. Zum Bau des Infraorbital-Foramens bei den Paulchoffatiidae (Multituberculata, Ober Jura). *Berl. Geowiss. Abh.* 60: 5–27.
1987. Neue Beobachtungen zum Schädel- und Gebiss-Bau der Paulchoffatiidae (Multituberculata, Ober-Jura). *Palaeo-vertebr. Montpellier* 17: 155–196.
1988. Die Ohr-region der Paulchoffatiidae (Multituberculata, Ober-Jura). *Ibid.* 18: 155–185.
1993. The systematic arrangement of the Paulchoffatiidae (Multituberculata) revisited. *Geol. Palaeontol.* 27: 201–214.
- Hahn, G., and R. Hahn
1994. Nachweis des Septomaxillare bei *Pseudobolodon krebsi* n. sp. (Multituberculata) aus dem Malm Portugals. *Berl. Geowiss. Abh.* E13: 9–29.
1999. Neue Beobachtungen an Plagiaulacoidea (Multituberculata) des Ober-Juras. 1. Zum Zahn-Wechsel bei *Kielanodon*. *Ibid.* E28: 1–7.
- Hahn, G., J. C. Lepage, and G. Wouters
1987. Ein Multituberculaten-Zahn aus der Ober-Trias von Gaume (S-Belgien). *Bull. Soc. Belg. Géol.* 96: 39–47.
- Hill, J. E.
1935. The cranial foramina in rodents. *J. Mammal.* 16: 121–129.
- Hill, J. P., and G. R. De Beer
1949. Development of the Monotremata. Part VII. The development and structure of the egg-tooth and caruncle in the monotremes and on the occurrence of vestiges of the egg-tooth and caruncle

- in marsupials. *Trans. Zool. Soc. London* 26: 503–544.
- Hillenius, W. J.
1994. Turbinates in therapsids: evidence for Late Permian origins of mammalian endothermy. *Evolution* 48: 207–229.
- Hochstetter, F.
1896. Beiträge zur Anatomie und Entwicklungsgeschichte des Blutgefäßsystems der Monotremen. *Semon Zool. Forschungsreisen in Australien* 5: 189–243.
- Hopson, J. A., Z. Kielan-Jaworowska, and E. F. Allin
1989. The cryptic jugal of multituberculates. *J. Vertebr. Paleontol.* 9: 201–209.
- Hopson, J. A., and G. W. Rougier
1993. Braincase structure in the oldest known skull of a therian mammal: implications for mammalian systematics and cranial evolution. *In* P. Dodson and P. Gingerich (eds.), *Functional morphology and evolution*. *Am. J. Sci.* 293-A: 268–299.
- Hopson, J. A., and J. R. Wible
1993. Cranial vascular patterns in Multituberculata: the postglenoid foramen that wasn't there. *J. Vertebr. Paleontol.* 13 (suppl. 3): 42A.
- Hu, Y., Y. Wang, Z. Luo, and C. Li
1997. A new symmetrodont mammal from China and its implications for mammalian evolution. *Nature* 390: 137–142.
- Hurum, J. H.
1994. Snout and orbit of Cretaceous Asian multituberculates studied by serial sections. *Acta Palaeontol. Pol.* 39: 181–221.
1998a. The braincase of two Late Cretaceous Asian multituberculates studied by serial sections. *Ibid.* 43: 21–52.
1998b. The inner ear in two Late Cretaceous multituberculate mammals, and its implications for multituberculate hearing. *J. Mamm. Evol.* 5: 65–93.
- Hurum, J. H., R. Presley, and Z. Kielan-Jaworowska
1995. Multituberculate ear ossicles. *In* A. Sun and Y. Wang (eds.), *Sixth symposium on Mesozoic terrestrial ecosystems and biota, short papers: 243–246*. Beijing: China Ocean Press.
1996. The middle ear in multituberculate mammals. *Acta Palaeontol. Pol.* 41: 253–275.
- Jenkins, F. A., Jr.
1990. Monotremes and the biology of Mesozoic mammals. *Neth. J. Zool.* 40: 5–31.
- Jenkins, F. A., Jr., and C. R. Schaff
1988. The Early Cretaceous mammal *Gobicodon* (Mammalia, Triconodonta) from the Cloverly Formation in Montana. *J. Vertebr. Paleontol.* 8: 1–24.
- Jerzykiewicz, T., and D. A. Russell
1991. Late Mesozoic stratigraphy and vertebrates of the Gobi Basin. *Cretaceous Res.* 12: 345–377.
- Jerzykiewicz, T., P. J. Currie, D. A. Eberth, P. A. Johnston, E. H. Koster, and J.-J. Zheng
1993. Djadokhta Formation correlative strata in Chinese Inner Mongolia: an overview of the stratigraphy, sedimentary geology, and paleontology and comparisons with the type locality in the pre-Altai Gobi. *Can. J. Earth Sci.* 30: 2180–2195.
- Ji, Q., Z. Luo, and S. Ji
1999. A Chinese triconodont mammal and mosaic evolution of the mammalian skeleton. *Nature* 398: 326–330.
- Kallen, F. C.
1977. The cardiovascular system of bats: structure and function. *In* W. A. Wimsatt (ed.), *Biology of bats*, vol. 3: 289–483. New York: Academic Press.
- Kermack, K. A.
1963. The cranial structure of the triconodonts. *Philos. Trans. R. Soc. London* B246: 83–102.
1967. The interrelations of early mammals. *Zool. J. Linn. Soc.* 47: 241–249.
- Kermack, K. A., and Z. Kielan-Jaworowska
1971. Therian and non-therian mammals. *In* D. M. Kermack and K. A. Kermack (eds.), *Early mammals*. *Zool. J. Linn. Soc.* 50 (suppl. 1): 103–115.
- Kermack, K. A., F. Mussett, and H. W. Rigney
1981. The skull of *Morganucodon*. *Zool. J. Linn. Soc.* 71: 1–158.
- Kielan-Jaworowska, Z.
1969. Discovery of a multituberculate marsupial bone. *Nature* 222: 1091–1092.
1970. New Upper Cretaceous multituberculate genera from Bayn Dzak, Gobi Desert. *Palaeontol. Pol.* 21: 35–49.
1971. Skull structure and affinities of the Multituberculata. *Ibid.* 25: 4–41.
1974. Multituberculate succession in the Late Cretaceous of the Gobi Desert (Mongolia). *Ibid.* 30: 25–44.
1979. Pelvic structure and nature of reproduction in Multituberculata. *Nature* 277: 402–403.
1980. Absence of ptilodontoidean multituberculates from Asia and its palaeoge-

- graphic implications. *Lethaia* 13: 169–173.
1983. Multituberculate endocranial casts. *Palaeovertebr. Montpellier* 13: 1–12.
1986. Brain evolution in Mesozoic mammals. *In* K. M. Flanagan and J. A. Lillegraven (eds.), *Vertebrates, phylogeny, and philosophy*. *Contrib. Geol. Univ. Wyoming Spec. Pap.* 3: 21–34.
1992. Interrelationships of Mesozoic mammals. *Hist. Biol.* 6: 185–202.
1994. A new generic name for the multituberculate mammal '*Djadochtatherium*' *catopsaloides*. *Acta Palaeontol. Pol.* 39: 134–136.
1997. Characters of multituberculates neglected in phylogenetic analyses of early mammals. *Lethaia* 29: 249–266.
1998. Humeral torsion in multituberculate mammals. *Acta Palaeontol. Pol.* 43: 131–134.
- Kielan-Jaworowska, Z., and J. F. Bonaparte
1996. Partial dentary of a multituberculate mammal from the Late Cretaceous of Argentina and its taxonomic implications. *Mus. Argent. Cienc. Nat. "Bernardino Rivadavia" Inst. Nac. Invest. Cienc. Nat., n. ser.* 145: 1–9.
- Kielan-Jaworowska, Z., and D. Dashzeveg
1978. New Late Cretaceous mammal locality in Mongolia and a description of a new multituberculate. *Acta Palaeontol. Pol.* 23: 115–130.
- Kielan-Jaworowska, Z., and P. P. Gambaryan
1994. Postcranial anatomy and habits of Asian multituberculate mammals. *Fossils Strata* 36: 92 pp.
- Kielan-Jaworowska, Z., and J. H. Hurum
1997. *Djadochtatheria* - a new suborder of multituberculate mammals. *Acta Palaeontol. Pol.* 42: 201–242.
- Kielan-Jaworowska, Z., and T. Qi
1990. Fossorial adaptations of a taeniolabidoid multituberculate mammal from the Eocene of China. *Vertebr. Palasiat.* 28: 81–94.
- Kielan-Jaworowska, Z., and R. E. Sloan
1979. *Catopsalis* (Multituberculata) from Asia and North America and the problem of taeniolabidoid dispersal in the Late Cretaceous. *Acta Palaeontol. Pol.* 24: 187–197.
- Kielan-Jaworowska, Z., and A. V. Sochava
1969. The first multituberculate from the Uppermost Cretaceous of the Gobi Desert (Mongolia). *Ibid.* 14: 356–367.
- Kielan-Jaworowska, Z., and B. A. Trofimov
1980. Cranial morphology of the Cretaceous eutherian mammal *Barunlestes*. *Ibid.* 25: 167–185.
- Kielan-Jaworowska, Z., C. Poplin, R. Presley, and A. de Ricqlès
1984. Preliminary note on multituberculate cranial anatomy studied by serial sections. *In* W.-E. Reif and F. Westphal (eds.), *Third symposium on Mesozoic terrestrial ecosystems: 123–128*. Tübingen: Attempto Verlag.
- Kielan-Jaworowska, Z., R. Presley, and C. Poplin
1986. The cranial vascular system in taeniolabidoid multituberculate mammals. *Philos. Trans. R. Soc. London B313*: 525–602.
- Kielan-Jaworowska, Z., D. Dashzeveg, and B. A. Trofimov
1987. Early Cretaceous multituberculates from Mongolia and a comparison with Late Jurassic forms. *Acta Palaeontol. Pol.* 32: 3–47.
- Kielan-Jaworowska, Z., M. J. Novacek, B. A. Trofimov, and D. Dashzeveg
2000. Mammals from the Mesozoic of Mongolia. *In* M. J. Benton, E. N. Kurochkin, M. A. Shishkin, and D. M. Unwin (eds.), *The age of dinosaurs in Russia and Mongolia*. London: Cambridge Univ. Press.
- Krause, D. W., and F. E. Grine
1996. The first multituberculates from Madagascar: implications for Cretaceous biogeography. *J. Vertebr. Paleontol.* 16 (suppl. 3): 46A.
- Krause, D. W., and Z. Kielan-Jaworowska
1993. The endocranial cast and encephalization quotient of *Ptilodus* (Multituberculata, Mammalia). *Palaeovertebr. Montpellier* 22: 99–112.
- Krause, D. W., Z. Kielan-Jaworowska, and J. F. Bonaparte
1989. *Ferugliotherium* Bonaparte, the first known multituberculate from South America. *J. Vertebr. Paleontol.* 12: 351–376.
- Krause, D. W., G. V. Prasad, W. von Koenigswald, A. Sahni, and F. E. Grine
1997. Cosmopolitanism among Gondwanan Late Cretaceous mammals. *Nature* 390: 504–507.
- Kristhalka, L., R. J. Emry, J. E. Storer, and J. F. Sutton
1982. Oligocene multituberculates (Mammalia: Allotheria): youngest known record. *J. Paleontol.* 56: 791–794.
- Kuhn, H.-J.
1971. Die Entwicklung und Morphologie des Schädels von *Tachyglossus aculeatus*.

- Abh. Senckenb. Naturforsch. Ges. 528: 1–192.
- Kuhn, H.-J., and U. Zeller
1987. The cavum epiptericum in monotremes and therian mammals. *In* H.-J. Kuhn and U. Zeller (eds.), *Morphogenesis of the mammalian skull*. Mamm. Depicta 13: 50–70.
- Kühne, W. G.
1956. The Liassic therapsid *Oligokyphus*. London: Brit. Mus.
- Lillegraven, J. A., and G. Hahn
1993. Evolutionary analysis of the middle and inner ear of Late Jurassic multituberculates. *J. Mamm. Evol.* 1: 47–74.
- Lillegraven, J. A., and G. Krusat
1991. Cranio-mandibular anatomy of *Haldanodon exspectatus* (Docodonta; Mammalia) from the Late Jurassic of Portugal and its implications to the evolution of mammalian characters. *Contrib. Geol. Univ. Wyoming* 28: 39–138.
- Lillegraven, J. A., S. D. Thompson, B. K. McNab, and J. L. Patton
1987. The origin of eutherian mammals. *Biol. J. Linn. Soc.* 32: 281–336.
- Lucas, S. G., and Z. Luo
1993. *Adelobasileus* from the Upper Triassic of west Texas: the oldest mammal. *J. Vertebr. Paleontol.* 13: 309–334.
- Luckett, W. P.
1993. An ontogenetic assessment of dental homologies in therian mammals. *In* F. S. Szalay, M. J. Novacek, and M. C. McKenna (eds.), *Mammal phylogeny: Mesozoic differentiation, multituberculates, monotremes, early therians, and marsupials*: 182–204. New York: Springer.
- Luo, Z.
1989. Structure of the petrosals of Multituberculata (Mammalia) and morphology of the molars of early arctocyonids (Condylarthra, Mammalia). Ph.D. diss., Univ. California, Berkeley, 426 pp.
1994. Sister-group relationships of mammals and transformations of diagnostic mammalian characters. *In* N. C. Fraser and H.-D. Sues (eds.), *In the shadow of the dinosaurs — early Mesozoic tetrapods*: 98–128. Cambridge: Cambridge Univ. Press.
1996. Phylogenetic implications of the petrosal features on the relationships of the multituberculata families of the Late Cretaceous. *J. Vertebr. Paleontol.* 16 (suppl. 3): 49A.
- Luo, Z., and D. R. Ketten
1991. CT scanning and computerized reconstructions of the inner ear of multituberculata mammals. *J. Vertebr. Paleontol.* 11: 220–228.
- MacIntyre, G. T.
1972. The trisulcate petrosal pattern of mammals. *In* T. Dobzhansky, M. K. Hecht, and W. C. Steere (eds.), *Evolutionary biology*, 6: 275–303. New York: Appleton-Century-Crofts.
- MacPhee, R.D.E.
1981. Auditory region of primates and eutherian insectivores. *Contrib. Primatol.* 18: 282 pp.
1994. Morphology, adaptations, and relationships of *Plesiorcycteropus*, and a diagnosis of a new order of eutherian mammals. *Bull. Am. Mus. Nat. Hist.* 220: 214 pp.
- MacPhee, R.D.E., and M. Cartmill
1986. Basicranial structures and primate systematics. *In* D. R. Swindler and J. Erwin (eds.), *Comparative primate biology, vol. 1. Systematics, evolution, and anatomy*: 219–275. New York: Alan R. Liss.
- Maier, W.
1987. The ontogenetic development of the orbitotemporal region in the skull of *Monodelphis domestica* (Didelphidae, Marsupialia), and the problem of the mammalian alisphenoid. *In* H.-J. Kuhn and U. Zeller (eds.), *Morphogenesis of the mammalian skull*. Mamm. Depicta 13: 71–90.
- Marshall, L. G., J. A. Case, and M. O. Woodburne
1990. Phylogenetic relationships of the families of marsupials. *Curr. Mamm.* 2: 433–502.
- Marshall, L. G., and C. de Muizon
1995. Part II: The skull. *In* C. de Muizon (ed.), *Pucadelphys andinus* (Marsupialia, Mammalia) from the early Paleocene of Bolivia. *Mém. Mus. Natl. Hist. Nat.* 165: 21–90.
- Martinson, G. G.
1982. Pozdnemelovye molliuski Mongolii (The Upper Cretaceous mollusks of Mongolia). *Joint Soviet-Mongolian Paleontol. Exped. Trans.* 17: 5–76. [in Russian].
- McDowell, S. B., Jr.
1958. The Greater Antillean insectivores. *Bull. Am. Mus. Nat. Hist.* 115: 113–214.

- McFarland, W. L., M. S. Jacobs, and P. J. Morgan
1979. Blood supply to the brain of the dolphin, *Tursiops truncatus*, with comparative observations on special aspects of the cerebrovascular supply of other vertebrates. *Neurosci. Biobehav. Rev.* 3 (suppl. 1): 1–93.
- McKenna, M. C., and S. K. Bell
1997. Classification of mammals above the species level. New York: Columbia Univ. Press.
- Meng, J.
1992. The stapes of *Lambdopsalis bulla* (Multituberculata) and transformational analyses on some stapedial features in Mammaliaformes. *J. Vertebr. Paleontol.* 12: 459–471.
- Meng, J., and A. R. Wyss
1995. Monotreme affinities and low frequency hearing suggested by multituberculate ear. *Nature* 377: 141–144.
1996. Multituberculate phylogeny. *Ibid.* 379: 407.
- Miao, D.
1986. Dental anatomy and ontogeny of *Lambdopsalis bulla* (Mammalia, Multituberculata). *Contrib. Geol. Univ. Wyoming* 24: 65–76.
1988. Skull morphology of *Lambdopsalis bulla* (Mammalia, Multituberculata) and its implications to mammalian evolution. *Contrib. Geol. Univ. Wyoming Spec. Pap.* 4: 1–104.
1993. Cranial morphology and multituberculate relationships. In F. S. Szalay, M. J. Novacek, and M. C. McKenna (eds.), *Mammal phylogeny: Mesozoic differentiation, multituberculates, monotremes, early therians, and marsupials*: 63–74. New York: Springer.
- Miao, D., and J. A. Lillegraven
1986. Discovery of three ear ossicles in a multituberculate mammal. *Natl. Geogr. Res.* 2: 500–507.
- Monastersky, R.
1996. The lost tribe of mammals. *Sci. News* 150: 378–379.
- Moore, W. J.
1981. *The mammalian skull*. Cambridge: Cambridge Univ. Press.
- Nomina Anatomica, 5th ed.
1983. Baltimore: Williams & Wilkins.
- Nomina Anatomica Veterinaria, 2nd ed.
1973. Vienna: Adolf Holzhausen's Successors.
- Novacek, M. J.
1977. Aspects of the problem of variation, origin and evolution of the eutherian auditory bulla. *Mammal Rev.* 7: 131–149.
1986. The skull of leptictid insectivorans and the classification of eutherian mammals. *Bull. Am. Mus. Nat. Hist.* 183: 1–112.
1993. Patterns of skull diversity in the mammalian skull. In J. Hanken and B. K. Hall (eds.), *The skull, vol. 2, Patterns of structural and systematic diversity*: 438–545. Chicago: Univ. Chicago Press.
1997. Mammalian evolution: an early record bristling with evidence. *Curr. Bio.* 7: R489–R491.
- Novacek, M. J., M. Norell, M. C. McKenna, and J. Clark
1994. Fossils of the Flaming Cliffs. *Sci. Am.* 271: 60–69.
- Novacek, M. J., M. A. Norell, L. Dingus, and D. Dashzeveg
1996. Dinosaurs, mammals, birds, and lizards from the Late Cretaceous Ukhaa Tolgod fauna, Mongolia. *J. Vertebr. Paleontol.* 19 (suppl. 3): 56A.
- Novacek, M. J., G. W. Rougier, J. R. Wible, M. C. McKenna, D. Dashzeveg, and I. Horovitz
1997. Epipubic bones in eutherian mammals from the Late Cretaceous of Mongolia. *Nature* 389: 483–486.
- Oelrich, T. M.
1956. The anatomy of the head of *Ctenosaura pectinata* (Iguanidae). *Misc. Publ. Mus. Zool. Univ. Michigan* 94: 122 pp.
- Parrington, F. R.
1946. On the cranial anatomy of cynodonts. *Proc. Zool. Soc. London* 116: 181–197.
- Parrington, F. R., and T. S. Westoll
1940. The evolution of the mammalian palate. *Proc. R. Soc. London B230*: 305–355.
- Pascual, R., F. J. Goin, D. W. Krause, E. Ortiz-Jaureguizar, and A. A. Carlini
1999. The first gnathic remains of *Sudamerica*: implications for gondwanathere relationships. *J. Vertebr. Paleontol.* 19: 373–382.
- Patterson, B., and E. C. Olson
1961. A triconodontid mammal from the Triassic of Yunnan. In G. Vandebroek (ed.), *International colloquium on the evolution of lower and specialized mammals*: 129–191. Brussels: K. Vlaamse Acad. Wettensch., Lett. Schone Kunsten België.
- Paulli, S.
1900. Über die Pneumaticität des Schädels

- bei den Säugetieren. I. Über den Bau des Siebbeins. Über die Morphologie des Siebbeins und die der Pneumaticität bei den Monotremen und den Marsupialiern. Gegenbaurs Morphol. Jahrb. 28: 147–178.
- Presley, R.
1981. Alisphenoid equivalents in placentals, marsupials, monotremes and fossils. *Nature* 294: 668–670.
- Presley, R., and F.L.D. Steel
1978. The pterygoid and ectopterygoid in mammals. *Anat. Embryol.* 154: 95–110.
- Prothero, D. R., and C. Swisher III
1992. Magnetostratigraphy and geochronology of the terrestrial Eocene–Oligocene transition in North America. In D. R. Prothero and W. A. Beggren (eds.), *Eocene–Oligocene climatic and biotic evolution*: 46–73. Princeton: Princeton Univ. Press.
- Rose, K. D., and H.-D. Sues
1996. Vertebrate paleontology. *Geotimes* (Feb.): 31–34.
- Rougier, G. W.
1993. *Vincelestes neuquenianus* Bonaparte (Mammalia, Theria) un primitivo mamífero del Cretácico Inferior de la Cuenca Neuquina. Ph.D. diss., Univ. Buenos Aires, 720 pp.
- Rougier, G. W., J. R. Wible, and J. A. Hopson
1992. Reconstruction of the cranial vessels in the Early Cretaceous mammal *Vincelestes neuquenianus*: implications for the evolution of the mammalian cranial vascular system. *J. Vertebr. Paleontol.* 12: 188–216.
- 1996a. Basicranial anatomy of *Priacodon fruitaensis* (Triconodontidae, Mammalia) from the Late Jurassic of Colorado, and a reappraisal of mammaliaform interrelationships. *Am. Mus. Novitates* 3183: 38 pp.
- Rougier, G. W., J. R. Wible, and M. J. Novacek
1996b. Multituberculate phylogeny. *Nature* 379: 406.
- 1996c. Middle-ear ossicles of *Kryptobaatar dashzevi* (Mammalia, Multituberculata): implications for mammalian relationships and the evolution of the auditory apparatus. *Am. Mus. Novitates* 3187: 43 pp.
- Rougier, G. W., M. J. Novacek, and D. Dashzeveg
1997a. A new multituberculate from the Late Cretaceous locality Ukhaa Tolgod, Mongolia. Considerations on multituberculate interrelationships. *Am. Mus. Novitates* 3191: 26 pp.
- Rougier, G. W., J. R. Wible, and M. J. Novacek
1997b. Nasal and endocranial morphology of Late Cretaceous multituberculates from Ukhaa Tolgod, Mongolia. *J. Vertebr. Paleontol.* 13 (suppl. 3): 72A.
- Rowe, T.
1988. Definition, diagnosis and origin of Mammalia. *J. Vertebr. Paleontol.* 8: 241–264.
1993. Phylogenetic systematics and the early history of mammals. In F. S. Szalay, M. J. Novacek, and M. C. McKenna (eds.), *Mammal phylogeny: Mesozoic differentiation, multituberculates, monotremes, early therians, and marsupials*: 129–145. New York: Springer.
- Rowe, T., W. D. Carlson, and W. W. Bortorff
1995. *Thrinaxodon*: Digital atlas of the skull (CD-ROM). Austin: Univ. Texas Press.
- Säve-Söderbergh, G.
1947. Notes on the brain-case in *Sphenodon* and certain Lacertilia. *Zool. Bidr. Upps.* 25: 489–516.
- Segall, W.
1970. Morphological parallelisms of the bulla and auditory ossicles in some insectivores and marsupials. *Fieldiana Zool.* 51: 169–205.
- Sereno, P. C., and M. C. McKenna
1995. Cretaceous multituberculate skeleton and the early evolution of the mammalian shoulder girdle. *Nature* 377: 144–147.
1996. Multituberculate phylogeny. *Ibid.* 379: 406–407.
- Shaner, R. F.
1926. The development of the skull of the turtle, with remarks on fossil reptile skulls. *Anat. Rec.* 32: 343–367.
- Shiino, K.
1914. Studien zur Kenntnis des Wirbeltierkopfes. I. Das Chondrocranium von *Crocodylus* mit Berücksichtigung der Gehirnnerven und der Kopfgefäße. *Anat. Hefte* 50: 253–382.
- Shindo, T.
1914. Zur vergleichenden Anatomie der arteriellen Kopfgefäße der Reptilien. *Anat. Hefte* 51: 267–356.
1915. Über die Bedeutung des Sinus cavernosus der Säuger mit vergleichenden anatomischer Berücksichtigung anderer Kopfvenen. *Ibid.* 52: 319–495.
- Sigogneau-Russell, D.
1991. First evidence of Multituberculata (Mammalia) in the Mesozoic of Africa.

- Neues Jahrb. Geol. Paläontol. Mh. 1991: 119–125.
- Sigogneau-Russell, D., R. Frank, and J. Hemmerle
1986. A new family of mammals from the lower part of the French Rhaetic. In K. Padian (ed.), The beginning of the age of dinosaurs, faunal change across the Triassic–Jurassic boundary: 99–108. Cambridge: Cambridge Univ. Press.
- Simmons, N. B.
1993. Phylogeny of Multituberculata. In F. S. Szalay, M. J. Novacek, and M. C. McKenna (eds.), Mammal phylogeny: Mesozoic differentiation, multituberculataes, monotremes, early therians, and marsupials: 146–164. New York: Springer.
- Simpson, G. G.
1925. A Mesozoic mammal skull from Mongolia. Am. Mus. Novitates 201: 12 pp.
1937. Skull structure of the Multituberculata. Bull. Am. Mus. Nat. Hist. 73: 727–763.
- Sloan, R. E.
1979. Multituberculata. In R. W. Fairbridge and D. Jablonski (eds.), The encyclopedia of paleontology: 492–498. Stroudsburg, PA: Dowden, Hutchinson & Ross.
1981. Systematics of Paleocene multituberculataes from the San Juan Basin, New Mexico. In S. G. Lucas, J. K. Rigby, Jr., and B. S. Kues (eds.), Advances in San Juan Basin paleontology: 127–160. Albuquerque, Univ. New Mexico Press.
- Starck, D.
1967. Le crâne des mammifères. In P.-P. Grasset (ed.), Traité de Zoologie, vol. 16, pt. 1: 405–549, 1095–1102. Paris: Masson.
1978. Das evolutive Plateau Säugetier. Sonderb. Naturwiss. Ver. Hamb. 3: 7–33.
1995. Lehrbuch der speziellen Zoologie. Band II: Wirbeltiere. Teil 5/1: Säugetiere. Jena: Gustav Fischer.
- Tandler, J.
1899. Zur vergleichenden Anatomie der Kopfarterien bei den Mammalia. Denkschr. K. Akad. Wiss. Wien Math.-Natwiss. Kl. 67: 677–784.
1901. Zur vergleichenden Anatomie der Kopfarterien bei den Mammalia. Anat. Hefte 18: 327–368.
1902. Zur Entwicklungsgeschichte der Kopfarterien bei den Mammalia. Gegenbaurs Morphol. Jahrb. 30: 275–373.
- Thewissen, J. G. M.
1989. Mammalian frontal diploic vein and the human foramen caecum. Anat. Rec. 223: 242–244.
- Toeplitz, C.
1920. Bau und Entwicklung des Knorpelschädels von *Didelphis marsupialis*. Zoologica (Stuttg.) 27: 1–84.
- Trofimov, B. A.
1975. New data on *Buginbaatar* Kielan-Jaworowska et Sochava, 1969 (Mammalia, Multituberculata) from Mongolia. Joint Soviet-Mongolian Paleontol. Exped. Trans. 2: 7–13. [In Russian].
- Voit, M.
1909. Das Primordialcranium des Kaninchens unter Berücksichtigung der Deckknochen. Anat. Hefte 38: 425–616.
- Wahlert, J. H.
1974. The cranial foramina of protrogomorphous rodents; an anatomical and phylogenetic study. Bull. Mus. Comp. Zool. 146: 363–410.
- Wall, C. E., and D. W. Krause
1992. A biomechanical analysis of the masticatory apparatus of *Ptilodus* (Multituberculata). J. Vertebr. Paleontol. 12: 172–187.
- Watson, D.M.S.
1911. The skull of *Diademodon*, with notes on those of some other cynodonts. Ann. Mag. Nat. Hist. 8: 293–330.
1920. On the Cynodontia. Ibid. 9: 506–524.
- Wible, J. R.
1983. The internal carotid artery in early eutherians. Acta Palaeontol. Pol. 28: 281–293.
1984. The ontogeny and phylogeny of the mammalian cranial arterial pattern. Ph.D. diss., Duke Univ., Durham, NC, 705 pp.
1986. Transformations in the extracranial course of the internal carotid artery in mammalian phylogeny. J. Vertebr. Paleontol. 6: 313–325.
1987. The eutherian stapedia artery: character analysis and implications for superordinal relationships. Zool. J. Linn. Soc. 91: 107–135.
1989. Vessels on the side wall of the braincase in cynodonts and primitive mammals. In H. Splechtna and H. Hilgers (eds.), Trends in vertebrate morphology. Fortschr. Zool. 35: 406–408.
1990. Late Cretaceous marsupial petrosal bones from North America and a cladistic analysis of the petrosal in therian mammals. J. Vertebr. Paleontol. 10: 183–205.

1991. Origin of Mammalia: the craniodental evidence reexamined. *Ibid.* 11: 1–28.
- Wible, J. R., and D. L. Davis
2000. Ontogeny of the chiropteran basicranium, with reference to the Indian false vampire bat *Megaderma lyra*. In R. A. Adams and S. C. Pedersen (eds.), *Ontogeny, functional ecology and evolution of bats*: 214–246. New York: Cambridge Univ. Press.
- Wible, J. R., and J. A. Hopson
1993. Basicranial evidence for early mammal phylogeny. In F. S. Szalay, M. J. Novacek, and M. C. McKenna (eds.), *Mammal phylogeny: Mesozoic differentiation, multituberculates, monotremes, early therians, and marsupials*: 45–62. New York: Springer.
1995. Homologies of the prootic canal in mammals and non-mammalian cynodonts. *J. Vertebr. Paleontol.* 15: 331–356.
- Wible, J. R., D. Miao, and J. A. Hopson
1990. The septomaxilla of fossil and Recent synapsids and the problem of the septomaxilla of monotremes and armadillos. *Zool. J. Linn. Soc.* 98: 203–228.
- Wible, J. R., G. W. Rougier, M. J. Novacek, M. C., McKenna, and D. Dashzeveg
1995. A mammalian petrosal from the Early Cretaceous of Mongolia: implications for the evolution of the ear region and mammalian interrelationships. *Am. Mus. Novitates* 3149: 19 pp.
- Williams, P. L., R. Warwick, M. Dyson, and L. H. Bannister (eds.)
1989. *Gray's anatomy*, 37th ed. Edinburgh: Churchill-Livingstone.
- Wilson, J. T.
1900. On the skeleton of the snout and os carunculae of the mammary foetus of the monotremes. *Proc. Linn. Soc. N.S.W.* 25: 58–59.
- Witmer, L. M.
1995. The extant phylogenetic bracket and the importance of reconstructing soft tissues in fossils. In J. Thomason (ed.), *Functional morphology in vertebrate paleontology*: 19–33. New York: Cambridge Univ. Press.
- Zeller, U.
1985. Die Ontogenese und Morphologie der Fenestra rotunda und des Aquaeductus cochleae von *Tupaia* und anderen Säugern. *Gegenbaurs Morphol. Jahrb.* 131: 179–204.
1988. The lamina cribrosa of *Ornithorhynchus* (Monotremata, Mammalia). *Anat. Embryol.* 178: 513–519.
1989. Die Entwicklung und Morphologie des Schädels von *Ornithorhynchus anatinus* (Mammalia: Prototheria: Monotremata). *Abh. Senckenb. Naturforsch. Ges.* 545: 1–188.
1991. Foramen perilymphaticum und Recessus scalae tympani von *Ornithorhynchus anatinus* (Monotremata) und anderen Säugern. *Verh. Anat. Ges.* 84: 441–443.
1993. Ontogenetic evidence for cranial homologies in monotremes and therians. In F. S. Szalay, M. J. Novacek, and M. C. McKenna (eds.), *Mammal phylogeny: Mesozoic differentiation, multituberculates, monotremes, early therians, and marsupials*: 95–128. New York: Springer.
- Zeller, U., J. R. Wible, and M. Elsner
1993. New ontogenetic evidence on the septomaxilla of *Tamandua* and *Choloepus* (Mammalia, Xenarthra), with a reevaluation of the problem of the mammalian septomaxilla. *J. Mamm. Evol.* 1: 31–46.

GLOSSARY

Given that usages of anatomical terms vary among researchers, we include a glossary specifying our usages for the cranial foramina and canals. The English form is given, followed by the Latin equivalent in parentheses where appropriate based on the *Nomina Anatomica* (1983) and/or *Nomina Anatomica Veterinaria* (1973). For many terms, we have used the morphology of the dog *Canis familiaris* as the basis for our discussion, relying on the detailed treatment of dog anatomy by Evans and Christensen (1979). Considering the

numerous plesiomorphies retained by monotremes (Zeller, 1989, 1993; Jenkins, 1990) and multituberculates (Kielan-Jaworowska, 1992; Lillegraven and Hahn, 1993; Kielan-Jaworowska and Gambaryan, 1994), the former might represent a suitable model for evaluating multituberculate morphology; however, the details of monotreme cranial anatomy, although well known (e.g., Kuhn, 1971; Zeller, 1989), are not described and illustrated to the same degree as for the dog.

ACCESSORY PALATINE FORAMEN (FORAMEN PALA-

TINUM ACCESSORIUS). In the dog (Evans and Christensen, 1979), the accessory palatine nerve and artery (branches of the major palatine nerve and artery, respectively) travel in an accessory palatine canal to supply the caudal portion of the mucosa on the hard palate; oddly enough, their foramen of exit on the palate is called the minor palatine foramen. In *Kryptobaatar*, there are four or five small foramina in the lateral margin of the palatine (minor palatine foramina of Kielan-Jaworowska, 1970), behind the major palatine foramen, that we interpret as for the accessory palatine nerves and arteries. Unlike the terminology in the dog, we call the apertures that transmitted these nerves and arteries the accessory palatine foramina and reserve the term minor palatine foramen for the more posterior aperture that transmitted the minor palatine nerve and artery.

ASCENDING CANAL (CANALIS ASCENDENS). First used by Kielan-Jaworowska et al. (1986) for the intramural canal in multituberculates within the suture between the anterior lamina and the squamosal. These authors suggested that this canal was more widespread among Mesozoic and extant taxa, and a more detailed evaluation of its homologies was completed by Rougier et al. (1992). The major occupants were the ramus superior of the stapedial artery and accompanying veins (Wible, 1989; Rougier et al., 1992; Wible and Hopson, 1995). The canal was further subdivided into dorsal and ventral ascending canals by Rougier et al. (1992), based on the positional relationship to the posttemporal canal.

BUCCINATOR FORAMEN (FORAMEN BUCCINATORIUM). Aperture in the alisphenoid, on the side wall of the braincase, transmitting the buccal branch of the mandibular nerve in some rodents (Hill, 1935; Wahlert, 1974). Despite the implication of the name, the buccal branch of the mandibular nerve is not the motor nerve to the buccinator muscle, but is sensory to the skin and mucosa associated with that muscle (Evans and Christensen, 1979; Williams et al., 1989). Used in *Kryptobaatar* for the anteriorly directed aperture in the pterygoid fossa of the alisphenoid between that bone and the anterior lamina.

CANAL FOR RAMUS INFERIOR (CANALIS RAMUS INFERIUS). Following Wible and Hopson (1995), the horizontal canal dorsal to the epitympanic recess and lateral flange that connects the middle ear and cavum epiptericum in multituberculates. Transmitted the ramus inferior of the stapedial artery and perhaps the post-trigeminal vein. In *Kryptobaatar*, the canal for the ramus inferior has a common tympanic aperture with the secondary facial foramen. Equivalent to the canal for the ?maxillary artery of Kielan-Jaworowska et al.

(1986) and the post-trigeminal canal of Rougier et al. (1996a, 1996c).

CAROTID CANAL (CANALIS CAROTICUM). In humans (Williams et al., 1989), the internal carotid artery and nerves run from the skull base to the cranial cavity through a perbullar carotid canal (Wible, 1986) in the petrosal (petrous temporal). In *Kryptobaatar*, the internal carotid artery and nerves first ran through the middle ear in a groove on the promontorium of the petrosal and then entered a carotid canal via a foramen between the petrosal and alisphenoid at the anterolateral pole of the promontorium. From this aperture, the carotid canal runs anteromedially and dorsally across the anterior pole of the promontorium between the petrosal, alisphenoid, and probably the pterygoid. The canal ends at the carotid foramen in the basisphenoid, which opens endocranially in the posterolateral part of the hypophyseal fossa. Branching off the ventromedial part of the carotid canal is the pterygoid canal.

DORSAL ASCENDING CANAL (CANALIS ASCENDENS DORSALIS). Following Rougier et al. (1992), the segment of the ascending canal dorsal to its communication with the posttemporal canal, transporting the ramus superior of the stapedial artery to the orbitotemporal channel. In *Kryptobaatar*, the dorsal ascending canal is an intramural passageway between the squamosal and petrosal. However, the equivalent channel can be endocranial, as in lipotyphlans, or an extracranial sulcus, as in the non-mammalian cynodont *Probainognathus* (Rougier et al., 1992).

ETHMOIDAL FORAMEN (FORAMEN ETHMOIDALE). In the dog (Evans and Christensen, 1979), two ethmoidal foramina connect the orbit and cranial cavity; the smaller, ventral one is in the suture between the frontal and orbitosphenoid, and the other is entirely in the frontal. The ventral foramen transmits the ethmoidal nerve, a branch of the ophthalmic, and the dorsal transmits the external ethmoidal artery, a branch of the maxillary, and an accompanying vein. Humans (Williams et al., 1989) have anterior and posterior ethmoidal foramina, which transmit the anterior and posterior ethmoidal nerves and vessels, respectively, with the former nerve being equivalent to the ethmoidal nerve of the dog. The foramina in humans are either in the frontoethmoidal suture or in the frontal. In *Kryptobaatar*, there is a single ethmoidal foramen between the frontal and orbitosphenoid, which accommodated the ethmoidal nerve and vessels.

FENESTRA VESTIBULI (FENESTRA VESTIBULI). Term in the *Nomina Anatomica* (1983) for the oval window, the opening in the petrosal (petrous temporal) that accommodates the footplate of the stapes.

FORAMEN FOR FRONTAL DIPLOIC VEIN (FORAMEN VENA DIPLOËTICA FRONTALIS). In the dog (Evans and Christensen, 1979), a small unnamed foramen in the orbital surface of the postorbital (zygomatic) process of the frontal transmits the frontal diploic vein, an emissary vein from the diploë of the frontal to the ophthalmic vein. In the few eutherians for which this vein has been described, it connects either the superior (dorsal) sagittal sinus or the frontal paranasal air sinus and the frontal diploë with the ophthalmic vein (Thewissen, 1989). Zeller (1989: fig. 55) reported a frontal diploic vein in *Ornithorhynchus*, and his illustration of the adult skull shows an unnamed foramen in the frontal in the same position as that transmitting the frontal diploic vein in the dog. A similarly placed foramen in the frontal in *Tachyglossus* accommodates diploic vessels according to Kuhn (1971) and, as interpreted here, in *Kryptobaatar*. To facilitate description, we designate the aperture in monotremes and *Kryptobaatar* the foramen for the frontal diploic vein.

FORAMEN FOR RAMUS TEMPORALIS (FORAMEN RAMUS TEMPORALIS). Openings in the squamosal and parietal of various extant therians that transmit temporal rami of the ramus superior of the stapedia artery and accompanying veins into the temporal fossa (Wible, 1987). Similar foramina are found in or along the anterior lamina of *Kryptobaatar* and are presumed to have had the same function. Included are the supraglenoid foramen in the anterior lamina in front of the root of the zygoma, the foramen of the dorsal ascending canal between the anterior lamina and the squamosal at their superior limits, and an unnamed foramen between the anterior lamina and squamosal above the root of the zygoma.

FORAMEN FOR PITUITO-ORBITAL VEIN (FORAMEN VENA PITUITO-ORBITALIS). In *Kryptobaatar*, the foramen in the anterolateral wall of the hypophysal fossa connecting to the orbitotemporal fossa, which transmitted a vein between the pituitary (hypophysis) and the orbit.

FORAMEN OF DORSAL ASCENDING CANAL (FORAMEN CANALIS ASCENDENS DORSALIS). Miao (1988) coined the term ascending canal foramen for the opening into the dorsal ascending canal between the anterior lamina, squamosal, and parietal in *Lambdopsalis*. This aperture was interpreted by Rougier et al. (1992) as having housed a temporal branch of the ramus superior of the stapedia artery. Miao's (1988) term is modified here to foramen of the dorsal ascending canal to distinguish it from other foramina on the ventral ascending canal. In *Kryptobaatar*, the foramen of the dorsal ascending canal is between the anterior lamina and squamosal at their superior limits.

FORAMEN OVALE INFERIUM (FORAMEN OVALE IN-

FERIUM). In *Ptilodus*, Simpson (1937) reported two openings in the area where the foramen ovale was expected. He interpreted both openings as for the mandibular nerve and named them the foramen masticator and foramen ovale inferius. As a model he offered the condition in some extant rodents where as many as three separate apertures transmitting branches of the mandibular nerve were reported by Hill (1935). Following Kielan-Jaworowska et al. (1986), we employ the term foramen ovale inferium for the more medial of the apertures that transmitted the mandibular nerve through the anterior lamina in multituberculates. In *Kryptobaatar*, the foramen ovale inferium lies in the anterior part of the epitympanic recess.

HYPOGLOSSAL CANAL (CANALIS HYPOGLOSSI). In the dog (Evans and Christensen, 1979), the opening in the exoccipital that transmits the hypoglossal nerve and the vein of the hypoglossal canal, which connects the condyloid and vertebral veins. In *Kryptobaatar*, only one hypoglossal foramen seems to be present; it is deep within the jugular fossa and completely encircled by the exoccipital.

INCISIVE FORAMEN (FORAMEN INCISIVUM). In the dog (Evans and Christensen, 1979), a large aperture (palatine fissure) in the anterior palate between the premaxilla and maxilla transmits the septal branch of the caudal nasal nerve, the rostral septal branch of the major palatine artery, and the nasopalatine (incisive) duct, which connects the nasal and oral cavities with the vomeronasal (Jacobson's) organ. We call the equivalent aperture in *Kryptobaatar* the incisive foramen following the *Nomina Anatomica* (1983). It likely transmitted the same structures as the palatine fissure in the dog; there is no bony evidence other than the incisive foramen for the nasopalatine duct and vomeronasal organ, but their presence is inferred for *Kryptobaatar* from the widespread distribution of these structures among extant amniotes (Gauthier et al., 1988; Eisthen, 1992).

INFRAORBITAL FORAMEN (FORAMEN INFRAORBITALE). In the dog (Evans and Christensen, 1979), the opening in the maxilla dorsal to the fourth premolar at the anterior end of the infraorbital canal that connects the orbit and snout and accommodates the infraorbital nerve, artery, and vein. In the floor of the infraorbital canal are several small alveolar canals, and in the medial wall is the incisivomaxillary canal; alveolar branches of the infraorbital nerve and vessels are transmitted to the premolars by the former and to the canine and incisors by the latter. In *Kryptobaatar*, the infraorbital foramen is dorsoventrally compressed, visible in ventral view, and above the embrasures of the first and second premolars or slightly posterior to them. In the right side of PSS-MAE 113, two openings leading medially into the maxilla

(either to the maxillary sinus or nasal cavity) are visible. As noted by Rougier et al. (1997a), these may be apertures to the alveolar canals.

INTERNAL ACOUSTIC MEATUS (MEATUS ACUSTICUS INTERNUS). In the dog (Evans and Christensen, 1979), the recess on the endocranial surface of the petrosal accommodating the facial and vestibulocochlear nerves as well as the labyrinthine artery off the basilar. A transverse crest divides the meatus into a dorsal part for the facial nerve and part of the vestibular nerve, and a ventral part for the rest of the vestibular nerve and for the cochlear nerve. In *Kryptobaatar*, the meatus is divided by a low transverse crest with a single aperture on either side.

JUGULAR FORAMEN (FORAMEN JUGULARE). In the dog (Evans and Christensen, 1979), the opening between the petrosal, basioccipital, and exoccipital that connects the cranial cavity and skull base and transmits the glossopharyngeal, vagus, and accessory nerves along with the sigmoid sinus. In *Kryptobaatar*, the jugular foramen lies between the petrosal and exoccipital, and in light of its small size likely transmitted nerves only; the sigmoid sinus and perhaps the inferior petrosal sinus exited the cranial cavity via the foramen magnum as, for example, in *Tachyglossus* (Wible and Hopson, 1995).

LACRIMAL FORAMEN (FORAMEN LACRIMALE). In the dog (Evans and Christensen, 1979), the opening into the nasolacrimal (lacrimal) canal lies within a depression in the orbital surface of the lacrimal bone called the fossa for the lacrimal sac. Accompanying the nasolacrimal duct into the canal is a delicate branch of the malar artery, off the infraorbital. "In about 50 per cent of dogs, the nasolacrimal duct has two openings (Evans and Christensen, 1979: 1105)." In *Kryptobaatar*, the small opening into the nasolacrimal canal, which we call the lacrimal foramen following, for example, Novacek (1986), is in the lacrimal high on the orbital rim, near the suture with the facial process of the maxilla.

MANDIBULAR CANAL (CANALIS MANDIBULARIS). In the dog (Evans and Christensen, 1979), the canal opening posteriorly in the ramus of the mandible and anteriorly via the mental foramen that accommodates the inferior alveolar nerve off the mandibular nerve and accompanying vessels from the maxillary artery and vein. In *Kryptobaatar*, the canal for the inferior alveolar nerve and vessels opens posteriorly just behind the level of the second molar.

MASTICATORY FORAMEN (FORAMEN MASTICATORIUM). Aperture in the alisphenoid, on the side wall of the braincase, transmitting the masticatory branch of the mandibular nerve in some rodents (Hill, 1935; Wahlert, 1974). Following Simpson

(1937), the term is used for the more lateral of the two foramina in the anterior lamina that transmitted branches of the mandibular nerve in multituberculates (see foramen ovale inferium). On one side of one specimen of *Kryptobaatar* (PSS-MAE 113), the masticatory foramen is bifurcated by the lateral flange, which produces a ventral opening into the epitympanic recess and a lateral opening into the temporal fossa.

MAJOR PALATINE FORAMEN (FORAMEN PALATINUM MAJOR). In the dog (Evans and Christensen, 1979), the major palatine nerve and artery (branches of the maxillary nerve and artery, respectively) leave the orbit in the palatine canal in the maxilla that opens at the major palatine foramen on the palate between the maxilla and palatine. In *Kryptobaatar*, the major palatine nerve and artery left the orbit via the sphenopalatine foramen and appeared on the hard palate via the major palatine foramen in the anteromedial corner of the suture between the maxilla and palatine at the level of the P4/M1 embrasure; the presence of the dorsal aperture of the palatine canal cannot be determined.

MENTAL FORAMEN (FORAMEN MENTALE). In the dog (Evans and Christensen, 1979), there are usually three mental foramina, each of which transmits nervous and vascular branches of the inferior alveolar nerves and vessels from the mandible to the chin. In *Kryptobaatar*, the single mental foramen is anterolaterally directed and in the diastema between the incisor and third premolar, closer to the superior than the inferior margin of the bone.

METOPTIC FORAMEN (FORAMEN METOPTICUM). The aperture occurring in most extant sauropsids between the pilae metoptica and antotica that transmits the oculomotor nerve and in some instances also the trochlear nerve, ophthalmic artery, and/or pituito-orbital vein (De Beer, 1926, 1937; Bellairs and Kamal, 1981). A metoptic foramen is not present in the chondrocranium or bony skull of any extant mammal, because the pilae metoptica and antotica do not co-occur; however, one is generally held to have been present in the chondrocranium of the common ancestor of Mammalia (Kuhn, 1971; Kuhn and Zeller, 1987; Zeller, 1989). In *Lambdopsalis*, Miao (1988) described an aperture at the anterolateral corner of the hypophyseal fossa as the metoptic foramen and placed within it the oculomotor nerve, ophthalmic artery, and pituitary vein (pituito-orbital vein), citing De Beer (1937). Following Miao, and in light of the morphology in *Tachyglossus* (see Gaupp, 1908) and *Ornithorhynchus* (personal obs.), we restore the oculomotor nerve in the similarly placed foramen in *Kryptobaatar*, but not the ophthalmic artery and pituito-orbital

vein. Although the ophthalmic artery accompanies the oculomotor nerve in some sauropsids (Shiino, 1914; Bellairs and Kamal, 1981), in others and in mammals, the ophthalmic artery runs with the optic nerve (Tandler, 1899; Hafferl, 1933; Wible, 1984). The pituito-orbital vein in *Kryptobaatar* occupied its own foramen.

MINOR PALATINE FORAMEN (FORAMEN PALATINUM MINUS). In the dog (Evans and Christensen, 1979), the minor palatine nerve and artery (branches of the maxillary nerve and artery, respectively) leave the orbit and reach the soft palate via an unnamed notch, rarely closed to form a foramen, in the back edge of the maxilla and palatine. In *Kryptobaatar*, the minor palatine nerve and artery left the orbit via a foramen in the posterior limit of the orbital process of the maxilla and traversed the minor palatine canal, which opens on the back edge of the palate between the palatine, maxilla, and alisphenoid. We designate the opening on the palate the minor palatine foramen.

NASAL FORAMEN (FORAMEN NASALE). First used by Simpson (1937) for the two pairs of foramina visible on the dorsum of the nasals in *Ptilodus*, suggested to have been vascular in function. Kielan-Jaworowska (1971) proposed the lateral ethmoidal nerve as an alternative occupant. Both nervous and vascular functions seem likely. Similar foramina in the nasal of the iguanid *Ctenosaura pectinata* accommodate the dorsal cutaneous branch of the lateral ethmoidal nerve, as pointed out by Kielan-Jaworowska (1971), and venous tributaries to the orbital sinus (Oelrich, 1956). In the dog (Evans and Christensen, 1979), the external nasal nerve, off the ethmoidal nerve, and branches of the external ethmoidal artery run ventral to the nasal bone and emerge at that bone's anterior limit to supply the muzzle; these seem likely occupants for the nasal foramina in multituberculates. In the specimens of *Kryptobaatar* described here, the number of nasal foramina is uncertain because of damage; there are two foramina arranged asymmetrically between the two sides in PSS-MAE 101.

OPTIC FORAMEN (FORAMEN OPTICUM). In the dog (Evans and Christensen, 1979), the opening in the orbitosphenoid that connects the cranial cavity and orbit and transmits the optic nerve and the ophthalmic branch of the internal carotid artery. A similar opening occurs in the orbitosphenoid of *Kryptobaatar*. The embryological precursor of the optic foramen is in the chondrocranium between the pilae preoptica and metoptica (Starck, 1967; Moore, 1981).

ORBITOTEMPORAL CANAL (CANALIS ORBITOTEMPORALIS). Following Rougier et al. (1992), the channel in the side wall of the braincase connect-

ing the dorsal ascending canal with the orbit and transmitting the ramus superior of the stapedia artery, its continuation the ramus supraorbitalis, and accompanying veins. In *Kryptobaatar*, this channel is largely endocranial, bounded laterally by the parietal, except anteriorly where there is a short intramural course between the parietal and frontal; the anterior opening of the orbitotemporal canal is beneath the postorbital process, between the parietal, frontal, and anterior lamina. The orbitotemporal canal, also called the sinus canal (Watson, 1911) and internal parietal groove (Kielan-Jaworowska et al., 1986), may be wholly extracranial as, for example, in the non-mammalian cynodont *Probainognathus* (Rougier et al., 1992).

PERILYMPHATIC FORAMEN (FORAMEN PERILYMPHATICUM). Following Kuhn (1971) and Zeller (1989, 1991), the aperture in monotremes in the back of the promontorium of the petrosal that transmits the perilymphatic duct into the inner ear and provides support for the secondary tympanic membrane. In therians, the perilymphatic duct becomes enclosed in a separate canal, the cochlear aqueduct, by the processus recessus; the enclosure of the perilymphatic duct leaves a separate aperture for the secondary tympanic membrane, the fenestra cochleae (Zeller, 1985). In *Kryptobaatar*, a cochlear aqueduct is lacking and, therefore, the aperture on the back of the promontorium is a perilymphatic foramen.

POSTTEMPORAL CANAL (CANALIS POSTTEMPORALIS). Following Rougier et al. (1992), the vascular canal between the petrosal and squamosal and/or parietal connecting the ascending canal with the occiput and transmitting the arteria and vena diploëtica magna. In *Kryptobaatar*, the posterior opening is at the lateral margin of the occiput, entirely within the mastoid exposure of the petrosal.

PRIMARY FACIAL FORAMEN (FORAMEN FACIALIS PRIMARIUM). Following Wible (1990) and Wible and Hopson (1993), the opening for the facial nerve in the endocranial surface of the petrosal that connects the internal acoustic meatus with the cavum supracochleare or cavum epiptericum. In *Kryptobaatar*, the primary facial foramen shares a common aperture in the internal acoustic meatus with that for the vestibular nerve, and it opens into the back of the cavum epiptericum.

PROOTIC CANAL (CANALIS PROOTICUS). First used by Gaupp (1908) for the canal in the petrosal of the echidna *Tachyglossus aculeatus*, transmitting the prootic sinus from the cranial cavity to the middle ear where it joins the post-trigeminal vein to form the lateral head vein. In *Kryptobaatar*, the endocranial aperture of the prootic canal is ventral to the lower margin of the subarcuate fossa; the ventral aperture is in a recess medial to

the crista parotica along with the foramen for the ramus superior.

PROOTIC FORAMEN (FORAMEN PROOTICUM). The opening in the orbitotemporal region of the chondrocranium between the pila antotica and the otic capsule. In extant mammals, a complete pila antotica and, therefore, the prootic foramen are found only in the chondrocrania of monotremes (Kuhn, 1971; Zeller, 1989). Transmitted are the fourth through sixth cranial nerves, the prootic vein (Wible and Hopson, 1995) and inferior petrosal sinus (Shindo, 1915) between the cavum epiptericum and the cranial cavity. This foramen is altered in adult monotremes by the resorption of all but the base of the pila antotica (Kuhn and Zeller, 1987) and the enclosure of the prootic sinus into a separate prootic canal (Wible and Hopson, 1995). The comparable region of the endocranium in *Kryptobaatar* is posterior and lateral to the ossified pila antotica, medial to the anterior lamina, and anterior to the petrosal. Transmitted through this gap were the fourth through sixth cranial nerves and the inferior petrosal sinus. The prootic sinus was enclosed in a separate canal in the anterior lamina and petrosal.

PTERYGOID CANAL (CANALIS PTERYGOIDEUS). In the dog (Evans and Christensen, 1979), the pterygoid canal is in the suture between the pterygoid and basisphenoid and transmits the nerve and artery of the pterygoid canal from the basicranium to the posteroinferior floor of the orbit. The nerve enters the basicranial end of the canal and is formed by sympathetic fibers from the internal carotid (deep petrosal) nerve and parasympathetic fibers from the greater (major) petrosal nerve; the artery is a branch of the maxillary that enters the orbital end of the canal. In *Kryptobaatar*, a canal resembling the pterygoid canal of the dog originates from the carotid groove or canal and is enclosed between the pterygoid and alisphenoid; the location of the orbital aperture could not be found. Given the size of this pterygoid canal and its intimate relationship to the carotid canal, the artery of the pterygoid canal was present, probably as a branch of the internal carotid as occurs in some lipotyphlans (McDowell, 1958; MacPhee, 1981). Whereas both the deep petrosal nerve and the artery of the pterygoid canal entered the pterygoid canal from the carotid canal in *Kryptobaatar*, the greater petrosal nerve must have entered from the cavum epiptericum; there are no tympanic apertures for the greater petrosal nerve that position it to enter the carotid canal. Consequently, the pterygoid canal of *Kryptobaatar* is not strictly homologous with that of the dog.

SECONDARY FACIAL FORAMEN (FORAMEN FACIALIS SECUNDARIUM). Following Wible (1990) and Wible and Hopson (1993), the opening in the tym-

panic surface of the petrosal by which the hyomandibular branch of the facial nerve enters the middle ear from the cavum supracochleare or cavum epiptericum. In *Kryptobaatar*, the secondary facial foramen appears to connect with the cavum epiptericum and has a common tympanic aperture with the canal for the ramus inferior of the stapedial artery.

SPHENORBITAL FISSURE (FISSURA SPHENORBITALIS). The term sphenorbital fissure (orbital fissure or anterior lacerate foramen) has been used for the gap walled medially by the orbitosphenoid and laterally by the alisphenoid or anterior lamina that transmits the contents of the cavum epiptericum anteriorly into the orbit (Simpson, 1937; McDowell, 1958; Kielan-Jaworowska et al., 1986). The nervous and vascular contents of the gap so defined vary dramatically among extant mammals and may include some combination of the following: the optic, oculomotor, trochlear, ophthalmic, maxillary, and abducens nerves; the ramus infraorbitalis, arteria anastomotica, and ophthalmic artery; and the ophthalmic veins. In *Kryptobaatar*, the sphenorbital fissure lies between the orbitosphenoid ventromedially, the frontal dorsomedially, the anterior lamina laterally, and probably the maxilla ventrally; it transmitted the trochlear, ophthalmic, and maxillary nerves, the ophthalmic veins, and probably the ramus infraorbitalis.

SPHENOPALATINE FORAMEN (FORAMEN SPHENOPALATINUM). In the dog (Evans and Christensen, 1979), the opening in the palatine that connects the orbit and the nasal fossa and transmits the caudal nasal nerve and the sphenopalatine artery and vein, branches of the maxillary nerve, artery, and vein, respectively. The sphenopalatine foramen lies immediately dorsal to the caudal palatine foramen, by which the major palatine nerve and artery enter the palatine canal. In *Kryptobaatar*, the sphenopalatine and caudal palatine foramina that occur in the dog are fused into a single opening either within the maxilla or between the maxilla and frontal. We call this common opening the sphenopalatine foramen, following, for example, Kielan-Jaworowska et al. (1986).

STYLOMASTOID FORAMEN (FORAMEN STYLOMASTOIDEUM). In the dog (Evans and Christensen, 1979), the opening between the petrosal, the osseous bulla, and the tympanohyal (tympanohyoid) cartilage by which the facial nerve (hyomandibular branch) leaves the middle ear and the stylo-mastoid artery off the posterior (caudal) auricular enters. In *Kryptobaatar*, only a stylo-mastoid notch formed by the petrosal, including the ossified hooklike tympanohyal, is evident. In addition to the facial nerve, the notch probably accommodated a stylo-mastoid artery, because that vessel is widely distributed in extant mammals (Wible,

1987). However, whether that artery was derived from the stapedia system as a ramus posterior or from the external carotid system is uncertain.

SUPRAGLENOID FORAMEN (FORAMEN SUPRAGLENOIDALE). First used by Cope (1880) for the presumed venous aperture perforating the base of the zygomatic process of the squamosal from above that occurs in a variety of extant therians. Simpson (1937) applied the name to the aperture in *Ptilodus* in front of the base of the zygomatic process of the squamosal that faces anterolaterally into the temporal fossa; however, he noted this opening does not correspond exactly with the supraglenoid foramen of therians and questioned the homology of the two. In *Kryptobaatar*, the supraglenoid foramen is in the anterior lamina slightly posterior and dorsal to the foramen masticatorium. Following Rougier et al. (1992) and Wible and Hopson (1995), we reconstruct as the principal vessel in it an arterial branch to the temporalis muscle off the ramus superior of the stapedia, known as a ramus temporalis.

TRANSVERSE CANAL (CANALIS TRANSVERSUS). Term used by Gregory (1910) for the venous canal in the basisphenoid crossing the midline in some extant therians. In *Kryptobaatar*, the transverse canal is a large channel in the sphenoid complex immediately in front of the hypophyseal fossa, connecting the left and right sphenorbital recesses.

VENTRAL ASCENDING CANAL (CANALIS ASCENDENS VENTRALIS). Following Rougier et al. (1992), the ventral part of the ascending canal between its tympanic opening (equivalent to the pterygoparoccipital foramen, see Rougier et al., 1992; Wible and Hopson, 1995) and the posttemporal canal, transporting the ramus superior of the stapedia artery. In *Kryptobaatar*, the ventral ascending canal is horizontal, posterolaterally directed, and presumably entirely within the anterior lamina; its tympanic opening shares a common recess with the prootic canal. The equivalent channel can be more vertical and either endocranial, as in lipotyphlans, or extracranial, as in *Morganucodon* (Rougier et al., 1992).

INDEX OF ANATOMICAL TERMS

- aqueducts
 cochlear, 39, 55, 118
 vestibular, 55
- arteries
 accessory palatine, 77, 114–115
 diploëtica magna, 67, 71, 91–92, 118
 ethmoidal, 50, 72, 115, 118
 external carotid, 67–68
 frontal, 23, 72
 infraorbital, 70, 116
 internal carotid, 31, 36–37, 68, 89–90, 102, 115
 lacrimal, 72
 major palatine, 70, 117, 119
 maxillary, 68
 minor palatine, 70, 115, 118
 ophthalmic, 50–51, 58, 72, 119
 of pterygoid canal, 38, 72, 92, 119
 ramus inferior, 41, 65, 68–70, 88, 91, 115
 ramus infraorbitalis, 55, 68–70, 96, 119
 ramus mandibularis, 68
 ramus orbitalis, 72
 ramus superior, 41, 67–72, 91–92, 115
 ramus supraorbitalis, 23, 67–72, 92, 118
 ramus temporalis, 42–43, 45, 71, 91–92, 116, 120
 sphenopalatine, 119
 stapedial, 37, 38–39, 42, 67, 70, 90, 102
 vertebral, 67, 68, 90
- auditory tube, 84, 101
- bones
 alisphenoid, 33–36, 85, 100
 anterior lamina, 36, 42–43, 55–56, 79, 100
 basioccipital, 48, 51–53
 basisphenoid, 31, 56, 98
 ectopterygoid, 84–85, 100
 ectotympanic, 99
 exoccipital, 47–48, 51
 frontal, 21–23, 79–80
 incus, 40, 94
 interparietal, 46
 jugal, 43, 83, 99–100
 lacrimal, 20–21, 78–79
 malleus, 40, 99
 mandible, 59–62
 maxilla, 23–28, 79–80
 nasal, 19–20, 76–77, 83
 orbitosphenoid, 31–33, 58, 79, 81
 palatine, 28–29, 79, 100
 parietal, 46, 82–83, 101
 petrosal, 36–43, 53–56, 93–96
 premaxilla, 16–19, 72–74
 presphenoid, 31
 pterygoid, 30–31, 84
 septomaxilla, 16, 74–76, 100
 squamosal, 43–46
 stapes, 40, 70, 90, 94, 99, 102
 supraoccipital, 46–47
 vomer, 31, 83
- canals
 accessory palatine, 114
 alisphenoid, 85, 91, 97
 alveolar, 25, 77, 116
 ascending, 67, 115
 carotid, 31, 37–38, 68, 89–90, 92, 115
 dorsal ascending, 43, 70–71, 115
 facial, 70
 hypoglossal, 116
 infraorbital, 23, 25, 70, 116
 mandibular, 62, 117
 of ?maxillary artery, 88, 115
 minor palatine, 27, 78, 101, 118
 orbitotemporal, 23, 42, 67, 70–71, 101, 118
 palatine, 26, 117, 119
 posttemporal, 43, 67, 70–72, 91–92, 118
 post-trigeminal, 88, 90, 115
 prootic, 41, 55, 65, 88, 91, 102, 118
 pterygoid, 38, 72, 92–93, 119
 for ramus inferior, 70, 88, 90, 115
 semicircular, 36, 39
 sinus, 118
 sphenoparietal, 97
 transverse, 59, 65–66, 89, 100, 120
 ventral ascending, 41, 70–71, 91, 115, 120
- cava
 epiptericum, 49, 53, 55, 70, 95, 96–98
 supracochleare, 55, 95
- cerebellum
 paraflocculus, 53
 vermis, 63
- cerebrum, 63
- choana, 28, 29, 30, 31, 34
- cochlea, 36
- condyles
 of mandible, 61
 occipital, 47
- crests
 condyloid, 60
 masseteric, 60
 nuchal, 45, 46, 47
 orbitosphenoidal, 58

- pterygoid, 62
 sagittal, 46
 supraorbital, 22, 46
 cribriform plate, 59, 99
 cristae
 interfenestralis, 39, 94
 parotica, 40, 93, 94
 petrosa, 53
 dorsum sellae, 56, 64, 98
 ducts
 endolymphatic, 55
 nasolacrimal, 59, 117
 perilymphatic, 39, 55, 93, 118
 egg-tooth, 74
 fenestrae
 cochleae, 118
 sphenoparietal, 51
 vestibuli, 39, 70, 115
 foramina
 for abducens nerve, 58
 accessory palatine, 28, 77–78, 114–115
 buccinator, 36, 85, 115
 carotid, 37, 56, 68, 89–90, 102, 115
 for cochlear nerve, 55, 98
 of dorsal ascending canal, 43, 92, 116
 ethmoidal, 23, 33, 58–59, 81, 115
 for frontal diploic vein, 23, 80, 82, 115–116
 hypoglossal, 47–48, 96, 116
 incisive, 19, 116
 infraorbital, 23, 77, 116
 jugular, 33, 47, 51, 55, 63, 87–88, 117
 lacrimal, 21, 80, 117
 magnum, 47, 48, 63, 102
 major palatine, 27, 77–78, 117
 masticatorium, 36, 41, 86, 117
 mental, 59, 117
 metoptic, 33, 49, 50–51, 57–58, 81, 88, 96–97, 100, 117
 minor palatine, 27, 34, 70, 77–78, 101, 118
 nasal, 19–20, 76–77, 118
 optic, 33, 49, 50–51, 58, 72, 81, 97, 100, 118
 orbitonasal, 49, 50
 ovale, 36
 ovale accessorius, 36
 ovale inferium, 41, 86, 116
 perilymphatic, 39, 118
 for pituito-orbital vein, 56, 88, 100, 102, 116
 primary facial, 50, 55, 95, 118
 prootic, 49, 50–51, 65, 118–119
 pseudoptic, 50–51
 pterygoparoccipital, 41, 91, 120
 for ramus temporalis, 43, 45, 46, 71, 92, 116
 secondary facial, 41, 118
 sphenopalatine, 25–26, 70, 80, 119
 sphenoparietal, 51
 stylomastoid, 119
 supraglenoid, 42, 70, 91, 119–120
 for vestibular nerve, 55
 fossae
 atlantal, 43, 47
 glenoid, 46
 hypochiasmatica, 98
 hypophyseal, 38, 56–57, 98, 102
 incudis, 40
 jugular, 39, 40, 47–48, 53, 93, 101
 masseteric, 59–60
 orbitonasal, 22
 pterygoid, of alisphenoid, 35–36, 86–87
 pterygoid, of mandible, 61–62
 stapedius, 40
 subarcuate, 53
 tensor tympani, 39, 95
 trigeminal, 55
 foveae
 masseteric, 59
 pterygoid, 62
 ganglia
 facial, 49, 55, 95, 96
 trigeminal, 49, 55, 96
 grooves
 ethmoidal, 33
 internal carotid, 36–38, 68, 89, 92, 102, 115
 internal parietal, 118
 sphenopalatine, 26–27, 70
 stapedial, 37, 38, 70, 90, 102
 temporal, 60
 hamulus, of pterygoid, 31, 84
 hiatus Fallopii, 92
 jugum sphenoidale, 58, 98–99
 laminae
 infracribrosa, 58, 99
 obturans, 36
 lateral flange, 40, 70, 90, 94
 meatuses
 external acoustic, 40, 45
 internal acoustic, 53, 55, 116–117
 muscles
 incisivus superioris, 18

- lateral pterygoid, 36, 42, 62
- medial masseter, pars anterior, 22, 59, 79
- medial pterygoid, 39, 62, 84
- sternomastoid, 43
- superficial masseter, pars anterior, 23, 24
- superficial masseter, pars posterior, 46
- temporalis, 43, 60, 70, 82
- tensor tympani, 39, 95
- tensor veli palatini, 84

- nasal overhang, 20, 76
- nerves
 - abducens (VI), 49, 51, 58, 96
 - accessory palatine, 77, 114
 - buccal, of V, 36, 86–87, 115
 - caudal nasal, 119
 - cochlear, 55, 117
 - deep petrosal, 38, 92–93, 119
 - deep temporal, 86
 - ethmoidal, 23, 33, 49, 59, 115, 118
 - facial (VII), 40, 41, 49, 55, 117, 118, 119
 - frontal, 23
 - glossopharyngeal (IX), 117
 - greater petrosal, 38, 93, 96, 119
 - inferior alveolar, 117
 - infraorbital, 25, 116
 - internal carotid, 38, 68, 115
 - major palatine, 26–27, 77, 117, 119
 - mandibular (V₃), 36, 41, 68, 86, 116, 117
 - maxillary (V₂), 55, 68
 - minor palatine, 27, 77, 118
 - oculomotor (III), 49, 51, 55, 58, 88, 97, 117
 - ophthalmic (V₁), 55, 68
 - optic (II), 49, 51, 58, 72, 118
 - of pterygoid canal, 38, 72, 119
 - spinal accessory (XI), 48, 117
 - trigeminal (V), 49, 51, 96
 - trochlear (IV), 49, 51, 55, 96
 - vagus (X), 117
 - vestibular, 55, 117
- notches
 - anterior nasal, 20, 76
 - odontoid, 47, 48
 - palatonasal, 78
 - stylomastoid, 40, 119
 - supraorbital, 22, 23, 46

- occipital plane, 47
- olfactory bulbs, 58
- orbital pocket, 22–23, 79–80
- orbital wing, 58
- os carunculae, 74

- pilae
 - antotica, 49, 50–51, 57–58, 97–98, 100
 - metoptica, 49, 50–51, 58, 97–98, 100
 - preoptica, 49, 50–51, 58, 97
- postpalatine torus, 29
- prefacial commissure, 50, 53
- processes
 - caudal tympanic, of petrosal, 40, 94
 - coronoid, 60–61
 - facial, of lacrimal, 20, 78
 - orbital, of palatine, 28, 79, 100
 - paroccipital, of petrosal, 40, 94
 - posterodorsal, of premaxilla, 17
 - postorbital, of frontal, 82–83, 101
 - postorbital, of parietal, 46, 82–83, 101
 - prenasal, of premaxilla, 17, 72–74, 100
 - rostral tympanic, of petrosal, 39
- promontorium, of petrosal, 36

- recesses
 - epitympanic, 35, 40–41, 86, 94–95
 - post-promontorial tympanic, 94
 - scala tympani, 93–94
 - sphenorbital, 25, 35
- ridges
 - anterior zygomatic, 24–25
 - intermediate zygomatic, 46
 - orbital, 22
 - posterior zygomatic, 46
 - pterygopalatine, 30–31, 83–84, 101
 - temporal, 46

- sinuses
 - anterior intercavernous, 50, 51
 - cavernous, 63
 - inferior petrosal, 50–51, 53, 63–64, 87–88, 117
 - maxillary, 25, 77, 116
 - posterior intercavernous, 51, 64
 - prootic, 41, 50–51, 55, 63, 65, 88, 118
 - sigmoid, 51, 53, 63, 87, 117
 - superior sagittal, 63, 87
 - tentorial, 63
 - transverse, 63, 86
- sphenoobturator membrane, 36
- sphenorbital fissure, 25, 33, 55, 70, 81–82, 119
- stylohyal, 36, 99
- subarcuate fenestration, 67
- sulci
 - chiasmatic, 58, 98
 - facial, 41
 - for inferior petrosal sinus, 53, 64, 87

- for nasolacrimal duct, 59
- for pituito-orbital vein, 56, 66
- for prootic sinus, 55
- for sigmoid sinus, 51, 63
- symphysis, mandibular, 61

- taenia clino-orbitalis, 57
- thickening, of premaxilla, 19
- transversal elevation, 62
- troughs
 - lateral, of petrosal, 40–41
 - pterygopalatine, 30–31, 34, 83–84, 101
- tuberculum sellae, 58, 98
- turbinals, 59
- tympanohyal, 40, 119

- veins
 - capsuloparietal emissary, 51
 - frontal diploic, 23, 115–116
 - internal jugular, 65, 88
 - lateral head, 50, 64–65, 88, 118
 - middle cerebral, 50
 - ophthalmic, 55, 63, 96
 - pituitary, 50, 117
 - pituito-orbital, 50, 56, 66, 88–89, 116, 117–118
 - post-trigeminal, 41, 65, 70, 88, 115, 118
 - prootic, 50
 - transverse canal, 59, 65–66, 89, 120
 - vertebral, 64, 87
 - vestibule, 36, 95–96
 - vomeronasal organ, 116